Talc Characterization: A Provenance Study

A Dissertation

Presented in Partial Fulfillment of the Requirements for the

Degree of Doctorate of Philosophy

with a

Major in Geology

in the

College of Graduate Studies

University of Idaho

by

Marian E. Buzon

Major Professor: Mickey E. Gunter, Ph.D.

Committee Members: Peter Larson, Ph.D.; Owen Neill, Ph.D.; Thomas Williams, Ph.D.

Department Administrator: Mickey E. Gunter, Ph.D.

August 2016

Authorization to Submit Dissertation

This dissertation of Marian E. Buzon, submitted for the degree of Doctorate of Philosophy with a Major in Geology and titled "Talc Characterization: A Provenance Study," has been reviewed in final form. Permission, as indicated by the signatures and dates below, is now granted to submit final copies to the College of Graduate Studies for approval.

Major Professor: _____ Date: _____

Mickey E. Gunter, Ph.D.

Committee Members: _____ Date: _____

Peter Larson, Ph.D.

_____ Date: _____

Owen Neill, Ph.D.

_____ Date: _____

Thomas Williams, Ph.D.

Department

Administrator: _____ Date: _____

Mickey E. Gunter, Ph.D.

Abstract

Talc is a useful mineral in many industries and therefore has a high probability that consumers are exposed to it and other minerals present in ores. Some of these accessory minerals may be classified as asbestos while others are known to be harmless. The conditions of talc formation at a given deposit determine the resulting mineralogy. In many instances, asbestos is "identified" in talc ores and products based on crude assumptions, misunderstanding of nomenclature, or improper interpretations of analytical results. Purported asbestos content in talc ores and products has been the focus of recent civil litigation, typically brought by victims of mesothelioma, a cancer that is causally associated with asbestos exposure but is not linked specifically to talc itself. The general geology of many economic talc deposits is well known, leading us to wonder if commercial talc could be traced back to the type of deposit in which it formed. Furthermore, could this information be used in litigation to support or deny the likelihood of asbestos in talc products with a known source?

This project involves the use of a suite of analytical methods to determine 1) what mineral phases are present in talc ores, 2) the bulk major and trace element concentrations of ores from a selected talc deposit and how the compositions relate to the mineral content, and 3) what, if any, compositional or morphological differences exist between talc that has formed from different protoliths and processes? We are considering provenance in the context of the location the talc is from and more importantly the processes that were involved in talc formation. The resulting information will be compiled in a database including results from powder x-ray diffraction, electron micro-probe, x-ray fluorescence spectroscopy, and stable isotope analyses.

Chapters 1 and 3 include the mineralogy, compositions, and morphologies of our commercial talc samples. Chapter 2 is a more focused view of all the data for talc from southwest Montana, which is a highly producing talc mining region, and the issues resulting from asbestos-related litigation.

Acknowledgements

I would like to thank those who contributed talc samples to this project including Richard Berg, Imerys Talc, Barretts Minerals Inc., and other anonymous personal contributors. I would also like to thank the Washington State University Geo-Analytical Lab for running analyses, allowing access to their facilities, and for training me in a variety of analytical methods. On a similar note, thank you to my committee members Peter, Owen, and Tom for their advice, expertise, and training in their respective fields. Most importantly I would like to thank Mickey, for everything.

Table of Contents

List of Figures

List of Tables

Chapter 1: Determining the provenance of commercial talc based on composition and mineralogy

Abstract

Talc is famously the softest mineral on Mohs hardness scale and is easily ground to a brilliant white powder, making it useful in many industries. We are creating a compositional database of talc ore, talc products, and monomineralic talc from known locations by using a suite of analytical techniques, including but not limited to electron microprobe analyses, powder x-ray diffraction and x-ray fluorescence spectrometry along with data published by other workers. This database will hopefully help us to source talc based on composition and on the principles of talc formation. Due to the lack of compositional variation in the mineral talc, we can use significant concentrations of major cations other than Si and Mg in ores and products as proxies for the content of common accessory minerals. These determinations are cross-checked with powder XRD data in order to confirm bulk mineral content. Trace element concentration applications via bulk XRF vary depending on the accessory mineral content in ores. Applications for these data might include sourcing commercial talcs to their type of deposit, and better understanding the compositional and mineralogical variations in talc deposits as often needed in the regulatory and legal arenas.

Introduction

Talc is a sheet silicate with a composition known to vary little from the empirical formula, $Mg_3Si_4O_{10}(OH)_2$. Industrially, talc may refer to an ore that contains as little as 20% of the mineral talc (McCarthy et al., 2006). Accompanying minerals in talc ores may include amphiboles (most likely tremolite, anthophyllite, actinolite) clinochlore, serpentine group minerals, calcite, dolomite, magnesite, and quartz (Chidester, 1962). Some ores contained a significant amount of tremolite but were still referred to as talc or tremolitic talc because of their commercial applications (Wright, 1968). Trade names such as “soapstone” and “steatite” have been used to describe commercial materials. “Soapstone” is a trade name for a carving or dimension stone made of about 30-50% talc, accompanied by clinochlore or serpentine group minerals. The term “steatite” designates very pure talc rocks, containing

upwards of 80% talc. Industrially, steatite indicates a relatively pure talc rock that has specific applications in ceramic insulating bodies (Chidester et al., 1964). These polymineralic talcs fill, or have filled industrial niches. For example the amphibole content in talc sourced from talc mines in New York was particularly useful in making paint and resin fillers while talc used in cosmetic products is nearly monomineralic and from different sources. Products categorized as “industrial talc” are often blends of several minerals to result in desired physical and chemical properties. Talc is useful due to its softness, white streak, ability to adsorb pigments, hydrophobic properties, chemical inertness, and heat resistance. Common production and uses of talc in the U.S. have applications in the ceramics, paper, paint, plastics, roofing, cosmetics, and rubber industries. Primary imports of talc to the U.S. are from Pakistan, Canada, China and Japan but Finland and other countries have contributed as well. The global leading producers and reserves for talc are the United States, Brazil, China, France, Finland, India, Japan and the Republic of Korea. Domestic U.S. sources in decreasing order are from Montana, Texas, Vermont and Virginia although New York, North Carolina, and California were major sources of talc over the last few decades (Flanagan, 2016).

It is highly likely that most consumers come in contact with talc-containing products on a daily basis, and many individuals experience occupational exposure. Although there is not much concern for the health effects of respirable talc, there is concern for exposure to asbestos via products with purported asbestos content. The magnesium-rich asbestos minerals including tremolite asbestos, and chrysotile are the most common of the regulated six to be purported to be in talc products. The identification of asbestos from a mineralogical perspective needs to be confirmed by composition of the phases, structure of the phases, and an asbestiform habit. Currently most popular press and medical websites link talcum powder to mesothelioma or ovarian cancer. Although the link between asbestos and or talc with ovarian cancer is not completely understood, it is well understood that mesothelioma is typically caused by prolonged exposure to respirable asbestos (Kane, 1993). This has resulted in an increase of civil litigation in which parties are arguably liable for damages incurred by individuals who purportedly have been exposed to asbestos. There are no asbestos companies left to sue so the talc industry has absorbed many of these claims. These

defendants may include mining companies, production plants or retailers of products with purported asbestos content. The most common of these products is body powders. Thus, there is a need to be able to systematically confirm or rule out whether an individual experienced asbestos exposure from these talc products. We are concerned with determining the composition and mineral content of commercial talc in order to trace talc ores and products back to the deposit, or type of deposit in which they formed along with determining if they contain minerals that may occur in the asbestiform habit.

Geologic context

Manganese, Ni and Cr may occur in trace concentrations substituting for Mg^{2+}, and Ti may occupy the tetrahedral site in talc and will only occur in significant concentrations in a Si-depleted environment. Aluminum and iron are most likely to be present in up to minor concentrations; ferrous (Fe^{2+}) iron content may span a range from a fraction of a formula unit to 1.22 atoms per three octahedral sites, but these compositions are not all necessarily from economic grade talcs. Fluorine and Cl commonly substitute for OH^- (Evans and Guggenheim, 1988 and references within). Concentrations of Ca, K, and Na are generally negligible and likely indicate the presence of interlayer cations or inclusions rather than site occupancies. Metamorphic rocks may retain compositional traits from their protolith, and from the processes that formed them. Most talc-forming mechanisms that create mineable deposits involve metasomatism, during which ions in solution completely, volume-by-volume, alter the protolith. However, in cases of pervasive hydrothermal alteration the composition of the altering fluids may overprint the compositional traits of the protolith.

The mineral talc is known to form in many geologic environments but mineable talc deposits form by the alteration of two compositionally distinct protoliths; those of carbonate origin and those of mafic/ultramafic origin. In many cases the increase in SiO_2 required to form talc from these lithologies comes from the surrounding rocks. Deposits also may be categorized by the mechanisms that formed them. McCarthy et al. (2006) defined four distinct types of economic talc deposits. Type 1 and Type 2 deposits are serpentinized, and subsequently carbonitized ultramafic and mafic rocks respectively. These types of deposits

account for about 30-40 percent of economic talc deposits (Boschi et al., 2006; Moine et al., 1989). The talc-forming processes are associated with regional metamorphism and alteration by fluids in varying degrees. Accessory minerals in regionally metamorphosed ultramafic-hosted talc ores typically include carbonates but expected assemblages may include talc ± serpentine ± chlorite ± tremolite ± carbonate (Moine et al., 1989). These deposits form in pods in which there are concentric zones of alteration. As a result, serpentine group minerals are often proximally associated with these deposits and are located in the innermost pod as seen in Figure 1a from Chidester et al. (1951) and Figure 1b from Karlsen et al. (2000). The composition of the ultramafic, or less commonly the mafic protolith is similar to that of the resulting talc ore indicating minimal fluid interaction with the protolith. Thus, compositional traits from an ultramafic rock, such as relatively high Ni and Cr concentrations tend to remain in the talc ores hosted in both accessory phases and the talc. Economic talc deposits formed from altered ultramafic rocks are located in Johnson and Ludlow, Vermont; the Llano mining district, Texas; and include all the known economic occurrences of talc in Norway and Finland.

Most economic talc has formed after altered carbonates (Moine et al., 1989). Ross et al. (1968) determined that of the twenty two worldwide talcs they analyzed, those with a carbonate origin had higher fluorine concentrations ranging from 0.11-0.48 weight percent F-, while those derived from ultramafic or mafic rocks had lower than 0.04 weight percent fluorine. McCarthy et al.(2006) defined type 3 deposits as those formed by the hydrothermal alteration of dolomites by a silica rich fluid. Economically important hydrothermally altered carbonate deposits are located in southwest Montana; northwest region Death Valley, California; Van Horn (Allamoore mining district), Texas; Trimouns deposit in the French Pyrenees, and the Puebla de Lillo deposits of Northern Spain. Van Gosen et al. (2003) observed that talc deposits formed after carbonates altered by fluids heated at depth generally lack amphiboles, and have very low accessory mineral content. Fluid inclusion studies of these deposits also have shown that the talc-forming process involved highly saline SiO_2-rich CO_2-poor fluids, temperatures <400° C, and relatively low pressures. Type 4 deposits are formed through contact or regional metamorphism of dolomitic marbles, and are more

likely to contain amphiboles, which through retrograde conditions and an increase in the SiO_2 content often alter to talc. Talc deposits in southeast Death Valley region, California; central western New York; and those in North Carolina are formed by mechanisms most closely associated with 4 deposits. It is common for metasomatism to accompany metamorphism making the boundary between type 3 and type 4 deposits gradational. The four "types" of deposits place helpful labels on talc forming process, but also assume that end-member mechanisms have resulted in these deposits while realistically a combination of processes has contributed to the resulting mineralogy. It is also important to recognize that because talc is thought to be stable in these deposits that it most likely formed in the latest stage of alteration, but most of these deposits have polymetamorphic histories creating compositional or structural boundaries that are unique to that location. For this reason we will not categorize talc deposits by the aforementioned "types" in our discussion, but will place most of our focus on the influence of protolith composition, fluid composition and mobilization, and pressure and temperature on the talc forming processes.

Methods and Data

Van Gosen et al. (2003) analyzed talc from commercial deposits primarily via powder XRD and scanning electron microscopy (SEM) with energy-dispersive spectroscopy (EDS); some of the samples were analyzed with wavelength-dispersive spectroscopy (WDS). Our project partly revisits the overarching theme of their paper, but we are concerned with using multiple analytical methods on more samples in order to address composition on a number of scales as well as non-U.S. samples. On a similar note, much of the existing compositional data published by earlier researchers is from bulk analyses of rocks that were not necessarily monomineralic or from in situ EDS analyses that are not precise enough to determine chemical formulas. As stated earlier, talc does not have a wide compositional range but we expect subtle and reproducible trends described in the previous section. The U.S. Geological Survey provided a thorough collection of wet chemical analyses on talc samples (Chidester et al., 1964). Again, excluding the data from McNamee and Gunter (2014), and Karlsen et al.

(2000), shown in Table 1, most of the existing compositional data are not precise enough to determine stoichiometric variations.

Composition in our paper, as suggested above, includes identified mineral phases via powder XRD, precise weight percent oxide compositional data via WDS, and trace element data via XRF-WDS for most samples. Sample grain sizes limited the ability to analyze some samples via EPMA. Our goal is to determine whether, and how significant of a relationship exists between composition and the geologic environment for each sample.

The samples for this project are talc ores, proprietary powders, and consumer-ready talc products. Ores include talc rock that is extracted for profit. Proprietary powders are milled and beneficiated ores that have an intended mineral content that directly relates to an industrial niche. Mining companies have unique and somewhat secretive methods in beneficiating and classifying these products. All samples have undergone powder XRD and XRF analyses. We did EPMA on fewer samples due to sample grain size limitations. We have acquired samples from numerous worldwide locations and have labeled samples using the following format: COUNTRY_state/province_mine/mill. The ore samples are labeled with their respective grades (HG=high grade, LG=low grade, or G#=specific grade of ore where 1 is the highest quality, and higher numbers indicate lower quality). We have samples from countries including Austria (AUSTRIA), Australia (AUS), Brazil (BRA), Canada (CAN), China (CHI), Finland (FIN), India (IND), Italy (ITA), Korea (KOR), Morocco (MOR), Norway (NOR), Spain (SPA) and the United States (USA). The abbreviation CT is used for commercial talc samples, indicating that the sample needs no further beneficiating in order for it to be sold as a product either to consumers or distributors; these include cut soapstone items, body or baby powders, paint/resin fillers, anticaking/releasing agents and pharmaceutical talc. Most samples were collected by us or were given to us with a relatively specific known location (city or mine). Other samples were treated as unknowns, or partial unknowns if they are commercial samples with unknown geologic origin (consumer-ready products) or if we only know the country the sample came from but have no other information (samples from Finland, Norway, Spain, “Korea” and one from China). In the case of the latter, the results are cautiously compared with what we would expect from the talc-forming environments in that

country. One critical view of this project is the assumption of homogeneity among all samples from the same deposit. Our efforts at addressing this issue are two-fold; we are comparing our compositional data with pre-existing data to determine whether our results are reasonable and representative of the composition of a deposit on a larger scale, and when possible, we analyzed multiple samples from the same deposit/mining region.

Preparation for bulk XRF and powder XRD

Approximately four grams of each talc ore sample, and non-powdered product were ground with a porcelain mortar and pestle until fragments were about 1mm in diameter. We ground the fragments with a McCrone micronizing mill using corundum beads and 95% ethanol for about twelve minutes. The slurry was rinsed into a glass dish with ethanol until the contents poured out clear. We left the dish in a fume hood until the ethanol evaporated. The dry powdered sample was removed from the glass dish. Samples that we acquired in powders were used in analyses as-is and were not processed any further.

Powder XRD

For each sample we prepared a backfilled powder mount and supported the bottom of the sample with a microscope slide. We analyzed samples with the Siemens D5000 powder x-ray diffractometer at the University of Idaho from 2°-52°, for 20 seconds for each step of 0.020°, using Cu kα radiation. Phases were identified using the Jade software and accompanying database. The Jade software only has a diffraction spectrum for monoclinic talc despite there being very little evidence that this structure exists. We cannot confirm with the diffraction data that we have whether the samples are monoclinic or triclinic and for consistency with the database and other references, all further discussion of diffraction data will reference dimensions of the monoclinic cell (a=5.3Å , b=9.1Å, c=18.8Å, β=80° (Akizuki and Zussman, 1978 and references within). All unlabeled difractograms are included in Appendix A. Labeled diffractograms for phases identified in our samples are also included for reference.

Table 2 includes a summary of the phases identified in each sample, the morphology index defined by Holland and Murtagh (2000) which also references a monoclinic cell and will

be discussed later, and the protolith. This talc-forming mechanism is included in this part of our results because most samples were able to be analyzed via XRD but may not have been suitable for analyses by other methods. The phases in unprocessed geologic samples determined by powder XRD are talc, chlorite, amphiboles, dolomite, calcite, magnesite, serpentine group minerals, muscovite, biotite and quartz. These data alone cannot be used to determine which mineral species are present from the amphibole, serpentine, chlorite or biotite group minerals.

The spectra for almost all the samples have two peaks at approximately 4.9° and 14.5° 2Θ. The intensities of these peaks are slightly above background radiation intensities and the 4.9° peak always has a higher intensity. The very low 2Θ value indicates that this diffraction is caused by a phase with large d-spacing.

XRF

The powdered samples were used to make fused glass beads for bulk XRF analyses using the ThermoARL X-ray fluorescence spectrometer at Washington State University's GeoAnalytial Laboratory. Each bead required a minimum of 2.0 grams of powdered sample mixed with a powdered Li-tetraborate ($Li_2B_4O_7$) flux in a ratio of 2:1. The sample and flux were thoroughly mixed, poured into a graphite crucible and heated in a furnace with an internal temperature of 1000°C. After the crucible contents melted the slab was removed from the furnace, samples fused into glass beads, were removed from the crucibles, reground, and refused in order to ensure homogeneity. Ten major rock-forming elements and 19 trace elements were analyzed. The detailed procedure and analytical parameters can be found in Johnson et al. (1999). Samples for which we did not have enough powder to fuse a standard sized bead were made into half-sized beads. Bulk XRF results are presented as weight percent oxides for major, rock-forming elements. The trace elements are reported in element concentrations of parts per million. Results are included in Appendix B.

EPMA

Individual mineral grains and thin sections were analyzed in prepared thin sections using a JEOL JXA-8500f field emission electron microprobe at Washington State University's GeoAnalytical Laboratory. Burnham Petrographics in Rathdrum, Idaho prepared thin sections an example of which is shown in Figure 2. Reference targets were marked on the thin sections with a pen and the samples were carbon-coated. The calibration standards and counting time conditions for each element are included in Table 3. The analytical routine was set up to analyze major rock-forming elements and elements that were suspected to be present in talc based on bulk XRF analyses. Standards were analyzed with a 10 µm beam. We used an accelerating voltage of 20kV, 30nA beam current, and 5 µm beam diameter on samples. Several points were analyzed for each of the three targets marked on every sample, and the resulting compositions were averaged for each mineral.

All talc microprobe data are reported in Appendix C. In agreement with our powder XRD results, we identified chlorites, amphiboles, micas, carbonates, serpentine group minerals, and quartz via microprobe analysis. The EPMA data for these phases (excluding quartz) are included in Appendix D following the data for talc. The EPMA data expressed as weight percent oxides are listed first, followed by APFU (atoms per formula unit) values calculated based on Table 10.6 from Dyar and Gunter (2008). Data are reported as averages of all the microprobe analyses of that specific mineral for that sample. The data for some analysis points were not included in the average calculations if the SiO_2/MgO ratio for an analysis was drastically different from ratios determined for other talc analyses in the same sample. Similarly, if the SiO_2/MgO ratio was very different from the ratio for the ideal chemical formula the points were not considered. In this case the spurious data are often the result of sampling two phases with one analysis point.

Discussion

Powder XRD

Talc ores from predominantly hydrothermally altered carbonate protoliths contain chlorite and talc. Amphiboles, when present, are present in samples from contact and

regionally metamorphosed rocks. Commercial talc powders that are a mixture of minerals typically contain talc and chlorite. Additionally, some of the powdered products (CT samples) might not reflect the mineralogical assemblage of a single ore used to make the product, but rather a mixture of minerals from multiple sources.

The morphology index ,($M=I_{(002)}/(I_{(002)}+I_{(040)})$) defined by Holland and Murtagh (2000) is a ratio of the intensities of the (002) reflection peak, which is along the preferred orientation for talc, and the sum of the intensities of the (002) and (040) reflection peaks. Lower morphology indices described powders that contain more finely grained talc particles, therefore both reducing the effect of preferred orientation along (002) and increasing the probability of particles oriented on (040). Particles in more coarse powders are more likely to lie on (002), and any (00*l*) for that matter, and therefore have much higher morphology indices. The morphology index values are plotted in increasing order in Figure 3 for all the samples with each sample labeled with its formation mechanism (H=hydrothermally altered, R=regional metamorphism, C=contact metamorphism, U=unknown). For comparison, the morphology indices from Murtagh and Holland range from 0.38-0.97 and the range for samples in this project is 0.23-0.98. The talc from regionally metamorphosed terrains generally formed in coarse sheets that were difficult to grind into a fine powder, despite all samples being ground in a micronizing mill. Therefore, the samples that exhibit foliation in hand sample are also the majority of the samples that have a high morphology index. The samples of microcrystalline talc that are very easily ground to a micron- to tens of microns-scale were expected to have relatively low morphology ratios. These generally include samples that formed in hydrothermally altered or contact metamorphosed terrains. Under the same sample preparation conditions, the morphology ratios for our talc samples indicate each sample's resistance to grinding, and indirectly infers the degree of foliation in a sample. Morphology ratios of ores with known origin may be able to tell us about the source of samples with unknown origin. Several samples in our collection are body and powders. These products are often blends of powders from multiple locations worldwide. The morphology ratios for these powders are quite different from each other, suggesting two potential options: 1) the grinding methods used to process talc ores into fine powders are not sufficient

to create fine enough powders, 2) that grinding methods are sufficient yet some of the talc cannot be ground into a fine powder because of its morphology. The indices determined in this chapter are not conclusive as there is no critical index under which all the samples are hydrothermally altered or above which they are all regionally metamorphosed. These observations were very much an afterthought and we think with more attention on grinding times, grinding medium, and reproducibility of data that this information could be valuable in determining provenance in regards to the alteration mechanism. In practice this is inadvertently done as we know platy talcs versus massive talcs have very different industrial applications.

Soapstone and steatite

We have several samples that were advertised as soapstone items including an ice cube, shot glass, griddle, pizza stone, coaster and bowl. The shot glass and bowl are almost entirely chlorite, based on their respective diffractograms, and technically should not be described as soapstone. The rest of the "soapstone" products do contain talc as a major phase. The coaster appears to have a significant amount of talc in it but the XRF data indicate that the peaks that appear to be for talc are pyrophyllite. Similarly, a sample categorized as "steatite" from India is also almost entirely chlorite

Sample preparation and Cl^-

The microprobe analyses on powdered samples yielded low totals due to the fine grain sizes of the particles in the powder. The analytical parameters likely resulted in an excitation volume greater than the volume of the grain, therefore analyzing surrounding Cl-rich epoxy as well. This resulted in lower than expected detection of major elements and relatively high concentrations of Cl^-. Analyses for samples that were prepared as rock sections typically produced data that were very close to expected talc compositions (31.88 weight percent MgO and 63.37 weight percent SiO_2) but we still do not think the Cl^- data are reliable. Therefore Cl^- concentrations are not included in the APFU calculation but are listed in Appendix C and D for reference. The concentration of Cl^- in most samples is negligible and can be ignored without affecting the determination of the concentrations of major cations in talc

or other minerals. On a similar note, we will be relying on the APFU values when describing compositional variations rather than weight percent oxides because the relative values of oxides (SiO_2/MgO) remained reasonable (approximately 2 for talc) despite low oxide totals.

One talc sample does seem to contain "real" Cl^-. This sample, a grade 3 ore from Guangxi, China was analyzed twice on two different slides that were prepared similar to thin sections rather than grains mounted in epoxy. This is the only sample that repeatedly contains >.02 weight percent Cl^- which converts to >.002 APFU and is not significant. Based on the samples we analyzed, concentrations of Cl^- cannot be used to distinguish talc samples.

Using major and minor elements to distinguish ores

All iron is discussed as Fe^{2+} but we did not determine the oxidation state of Fe while analyzing any of our data. Variations in Al^{3+}, Fe^{2+}, and F^- are the most common based on the EPMA data based on the multivariate scatter plots in Figures 4a and 4b. Zn^{2+}, Ni^{2+}, Mn^{2+}, Ti^{4+}, Cr^{3+}, P^{5+}, and S^{6+} show no significant variation with respect to the other elements and will not be considered in distinguishing samples based on electron microprobe data. There is more apparent scatter in the plots from oxide values (4a) but the values for TiO_2, for example, range from -0.015- 0.03 weight percent, a range in which almost all the values are below the detection limit. It is for this reason that we will be relying on compositional differences based on APFU values (4b). The correlation coefficients that correspond to these plots are included in Tables 4a and 4b. Figure 5 is a dendrogram showing clusters based on composition when considering the values for major and minor elements such as Si^{4+}, Al^{3+}, Fe^{2+}, Mg^{2+}, Ca^{2+}, K^+, Na^+, and F^-. The key compositional differences that determined what cluster each sample falls into are described in detail below. Additionally data from XRF analyses will be discussed. Grouping based on ten clusters is appropriate as that categorizes about 80% of the data. A higher number of clusters creates smaller, more compositionally distinct groups, which is not so helpful because it isolates some samples into individual clusters.

The plot for Fe^{2+} and Mg^{2+} shows the two are inversely related indicating that Fe is present in one of the M sites in place of Mg^{2+}. This has been observed in numerous other studies. Generally, the talc from altered ultramafic rocks has 0.10-0.24 APFU Fe while the

talcs sourced from altered carbonate rocks (dolomitic marbles, altered limestones) tend to have lower Fe content ranging from 0.00-0.07 APFU. Figure 6 is a BSE image of a sample from North Karelia,Finland, for which the exact location is unknown, but we know is ultramafic-hosted. This sample is representative of ultramafic-hosted talcs in that magnesite is also present, confirmed by powder XRD data. Refer to **Table 5** for compositional data.

The talc from Montana is an exception to the Fe trends observed in carbonate-hosted talcs and has a range of 0.01-0.14 Fe, but in observing the data this range can easily be split into two categories with a high-Fe talc (0.09-0.14 APFU) and a low- Fe talc (0.01-0.07 APFU). It is for this reason that some of the talc samples from Montana cluster with samples from Vermont, Finland, and Llano, Texas when based on EPMA data. An example of this is included in Figure 7 and Table 6 for a grade 1 ore from the Treasure Mine. The apparent relationship between texture and composition, where the high Fe talc is localized, is observed in other samples from the same area, although not all samples. The composition of Montana talc is discussed in great detail in the following chapter.

The concentration of F detected in samples varies from non-detectable levels to 0.28 APFU. The samples from Finland, Llano, Texas, and Vermont, which are all known to have formed in altered ultramafic rocks have a maximum of 0.02 APFU fluorine. The sample with the most F is a Grade-3 ores from Guangxi China (sample 91) with 0.27-0.28 APFU F; these values when converted to weight percent oxides are an order of magnitude greater than any of the talcs analyzed by Ross et al. (1968). The high F sample has light and dark bands that are compositionally distinct based on low and high Al^{3+} respectively, and to a lesser extent the Na^{+}. It is debatable that the dark bands are a fine intergrowth of clinochlore and talc but the dark bands have oxide totals very close to that of talc and the diffractogram from powder XRD does not indicate that any chlorite phases are present. Also, if clinochlore was present in high enough concentrations to consistently be detected when we attempted to analyze talc, then the weight percent Al_2O_3 would be much higher. Figures 8 (a-d) are for this sample, including a diffractogram (a), photos of the cut and foliated faces (b), and BSE images of the dark and light bands (c-d) of this sample with compositional data listed in Tables 7a and 7b. Although it is difficult to see in Figure 8b, this sample is weakly foliated nearly perpendicular

to the banding. Most of the samples we analyzed have comparable F concentrations to those published in the Ross et al. study. Generally the samples with the highest concentrations of F are those that have a carbonate protolith. Compositions determined by McNamee and Gunter (2014) on talc from New York agree with this conclusion as they reported F content ranging from 0.01-0.15 APFU (refer to Table 1).

Excluding the high Al^{3+} sample from Guangxi, China, the rest of the talc samples have very little Al^{3+}, with a maximum of 0.05 APFU. This was expected because all of these samples are from geologic environments in which SiO_2 was available in excess. As stated earlier, had the talc formed in a Si-depleted environment, then we would see higher concentrations of Al as a result of it occupying the tetrahedral site. Instead, aluminum in these deposits is often hosted in clinochlore, the approximate concentration of which can be estimated using both microprobe and XRF data. This will be discussed in great detail in the following section.

The fluctuations of Ca^{2+}, Na^{+}, and K^{+} based on our electron microprobe analyses are very subtle but no less significant. Calcium and potassium content are weakly correlated and tend to have the highest concentrations (up to 0.01 APFU) in samples from regionally or metamorphosed carbonates, most notably those from eastern Death Valley, California.

Accessory mineral concentrations and compositions

This is done using the following calculation.

$$(Al_2O_{3\ XRF} - Al_2O_{3\ EPMA,\ talc}) = (Al_2O_{3\ bulk,\ clinochlore})$$

$$((Al_2O_{3\ bulk,clinochlore})/(Al_2O_{3\ EPMA,\ clinochlore})*100) = \text{weight percent clinochlore in sample}$$

This calculation is assuming that clinochlore is the only phase contributing alumina to the composition of the bulk sample (no micas). The “EPMA, clinochlore” term should be taken from the microprobe data for clinochlore in the same sample for which the Al_2O_3 from “EMPA, talc” is being used. However, due to slightly lower than ideal weight percent oxide values from the microprobe data, it is best to use the calculated APFU values and convert those to weight percent oxide values and then use these calculated values for the $Al_2O_{3\ EPMA,\ talc}$ and $Al_2O_{3\ EPMA,\ clinochlore}$. Table 8 shows the weight percent clinochlore in samples for which we have XRF, clinochlore microprobe data, and powder XRD data. Note that the alumina

content varies among these samples. The values for Al_2O_3 from microprobe analyses in Table 8 are slightly different than those listed in Appendix C and D because these concentrations are calculated based on APFU values. This same type of calculation can be used for any chemical component that serves as a proxy for a particular mineral of known composition (K_2O for micas or CaO for tremolite or calcite). We acknowledge that most researchers do not have access to microprobe facilities, and suggest that pairing powder XRD with bulk XRF data is a reliable way to infer the mineral content of commercial talc since there are typically very few phases in these ores and products. In looking closer at the chlorite microprobe data we see that SiO_2, Al_2O_3, MgO, FeO, and F^- follow similar trends to what we see in talc; chlorites from Vermont (ultramafic) have low F^- (0.00-0.02 APFU), and relatively high Fe (0.56-0.91 APFU). Also, all the chlorite from commercial talc samples is clinochlore. The samples from carbonate-hosted deposits have 0.09-.46 APFU Fe with the exception of samples from Montana that overlap with both carbonate and ultramafic compositions. The clinochlore in carbonate-hosted talc also have as much as 0.09 APFU F^-. The composition of clinochlore in commercial talc may be helpful in determining the geologic origin as chlorite has a wider compositional range than talc does. Clinochlore is the most common accessory phase in talc ores. It is not uncommon to see clinochlore forming from biotite, which can give the impression that the chlorite is K-rich. In this case it is important to analyze single grains at multiple points to determine the chlorite "end-member" composition. An example of this is included in the next section for sample CHI_94.

Amphibole species were determined based on the classification scheme in Leake et al. (1997). Most of the amphiboles analyzed have calcic compositions (actinolite and tremolite) with the exception of those from the Western Talc Mine in northeastern Death Valley region, which are richterite. Tremolite was found in a sample from North Carolina, one from China (we do not know the exact location), and one from Morocco. The tremolite from North Carolina (USA_NC_Murphy_129), shown in Figure 9a-c formed as prismatic porphyroblasts, showing no signs of a fibrous morphology. Compositions of talc and tremolite from Figure 9 are included in Tables 9a and 9b. This sample has undergone rigorous polishing during sample preparation, and likely would have resulted in splaying fibers if it is asbestos. Note that the

tremolite porphyroblasts are aligned approximately parallel to each other suggesting regional metamorphism occurred during or after tremolite crystallization. This was the only sample out of 11 from carbonate-hosted talc deposits in North Carolina that contained amphiboles. The acicular mineral in the sample from China (CHI_94) shown in Figure 10 is likely tremolite, but the APFU values in Table 10b show more Mg than is allowed in the structure, therefore these values are not included in Appendix B as reliable data. This is an example of a common issue with very narrow or fine grains within a matrix; in this case the excess Mg is from analyzing the surrounding talc. Most of the economically viable talc deposits in China formed after carbonates but we do not know anything else about the origin of the sample. The tremolite in the talc from Morocco, for which we do not have an exact location, has high Mg for the same reason as the sample from China. Actinolite is the primary phase in the ultramafic-hosted samples from Earnest, Georgia, which is not a major talc-producing region. The sample in Figure 11 is fibrous and would be considered asbestos. The talc in this sample is relatively Ca- and Fe-rich, which, again is probably due in part to its proximity to actinolite. Microprobe data for this sample are shown in Table 11. No anthophyllite was identified via EPMA in any of our samples.

Concentrations of K, Na, and Ca in are indicative of other minerals, as these cations cannot be accommodated in the talc structure. Similarly, the concentration of CaO in a bulk talc sample can be used as a proxy for tremolite as long as powder XRD results confirm whether it is present, and if it is the only calcic phase in the sample. Furthermore, if calcite is present, and if tremolite is a concern in the sample, the calcite should be removed via acid digestion before bulk XRF (Gunter et al., 2007). We did not do this because we are concerned with the composition of ores and the removal of carbonate phases would not have resulted in compositional data representative of the original ores. K_2O and Na_2O were not common components in ores based on bulk XRF data. The microprobe data support our expectation of K and Na being hosted in micas or amphiboles. We do not suggest using major oxides determined by XRF to estimate accessory mineral concentrations when the only available data are bulk XRF.

Bulk XRF concentrations of MnO vary from 0.00-0.22 weight percent in samples with known origin, and are highest in ultramafic samples. Based on the ultramafic microprobe data the Mn is being hosted in amphiboles (from Earnest, Georgia) and clinochlore (from Vermont). Due to how slightly the concentrations of MnO vary among bulk talc samples we do not suggest considering MnO in determining the provenance of samples.

Trace element concentrations

There are many samples that are compositionally indistinguishable based only on major element concentrations. Figure 12 is a dendrogram based on the trace element data. The samples cluster differently than in the dendrogram for APFU values (Figure 5) and possibly more accurately in terms of protolith. We again decided that ten clusters appropriately categorized samples without creating too many clusters. The largest cluster in this diagram contains carbonate-hosted talcs. The high-Fe talc from Montana is compositionally very similar to talc from ultramafic-hosted deposits when comparing the most variable components among talcs such as Al, Fe and F^- content. Generally, we observe that talc samples formed from the alteration of ultramafic deposits contain Ni on the order of 100s-1000s ppm. Almost all of these samples fall into the same cluster in the dendrogram. Trace element concentrations in talc, similar to those of major elements cannot be interpreted solely as those in talc. It is for this reason that the samples listed in Table 12 include major oxides determined by XRF analysis showing that these samples are almost entirely talc, and would not be contributing very high concentrations of trace elements from accessory phases. For example, the Al_2O_3 content is very low and the FeO concentrations among samples are comparable. The samples could arguably be distinguished based on F^- content but we do not recommend relying on one compositional trait to distinguish ores. The talc from Llano, Texas, that is thought to be hosted in a serpentinized ophiolite suite (Chidester, 1964), contains 0.01 APFU Ni. We were not expecting Ni to be present in high enough concentrations to be detected during microprobe analyses, and therefore only have EMPA data on three ultramafic-hosted talc samples, which were analyzed by EPMA after XRF data were obtained. We suspect that the samples from Vermont would yield detectable Ni if

analyzed by EPMA. Ni and Cr, when present, occur in such significant concentrations that ultramafic-hosted talc tend to have much higher trace element concentrations than carbonate-hosted talcs.

The samples from NY (Vanderbilt products), south/eastern Death Valley, California, Ontario, Canada, and one from Van Horn mining district in Texas have significantly higher Sr concentrations than the rest of the samples ranging from 98-2121ppm. Most of these also have higher concentrations of Ba and Rb. It is likely that these cations are substituting for Ca in calcite, which is present in all of these samples. The talc from western Death Valley, which is thought to have the same protolith as the talc in eastern Death Valley but was hydrothermally altered has almost negligible concentrations of these elements. In general, talc from pervasively hydrothermally altered environments tends to have very low trace element concentrations (all <30ppm).

The remaining trace element data do not show any correlative trends regarding protolith composition or mechanism of formation. Some samples have anomalously high values, even compared to other samples from the same deposit. This may be attributed to trace accessory phases.

Determining the provenance of “unknowns”

The sample that we acquired with the information that it was labeled “Cerbis, Norway” remains a mystery but based on its composition we know a few things. Also, “Cerbis” is not a location in Norway, and after seeking information from multiple sources never seems to have been a location, and the name is not related to anything in the talc industry in Norway. That being said, this sample has been treated as an unknown. Karlsen et al. (2000) stated that all major sources of talc in Norway are sourced form ultramafic rocks. The sample we have has absolutely no compositional indicators suggesting it is from an ultramafic source. The microprobe data for this sample, listed in Table 13, are quite different from those listed in Table 1 from Karlsen et al (2000). The bulk sample is almost entirely talc, lacking the expected carbonate accessory phases and chlorite. The purity of the bulk sample is also proven by the composition based on XRF data, which is nearly identical to the weight

percent oxide values determined by microprobe analyses. The very low concentrations of trace elements, particularly Ni and Cr indicate a carbonate origin. Lastly, this sample has pencil cleavage, indicating an influence of regional metamorphism, very much like the samples from North Carolina. Although determining the morphology index for individual powders was not conclusive talcs formed in different geologic environments do break into particles of differing length:width ratios. For comparison Figure 13 shows cleavage fragments for talc from "Norway", Yellowstone Mine in Montana, Talc City in California, and Hitchcock County, North Carolina. The fragments from the Montana talc broke apart into relatively equant particles while the talc from North Carolina and California formed elongate, pencil-like fragments.

The body and baby powder samples pose a couple challenges when determining provenance because of the fine grain sizes and the possibility that products are a mixture of talcs of high quality from multiple locations. We looked at Cashmere Bouquet Body Talc, Gold Bond body powder, Johnson's Baby Powder, Perlier Ricette Naturali talcum powder, and Safeway baby powder powders. It is likely that these are all from carbonate-hosted deposits.

The most telling data for these samples are the Ni concentrations, which are all <30ppm for. The Sr concentrations increase with CaO content, which is likely not that of talc but of a trace accessory phase not removed during beneficiation. Additionally, the talc microprobe data for Johnson's baby powder has relatively low Fe (0.04 APFU) and 0.03 APFU F^-. We only have one chlorite microprobe analysis from this sample but is also has low iron (0.16 APFU) and high aluminum (2.33 APFU). Dolomite was also found in this sample, accounting for the CaO. This is interesting from a historical perspective as Johnson's Baby Powder was among a group of powders that were reported on in a 1976 Washington Post article summarizing the conclusions of a Mt. Sinai's Department of Environmental Medicine study on 19 body and baby powders. The study determined that Johnson's Baby Powder had Ni concentrations ranging from below 710 ppm to 2200 ppm (Burros, 1976). These values are comparable to the Ni concentrations in the ultramafic-hosted talc ores from our study, indicating a change in the source location of these talcs over time. Three of the body powder samples have very high concentrations of Zn (1073-9024 ppm) of Zn. This is not a result of the

geology, but is an additive in baby powders as an active ingredient to treat diaper rash, and also increases the brightness of a powder.

The soapstone products that actually contained talc were analyzed by XRD and XRF but not with the electron microprobe. Tire talc was included in this category as well because all these samples were unknowns made of talc, chlorite, and possibly serpentine group minerals. The tire talc is used to keep a tire tube from folding or sticking to itself and its casing during installation. The powder XRD and XRF results are summarized in Table 14, below. We cannot determine whether these trace elements are hosted in the talc or accessory phases, but based on the lack of these elements in the ice cube it indicates that regardless of the phases present that the chlorite and talc in the ice-cube are not hosting Ni and Cr. The rest of these samples contain high concentrations of Ni and Cr, indicating high concentrations of Ni and Cr in the protolith. The presence of magnesite in the soapstone griddle is another indicator that these samples are made from ultramafic-hosted talc. The tire talc also contains magnesite, but because it is a powdered product there is no guarantee that all the minerals in this sample are representative of a mineralogical assemblage of a single ore.

Conclusions

The data collected for this chapter are in agreement with pre-existing data from similar studies. Talc compositions do not show much variability but talc from a carbonate (sedimentary) protolith tends to have lower Fe content, and higher F^- than talc from ultramafic-hosted deposits. Clinochlore is the most common accessory phase in talc ores and shows the same variations that we see in talc but on a more noticeable scale. Amphiboles in talc ores tend to be calcic with the exception of the sodic-calcic amphibole from eastern Death Valley. We found no anthophyllite in any of our samples. Amphiboles are more likely to be present in ores that have undergone regional or contact metamorphism. Ultramafic-hosted talc and the accessory minerals within have Ni concentrations orders of magnitude greater than those in carbonate-hosted talcs. Nickel and Cr trace element concentrations may be the most useful in determining the provenance of commercial talcs. Calcite and dolomite

are common in carbonate-hosted ores but magnesite is the major carbonate phase in ultramafic-hosted ores. We can use these broad compositional differences to differentiate between talc based on protolith. The data presented in this paper cannot be used to distinguish between talcs formed from the same protolith and altering mechanism (Spain and southwest Montana or Vermont and Finland). Stable isotope analyses for H and O may be sensitive enough to distinguish talc based on the composition of altering fluids present during the talc-forming process from multiple regions.

Acknowledgements

We would like to thank Owen Neill, Charles Knaack, Rick Conrey, Scott Buroughs and Tom Williams for their help in setting up and running analyses. Additionally we must thank Richard Berg, and current mining companies for their generous contribution of talc specimens.

References

Akizuki, M. and Zussman, J. (1978) The unit cell of talc. Mineralogical Magazine, 42, 107-110.

Anderson, D.L., Mogk, D.W., and Childs, J.F. (1990) Petrogenesis and timing of talc formation in the Ruby Range, southwestern Montana. Economic Geology, 85, 585-600.

Boschi, C., Fruh-Green, G.L., and Escartin, J. (2006) Occurrence and significance of serpentinite-hosted, talc- and amphibole-rich fault rocks in modern oceanic settings and ophiolite complexes: an overview, Ofioliti, 31 (2), 129-140.

Brady, J. B., Cheny, J. T., Rhodes, A., Vasquez, A., Green, C., Duvall, M., Kogut, A., Kaufman, L., Kovaric,D. (1998) Isotope geochemistry of Proterozoic talc occurrences in Archean Marbles of the Ruby Mountains, southwest Montana, U.S.A. Geological Materials Research, 1,2,1-41.

Burros, M. (1976) Asbestos fibers found in baby powder. Washington Post (extracted from Harris, D.D. (2004) Luzenac re: Comments on the talc nominations for the 12th RoC).

Chidester, A.H., Engel, E.J., and Wright, L.A. (1964) Talc Resources of the United States. Geological Survey Bulletin 1167.

Chidester, A.H. (1962) Petrology and geochemistry of selected talc-bearing ultramafic rocks and adjacent country rocks in north-central Vermont. Geological survey professional paper 345, United States Government printing office, Washington, U.S..

Dyar, M.D., Gunter, M.E. (2008) Mineralogy and Optical Mineralogy, 206 p, Mineralogical Society of America, Chantilly, VA.

Flanagan, Daniel M. (2016) Talc and Pyrophyllite. In U.S. Department of the Interior and U.S. Geological Survey Mineral Commodity Summaries 2016, p.164-165. U.S. Geological Survey, Reston, Virginia.

Gammons, C.H. and Matt, D.O (2002) Using fluid inclusions to help unravel the origin of hydrothermal talc deposits in southwest Montana. Northwest Geology, 31, 44-55.

Gunter, M.E., Belluso, E. and Mottana, A. (2007) Amphiboles: Environmental and health concerns. Reviews in Mineralogy and Geochemistry, 67, 453-516.

Holland H.J., and Murtagh M.J.,(2000). An XRD morphology index for talcs: The effect of particle size and morphology on the specific surface area. JCPDS-International centre for diffraction data, Advances in X-ray Anaysis, Vol. 42, pp 421-428.

Johnson, D.M., Hooper, P.R., and Conrey R.M. (1999) XRF analysis of rocks and minerals for major and trace elements on a single low dilution Li-tetraborate Fused Bead. JCPDS-International Centre for Diffraction Data, 843-867.

Kane, A.B. (1993) Epidemiology and pathology of asbestos-related diseases. In G.D. Guthrie Jr. and B.T. Mossman, Eds., Health Effects of Mineral Dusts, 28, p.347-359. Reviews in Mineralogy and Geochemistry, Mineralogical Society of America, Chantilly, Virginia.

Karlsen, T.A., Rain, E., and Olesen, O. (2000) Overview of talc resources in the Altermark talc province, northern Norway, and possible uses of the talc ore. Norges geologiske undersøkelse Bulletin, 436, 93-102.

Leake, B., Woolley, A.R., Arps, C.E.S., Birch, W.D., Gilbert, M.C., Grice, J.D., Hawthorne, F.C., Kato, A., Kisch, H.J., Krivovichev, V.G., Linthout, K., Laird, J., Mandarino, J.A., Maresch, W.V., Nickel, E.H., Rock, N.M.S., Schumbacher, J.C., Smith, D.C, Stephenson, N.C.N., Ungharetti, L., Whittaker, E.J.W., Youzhi, G. (1997) Nomenclature of amphiboles: Report of the subcommittee on amphiboles of the International Mineralogical Association, Commission on new minerals and mineral names. The Canadian Mineralogist, 35, 219-246.

McNamee, B.D. and Gunter, M.E. (2013) Compositional analysis and morphological relationships of amphiboles, talc and other minerals found in the talc deposits from the Gouverneur Mining District, New York (Part 1 of 2). The Microscope, 61:4, 147-161.

McNamee, B.D. and Gunter, M.E. (2014) Compositional analysis and morphological relationships of amphiboles, talc and other minerals found in the talc deposits from the Gouverneur Mining District, New York (Part 2 of 2). The Microscope, 62:1, 3-13.

Moine, B., Fortune, J., Moreau, P., and Viguier, F. (1989) Comparative mineralogy, geochemistry, and conditions of formation of two metasomatic talc and chlorite deposits: Trimouns (Pyrenees, France) and Rabenwald (Eastern Alps, Austria). Economic Geology, 84, 1398-1416.

Ross, M. and Ashton, W.H. (1968) Triclinic Talc and associated amphiboles form Gouverneur Mining District, New York. The American Mineralogist, 53, 751-769.

Tornos, F. and Spiro, B.F. (2000) The geology and isotope geochemistry of the talc deposits of Puebla de Lillo (Cantabrian Zone, Northern Spain), Economic Geology, 95, 1277-1296.

Van Gosen, B.S., Lowers, H.A., Sutley, S.J., and Gent, C.A. (2004) Using the geologic setting of talc deposits as an indicator of amphibole asbestos content. Environmental Geology, 45, 920-939.

Wright, L.A. (1968) Talc deposits of the southern Death Valley-Kingston Range region, California. California Division of Mines and Geology, Special Report 95, San Francisco 1968.

Van Gosen, B.S., Lowers, H.A., Sutley, S.J., and Gent, C.A. (2004) Using the geologic setting of talc deposits as an indicator of amphibole asbestos content. Environmental Geology, 45, 920-939.

Wright, L.A. (1968) Talc deposits of the southern Death Valley-Kingston Range region, California. California Division of Mines and Geology, Special Report 95, San Francisco 1968.

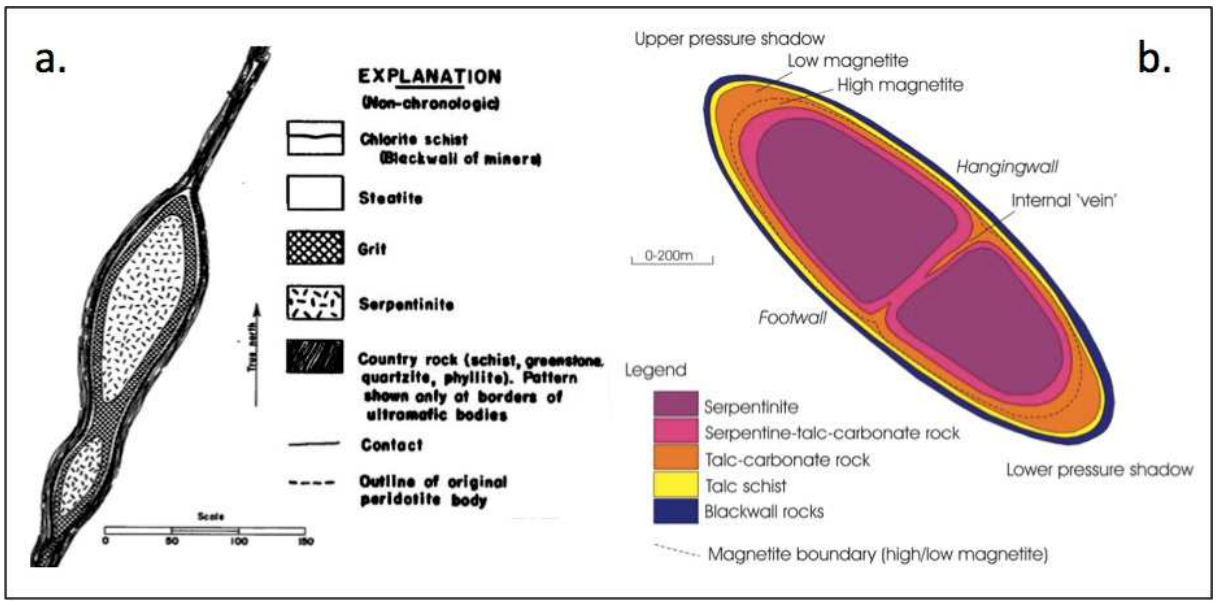

Figure 1: General geometry of serpentinite pod and concentric units from (a) Chidester et al. (1951) explaining talc-formation in Vermont and (b) Karlsen et al. (2000) explaining talc-formation in the Altermark talc deposits in Norway

Figure 2: Typical thin section used for EPMA, slide is 4.5mm long, 2.6mm wide; each sample is in a 9.0mm circle. Four different samples were mounted on a slide and three targets were created around points of interest. The back-scattered electron images referenced later are from a target, unless otherwise noted.

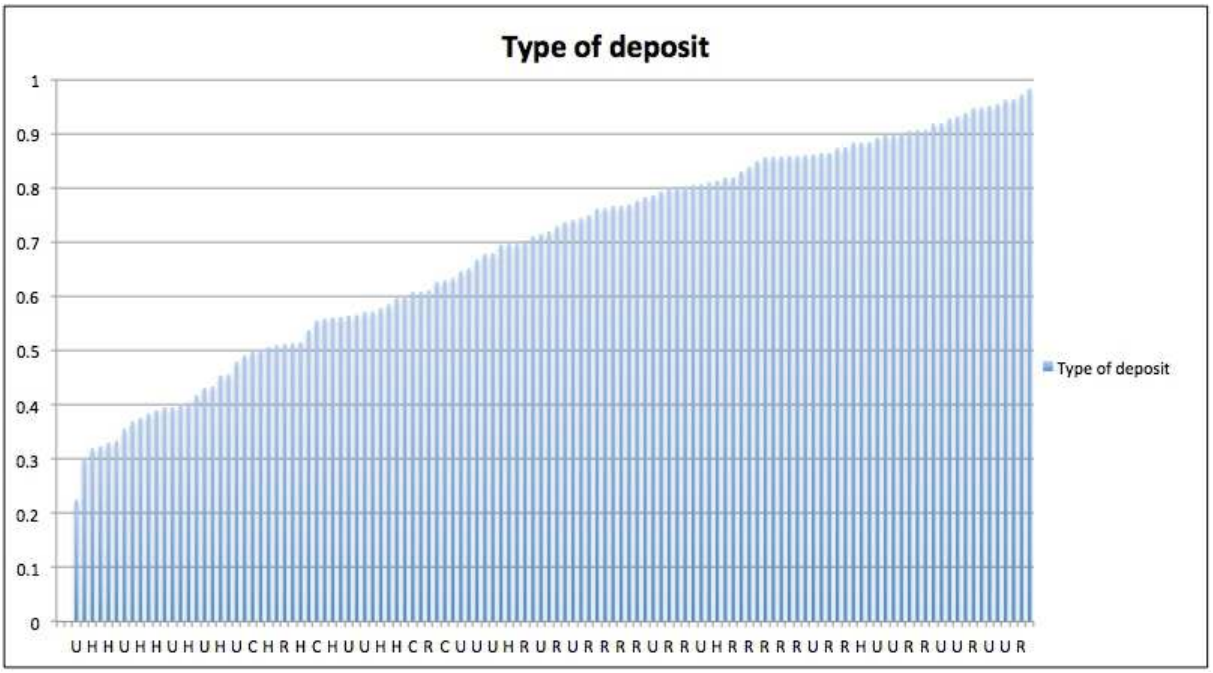

Figure 3: morphology indices for talc samples
Morphology index values are along the y-axis, with labels for the general talc-forming mechanism labeling the x-axis (H=hydrothermally altered, R=regionally metamorphosed, and C=contact metamorphosed, and U=unknown).

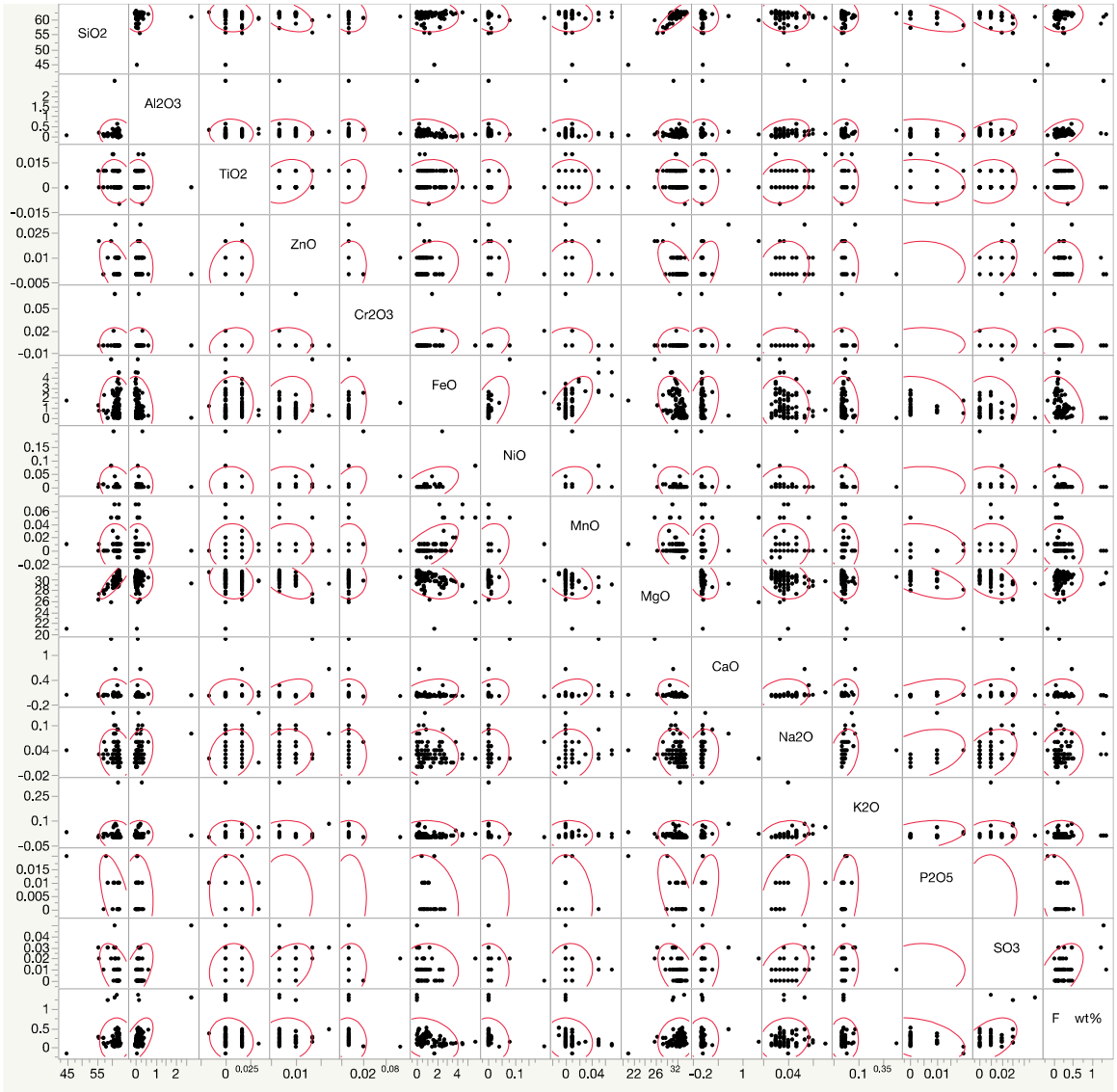

Figure 4a: Multivariate scatter plots based on weight percent oxide values from EPMA for talc. Each black do represents the composition of a sample based on two oxides. For example, the first row plots the weight percent SiO_2 of each sample versus its respective weight percent of Al_2O_3, and TiO_2, and so on. Note that some oxides do not vary significantly with respect to other oxide concentrations such as TiO_2, ZnO, Cr_2O_3, NiO, P_2O_5, and SO_3.

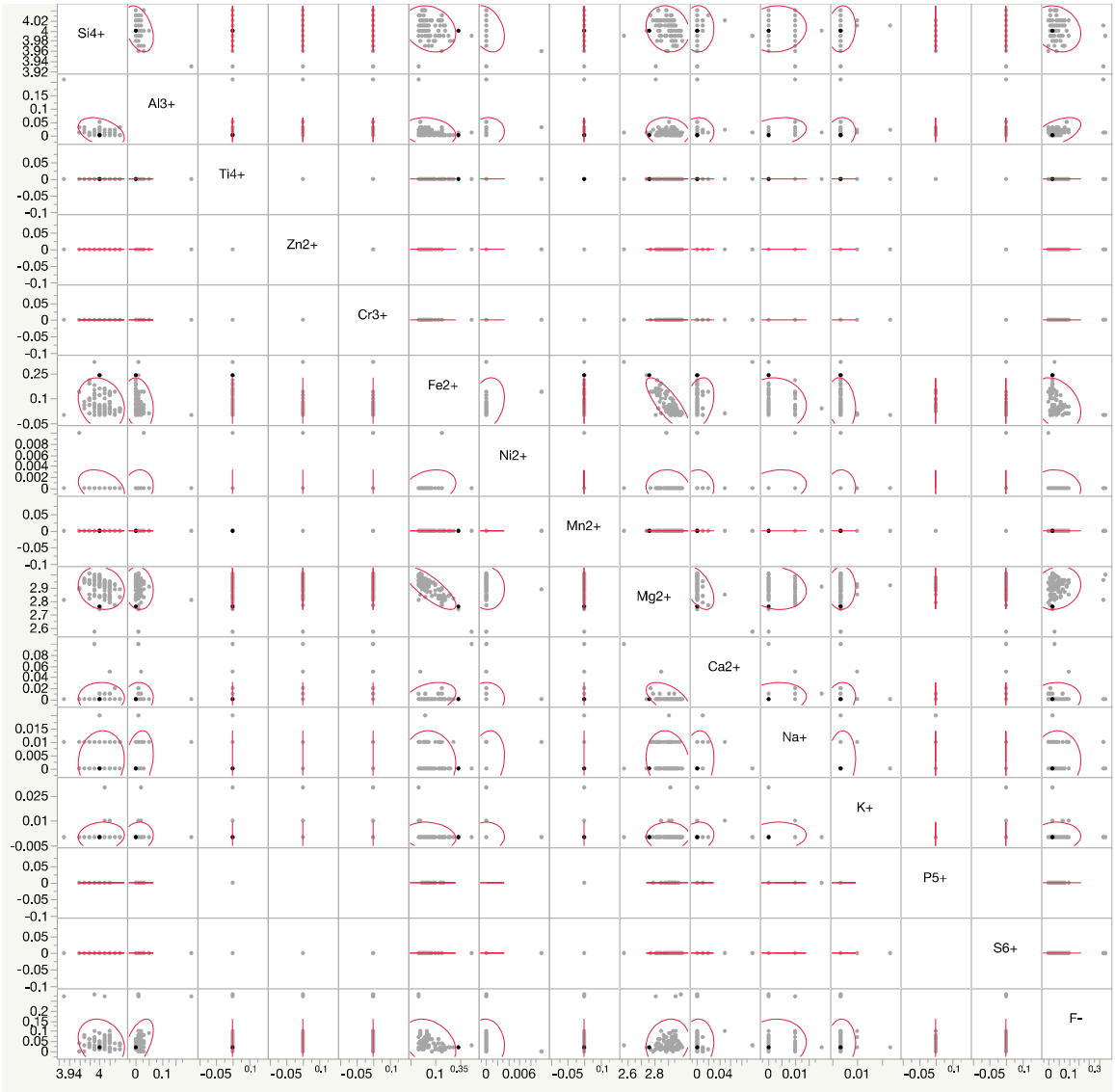

Figure 4b: Multivariate scatter plots for APFU values in talc. Refer to the caption for Figure 4b for explanation

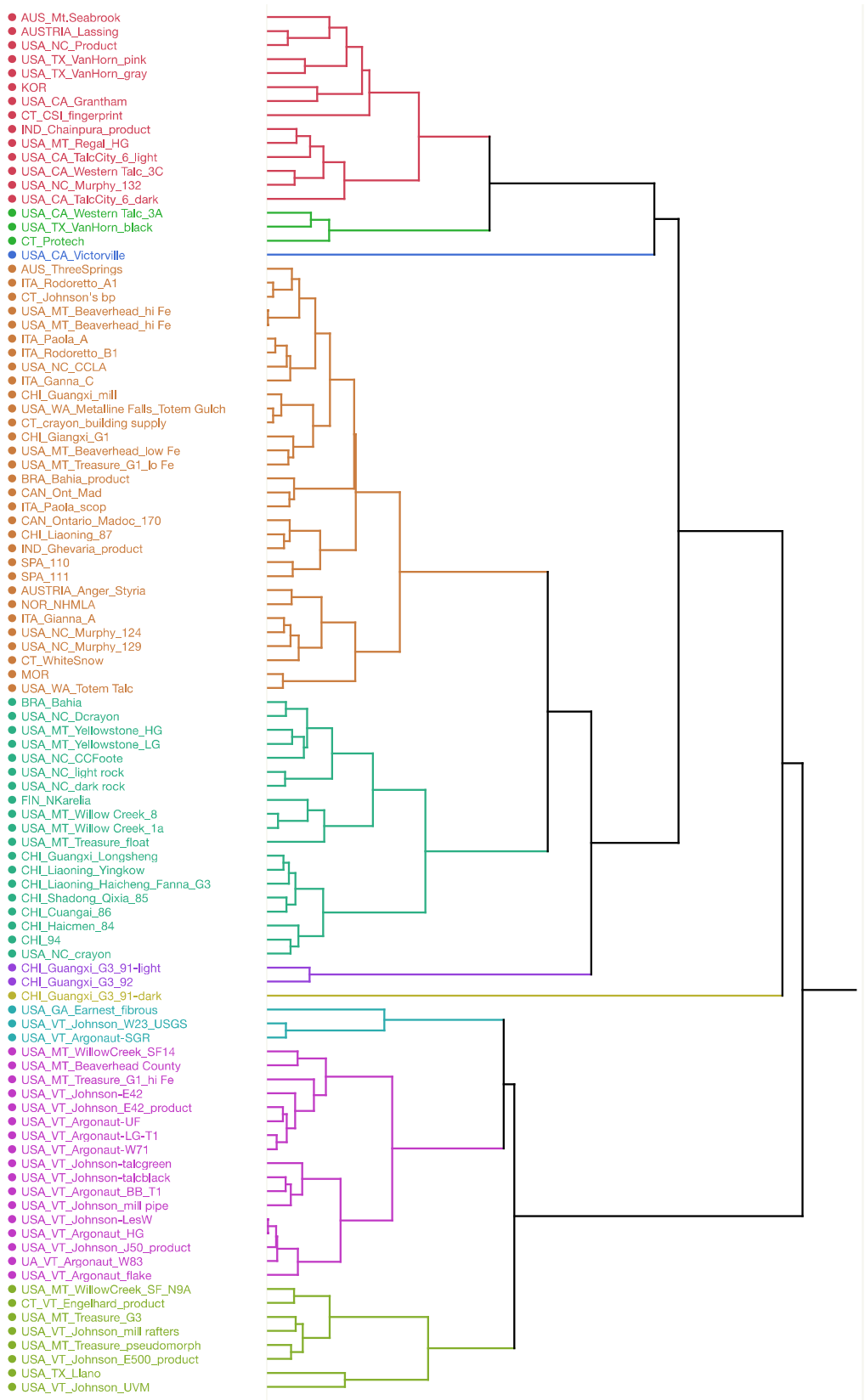
AUS_Mt.Seabrook
AUSTRIA_Lassing
USA_NC_Product
USA_TX_VanHorn_pink
USA_TX_VanHorn_gray
KOR
USA_CA_Grantham
CT_CSI_fingerprint
IND_Chainpura_product
USA_MT_Regal_HG
USA_CA_TalcCity_6_light
USA_CA_Western Talc_3C
USA_NC_Murphy_132
USA_CA_TalcCity_6_dark
USA_CA_Western Talc_3A
USA_TX_VanHorn_black
CT_Protech
USA_CA_Victorville
AUS_ThreeSprings
ITA_Rodoretto_A1
CT_Johnson's bp
USA_MT_Beaverhead_hi Fe
USA_MT_Beaverhead_hi Fe
ITA_Paola_A
ITA_Rodoretto_B1
USA_NC_CCLA
ITA_Ganna_C
CHI_Guangxi_mill
USA_WA_Metalline Falls_Totem Gulch
CT_crayon_building supply
CHI_Giangxi_G1
USA_MT_Beaverhead_low Fe
USA_MT_Treasure_G1_lo Fe
BRA_Bahia_product
CAN_Ont_Mad
ITA_Paola_scop
CAN_Ontario_Madoc_170
CHI_Liaoning_87
IND_Ghevaria_product
SPA_110
SPA_111
AUSTRIA_Anger_Styria
NOR_NHMLA
ITA_Gianna_A
USA_NC_Murphy_124
USA_NC_Murphy_129
CT_WhiteSnow
MOR
USA_WA_Totem Talc
BRA_Bahia
USA_NC_Dcrayon
USA_MT_Yellowstone_HG
USA_MT_Yellowstone_LG
USA_NC_CCFoote
USA_NC_light rock
USA_NC_dark rock
FIN_NKarelia
USA_MT_Willow Creek_8
USA_MT_Willow Creek_1a
USA_MT_Treasure_float
CHI_Guangxi_Longsheng
CHI_Liaoning_Yingkow
CHI_Liaoning_Haicheng_Fanna_G3
CHI_Shadong_Qixia_85
CHI_Cuangai_86
CHI_Haicmen_84
CHI_94
USA_NC_crayon
CHI_Guangxi_G3_91-light
CHI_Guangxi_G3_92
CHI_Guangxi_G3_91-dark
USA_GA_Earnest_fibrous
USA_VT_Johnson_W23_USGS
USA_VT_Argonaut-SGR
USA_MT_WillowCreek_SF14
USA_MT_Beaverhead County
USA_MT_Treasure_G1_hi Fe
USA_VT_Johnson-E42
USA_VT_Johnson_E42_product
USA_VT_Argonaut-UF
USA_VT_Argonaut-LG-T1
USA_VT_Argonaut-W71
USA_VT_Johnson-talcgreen
USA_VT_Johnson-talcblack
USA_VT_Argonaut_BB_T1
USA_VT_Johnson_mill pipe
USA_VT_Johnson-LesW
USA_VT_Argonaut_HG
USA_VT_Johnson_J50_product
UA_VT_Argonaut_W83
USA_VT_Argonaut_flake
USA_MT_WillowCreek_SF_N9A
CT_VT_Engelhard_product
USA_MT_Treasure_G3
USA_VT_Johnson_mill rafters
USA_MT_Treasure_pseudomorph
USA_VT_Johnson_E500_product
USA_TX_Llano
USA_VT_Johnson_UVM

Figure 5a:

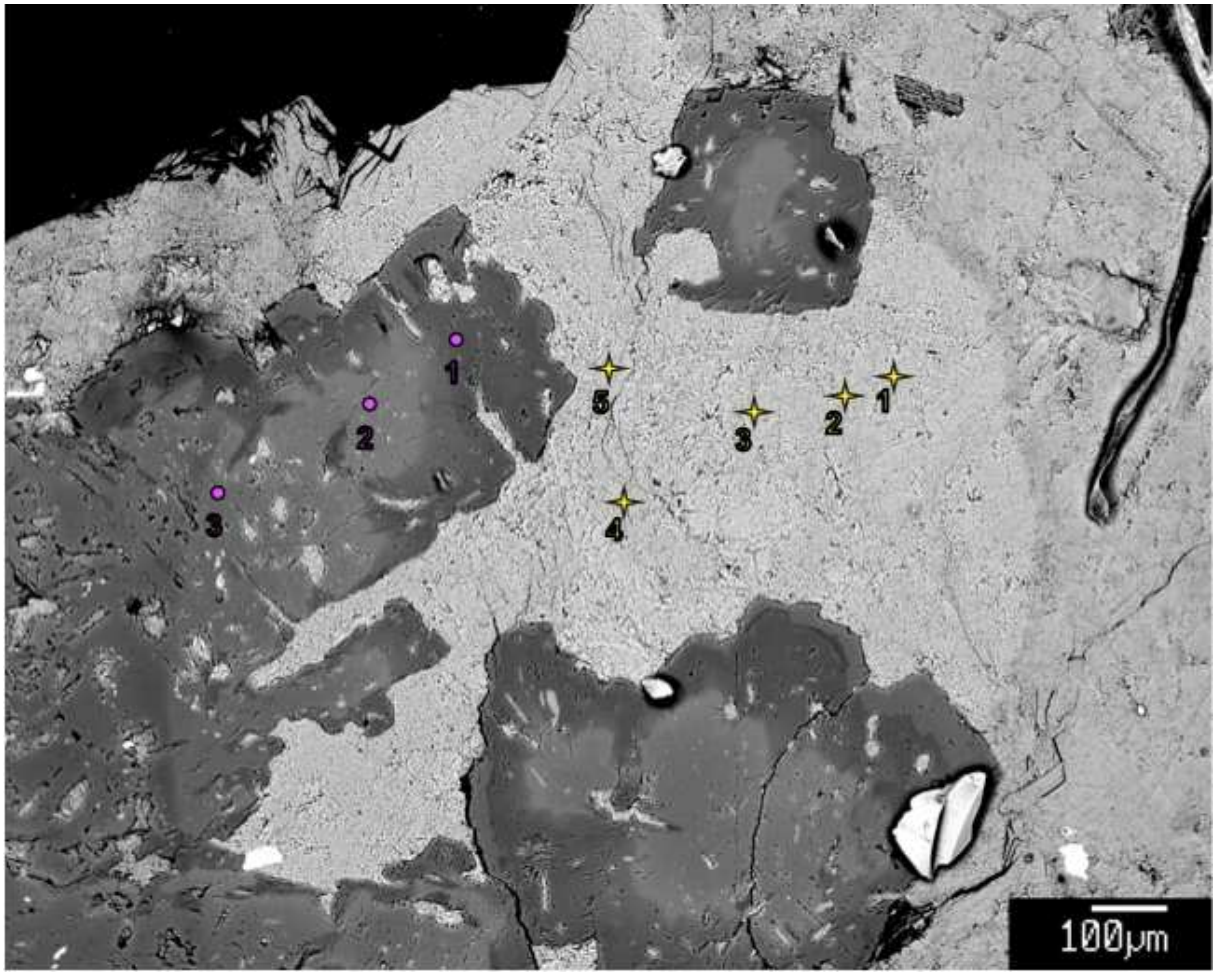

Figure 6: BSE image of FIN_NKarelia, yellow stars indicate talc analysis points, magenta circles indicate magnesite analysis points

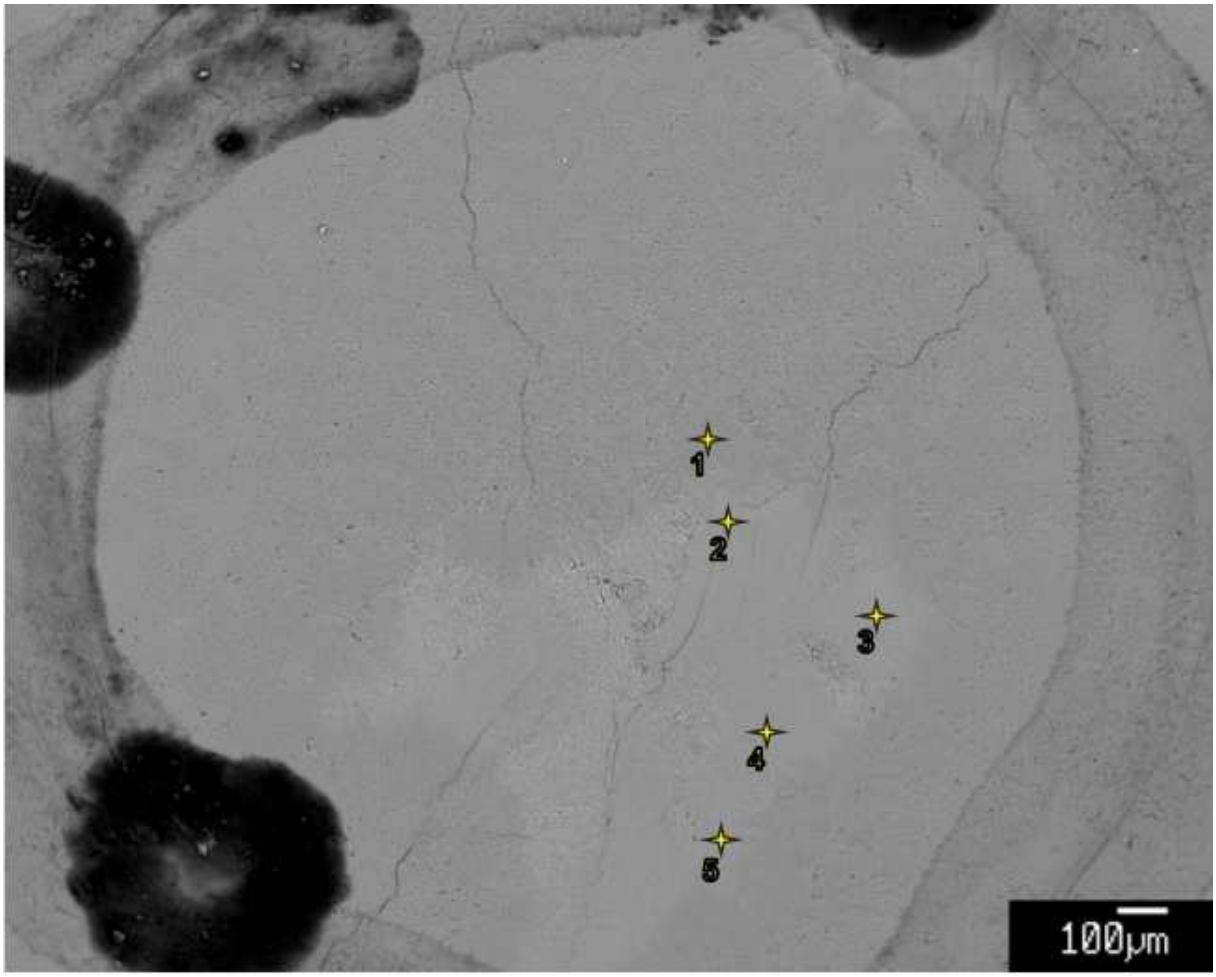

Figure 7: BSE image of USA_MT_Treasure_G1, yellow stars indicate talc analysis points. Points 2-5 have higher iron content than point 1

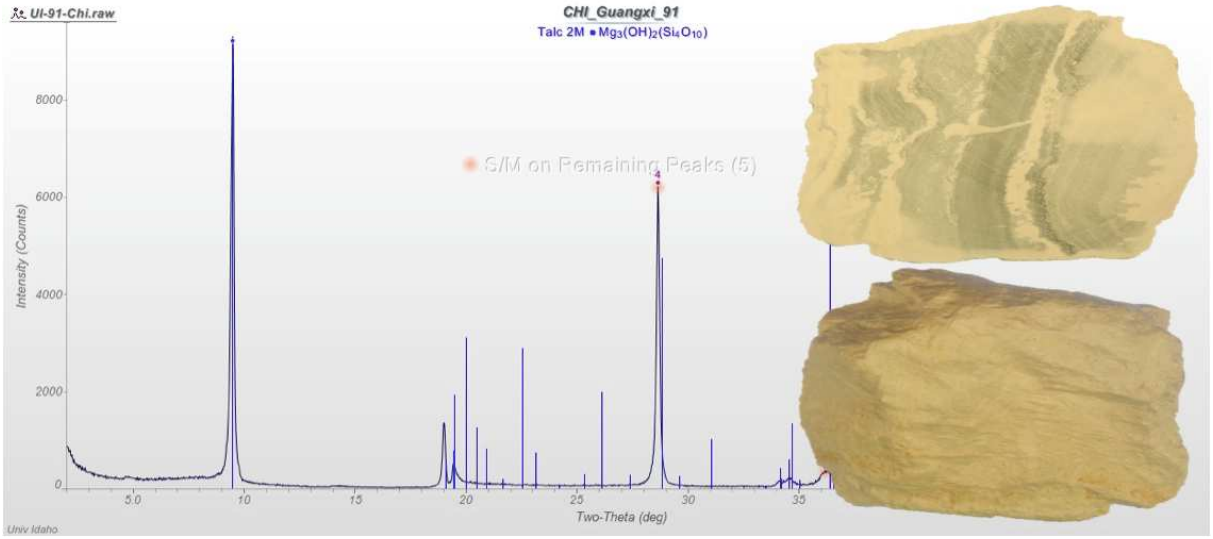

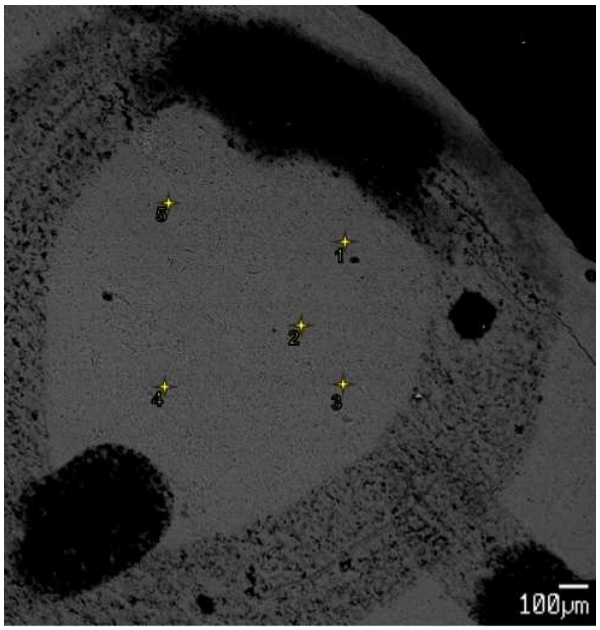

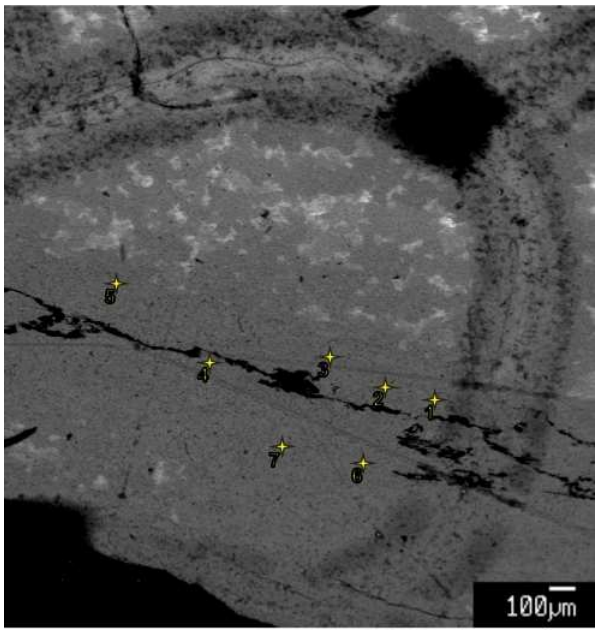

8a (top): Powder X-ray diffractogram for CHI_Guangxi_G3_91 indicating talc is the only major phase
Figure 8b: (top right) Photos of Sample 91, a grade 3 ore from Guangxi China, showing compositional banding (top) and foliation (bottom). Hand samples are 9cm across.
Figure 8c (left): BSE image for dark (Al-rich) bands in CHI_Guangxi_G3_91
Figure 8d (right): BSE image for light (Al-poor) bands, yellow stars are talc analysis points, lighter shades in top of 8d are a result of charging

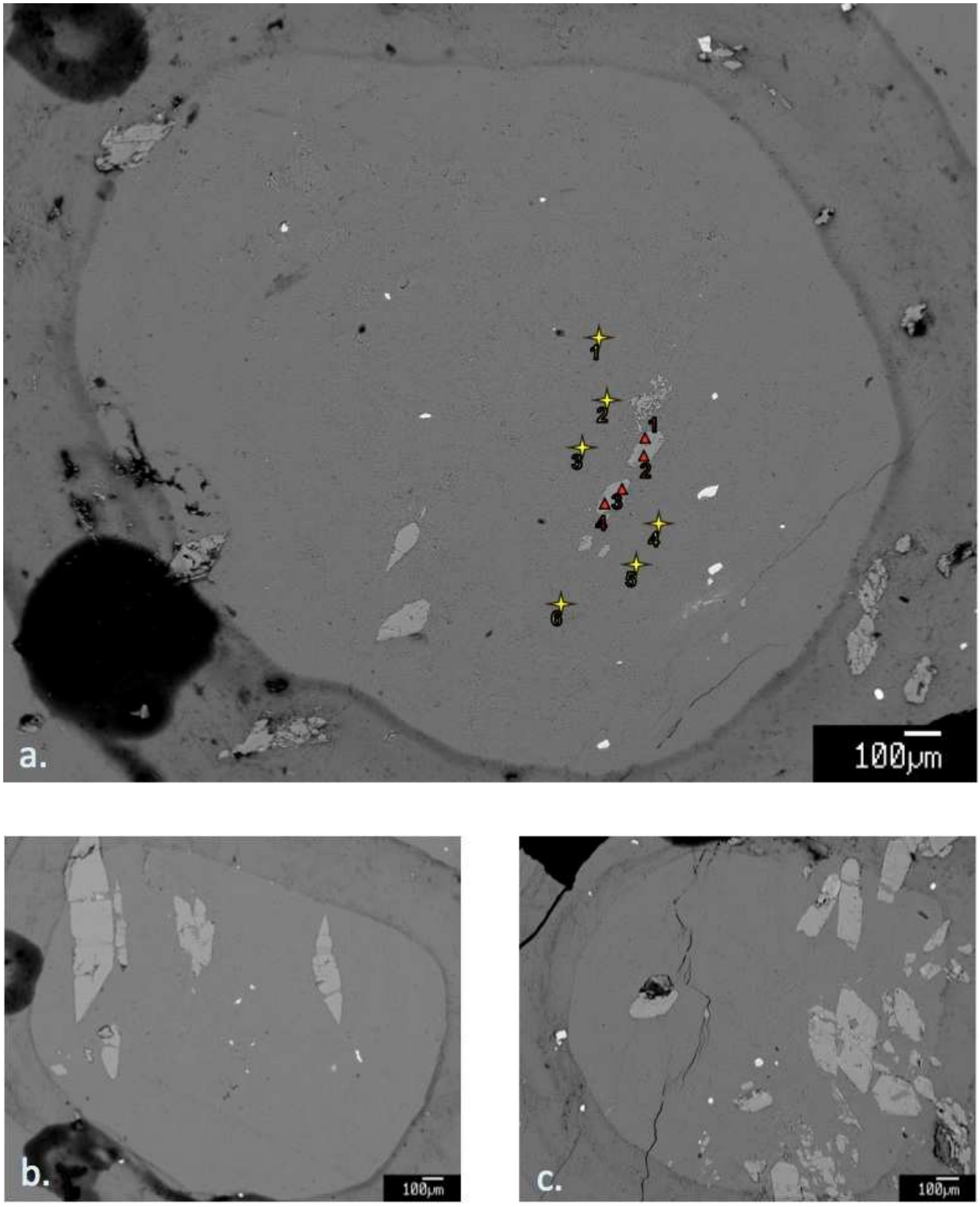

Figure 9: BSE images of USA_NC_Murphy_129; 9a showing marked analysis points, 9a-9c showing morphology of tremolite porphyroblasts in the three prepared targets. The composition of tremolite is comparable for all three targets. Yellow stars are talc analysis points, red triangles are amphibole analysis points

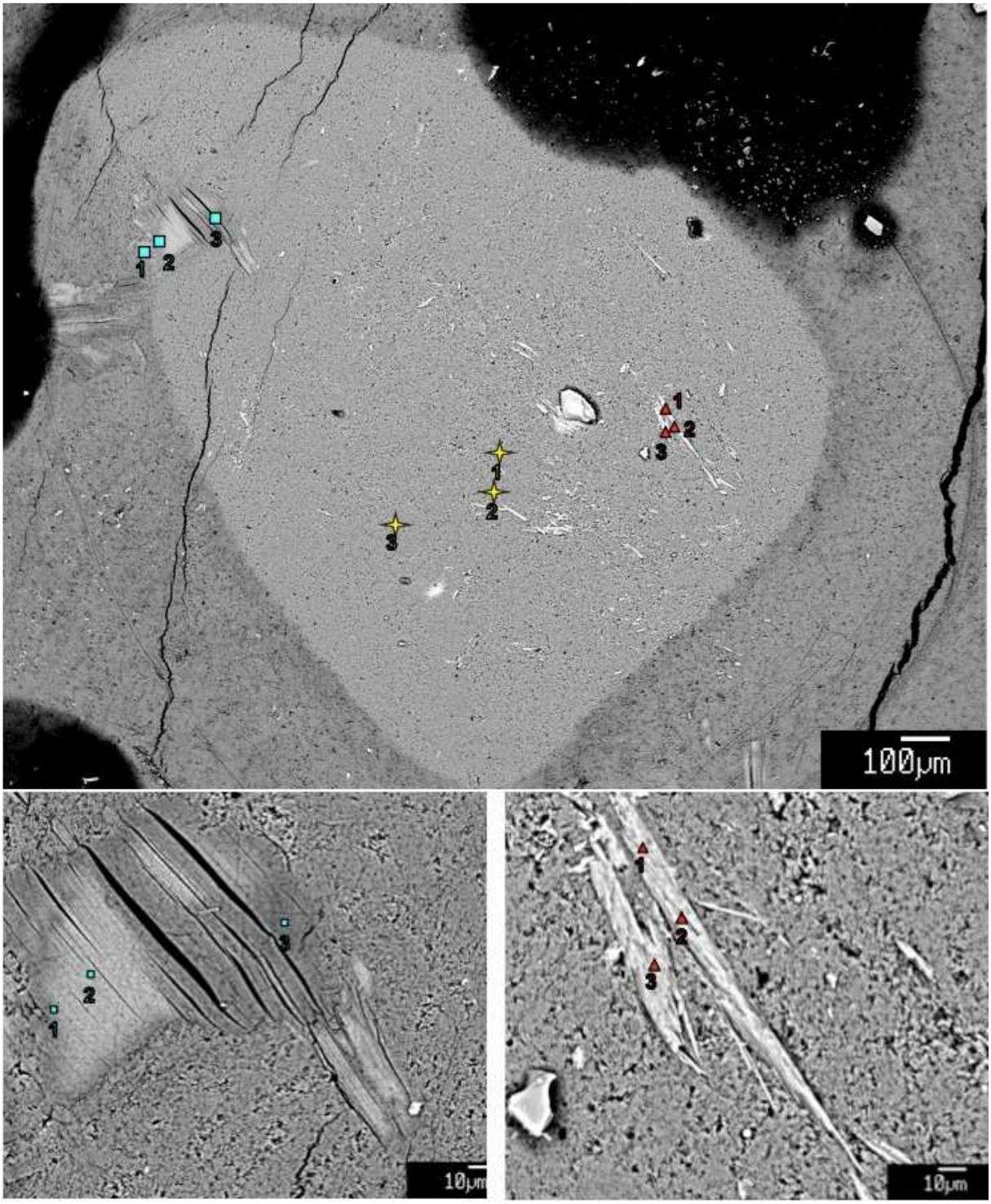

Figure 10: BSE image of CHI_94, talc analysis points are marked by yellow stars, amphibole analysis points are marked by red triangles, and chlorite analysis points are marked by blue squares.

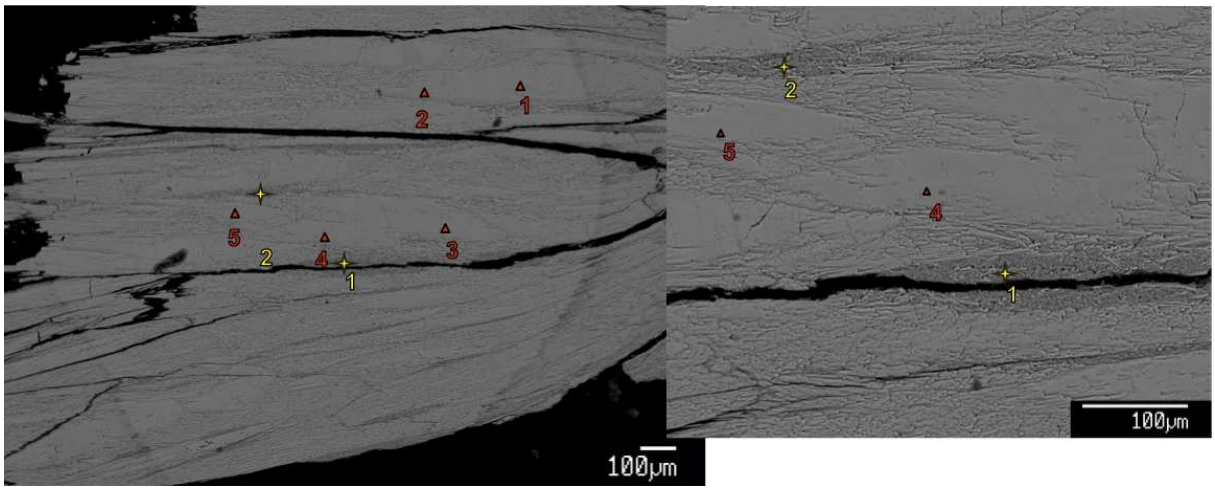

Figure 11: BSE image of USA_GA_Earnest_fib, talc analysis points are marked by yellow stars, amphibole analysis points are marked by red triangles

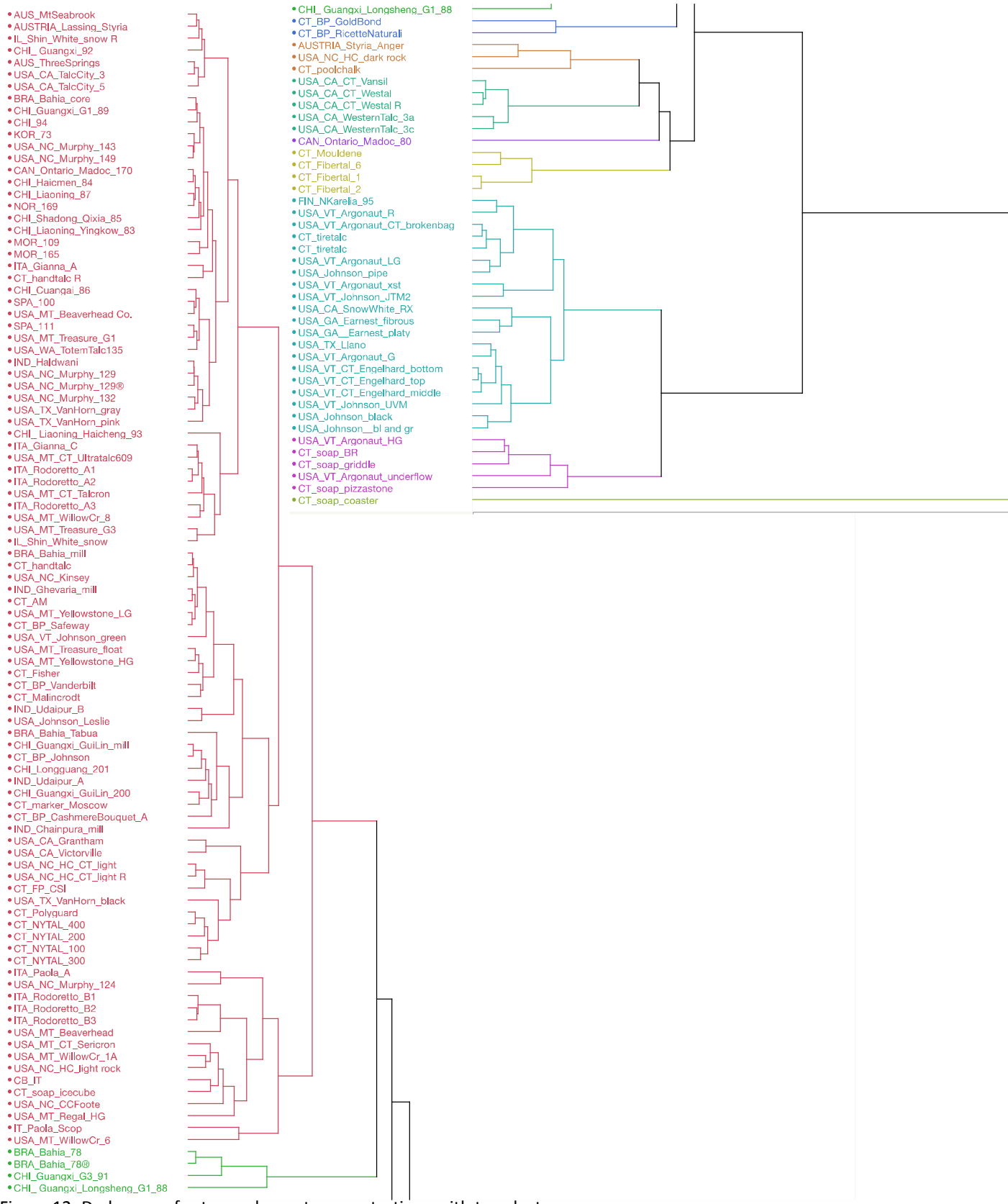

Figure 12: Dedrogram for trace element concentrations with ten clusters.

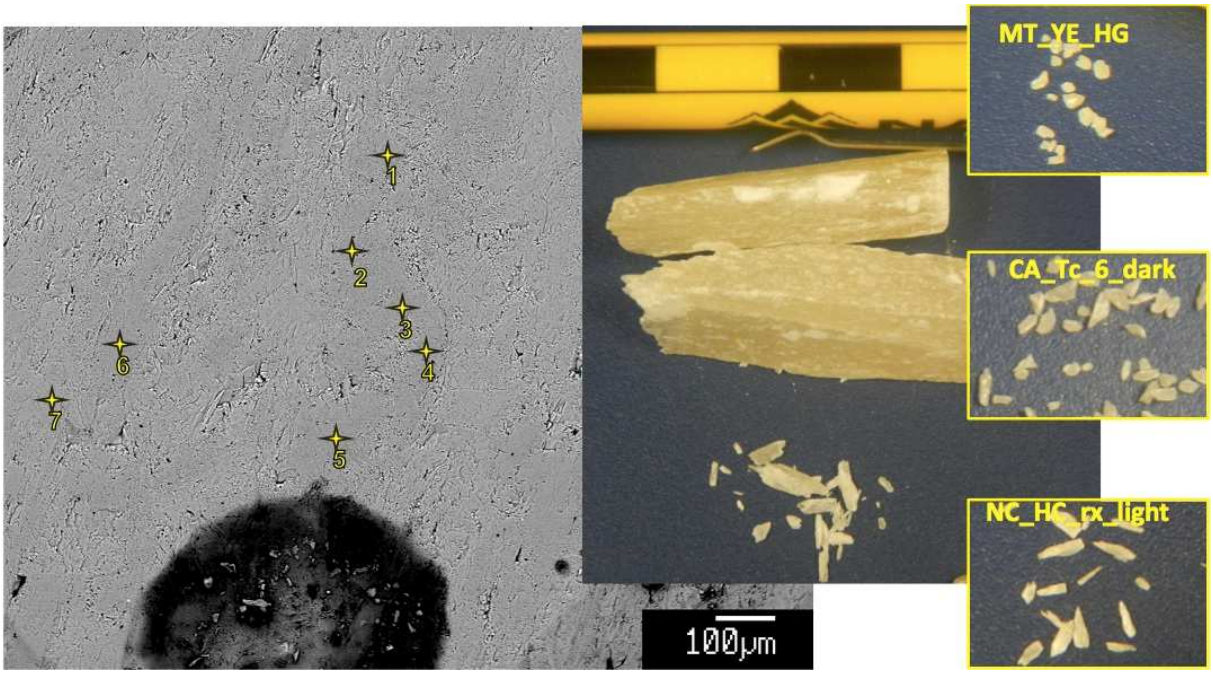

Figure 13: BSE image of talc from “Cerbis, Norway” (left), photo of handsample and cleavage fragments with cm scale (middle), and cleavage fragments from samples from other locations showing variability in length:width ratios for grains 20-48 mesh.

Table 1: Composition of talcs reported in APFU from McNamee and Gunter (2014) and Karlsen et al. (2001)
(*)Data were converted to APFU based on data from Karlsen et al (2000)
(**)Published values from McNamee and Gunter (2014)
(-) Not analyzed

Mine	Si4+	Al3+	Ti4+	Cr3+	Fe2+	Ni2+	Mn2+	Mg2+	Ca2+	Na+	K+	F-	OH-	Tet	Oct
Talc Mine, Norway*	3.95	0.00	0.00	0.00	0.18	0.01	0.00	2.90	0.00	0.00	0.00	0.00	2.00	3.96	3.09
St. Esjelk, Norway*	3.98	0.00	0.00	0.00	0.17	0.01	0.00	2.85	0.00	0.00	0.00	0.00	2.00	3.98	3.04
Nakkan, Norway*	3.94	0.00	0.00	0.00	0.04	0.01	0.00	3.06	0.00	0.00	0.00	0.00	2.00	3.94	3.11
Arnold Pit 15**	3.98	0.02	0.00	-	0.01	-	0.01	3.15	0.02	0.02	0.00	0.06	1.94	3.90	3.17
Arnold Pit 18**	4.01	0.02	0.00	-	0.04	-	0.01	2.86	0.03	0.01	0.00	0.03	1.97	4.01	2.94
Talcville 23**	4.04	0.01	0.00	-	0.01	-	0.04	2.86	0.00	0.01	0.00	0.06	1.94	4.04	2.91
Talcville 26**	3.91	0.02	0.00	-	0.01	-	0.01	3.08	0.05	0.02	0.00	0.15	1.85	3.93	3.09
Talcville 27**	4.05	0.01	0.00	-	0.01	-	0.00	2.84	0.04	0.00	0.00	0.01	1.99	4.05	2.89
Talcville 28**	3.92	0.01	0.00	-	0.01	-	0.01	3.10	0.03	0.02	0.00	0.15	1.85	3.93	3.11

Table 2: Phases identified from powder XRD analyses, protolith, and morphology indices

Sample #	Sample Name	XRF	EPMA	Protolith	M.I.	Phases Identified
AUSTRALIA						
75	AUS_ThreeSprings	y	y	carbonate	0.38	talc
76	AUS_MT.Seabrook	y	y	carbonate	0.43	talc, chlorite
AUSTRIA						
168	AUSTRIA_Styria_Anger	y	y	carbonate	0.54	talc, chlorite
77	AUSTRIA_Styria_Lassing		y	carbonate	0.32	talc, chlorite, biotite
BRAZIL						
2	BRA__Bahia_Magnesita_powder	y	y	carbonate	0.72	talc
78	BRA_Bahia_Casa Nova	y	y	carbonate	0.95	talc
203		y		carbonate	0.94	talc
CANADA						
80	CAN_Ontario_Madoc	y	y	carbonate	0.90	talc, dolomite, chlorite, biotite, amphibole
170	CAN_Ont_Madoc	y	y	carbonate	0.98	talc
CHINA						
94	CHI	y	y	carbonate	0.79	talc, chlorite, amphibole
86	CHI_Cuangai	y	y	carbonate	0.83	talc
3	CHI_Guangxi_GuiLin_mill	y	y	carbonate	0.73	talc, chlorite
88	CHI_ Guangxi_Longsheng_G1	y	y	carbonate	0.80	talc, chlorite
89	CHI_Guangxi_G1	y	y	carbonate	0.77	talc, chlorite
200	CHI_Guangxi_GuiLin	y		carbonate	0.87	talc, chlorite
201	CHI_Guangxi_Longguang	y		carbonate	0.68	talc, chlorite
91	CHI_Guangxi_G3	y	y	carbonate	0.56	talc
92	CHI_ Guangxi_G3	y	y	carbonate	0.49	talc
84	CHI_Hiacmen (Haichen?)	y	y	carbonate	0.57	talc
87	CHI_Liaoning	y	y	carbonate	0.70	talc, chlorite
90	CHI_ Liaoning_Liaoyang	y	y	carbonate		chlorite
93	CHI_ Liaoning_Haicheng_G3		y	carbonate	0.86	talc
83	CHI_Liaoning_Yingkow	y	y	carbonate	0.67	talc
85	CHI_Quixia		y	carbonate	0.93	talc
FINLAND						
95	FIN_Nka	y	y	ultramafic	0.91	talc, chlorite, magnesite
INDIA						
4	IND_Chainpura_mill	y	y	carbonate	0.86	talc, chlorite
5	IND_Ghevaria_mill	y	y	carbonate	0.71	talc, chlorite
204	IND_Haldwani	y		carbonate	0.88	talc, chlorite
ITALY						
180	ITA_Gianna_A	y	y	carbonate	0.86	talc
181	ITA_Gianna_C	y	y	carbonate	0.96	talc
99	ITA_Paola_A	y	y	carbonate	0.70	talc
100	ITA_Paola_scop	y	y	carbonate	0.86	talc
101	ITA_RodorettoMill_A1	y	y	carbonate	0.61	talc, chlorite
102	ITA_RodorettoMill_A2	y		carbonate	0.70	talc, chlorite
103	ITA_RodorettoMill_A3	y		carbonate	0.76	talc, chlorite
104	ITA_RdorettoMill_B1	y	y	carbonate	0.75	talc, chlorite
105	ITA_RodorettoMill_B2	y		carbonate	0.86	talc, chlorite
106	ITA_RodorettoMill_B3	y		carbonate	0.79	talc, chlorite
"KOREA"						
73	KOR	y	y	carbonate	0.82	talc
183	KOR_CT_IlShin_Whitesnow	y	y	carbonate	0.60	talc, serpentine
MOROCCO						
109	MOR	y	y	carbonate	0.86	talc, chlorite
165	MOR			carbonate	0.84	talc, chlorite
NORWAY						
169	NOR_Cerbis	y	y	"ultramafic"	0.89	talc
SPAIN						
110	SPA	y	y	carbonate	0.56	talc
111	SPA	y	y	carbonate	0.39	talc
USA		y				
20	USA_CA_CT_Vansil	y		carbonate	0.46	talc, calcite, amphibole, biotite
1	USA_CA_CT_Westal	y		carbonate	0.40	talc,calcite, biotite, amphibole
153	USA_CA_Grantham	y	y	carbonate	0.66	talc, calcite, biotite, quartz
152	USA_CA_Pfizer		y	carbonate	-	talc, amphibole, calcite, biotite
113	USA_CA_TalcCity_2			carbonate	0.38	talc, chlorite
114	USA_CA_TalcCity_3	y		carbonate	0.33	talc
115	USA_CA_TalcCity_4			carbonate	0.45	talc
116	USA_CA_TalcCity_5	y		carbonate	0.33	talc
117	USA_CA_TalcCity_6_dark		y	carbonate	0.40	talc, chlorite

Sample #	Sample Name	XRF	EPMA	Protolith	M.I.	Phases Identified
118	USA_CA_TalcCity_6_light		y	carbonate	0.56	talc, chlorite
119	USA_CA_TalcCity_7			carbonate	-	calcite, biotite
120	USA_CA_TalcCity_8			carbonate	0.30	talc, chlorite
14	USA_CA_WesternTalc_3A			carbonate	0.57	talc, biotite, amphibole, calcite
15	USA_CA_WesternTalc_3B			carbonate	0.63	talc, calcite, biotite, amphibole
16	USA_CA_WesternTalc_3C			carbonate	0.60	talc, amphibole, calcite, biotite
121	USA_GA_Earnest_fib		y	ultramafic	-	amphibole, talc, chlorite
122	USA_GA_Earnest_platy		y	ultramafic	-	amphibole, talc
123	USA_MT_Beaverhead	y	y	carbonate	0.70	talc, chlorite
136	USA_MT_Beaverhead Co._Benson ranch		y	carbonate	0.58	talc
172	USA_MT_CT_Sericron	y		carbonate	0.59	talc, chlorite
173	USA_MT_CT_Talcron	y		carbonate	0.52	talc, chlorite
174	USA_MT_CT_UltraTalc609	y		carbonate	0.37	talc, chlorite
175	USA_MT_Regal_HG	y	y	carbonate	0.51	talc, chlorite
7	USA_MT_Treasure_float	y	y	carbonate	0.54	talc
177	USA_MT_Treasure_G1	y	y	carbonate	0.61	talc, chlorite
184	USA_MT_Treasure_G3		y	carbonate	0.36	talc
9	USA_MT_WillowCreek_1A	y	y	carbonate	0.81	talc, chlorite
10	USA_MT_WillowCreek_1B			carbonate	0.88	talc, chlorite
11	USA_MT_WillowCreek_1C			carbonate	0.42	chlorite, talc
12	USA_MT_WillowCreek_2			carbonate	0.56	talc, chlorite
13	USA_MT_WillowCreek_3			carbonate	-	chlorite, talc
17	USA_MT_WillowCreek_6	y		carbonate	0.76	talc, calcite, chlorite
18	USA_MT_WillowCreek_7A			carbonate	0.51	talc
19	USA_MT_WillowCreek_8	y	y	carbonate	0.58	talc, chlorite
6	USA_MT_Yellowstone_HG	y	y	carbonate	0.39	talc
8	USA_MT_Yellowstone_LG	y	y	carbonate	0.32	talc
198	NY_CT_Nytal	y		carbonate	0.50	amphibole, quartz, serpentine, talc
199	NY_CT_Ceramital	y		carbonate	0.56	quartz,amphibole, serpentine, talc
36	USA_NC_Hitchcock_RX_LI	y	y	carbonate	0.86	talc, chlorite
37	USA_NC_Hitchcock_RX_DA	y	y	carbonate	0.78	chlorite, talc
39	USA_NC_CT_Hitchcock_Light	y		carbonate	0.39	talc, chlorite
40	USA_NC_Kinsey	y		carbonate	0.86	talc
41	USA_NC_Maltby			carbonate	0.87	talc, chlorite
42	USA_NC_Foote	y	y	carbonate	0.74	talc, chlorite
124	USA_NC_Murphy	y	y	carbonate	0.65	talc, chlorite
129	USA_NC_Murphy	y	y	carbonate	0.91	talc, amphibole
132	USA_NC_Murphy	y	y	carbonate	0.86	talc
143	USA_NC_Murphy	y		carbonate	0.77	talc
149	USA_NC_Murphy	y		carbonate	0.71	talc
125	USA_TX_Llano	y	y	ultramafic	0.96	talc, chlorite
156	USA_TX_VanHorn_pink	y	y	carbonate	0.90	talc, serpentine
157	USA_TX_VanHorn_gray	y	y	carbonate	0.90	talc
158	USA_TX_VanHorn_black	y	y	carbonate	0.84	talc, quartz
		y				
23	USA_VT_CT_Johnson_ENG_middle	y	y	ultramafic	0.43	talc, chlorite
26	USA_VT_Johnson_pipe	y	y	ultramafic	0.51	talc, magnesite, chlorite, serpentine
31	USA_VT_Johnson_JTM2	y		ultramafic	0.97	talc, chlorite
27	USA_VT_Johnson_green	y	y	ultramafic	0.80	talc
30	USA_VT_Johnson_black	y	y	ultramafic	0.82	talc, chlorite
33	USA_VT_CT_Johnson_J50		y	ultramafic	0.95	talc, chlorite, enstatite?
35	USA_Johnson_Leslie	y	y	ultramafic	0.93	talc
44	USA_VT_Argonaut_green	y	y	ultramafic	0.88	talc
45	USA_VT_Argonaut_underflow	y	y	ultramafic	0.74	talc, chlorite, magnesite
46	USA_VT_Argonaut_brokenbag	y	y	ultramafic	0.74	talc, magnesite, chlorite
49	USA_VT_Argonaut_R			ultramafic	0.90	talc, chlorite
50	USA_VT_Argonaut_HG	y	y	ultramafic	0.86	talc, magnesite, chlorite
43	USA_VT_Argonaut_LG	y	y	ultramafic	0.77	talc, magnesite, chlorite
53	USA_VT_Argonaut_xst	y	y	ultramafic	0.92	talc
135	USA_WA_TotemTalc	y	y	carbonate	0.81	talc
UNKNOWN						
55	CT_BP_Johnson	y	y	unknown	0.50	talc, chlorite
56	CT_BP_GoldBond	y		unknown	0.77	talc, chlorite
57	CT_BP_CashmereBouquet_A	y		unknown	0.85	talc, chlorite

Sample #	Sample Name	XRF	EPMA	Protolith	M.I.	Phases Identified
	CT_CashmereBouquet_B			unknown	0.81	talc, chlorite
	CT_CashmereBouquet_C			unknown	0.83	talc, chlorite
58	CT_BP_Safeway	y		unknown	0.23	talc
59	CT_BP_Ricette Naturali	y		unknown	0.92	talc, chlorite
21	CT_BP_Vanderbilt	y		unknown	0.81	talc, chlorite
60	CT_Malinkrodt	y		unknown	0.81	talc, chlorite
61	CT-1-AM	y		unknown	0.36	talc, chlorite
62	CT_poolchalk	y		unknown	-	gypsum, talc, kaolinite, quartz, calcite
63	CT_handtalc	y		unknown	0.63	talc, magnesite, quartz
64	CT_Fisher	y		unknown	0.74	talc
65	CT_tiretalc	y		unknown	0.95	talc, serpentine, chlorite, magnesite
66	CT_CB_IT	y		unknown	0.95	talc, chlorite
67	CT_FP_CSI_A	y	y	unknown	0.65	talc, chlorite,calcite, quartz
	CT_FP_CSI_B				0.74	talc, chlorite, calcite, quartz
188	CT_marker_MBS		y	unknown	0.80	talc, chlorite
190	CT_soap_BR	y		unknown	0.63	talc, chlorite
191	CT_soap_icecube	y		unknown	0.57	talc, chlorite
192	CT_soap_coaster	y		unknown	0.68	pyrophyllite, biotite, serpentine
193	CT_soap_bowl	y		unknown	-	chlorite, talc
194	CT_soap_griddle	y		unknown	0.65	talc, chlorite, magnesite
195	CT_soap_shotglass	y		unknown	-	chlorite, talc
196	CT_soap_pizzastone	y		unknown	0.80	talc, chlorite, amphibole
197	CT_Polyguard			unknown	0.48	talc, serpentine, amphibole

Table 3: EPMA standards

Element	Peak Counting Time (s)	Low Background Counting Time (s)	High Background Counting Time (s)	Analyzing Crystal	Calibration Standard
Si	15	5	5	TAP	Wollastonite #2 (C.M. Taylor)
Ti	90	45	45	PETJ	Sphene #1A (C.M. Taylor)
Zn	30	15	15	LiFH	Willemite #1 (C.M. Taylor)
Al	30	10	10	TAP	Albite #4 (C.M. Taylor)
Cr	30	15	15	LiFH	Chromite #5 (C.M. Taylor)
Fe	10	5	5	LiFH	VG-A99 (USNM 113498/1)
Ni	30	15	15	LiFH	Pentlandite (Astimex)
Mn	30	15	15	LiFH	Spessartine (C.M. Taylor)
Mg	15	5	5	TAP	Arenal Hornblende (USNM 111356)
Ca	30	15	15	PETJ	Arenal Hornblende (USNM 111356)
Na	30	10	10	TAP	Albite #4 (C.M. Taylor)
K	30	15	15	PETJ	Orthoclase OR-10 (C.M. Taylor)
S	80	40	40	PETJ	Pentlandite (Astimex)
Cl	80	40	40	PETJ	KCl (Fisher Sci.)
F	200	100	100	TAP	MgF_2 (C.M. Taylor)

Table 4a (top) and 4b (bottom): Correlation coefficients for multivariate scatter plots shown in Figures 4a (oxides determined by EPMA) and 4b (calculated APFU values).
Red font indicates a negative correlation between the two oxides; blue font indicates a positive correlation. The intensity of the color is proportional to the magnitude of the correlation. Correlation coefficients between 0.30 and -0.30 were not considered significant.

a.

Row	SiO2	Al2O3	TiO2	ZnO	Cr2O3	FeO	NiO	MnO	MgO	CaO	Na2O	K2O	P2O5	SO3	F wt%
SiO2	1.00	-0.01	-0.10	-0.49	-0.07	-0.03	-0.18	-0.04	0.87	-0.09	-0.14	-0.05	-0.61	-0.48	0.07
Al2O3	-0.01	1.00	-0.03	-0.01	0.00	-0.23	0.03	-0.05	-0.01	0.00	0.31	0.06	-0.08	0.51	0.54
TiO2	-0.10	-0.03	1.00	0.25	0.22	0.10	-0.06	0.04	-0.13	0.04	0.21	0.02	-0.15	0.11	-0.13
ZnO	-0.49	-0.01	0.25	1.00	0.10	0.26	0.07	0.09	-0.57	0.49	0.11	0.05	0.00	0.46	0.09
Cr2O3	-0.07	0.00	0.22	0.10	1.00	0.16	0.40	-0.02	0.03	-0.04	-0.03	-0.05	0.00	0.10	-0.13
FeO	-0.03	-0.23	0.10	0.26	0.16	1.00	0.51	0.62	-0.39	0.33	-0.10	-0.09	-0.25	-0.03	-0.32
NiO	-0.18	0.03	-0.06	0.07	0.40	0.51	1.00	0.22	-0.23	0.27	0.08	-0.05	0.00	-0.05	-0.13
MnO	-0.04	-0.05	0.04	0.09	-0.02	0.62	0.22	1.00	-0.30	0.34	0.06	-0.01	-0.16	0.05	-0.16
MgO	0.87	-0.01	-0.13	-0.57	0.03	-0.39	-0.23	-0.30	1.00	-0.33	-0.19	-0.07	-0.60	-0.44	0.16
CaO	-0.09	0.00	0.04	0.49	-0.04	0.33	0.27	0.34	-0.33	1.00	0.14	0.12	0.51	0.27	0.02
Na2O	-0.14	0.31	0.21	0.11	-0.03	-0.10	0.08	0.06	-0.19	0.14	1.00	0.29	0.35	0.36	0.15
K2O	-0.05	0.06	0.02	0.05	-0.05	-0.09	-0.05	-0.01	-0.07	0.12	0.29	1.00	0.34	0.16	-0.02
P2O5	-0.61	-0.08	-0.15	0.00	0.00	-0.25	0.00	-0.16	-0.60	0.51	0.35	0.34	1.00	0.00	-0.39
SO3	-0.48	0.51	0.11	0.46	0.10	-0.03	-0.05	0.05	-0.44	0.27	0.36	0.16	0.00	1.00	0.46
F wt%	0.07	0.54	-0.13	0.09	-0.13	-0.32	-0.13	-0.16	0.16	0.02	0.15	-0.02	-0.39	0.46	1.00

b.

Row	Si4+	Al3+	Ti4+	Zn2+	Cr3+	Fe2+	Ni2+	Mn2+	Mg2+	Ca2+	Na+	K+	P5+	S6+	F-
Si4+	1.00	-0.39	0.00	0.00	0.00	-0.21	-0.33	0.00	-0.14	0.01	0.06	0.09	0.00	0.00	-0.21
Al3+	-0.39	1.00	0.00	0.00	0.00	-0.22	0.07	0.00	-0.09	0.01	0.26	0.06	0.00	0.00	0.53
Ti4+	0.00	0.00	1.00	0.00	0.00	0.00	0.00	0.00	0.00	0.00	0.00	0.00	0.00	0.00	0.00
Zn2+	0.00	0.00	0.00	1.00	0.00	0.00	0.00	0.00	0.00	0.00	0.00	0.00	0.00	0.00	0.00
Cr3+	0.00	0.00	0.00	0.00	1.00	0.00	0.00	0.00	0.00	0.00	0.00	0.00	0.00	0.00	0.00
Fe2+	-0.21	-0.22	0.00	0.00	0.00	1.00	0.25	0.00	-0.80	0.33	-0.08	-0.18	0.00	0.00	-0.32
Ni2+	-0.33	0.07	0.00	0.00	0.00	0.25	1.00	0.00	-0.04	-0.03	0.19	-0.03	0.00	0.00	-0.11
Mn2+	0.00	0.00	0.00	0.00	0.00	0.00	0.00	1.00	0.00	0.00	0.00	0.00	0.00	0.00	0.00
Mg2+	-0.14	-0.09	0.00	0.00	0.00	-0.80	-0.04	0.00	1.00	-0.52	-0.13	0.03	0.00	0.00	0.16
Ca2+	0.01	0.01	0.00	0.00	0.00	0.33	-0.03	0.00	-0.52	1.00	0.10	0.10	0.00	0.00	0.01
Na+	0.06	0.26	0.00	0.00	0.00	-0.08	0.19	0.00	-0.13	0.10	1.00	0.09	0.00	0.00	0.02
K+	0.09	0.06	0.00	0.00	0.00	-0.18	-0.03	0.00	0.03	0.10	0.09	1.00	0.00	0.00	0.00
P5+	0.00	0.00	0.00	0.00	0.00	0.00	0.00	0.00	0.00	0.00	0.00	0.00	1.00	0.00	0.00
S6+	0.00	0.00	0.00	0.00	0.00	0.00	0.00	0.00	0.00	0.00	0.00	0.00	0.00	1.00	0.00
F-	-0.21	0.53	0.00	0.00	0.00	-0.32	-0.11	0.00	0.16	0.01	0.02	0.00	0.00	0.00	1.00

Table 5: APFU values for Figure 6, FIN_NKarelia

a. Talc (yellow stars)

Target	Si4+	Al3+	Fe2+	Ni2+	Mn2+	Mg2+	Ca2+	Na+	K+	S6+	F-	OH-	Tet	Oct
Ideal	4.00	0.00	0.00	0.00	0.00	3.00	0.00	0.00	0.00	0.00	0.00	2.00	4.00	3.00
T3_1	4.02	0.00	0.08	0.00	0.00	2.87	0.00	0.00	0.00	0.00	0.00	2.00	4.02	2.96
T3_2	3.99	0.00	0.07	0.00	0.00	2.93	0.00	0.00	0.00	0.00	0.01	1.99	3.99	3.01
T3_3	3.82	0.14	0.10	0.00	0.00	3.02	0.00	0.00	0.00	0.00	0.01	1.99	3.96	3.14
T3_4	3.59	0.31	0.13	0.00	0.00	3.17	0.00	0.00	0.00	0.00	0.00	2.00	3.90	3.34
T3_5	3.94	0.03	0.09	0.00	0.00	2.98	0.00	0.00	0.00	0.00	0.00	2.00	3.97	3.08

b. Magnesite (magenta circles)

Target	Si4+	Fe2+	Mg2+	Ca2+	S6+	F-	CO3	Oct
Ideal	0.00	0.00	2.00	0.00	0.00	0.00	2.00	0.00
T3_1	0.00	0.12	1.87	0.00	0.00	0.00	2.00	2.00
T3_2	0.00	0.23	1.75	0.00	0.00	0.00	2.00	2.00
T3_3	0.00	0.18	1.80	0.00	0.00	0.00	2.00	2.00

Table 6: APFU values for Figure 7, USA_MT_Treasure_G1
Talc (yellow stars)

Target	Si4+	Al3+	Fe2+	Ni2+	Mn2+	Mg2+	Ca2+	Na+	K+	S6+	F-	OH-	Tet	Oct
Ideal	4.00	0.00	0.00	0.00	0.00	3.00	0.00	0.00	0.00	0.00	0.00	2.00	4.00	3.00
T1_1	3.99	0.01	0.01	0.00	0.00	3.00	0.00	0.00	0.00	0.00	0.02	1.98	3.99	3.02
T1_2	4.01	0.00	0.12	0.00	0.00	2.85	0.00	0.00	0.00	0.00	0.04	1.96	4.01	2.97
T1_3	4.01	0.00	0.14	0.00	0.00	2.83	0.00	0.00	0.00	0.00	0.06	1.94	4.01	2.98
T1_4	4.03	0.00	0.11	0.00	0.00	2.82	0.00	0.00	0.00	0.00	0.06	1.94	4.03	2.93
T1_5	4.01	0.00	0.13	0.00	0.00	2.84	0.00	0.00	0.00	0.00	0.07	1.93	4.01	2.97

Table 7: APFU values for CHI_Guangxi_G3_91

a. dark bands, Figure 8c

Target	Si4+	Al3+	Fe2+	Ni2+	Mn2+	Mg2+	Ca2+	Na+	K+	S6+	F-	OH-	Tet	Oct
Ideal	4.00	0.00	0.00	0.00	0.00	3.00	0.00	0.00	0.00	0.00	0.00	2.00	4.00	3.00
T2_1	3.93	0.23	0.00	0.00	0.00	2.79	0.00	0.01	0.00	0.00	0.25	1.75	4.00	2.96
T2_2	3.96	0.12	0.00	0.00	0.00	2.89	0.00	0.01	0.00	0.00	0.29	1.71	4.00	2.98
T2_3	3.76	0.42	0.00	0.00	0.00	2.83	0.00	0.01	0.00	0.00	0.23	1.77	4.00	3.03
T2_4	3.91	0.30	0.00	0.00	0.00	2.72	0.00	0.01	0.00	0.00	0.28	1.72	4.00	2.94
T2_5	4.00	0.08	0.00	0.00	0.00	2.86	0.00	0.01	0.00	0.00	0.27	1.73	4.00	2.95

b. light bands, Figure 8d (values from point 6 were not used to calculate the average composition listed in Appendix C, thin section may have been too thin, resulting in sampling the glass slide)

Target	Si4+	Al3+	Fe2+	Ni2+	Mn2+	Mg2+	Ca2+	Na+	K+	S6+	F-	OH-	Tet	Oct
Ideal	4.00	0.00	0.00	0.00	0.00	3.00	0.00	0.00	0.00	0.00	0.00	2.00	4.00	3.00
T2_1	4.02	0.01	0.00	0.00	0.00	2.94	0.00	0.01	0.00	0.00	0.24	1.76	4.02	2.96
T2_2	4.02	0.01	0.00	0.00	0.00	2.94	0.00	0.00	0.00	0.00	0.26	1.74	4.02	2.95
T2_3	4.04	0.01	0.00	0.00	0.00	2.90	0.00	0.00	0.00	0.00	0.26	1.74	4.04	2.92
T2_4	4.01	0.01	0.00	0.00	0.00	2.95	0.00	0.00	0.00	0.00	0.25	1.75	4.01	2.97
T2_5	4.02	0.01	0.00	0.00	0.00	2.93	0.00	0.00	0.00	0.00	0.27	1.73	4.02	2.94
T2_6	4.10	0.01	0.00	0.00	0.00	2.77	0.00	0.01	0.00	0.00	0.23	1.77	4.10	2.80
T2_7	4.03	0.01	0.00	0.00	0.00	2.91	0.00	0.01	0.00	0.00	0.24	1.76	4.03	2.93

Table 8: Clinochlore content in commercial talc based on EPMA and XRF data

Sample	SiO2/MgO	Al2O3	Al2O3(talc)	XRF Al2O3-EPMA Al2O3	Al2O3 EPMA chlorite	wt % chlorite
AUS_MtSeabrook	2.00	1.18	0.32	0.86	18.32	4.67
AUSTRIA_Styria_Anger	1.57	9.13	0.33	8.79	22.03	39.91
AUSTRIA_Styria_Lassing	2.00	0.65	0.13	0.52	17.44	3.00
CHI_Guangxi_GuiLin_mill	1.97	1.07	0.03	1.04	21.67	4.80
ITA_Paola_A	2.02	0.71	0.15	0.56	20.95	2.66
USA_MT_Beaverhead_high Fe	1.99	0.42	0.06	0.36	12.85	2.82
USA_MT_Beaverhead_low Fe	1.99	0.42	0.19	0.23	12.85	1.81
USA_NC_HC_CT_light	1.98	0.97	0.16	0.81	20.95	3.85
USA_NC_HC_CT_light R	1.99	0.97	0.16	0.81	20.95	3.85
USA_NC_HC_RX_LI	1.94	2.87	0.38	2.49	23.54	10.57
USA_VT_Argonaut_underflow	0.29	1.30	0.05	1.25	16.81	7.44
USA_VT_CT_Argonaut_brokenbag	1.03	0.98	0.03	0.95	18.33	5.17
USA_VT_Johnson_black	2.05	1.36	0.02	1.34	17.28	7.78
USA_VT_Johnson_UVM	2.09	0.88	0.02	0.86	16.19	5.30
CT_BP_Johnson	1.94	1.44	0.08	1.36	21.17	6.41

Table 9: APFU values for Figure 9a, USA_NC_Murphy_129

a. Talc

Target	Si4+	Al3+	Fe2+	Ni2+	Mn2+	Mg2+	Ca2+	Na+	K+	S6+	F-	OH-	Tet	Oct
Ideal	4.00	0.00	0.00	0.00	0.00	3.00	0.00	0.00	0.00	0.00	0.00	2.00	4.00	3.00
T1_1	4.03	0.02	0.05	0.00	0.00	2.87	0.00	0.00	0.00	0.00	0.07	1.93	4.03	2.94
T1_2	4.04	0.02	0.05	0.00	0.00	2.84	0.00	0.00	0.00	0.00	0.08	1.92	4.04	2.91
T1_3	4.02	0.02	0.05	0.00	0.00	2.89	0.00	0.00	0.00	0.00	0.07	1.93	4.02	2.96
T1_4	4.01	0.02	0.05	0.00	0.00	2.90	0.00	0.00	0.00	0.00	0.07	1.93	4.01	2.98
T1_5	4.03	0.02	0.05	0.00	0.00	2.86	0.00	0.00	0.00	0.00	0.07	1.93	4.03	2.93
T1_6	4.03	0.02	0.05	0.00	0.00	2.86	0.00	0.00	0.00	0.00	0.08	1.92	4.03	2.93

b. Tremolite

Target	Si4+	Al3+	Fe2+	Ni2+	Mn2+	Mg2+	Ca2+	Na+	K+	S6+	F-	OH-	A	B	C	T
Ideal	8.00	0.00	0.00	0.00	0.00	5.00	2.00	0.00	0.00	0.00	0.00	2.00	0.00	2.00	5.00	8.00
T1_1	7.90	0.21	0.13	0.00	0.00	4.70	2.03	0.04	0.00	0.00	0.12	1.88	0.00	2.03	5.00	8.00
T1_2	7.93	0.19	0.12	0.00	0.00	4.69	2.02	0.03	0.00	0.00	0.12	1.88	0.00	2.02	5.00	8.00
T1_3	7.80	0.28	0.13	0.00	0.00	4.77	2.05	0.04	0.01	0.00	0.10	1.90	0.01	2.05	5.00	8.00
T1_4	8.04	0.26	0.13	0.00	0.00	4.37	2.00	0.03	0.01	0.00	0.10	1.90	0.01	2.00	5.00	8.04

Table 10: APFU values for Figure 10, CHI_94

a. Talc

Target	Si4+	Al3+	Fe2+	Ni2+	Mn2+	Mg2+	Ca2+	Na+	K+	S6+	F-	OH-	Tet	Oct
Ideal	4.00	0.00	0.00	0.00	0.00	3.00	0.00	0.00	0.00	0.00	0.00	2.00	4.00	3.00
T2_1	3.99	0.00	0.02	0.00	0.00	3.00	0.00	0.00	0.00	0.00	0.02	1.98	3.99	3.02
T2_2	4.02	0.00	0.01	0.00	0.00	2.94	0.00	0.00	0.00	0.00	0.02	1.98	4.02	2.96
T2_3	4.00	0.00	0.01	0.00	0.00	2.98	0.00	0.00	0.00	0.00	0.03	1.97	4.00	2.99

b. Tremolite

Target	Si4+	Al3+	Fe2+	Ni2+	Mn2+	Mg2+	Ca2+	Na+	K+	S6+	F-	OH-	A	B	C	T
Ideal	8.00	0.00	0.00	0.00	0.00	5.00	2.00	0.00	0.00	0.00	0.00	2.00	0.00	2.00	5.00	8.00
T2_1	7.72	0.01	0.04	0.00	0.00	6.26	1.25	0.00	0.01	0.00	0.05	1.95	0.01	2.55	5.00	7.72
T2_2	7.58	0.01	0.03	0.00	0.00	5.88	1.90	0.01	0.01	0.00	0.05	1.95	0.01	2.81	5.00	7.59
T2_3	7.72	0.01	0.03	0.00	0.00	5.50	2.00	0.01	0.01	0.00	0.05	1.95	0.01	2.53	5.00	7.73

c. Chlorite-biotite (mentioned in previous section)

Target	Si4+	Al3+	Fe2+	Ni2+	Mn2+	Mg2+	Ca2+	Na+	K+	S6+	F-	OH-	Tet	Oct	I
Ideal	3.00	1.00	0.00	0.00	0.00	3.00	0.00	0.00	1.00	0.00	0.00	2.00	4.00	4.00	1.00
T2_1	3.25	0.78	0.02	0.00	0.00	3.09	0.00	0.01	0.67	0.00	0.11	1.89	4.00	3.15	0.68
T2_2	3.18	0.75	0.01	0.00	0.00	3.03	0.00	0.01	0.68	0.00	0.14	1.86	3.93	3.04	0.69
Ideal	3.00	2.00	0.00	0.00	0.00	5.00	0.00	0.00	0.00	0.00	0.00	8.00	4.00	6.00	-
T2_3	3.71	1.06	0.06	0.00	0.00	4.87	0.01	0.00	0.06	0.00	0.08	7.92	4.00	5.71	-

Table 11: APFU values for Figure 11, USA_GA_Earnest_fib

a. Talc

Target	Si4+	Al3+	Fe2+	Ni2+	Mn2+	Mg2+	Ca2+	Na+	K+	S6+	F-	OH-	Tet	Oct
Ideal	4.00	0.00	0.00	0.00	0.00	3.00	0.00	0.00	0.00	0.00	0.00	2.00	4.00	3.00
T2_1	4.00	0.01	0.30	0.00	0.00	2.64	0.03	0.00	0.00	0.00	0.03	1.97	4.00	2.99
T2_2	3.97	0.01	0.33	0.01	0.00	2.59	0.11	0.00	0.00	0.00	0.02	1.98	3.98	3.04

b. Actinolite

Target	Si4+	Al3+	Fe2+	Ni2+	Mn2+	Mg2+	Ca2+	Na+	K+	S6+	F-	OH-	A	B	C	T
Ideal	8.00	0.00	2.5-1.0	0.00	0.00	2.5-4.0	2.00	0.00	0.00	0.00	0.00	2.00	0.00	2.00	5.00	8.00
T2_1	7.94	0.08	0.95	0.00	0.03	3.98	2.00	0.03	0.01	0.00	0.03	1.97	0.01	2.00	5.00	8.00
T2_2	7.96	0.06	0.94	0.01	0.04	3.98	2.00	0.02	0.01	0.00	0.05	1.95	0.01	2.00	5.00	8.00
T2_3	7.98	0.05	0.95	0.01	0.04	3.94	2.00	0.02	0.01	0.00	0.02	1.98	0.01	2.00	5.00	8.00
T2_4	7.99	0.04	1.01	0.01	0.04	3.88	2.00	0.01	0.01	0.00	0.04	1.96	0.01	2.00	5.00	8.00
T2_5	7.96	0.05	1.02	0.01	0.04	3.93	2.00	0.01	0.01	0.00	0.04	1.96	0.01	2.00	5.00	8.00

Table 12: APFU values for most variable elements in talc showing similarities in compositions

	EPMA, APFU			XRF, weight percent oxides			XRF, ppm	
Sample	Al3+	Fe2+	F-	SiO2/MgO	Al2O3	FeO	Ni	Cr
USA_MT_Treasure_float	0.01	0.14	0.04	2.08	0.19	2.79	12.32	10.20
USA_MT_Treasure_G1	0.00	0.12	0.06	2.01	0.04	0.50	27.86	2.24
USA_MT_Treasure_G3	0.01	0.12	0.04	2.05	0.16	2.43	87.08	8.68
USA_MT_WillowCr_8	0.00	0.10	0.03	2.03	0.05	1.34	16.26	22.12
USA_TX_Llano	0.03	0.14	0.00	2.08	0.34	3.79	1722.98	1261.12
USA_VT_Johnson_black	0.00	0.18	0.02	2.05	0.02	3.70	621.00	1043.00
USA_VT_Johnson_green	0.00	0.19	0.02	2.06	-0.01	3.45	407.00	59.00
USA_VT_Johnson_Leslie	0.00	0.13	0.01	2.08	-0.03	2.54	1049.00	19.00

Table 13: APFU values for Figure 13, “Cerbis, Norway”; point numbers correspond to those in Figure n, above. Note the Fe^{2+} and F^{-} values compared to those in Table 4 for the ultramafic talc from Finland

Target	Si4+	Al3+	Fe2+	Ni2+	Mn2+	Mg2+	Ca2+	Na+	K+	S6+	F-	OH-	Tet	Oct
Ideal	4.00	0.00	0.00	0.00	0.00	3.00	0.00	0.00	0.00	0.00	0.00	2.00	4.00	3.00
T3_1	4.05	0.01	0.03	0.00	0.00	2.86	0.00	0.00	0.00	0.00	0.03	1.97	4.05	2.90
T3_2	4.02	0.01	0.03	0.00	0.00	2.92	0.00	0.00	0.00	0.00	0.04	1.96	4.02	2.96
T3_3	4.02	0.01	0.03	0.00	0.00	2.90	0.00	0.00	0.00	0.00	0.04	1.96	4.02	2.95
T3_4	4.07	0.02	0.03	0.00	0.00	2.80	0.00	0.00	0.00	0.00	0.04	1.96	4.07	2.85
T3_5	4.00	0.01	0.02	0.00	0.00	2.95	0.00	0.00	0.00	0.00	0.04	1.96	4.00	2.99
T3_6	4.02	0.02	0.03	0.00	0.00	2.91	0.00	0.00	0.00	0.00	0.04	1.96	4.02	2.95
T3_7	4.04	0.02	0.03	0.00	0.00	2.86	0.00	0.00	0.00	0.00	0.05	1.95	4.04	2.91

Table 14: Compositional data for unknown talc and clinochlore products

	EPMA, APFU			XRF, weight percent oxides			XRF, ppm	
Sample	Al3+	Fe2+	F-	SiO2/MgO	Al2O3	FeO	Ni	Cr
USA_MT_Treasure_float	0.01	0.14	0.04	2.08	0.19	2.79	12.32	10.20
USA_MT_Treasure_G1	0.00	0.12	0.06	2.01	0.04	0.50	27.86	2.24
USA_MT_Treasure_G3	0.01	0.12	0.04	2.05	0.16	2.43	87.08	8.68
USA_MT_WillowCr_8	0.00	0.10	0.03	2.03	0.05	1.34	16.26	22.12
USA_TX_Llano	0.03	0.14	0.00	2.08	0.34	3.79	1722.98	1261.12
USA_VT_Johnson_black	0.00	0.18	0.02	2.05	0.02	3.70	621.00	1043.00
USA_VT_Johnson_green	0.00	0.19	0.02	2.06	-0.01	3.45	407.00	59.00
USA_VT_Johnson_Leslie	0.00	0.13	0.01	2.08	-0.03	2.54	1049.00	19.00

Chapter 2: Current issues with purported asbestos content in talc ores from southwest Montana

Abstract

Talc formed by hydrothermal alteration of preexisting carbonate rocks is known to be nearly monomineralic, and lacking in amphiboles. In southwest Montana, talc formed from hydrothermally altered dolomitic marbles, and is still actively mined. These talc deposits are typically in contact with quartzofeldspathic gneiss and marble. Accessory minerals vary between these rocks and the ore producing body; the identification and characterization of such minerals requires carefully selected analytical methods. Recent litigation and ensuing confusion over the petrology and asbestos content of these deposits challenges the talc mining industry in Montana, and elsewhere in the world.

Introduction

Commercial talc has been mined from the deposits in southwest Montana since the 1940s, and by 1956 the region had output 200,000 tons of talc ore (Chidester et al., 1964). Commercial talc refers to rocks containing more than 20% of the mineral talc (McCarthy et al., 2006); the ores from Montana typically contain upwards of 90% talc. This region remains the leading domestic source of talc in the U.S. partly due to the reserves in the area, and partly due to the diagnostic purity of the ore compared to that of other regions, some of which are no longer actively mined. The mineral talc, a sheet silicate, is expressed by the formula $Mg_3Si_4O_{10}(OH)_2$, and therefore forms in geologic environments that are rich in Mg, Si, O and water. The protolith for the talc deposits in southwest Montana is a dolomitic marble, but other common protoliths include siliceous dolimites and mafic/ultramafic rocks (McCarthy et al., 2006). The compositional data show mineral content of selected ores, and the major and trace element content of those minerals, specifically talc. Our electron microprobe (EPMA), powder x-ray diffraction (XRD) and x-ray fluorescence spectroscopy (XRF) data for samples from five mines in these three ranges provide continued evidence of the purity of the ores from Montana despite claims made during recent litigation that these ores contain asbestos. Cashmere Bouquet, a Colgate Palmolive product, is a talc body

powder that was sourced from talc mines in the Murphy Marble belt, North Carolina, Chisone Valley, Italy, and specifically the Willow Creek Mine in the Greenhorn Range, southwest Montana (Levin, 2015). The Willow Creek mine was the largest source of commercial talc in the Greenhorn Range. Some individuals who have used Cashmere Bouquet have also been diagnosed with mesothelioma, resulting in parties seeking restitution from Colgate Palmolive for exposure to asbestos (as asbestos exposure and mesothelioma are causatively linked). Both plaintiff and defense verdicts have been reached (Levin, 2015). In the following sections we describe the mechanism of talc formation in southwest Montana by focusing on talc deposits and surrounding rocks in the Ruby, Greenhorn, and Gravelly Ranges, and to relate the mechanism of formation to the composition of talc ores. We also discuss the identification of asbestos in these ores and unravel some confusion that we believe gives further motivation for asbestos litigation over ores from this region, and also cause issues in the regulatory community. The five mines that we discuss include the Beaverhead, Treasure, Regal, Willow Creek, and Yellowstone. (Figure 1.)

Southwest Montana talc formation

The talc deposits in southwest Montana have a long metamorphic history involving at least three events that will be referred to as M_1, M_2, and M_3. The talc formed in dolomitized marbles of the Cherry Creek rocks, which can be most simply described as Archean meta-sediments. Other Cherry Creek rock types include metamorphosed carbonates, mafic gneiss, banded iron formation, meta-pelites, and quartzites (Berg, 1979; Dahl, 1979). This group of rocks exists in multiple ranges through southwest Montana but is not easily traceable due to prominent foliation and isoclinal folds. The Dillon Gneiss has a quartzofeldspathic composition and conformably underlies the Cherry Creek dolomites. This gneiss was most likely a source of SiO_2 in the formation of talc. Despite the structural complexity of the area, it is generally assumed that the talc in southwest Montana all has similar, if not the same geologic history because it only occurs in Precambrian rocks, and is not found in Paleozoic dolomites. The ternary diagrams in Figures 3A-3B from Anderson et al. (1990) plot the bulk

compositions determined from XRF analyses of high-grade marbles (rock compositions formed from M_1), talc-bearing marbles (rock compositions formed from M_2), and massive talc bodies (rock compositions formed from M_3). These diagrams are helpful in describing the compositional variations that accompanied geologic events in the Ruby Range. H_2O and CO_2 are not included in these diagrams because they are mobile components. Again, due to the structural and lithological constraints on talc occurrences in southwest Montana, the deposits in the Ruby Range, Greenhorn Range, and Gravelly Range are understood to have very similar histories.

M_1

Approximately 2.7Ga upper-amphibolite facies metamorphism (M_1) of the Cherry Creek rocks (James and Hedge, 1980) resulted in the formation of high-grade marbles. Peak metamorphic conditions from this event based on mineral-pair geothermometers and geobarometers recorded in two areas in the Ruby Range span from 675 ± 45° - 745 ± 50°C and 0.5-0.8 GPa respectively (Dahl, 1979). This event also created the dominant northeast-trending, northwest dipping foliation and axial surfaces in isoclinal folds (Anderson et al., 1990**)**. The M_1 mineral assemblage in the marble included calcite – olivine – phlogopite ± dolomite ± garnet, with tremolite replacing olivine. The formation of tremolite is not completely understood but it is likely that it formed as a late M_1 mineral or an early M_2 mineral. (Anderson et al., 1990) The compositions for these rocks are plotted as squares in Figure 3A.

M_2

Retrograde greenschist metamorphism (M_2) occurred during the Meso-Paleoproterozoic and resulted in the formation of talc-bearing marbles from the alteration of high-grade marbles. Biotite and muscovite in the Dillon gneiss reveal K-Ar dates of 1.6±0.1Ga (Giletti, 1966**)** (M_2). Similar $^{39}Ar/^{40}Ar$ dates in phlogopite from marbles and amphibolites were recorded for ~1.7Ga (Brady et al., 1998). This event overprinted the earlier high-grade metamorphism and is associated with the increase in Mg in the region,

recorded by dolomitization of the high-grade marbles and clinochlore (chlorite Mg end-member) replacement of plagioclase and biotite in the Dillon Gneiss. This is shown by trend 1 in Figure 3B. Chloritization of the gneiss occurred where it is adjacent to the marbles or talc bodies, suggesting that the current compositions of the rocks resulted from the same process (Anderson et al., 1990). Another important point is that dolomitization of calcite would have resulted in a volumetric decrease due to the replacement of Ca^{2+} by Mg^{2+}. There is no evidence for volume loss indicating that Mg was present in excess. The question remains for what such a massive source for Mg would have been. Events M_2 and M_3 are gradational rather than recorded by specific dates. The inclusions of chlorite in the massive talc bodies indicate the two crystallized during the same or overlapping processes, but we know that the introduction of Mg to the system happened prior to the formation of the very pure talc. The bulk XRF data from Anderson et al. (1990) plot the talc-bearing marbles at a composition very close to pure dolomite. These rocks have not been completely altered to talc due to the lack of SiO_2. The mineral assemblage associated with these conditions is talc – dolomite – chlorite ± calcite. Accessory minerals include graphite, pyrite, manganese oxides, and quartz (Anderson et al., 1990). These rocks are not ore-quality.

M_3

The metasomatic event (M_3) is estimated to have occurred 1.6-1.1Ga. A series of mafic dikes and sills intruded the Archean rocks approximately 1.455Ga and 1.12-1.13 Ga, accompanied by extension associated with rifting of the overlying basin. These dikes are thought to be the heat source behind circulating the talc-forming fluids. Anderson et al. (1990) estimated the conditions for the talc-forming event from samples in the Ruby Range to be <400°C and 2Gpa, indicating a depth of about 6km. Volumetric water/rock ratios were calculated to be >600. Brady et al. (1998) determined stable C isotope ratios in carbonates and graphite in high-grade marbles and talc rocks from the Ruby Range. Their study determined that the ^{14}C values were indistinguishable and represented amphibolite-grade conditions (M_1). The talc-forming fluids did not affect the ^{14}C composition, indicating that the fluid was CO_2-poor. Differences in the ^{18}O in dolomite and calcite indicate the fluids were

H_2O-rich and thought to be derived from seawater. In the same study the temperatures of talc formation were constrained to 200°-300°C, at depths of 5-10 km. Their study also determined $^{40}Ar/^{39}Ar$ ages for muscovite intergrown with talc at 1.36Ga. This date coincides with the timing of the mafic intrusions. Gammons and Matt (2002) studied fluid inclusions in quartz samples that were contemporaneous with talc from the Gravelly Range. Their results indicate the talc-forming fluids were 7x saltier than modern day seawater and that trapping temperatures were 190°-250°C. Their suggested mechanism is that connate brines and Proterozoic seawater associated with the overlying Belt Basin were heated by mafic intrusions and were circulated toward the underlying Cherry Creek rocks. Circulation may have been aided by the high-pressure gradient due to the thick overlying Belt sequence and from the volume increase resulting from heating the brines. Estimated depths are from 3-10km. Figure 4, is a schematic of this process. Botryoidal talc has been found at the Yellowstone and other mines, which indicates crystallization in a shallow vug-like environment (Cerino et al., 2007; Underwood et al., 2014). It is possible that talc with this texture was formed in the waning stages of M_3 as a result of lower pressures, however significant decreases in pressure would have had to occur for small cavities to exist. This texture is not observed homogeneously throughout the deposits and may have been controlled by small-scale structural differences.

Despite differences in P-T estimates for formation of the massive talc bodies, it is agreed upon that the following reaction:

3 dolomite +4 $SiO_2(aq)$ + $4H_2O$ = 1 talc+ $3Ca^{2+}$ + $6HCO_3^-$, occurred, and that temperatures <400°C resulted in the pure talc mineralogy. Generally, the massive talc bodies lack carbonates and other Ca-rich phases, indicating that the fluid was not rich in CO_2 or Ca^{2+}. The $SiO_2(aq)$ was sourced from the quartzofeldspathic gneiss reacting with the seawater-brine fluid. Arrow 2 in Figure 3B illustrates the increasing amount of SiO_2 in the system. Trends 1 and 2 have different slopes, supporting the idea that the increase in MgO and increase in SiO_2 were two separate processes (Anderson et al., 1990).

One suggestion made during testimony and in a deposition by a plaintiff's expert in civil litigation is that the talc deposits in southwest Montana were formed by interactions

with the Yellowstone hot spot. The timescale for talc formation, for which there is an abundance of thermochronometric data, occurred on the scale of 1-2 Ga, and the Yellowstone hot spot has a history <20Ma, much closer to <5Ma if there would be any effects in southwest Montana. If the hot spot had resulted in alteration of these rocks we would see evidence of hydrothermal alteration in all the rocks older than 5Ma. The talc in this region is found in Archean dolomites, and not found in younger carbonates. This suggestion has no validity in describing the mechanism of talc formation in southwest Montana. There are many occurrences of talc around the world that have formed by hydrothermal or precipitate mechanisms (Evans and Guggenheim, 1988), but these are not in deposits at a mineable scale.

Willow Creek Mine

There have been recent claims in civil litigation that asbestiform tremolite, chrysotile, and anthophyllite have been found in this deposit and represent the mineralogy of the ores once mined here. Although this deposit is no longer a source for commercial talc, these claims have serious consequences for the entire talc-producing region. Also, Cyprus Mines Corporation reported occurrences of fibrous tremolite down dip from the former pit (Weeks, 1984); however, as is common, the authors of this study did not define fibrous. Recall during this time period an amphibole was considered a fiber if it met the 3:1 (length: width) counting criteria, regardless of its morphology. As pointed out in Gunter et al. (2016), OSHA clarified their definition to not include cleavage fragments, which would often meet this counting criteria. Also, as pointed out in Gunter et al. (2016) a countable fiber pre-1992 often was used synonymously to mean asbestos or asbestiform, or fibrous. We would like to address the occurrences of the abovementioned minerals, and give context for the importance of where these minerals occur. But before we provide our research, it is worth pointing out that to our knowledge in the published literature there are no reports of asbestos minerals occurring in talc formed in southwestern Montana in general or at Willow Creek specifically. In fact both Berg (1979) and Van Gosen et al. (2004) point out the former, while Berg (1979) points out the latter as well.

Asbestos content

The purity of a talc deposit is unique to the mechanism and composition of geologic materials from which it formed. For example talc mined from metamorphosed carbonate deposits can contain significant amounts of amphiboles. The regulatory definition of asbestos in the Code of Federal Regulations is, “chrysotile, amosite, crocidolite, tremolite asbestos, anthophyllite asbestos, actinolite asbestos, and any of these minerals that have been chemically treated and/or altered” (29CFR§1910.1001(b)). Although the word asbestos is used in the legal definition, “tremolite asbestos” is tremolite that displays a fibrous, or hair-like habit, the same goes for the other five asbestos minerals. These minerals are not regulated when they do not occur in a fibrous habit. Asbestos is a commercial term for minerals that have a fibrous morphology, high tensile strength, flexibility, are heat resistant, and most importantly lengthwise separable into fibers. These minerals are of concern in talc products because they are known to form in some economic talc deposits. However the question remains whether these amphiboles are truly asbestiform or are cleavage fragments; this distinction can be difficult once the products have been processed.

Tremolite ($Ca_2Mg_5Si_8O_{22}(OH)_2$) and anthophyllite ($Mg_7Si_8O_{22}(OH)_2$) are expected to be the most likely of the amphibole varieties to occur in talc deposits because of their composition. Although, recall from Chapter 1 that anthophyllite was not found in any of the commercial talc samples we analyzed. The deposits that do contain amphiboles in greater than trace concentrations have been formed by contact or regional metamorphism, at higher temperatures (>400°C) and/or higher pressures than what was required to form talc in a predominantly metasomatic zone (Van Gosen et al., 2004). An example of this would be the deposits in upstate/central New York that produced ores containing significant amounts of tremolite and anthophyllite. These deposits formed from regional metamorphism accompanied shortly after by related hydrothermal alteration (Chidester et al., 1964**).** Fluids are involved in nearly all metamorphic reactions, but unlike the deposits in New York, the deposits in southwest Montana have undergone extensive hydrothermal alteration. The tremolite identified in the deposit at Willow Creek is located in dolomitic and calcitic marbles, and not in the talc ore. These rocks do not represent M_3 mineral assemblages

associated with talc ores. Of the sixteen drill holes in the 1979-1984 study, only one was representative of talc ore, and it contained trace amounts of tremolite. Berg's (1979) observations of tremolite were limited to the marbles, and were not associated with the massive talc-body, which generally agrees with the results of the mine report. The presence of tremolite may serve as an indicator for the edge of the metasomatic zone at Willow Creek for three reasons: 1) tremolite is not stable in the temperature ranges estimated for the M_3 event, 2) the metasomatic fluids resulted in rocks with a much higher Si/Mg ratio, and lower Ca than what is suitable for tremolite to form, or 3) because the drill rig used re-circulated water, it can be difficult to determine the exact depth in the hole where a mineral was encountered.

The non-amphibole variety of asbestos, chrysotile ($Mg_3Si_2O_5(OH)_4$) is a serpentine-group mineral. There are three Mg-serpentine-group minerals, but chrysotile is the only one that is regulated. Serpentine is often seen replacing forsterite in metamorphic rocks, creating the classic mesh texture. Anderson et al. (1990) pointed this out in their petrographic descriptions of the high-grade marbles, which has an assemblage of minerals that reflect amphibolite-grade metamorphism. This reaction is not preserved in the massive talc bodies because of the high Si:Mg ratio introduced by the pervasive altering fluids, and the lower temperatures required to stabilize talc. The serpentine that has been found in association with the talc deposits in this region has not been found in the massive talc body, and therefore, regardless of morphology, has no commercial pathway that would be a concern for human exposure. We are not claiming that chrysotile, or another serpentine-group mineral does not occur anywhere in the altered Cherry Creek rocks, in fact Berg (1979) reported chrysotile at Willow Creek, but in the country rocks and not in the mineable talc ore.

Sepiolite ($Mg_8Si_{12}O_{30}(OH)_4(H_2O)_{12}$), is a sheet silicate that has been identified at the Willow Creek Mine by Berg (1979) and by us, but has never warranted much attention until recently. It occurs in a fibrous habit, and some samples have a waxy, plastic-like appearance that could easily be mistaken for an asbestos variety without close observation and the application of appropriate analytical methods. For example, energy-dispersive spectroscopy

(EDS), a commonly used semi-quantitative compositional technique yields, element concentrations as the area under peaks (often simplified to peak height). The Mg/Si ratio in anthophyllite is 7/8 and sepiolite is 2/3, making the two difficult to confidently distinguish based on EDS because the relative Mg and Si peak heights will be similar for these two minerals. Therefore it is important to obtain EDS spectra for sufficient count times so that the intensity of peaks are on the order of 1000s, not 100 counts, and even that might not be sufficient to distinguish minerals of such similar composition such as sepiolite, serpentine, and anthophyllite. However, the more precise WDS data can be used to accomplish this. Structurally sepiolite and anthophyllite are distinct, but both have a 5.3 Å repeat (along the polymerized chains of silicon tetrahedra from which they form- double chains for anthophyllite and triple chains for sepiolite), so SAED patterns, and grain orientation can also lead to misidentifying these phases. Claims of sepiolite and chrysotile in bundles together bring up the same consideration. Because the two are both sheet silicates (like talc) they have the structural similarity of ~5.3 Å repeat along the a-axis. This could make the two difficult to distinguish without other crystallographic identifiers.

Samples and mines

The samples at the focus of this paper are talc-rich, commercial grade rocks. The Willow Creek Mine and Beaverhead Mine, last operated by Cyprus Industrial Minerals are no longer actively mined. The mine site at Willow Creek has been reclaimed, but representative talc samples were collected in the area of the former, now a collapsed pit (WC_1a and WC_8). The sample from the Beaverhead Mine (BH) was a split that was provided by Richard Berg. Samples from the Yellowstone Mine, operated by Imerys include a low-grade (YE_low) and high-grade ore (YE_high). The Treasure and Regal Mines, operated by Barretts Minerals Inc., a subsidiary of Minerals Technologies Inc., are also currently operating. The samples from these two mines range in quality from float (TR_float) to high-grade ores (Tr_G1, RE).

Methods

Eight samples will be discussed in this paper. All were prepared for electron probe micro-analysis and for powder x-ray diffraction. Five were prepared for x-ray fluorescence spectrometry.

Powder XRD

Approximately four grams of each talc sample were ground with a mortar and pestle until fragments were ~2mm in diameter. Samples were then ground in a polyethelene canister with corundum milling beads using a McCrone micronizing mill for 12 minutes with 95% ethanol. The slurry was rinsed into a glass dish and the powdered contents were scratched from the glass dish after the ethanol evaporated. We prepared backfilled powder mounts and analyzed samples with the Siemens D5000 powder x-ray diffractometer at the University of Idaho from 2°-52°, for 20 seconds for each step of 0.020°, with Cu kα radiation. Phases were identified using the EVA software and accompanying database. The same powders were used for bulk x-ray fluorescence (XRF) analyses.

Bulk XRF

The powdered samples were used to make fused glass beads for bulk XRF analyses using the ThermoARL X-ray fluorescence spectrometer at Washington State University's GeoAnalytial Laboratory. Each bead required 2.0-3.5 grams of powdered sample, along with a powdered Li-tetraborate flux; a sample-to-flux ratio of 1:2 was required. The sample and flux were weighed and combined in a plastic mixing jar, and were thoroughly mixed. The contents of the jar were poured into a graphite crucible which was put on a silica slab and placed in a furnace with an internal temperature of 1000 °C. After the crucible contents melted the slab was removed from the furnace, the samples were allowed to cool into fused glass beads and were removed from the crucibles. Samples were ground in a tungsten-carbide mill and re-fused into homogenous glass beads. The procedure we followed is detailed in Johnson et al. (1999).

EPMA

Individual mineral grains were analyzed in polished grain mounts by the JEOL JXA-8500f field emission electron microprobe at Washington State University. The polished grain mounts were prepared by Burnham Petrographics from Rathdrum, Idaho; four ~1cm wide samples were mounted on one standard sized thin section slide. The slides were inspected using a polarized light microscope, and reference targets were marked on the thin sections with a fine-point felt pen. This is the dark rim in many of the BSE and XPL images. The electron beam was set to 20kV accelerating voltage and 30nA beam current. Samples were analyzed with a 5µm beam and standards were analyzed with a 10µm beam. BSE images were collected for all targets and are shown in Figures 6-13.

Results and discussion

Powder XRD

Figure 5A (Yellowstone and Willow Creek Mines) and 5B (Ruby Range Mines) include powder x-ray diffraction spectra for eight samples. Predominant peaks for clinochlore and talc are labeled. Only talc was detected in the high- and low-grade ores from the Yellowstone Mine. Willow Creek_1a is mostly talc but does have a detectable amount of clinochlore in it. Only talc was detected in sample 8 from Willow Creek. The four samples from the Ruby Range are predominantly talc as well, with only a trace amount of clinochlore detected in the samples from the Regal and the Beaverhead Mines. Most of these samples were obtained with the idea that they were ore quality, so these results were expected. Sample 1a from Willow Creek might not be the best representation of a high-grade ore from this deposit, although it is difficult to say since the mine is no longer operating. No amphiboles or serpentine-group minerals were detected in these samples via powder XRD.

Bulk XRF

Bulk XRF results are presented as major and minor rock-forming oxides in Table 1. A rock entirely composed of talc would have 63.37 weight percent SiO_2 and 31.88 weight percent MgO. In general, the results for these five samples show small deviations from pure

talc. The values for Al_2O_3 in all the samples relate to the clinochlore content in the sample. Aluminum may substitute for Si in Si-deficient environments, but we know the talc-forming fluids were Si-rich so this scenario does not apply. Clinochlore, represented as $Mg_5Al(AlSi_3)O_{10}(OH)_8$, also may be responsible for the higher loss on ignition (LOI) values. The LOI values indicate the weight percent of the sample that was volatized during sample preparation in the furnace; in the case of talc and clinochlore, the samples de-hydroxylated. The FeO detected represents ferric and ferrous iron combined, and is present in all samples from 1.26-2.79 weight percent. These values are not unusual in talc, which can have minor substitutions of Fe in the octahedral site for Mg. The rest of the oxides are present in negligible concentrations and do not indicate the presence of any other phases.

The trace element concentrations, reported in ppm, are included in Table 2. Trace elements are often helpful in determining provenance or understanding geologic processes. Due to the intense hydrothermal alteration of these rocks, it is likely that trace element concentrations would be more representative of the process rather than the protolith. It is worth noting that the data for the five samples are relatively uniform. This may not be surprising for samples from the same mine, but values do not vary between samples from different ranges, suggesting that the same process controlled the trace element concentrations within these deposits.

EPMA

Figures 6-13 are BSE and XPL images of the points that were analyzed by the electron microprobe. The ink circles have 2-3mm diameters, and a 100µm scale-bar is in each BSE image. In all sets of photos, the BSE images are on the top and XPL images are on the bottom. Yellow triangles indicate sampling points for talc and blue squares indicate analyses for clinochlore. The average atomic number of each phase is related to the shade of gray in the BSE images. Minerals with a higher average atomic number are lighter in the images. This is helpful in distinguishing clinochlore from talc in the sample from the Beaverhead Mine (Figure 13). One calcite grain was analyzed, indicated by the red dot in Figure 13, but the data for that point are not included in this paper. Some of the images have minute

differences in shades of gray, which is a result from an uneven polish on the talc due to its softness.

The compositional data from EPMA are compiled in Table 3. Corresponding atoms per formula unit (APFU) values are listed in Table 4**.** APFU values indicate that all the talc analyzed has near end-member compositions. The low values for Al_2O_3 compared with the XRF values indicate that the Al is definitely in the clinochlore, and not substituting for Si in talc. The FeO in the talc correlates fairly well with the bulk XRF data for FeO, indicating that all the Fe is in the talc, substituting for Mg^{2+}. The clinochlore data from the Beaverhead Mine also indicate a near end-member composition. Similar to the talc, trace amounts of Fe are substituting for Mg^{2+}. We were not expecting Fe to be present in detectable quantities in this talc because of its carbonate origin. Potential sources for Fe in the talc and clinochlore may be from adjacent rocks (similar to how the gneiss provided Si, the Fe from biotite may have been released during the influx of Mg during M_2), or the initial limestone. Before M_1, the protolith may have contained some clays, which would have provided Fe and Al for the chlorite inclusions as well.

These samples are coarse to very fine grained, have irregularly shaped grains, and lack of foliation. The samples from the Beaverhead, Regal, Treasure, and Willow Creek mines (Figures 6, 7, 10-13) have a random distribution of medium to very fine- grained talc. The samples from the Yellowstone Mine (Figures 8 and 9) are both very fine-grained. These differences may be due to the textures present in the high-grade marbles that have been preserved despite the thorough talc mineralization. The samples from the Willow Creek Mine are texturally distinct in that there are halos of very fine talc that are relatively optically continuous (sections of each halo go extinct together). Although these rocks have endured multiple stages of alteration, this texture suggests talc pseudomorphs after olivine porphyroblasts from the high-grade marbles formed during M_1. This is best seen in Figure 7, and is common throughout the rest of the thin section. However, no olivine remnants were found in this grain mount; again this is evidence of complete replacement of the preexisting rock to form talc.

Plaintiff's expert's samples

We also analyzed samples collected by the aforementioned expert witness for the plaintiffs involved in Cashmere Bouquet litigation. Many of these samples were not within the mined area, and do not represent ores from the Willow Creek deposit. We did identify tremolite based on electron microprobe data in sample WC_SF_N9A, along with clinochlore, serpentine, dolomite, calcite, and minor talc. The tremolite does not appear to be fibrous. Back-scattered electron images of these sections of the rock are in Figures 14-16. The traces of talc in this sample are always in contact with tremolite(shown in Figures 14 and 15), suggesting the talc has formed after the amphibole, which has been documented in the unaltered amphibolite-grade marbles (Berg, 1979). The texture and mineral assemblage of this sample indicates that is has not been hydrothermally altered and likely represents M_1. We did not find calcite or dolomite in any of the ore-grade samples from Montana yet the two phases are abundant in this sample. The serpentine in this sample formed at the edges of clinochlore and appears to be a sheet-like pseudomorph after it (Figure 16). The talc in this sample has 0.14 APFU Fe. The sepiolite from this area is the only mineral that, without a doubt, has a fibrous morphology; a BSE image of sample WC_sep in Figure 17 shows this. We did not find any anthophyllite in the samples from this expert witness, or in the samples that we collected. The plaintiff's expert's samples were collected with the purpose of being used as evidence to show that the talc ores from this mine contain asbestos. It may seem obvious to a mineralogist or petrologist that these samples are not in any way representative of talc ores. However, this is not as obvious to a jury that has the responsibility of deciding whether Colgate-Palmolive is liable for asbestos related diseases, related costs, or possibly punitive damages. This system encourages advocacy and, although it procedurally does not set precedent, it likely does influence the outcome of other civil litigation through popular press articles linking talc and asbestos.

Conclusions

Microprobe data easily differentiate sepiolite from talc or serpentine group minerals, while EDS data may limit the confidence with which these minerals can be distinguished.

We conclude that commercial talc from southwest Montana is pure in that it is nearly monomineralic, and there are very low concentrations of trace elements. Our samples from the Yellowstone, Regal, and Beaverhead mines have low Fe content (≤0.07 APFU) while the samples from Willow Creek and Treasure mine have both low-Fe talc and higher Fe-talc (up to 0.20 APFU Fe). The talc associated with tremolite at Willow Creek has 0.14 APFU Fe. Other than the variations in iron the talc from Montana represents near-end member compositions. Although the deposits can be as far as 60 miles from each other, they share the same geologic history. The occurrences of tremolite in close proximity to the mineable bodies represent higher-grade metamorphic conditions, and do not represent the mineralogy produced by M_3.

Acknowledgements

We would like to thank Richard Berg, Imerys Talc, and Barretts Minerals for providing samples for this project; Sandra Underwood, John Childs, Chad Walby, Helen Lynn, Zachary Wall, Mike Cerino and Ericka Bartlett for organizing a very informative GSA field trip to the Regal and Yellowstone Mines; Cody Steven for help with sample preparation; and Owen Neil and Rick Conrey for their help with analyzing these samples.

Disclosure

M.E. Gunter is currently working with past and current producers of talc, and has served as an expert witness for their defense; however, no funds or input from any source was directly used for the preparation of this manuscript.

References

Anderson, Dale L., Mogk, David W., and Childs, J.F. (1990) Petrogenesis and Timing of Talc Formation in the Ruby Range, Southwestern Montana, Economic Geology, Vol. 85, pp. 585-600.

Berg, Richard B. (1979) Talc and chlorite deposits in Montana, Montana Bureau of Mines and Geology, Memoir 45.

Brady, J.B., Cheny, J.T., Rhodes, A.L., Vasquez, A., Green, C., Duvall, M., Kogut, A., Kaufman, L., and Kovaric, D. (1998) Isotope geochemistry of Proterozoic talc occurrences in Archean marbles of the Ruby Range Mountains, southwest Montana, U.S.A. Geological Materials Research Vol.1, n.2, pp. 1-41.

Cerino, M.T., Childs, J.F., and Berg, R. (2007) Talc in southwestern Montana, Northwest Geology, Vol. 36, pp. 9-22.

Chidester, A. H., Engel, A. E. J., and Wright, L.A. (1964) Talc Resources of the United States, Geological Survey Bulletin 1167.

Code of Federal Regulations, 29CFR§1910.1001(b).

Dahl, Peter S. (1979) Comparative geothermometry based on major-element and oxygen isotope distributions in Precambrian metamorphic rocks from southwestern Montana, American Mineralogist, Vol. 64, pp. 1280-1293.

Gammons, C.H. and Matt, D.O (2002) Using fluid inclusions to help unravel the origin of hydrothermal talc deposits in southwest Montana, Northwest Geology, Vol. 31, pp. 44-55.

Giletti, B.J. (1966) Isotopic ages from southwestern Montana, Journal of Geophysical Research", Vol. 71, Issue 16, pp. 4029-4036.

Gunter, M.E., Buzon, M.E., and McNamee, B.D. (2016) Current issues with purported "asbestos" content of talc: Part 1, Introduction and examples in metamorphic and ultramafc hosted talc ores.

James, H.L. and Hedge, C.E. (1980) Age of basement of southwestern Montana, Geological Society of America Bulletin, Vol. 91, pt. 1, pp. 1-11.

Johnson, D.M., Hooper, P.R., and Conrey, R.M. (1999) Analysis of Rocks and Minerals for Major and Trace Elements on a Single Low Dilution Li-tetraborate Fused Bead, Advances in X-ray Analysis, Vol. 41, pp. 838-876.

Levin, Myron (2015) Colgate-Palmolive suffers courtroom loss in asbestos-talc powder case. Fair Warning Reports. April 29, 2015,

McCarthy, E.F., Genco, N.A., and Reade, E.H. Jr. (2006) Talc: Ch. in, Industrial Minerals and Rocks, 7th Ed., pp. 971-986.

Moine, B., Fortune, J., Moreau, P., and Viguier, F. (1989) Comparative mineralogy, geochemistry and conditions of formation of two metasomatic talc and chlorite deposits: Trimouns (Pyrenees, France) and Rabenwald (Eastern Alps, Austria), Economic Geology, Vol. 84, pp. 1398-1416.

Tornos, Fernando and Spiro, Baruch F. (2000) The geology and isotope geochemistry of the talc deposits of Puebla de Lillo (Cantabrian Zone, Northern Spain) Economic Geology, Vol. 95, pp. 1277-1296.

Underwood, S.J., Childs, J.F., Walby, C.P., Lynn, H.B., Wall, Z.S., Cerino, M.T. and Bartlett, E. (2014) The Yellowstone and Regal talc mines and their geologic setting in southwestern Montana, Geologic Society of America Field Guides, 37: pp. 161-187.

Van Gosen, B.S., Lowers, H.A., Sutley, S.J., and Gent, C.A. (2004) Using the geologic setting of talc deposits as an indicator of amphibole asbestos content, Environmental Geology, Vol. 45, pp. 920-939.

Virta, Robert L., (2015) Talc and Pyrophyllite, Mineral Commodity Summaries, pp 158-159.
Weeks, R.L., 1984, Willow Creek Mine Evaluation.

Zharikov, V.A., Pertsev, N.N., Rusinov, V.L., Callegari, E., and Fettes, D.J. (2007) A systematic nomenclature for metamorphic rocks 9: Metasomatism and metasomatic rocks, Recommendation by the IUGS Subcommission on the Systematics of Metamorphic Rocks, web version of 01.01.07.

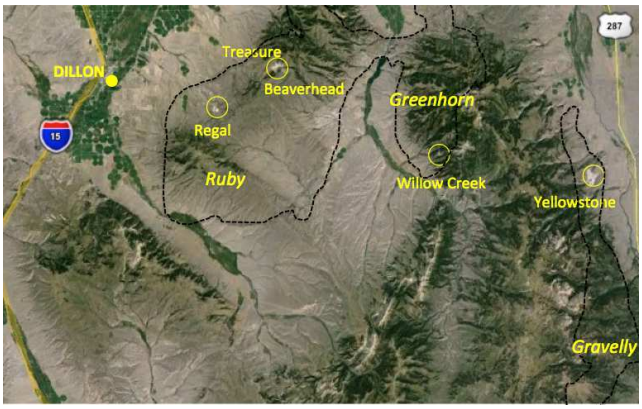

Figure 1. The five mine locations are labeled on the Google Earth image of Madison County, Montana. The width of the image is approximately 57 miles. Dashed lines based on Dahl (1979) indicate Precambrian rocks. The Beaverhead, Treasure and Regal Mines are in the Ruby Range. The Beaverhead and Treasure Mines are adjacent, and are located in the same circle in this diagram. Beaverhead is to the southeast of Treasure. The Willow Creek and Yellowstone Mines are located in the Greenhorn and Gravelly Ranges, respectively.

Figure 2. The rhombohedral cleavage is still dominant in this talc sample collected in the Treasure Mine (Ruby Range). The scale on the pencil is in cm.

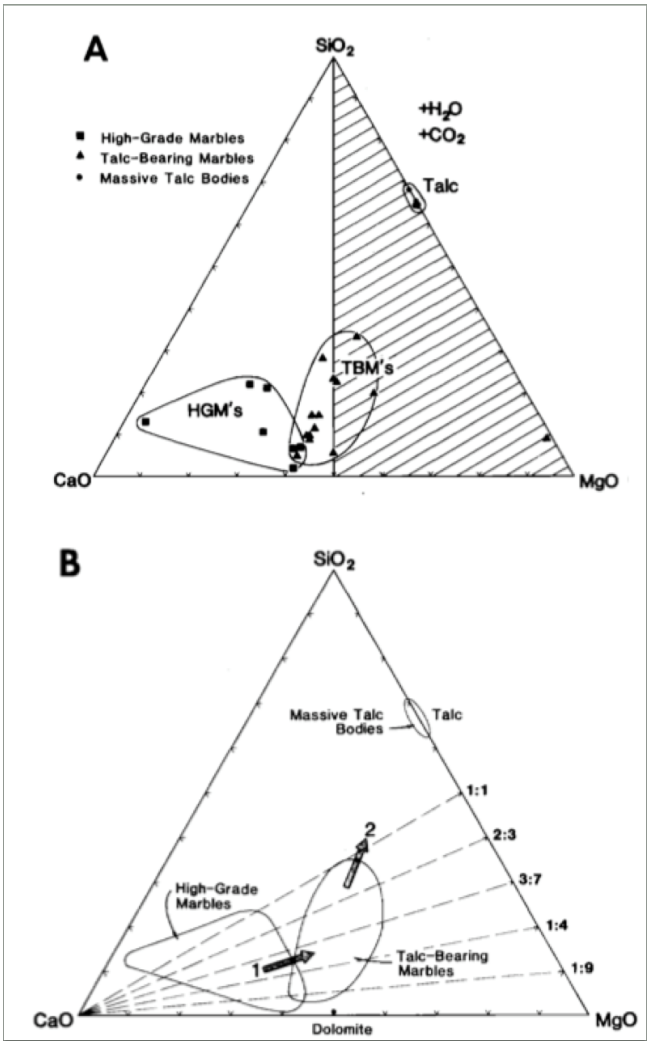

Figures 3A-3B. (Figure 11 from Anderson et al., 1990) A: High-grade marbles (HGM), talc-bearing marbles (TBM) and massive talc bodies (talc) plotted in the CaO-MgO-SiO_2 ternary diagram based on bulk XRF analyses (Table 2 in Anderson et al., 1990). There is little overlap between fields. B: Arrow 1 follows the compositional trend from HGM to TBM, increase in MgO/CaO. Arrow 2 follows compositional trend from TBM-talc, increase in SiO_2/MgO.

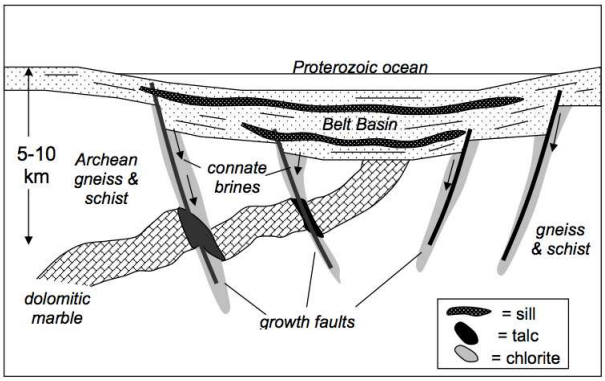

Figure 4. (Gammons and Matt, 2002, Figure 6) Schematic of talc-forming mechanism.

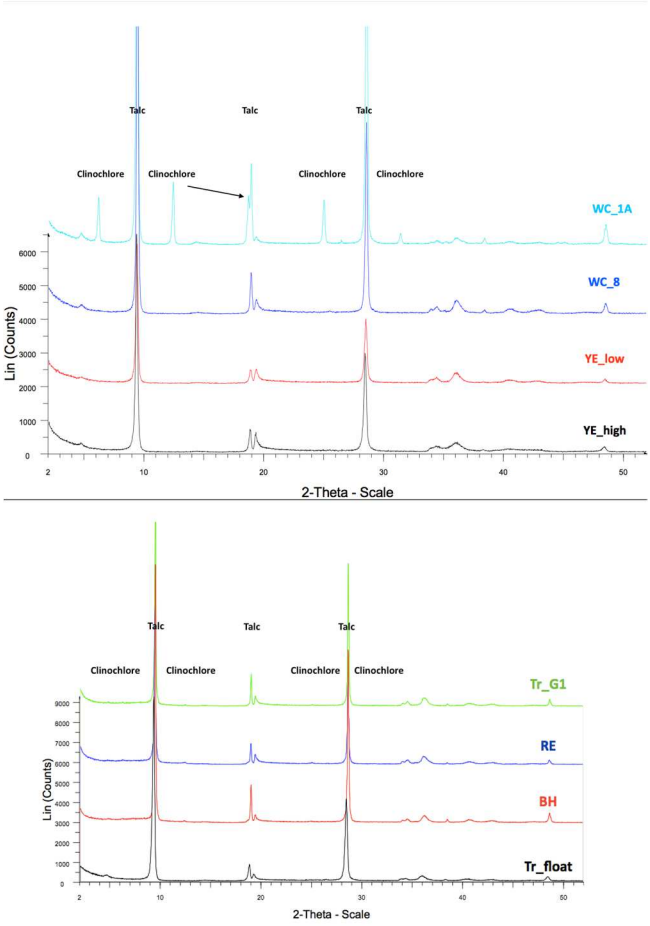

Figure 5A(top): Powder XRD spectra for samples from the Yellowstone and Willow Creek Mines
Figure 5B(bottom): Powder XRD spectra for samples from Regal, Beaverhead and Treasure Mines.

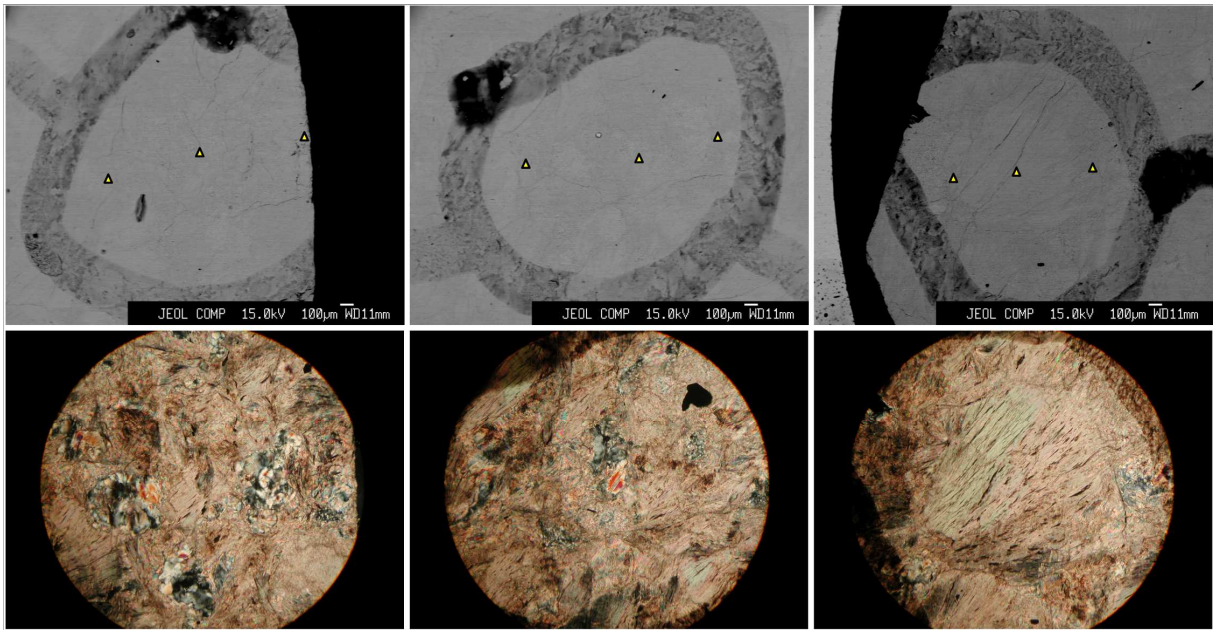

Figure 6. BSE (top) and XPL (bottom) images for WC_1a. Note the variability in grain sizes. The iron content on the talc from this sample varies from 0.05-0.13 APFU.

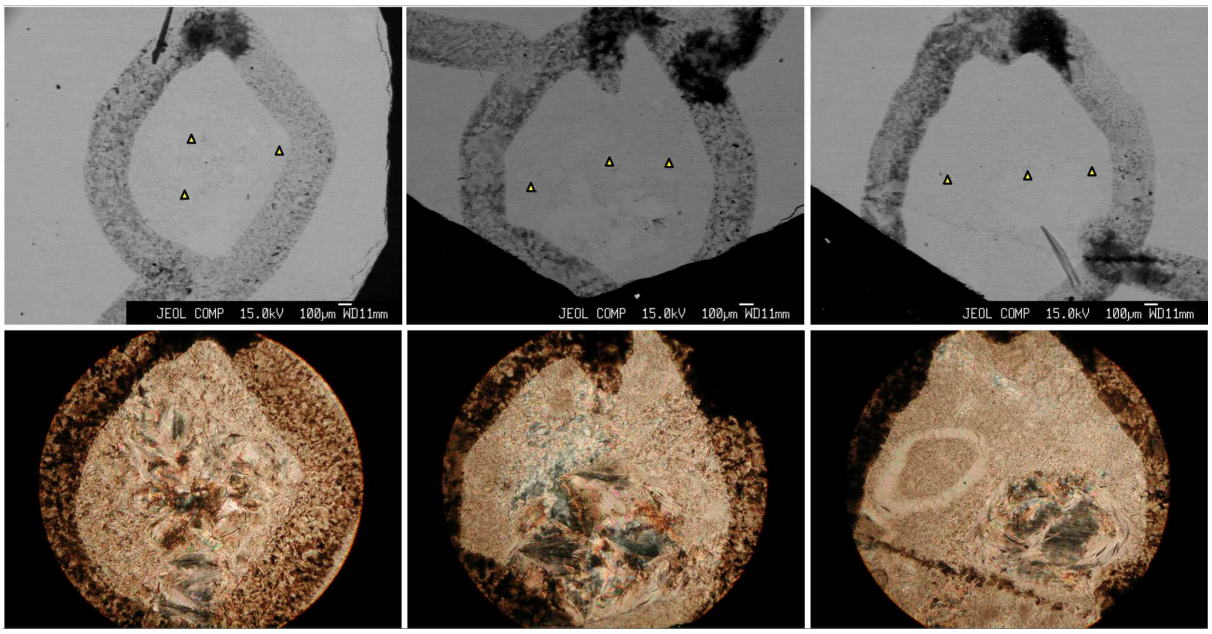

Figure 7. BSE (top) and XPL (bottom) images for WC_8. Note the variability in grain sizes and the talc halo. The iron content in this sample varies from 0.06-.12 APFU Fe.

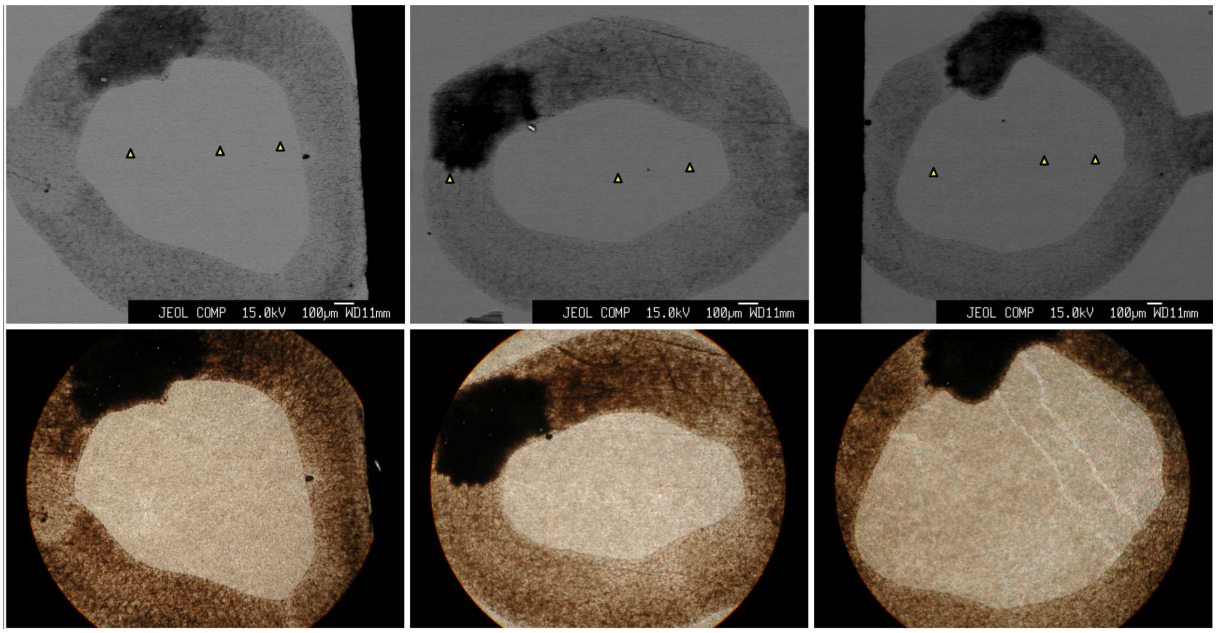

Figure 8. BSE (top) and XPL (bottom) images for YE_high. Note the very fine and uniform grain sizes. All of the talc analyzed in this sample has 0.06 APFU Fe.

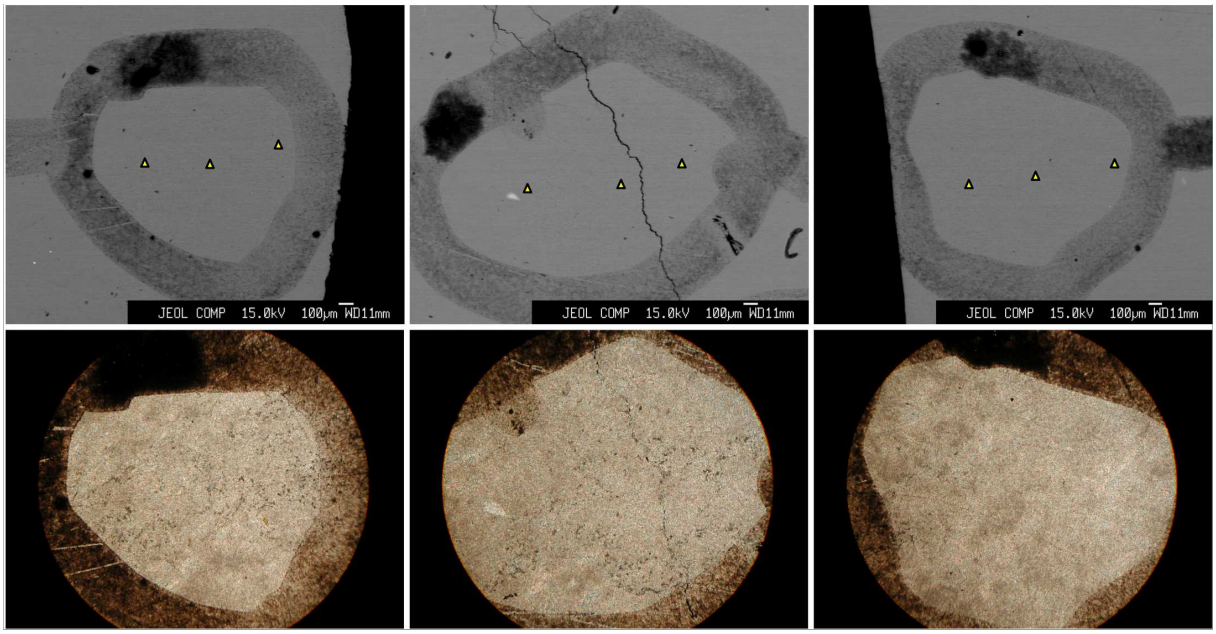

Figure 9. BSE (top) and XPL (bottom) images for YE_low. Note the very fine and uniform grain sizes. All the talc analyzed in this sample has 0.07 APFU Fe.

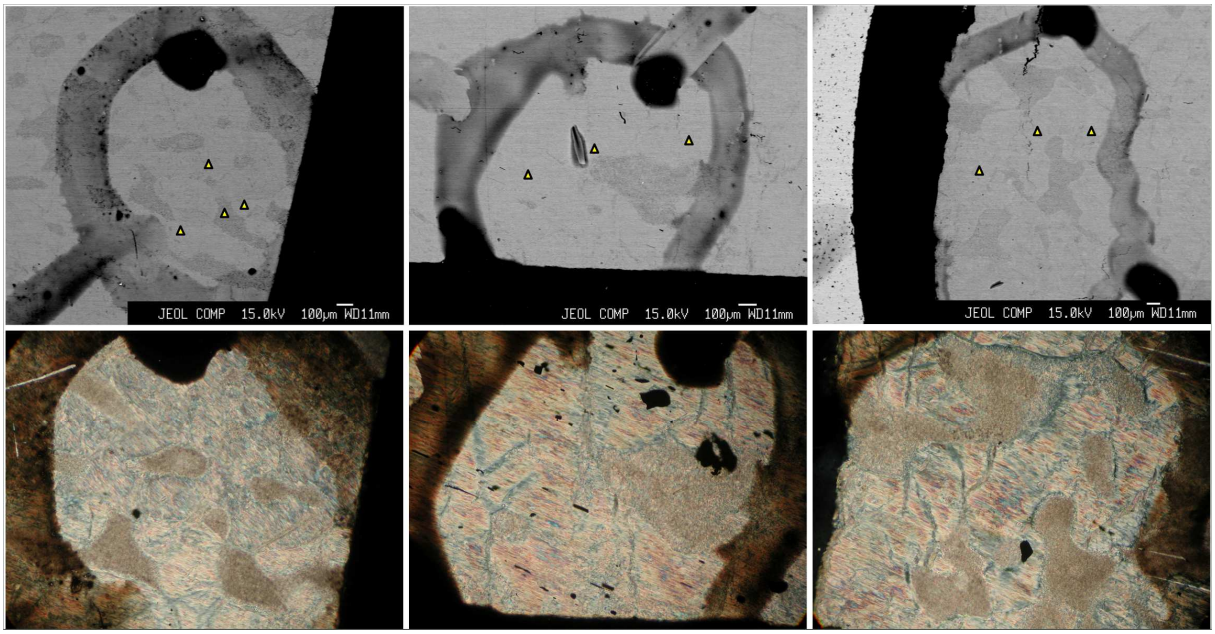

Figure 10. BSE (top) and XPL (bottom) images for TR_float. This sample has high iron content with Fe APFU ranging from 0.11-0.20.

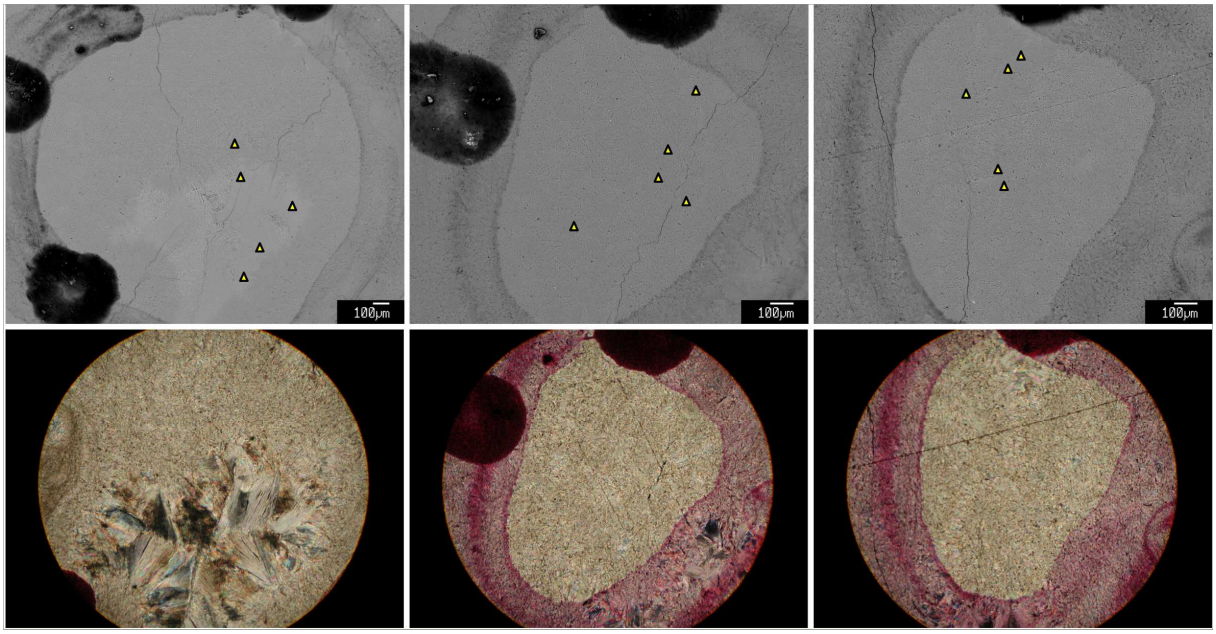

Figure 11. BSE (top) and XPL (bottom) images for TR_G1. The talc in target 1 (far left) has high iron content, with 0.12 APFU Fe. The second and third targets contain talc with 0.01-0.03 APFU Fe.

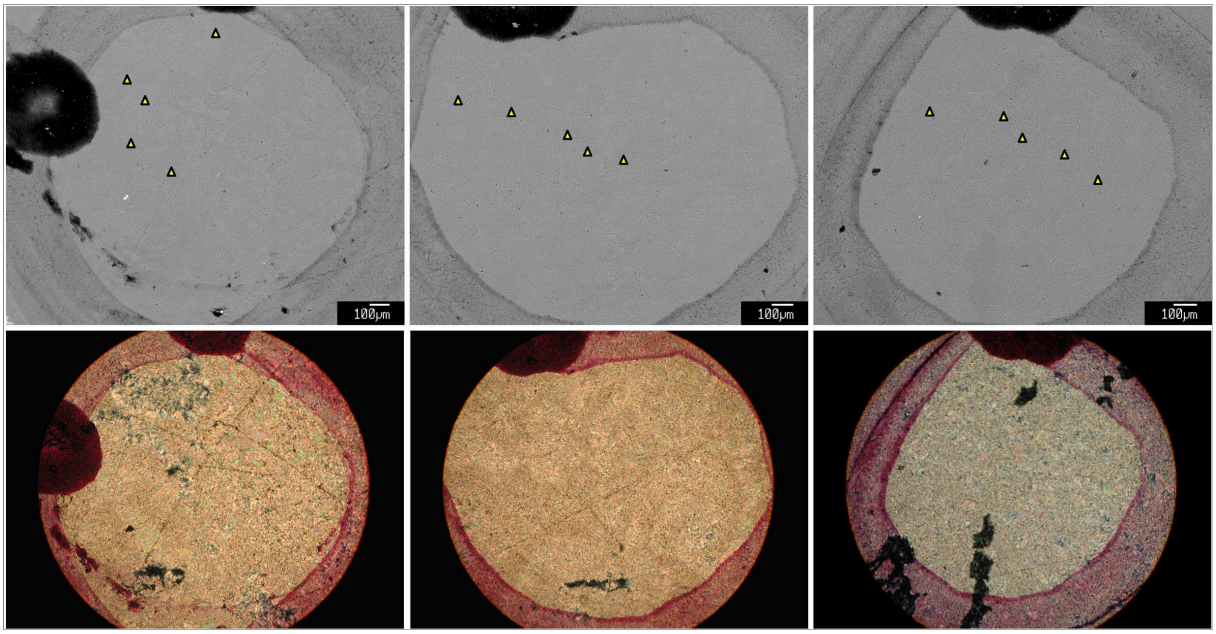

Figure 12. BSE (top) and XPL (bottom) images for RE. All of the analyses for this sample show that the Fe content is between 0.02-0.04 APFU.

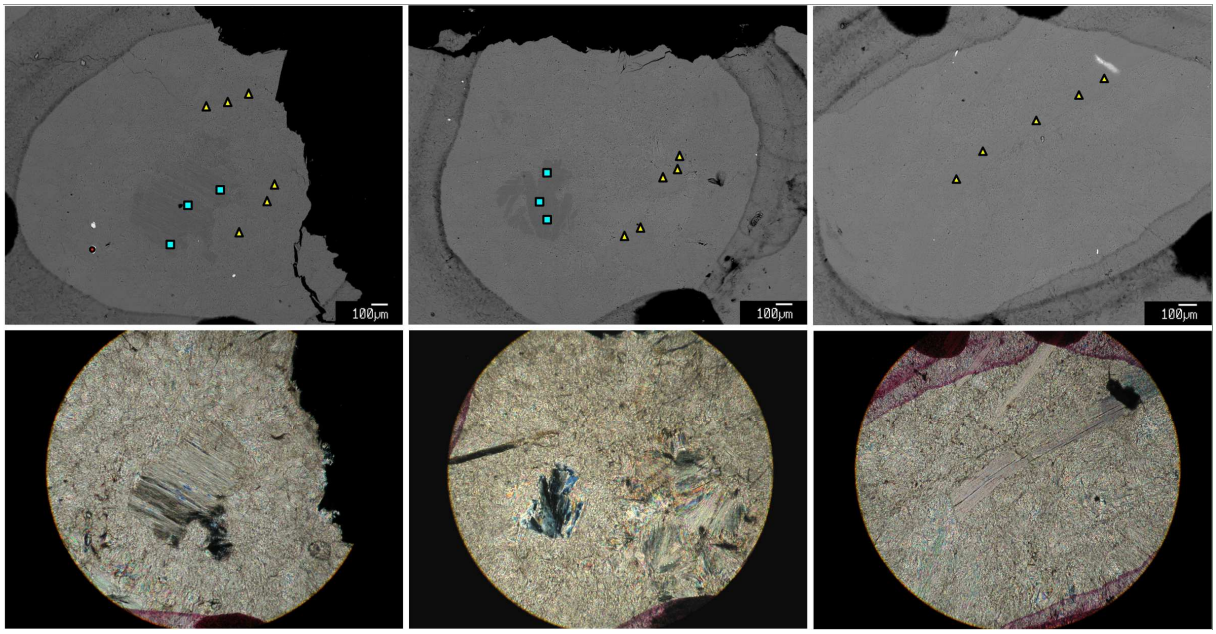

Figure 13. BSE (top) and XPL (bottom) images for BH. There are two populations of talc among the Montana samples. The talc in the first and third targets (far left and far right) has 0.01 APFU Fe, the talc in the second target has 0.06 APFU Fe.

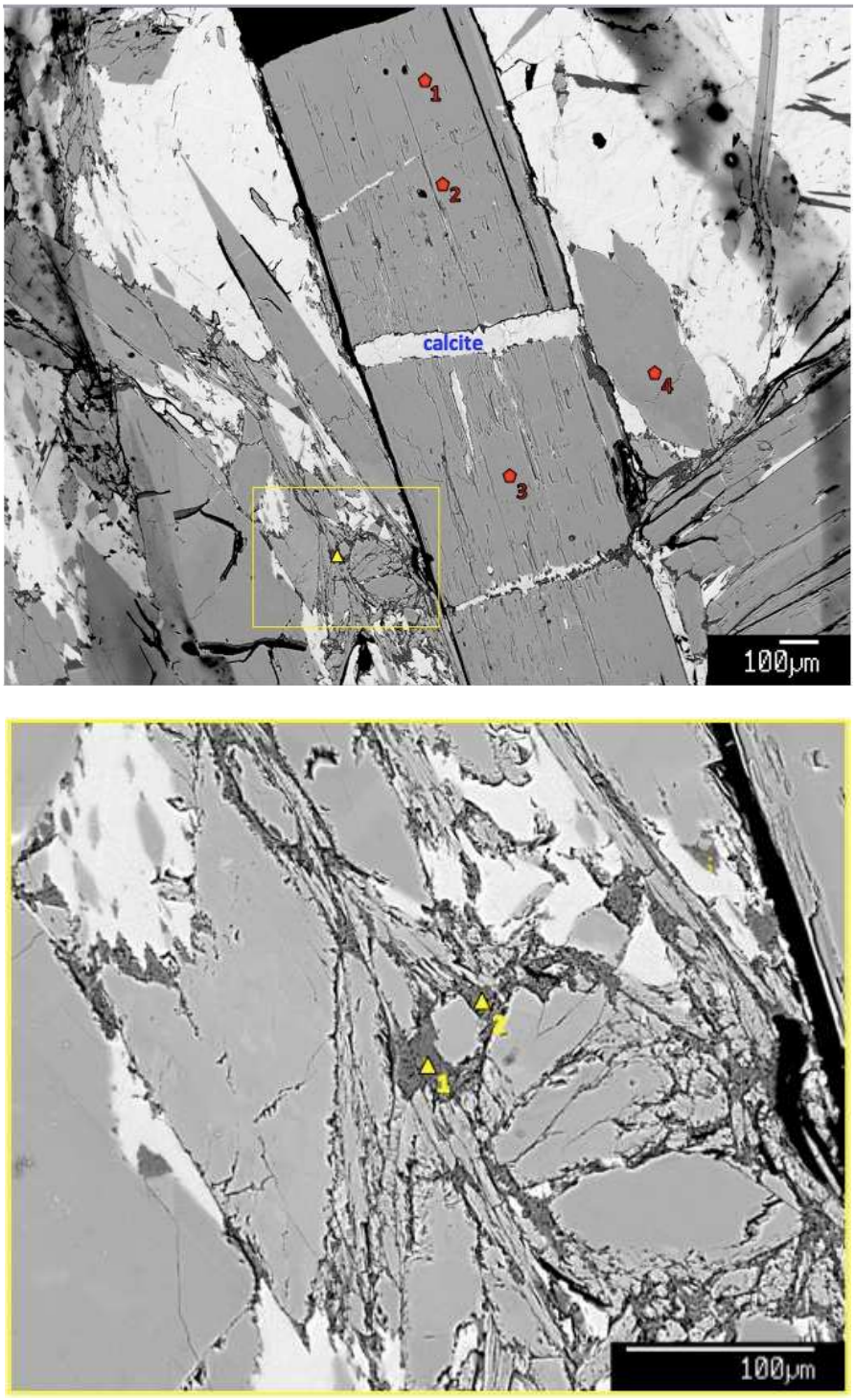

Figure 14: BSE images of SF_WC_N9A showing calcite and analysis points for tremolite (red pentagons) and talc (yellow triangles). Note that talc is not a major phase. Bottom image is a BSE image of the area in the yellow box in the top image.

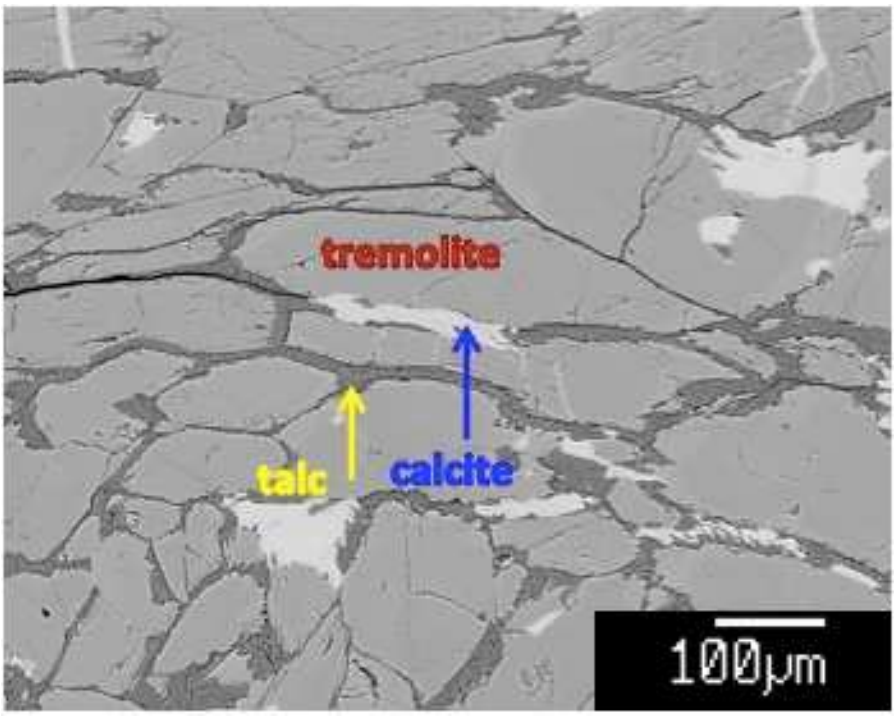

Figure 15: BSE image of WC_SF_N9A showing tremolite, calcite and talc. This sample does not represent a hydrothermally altered rock, and certainly does not represent an ore from this region.

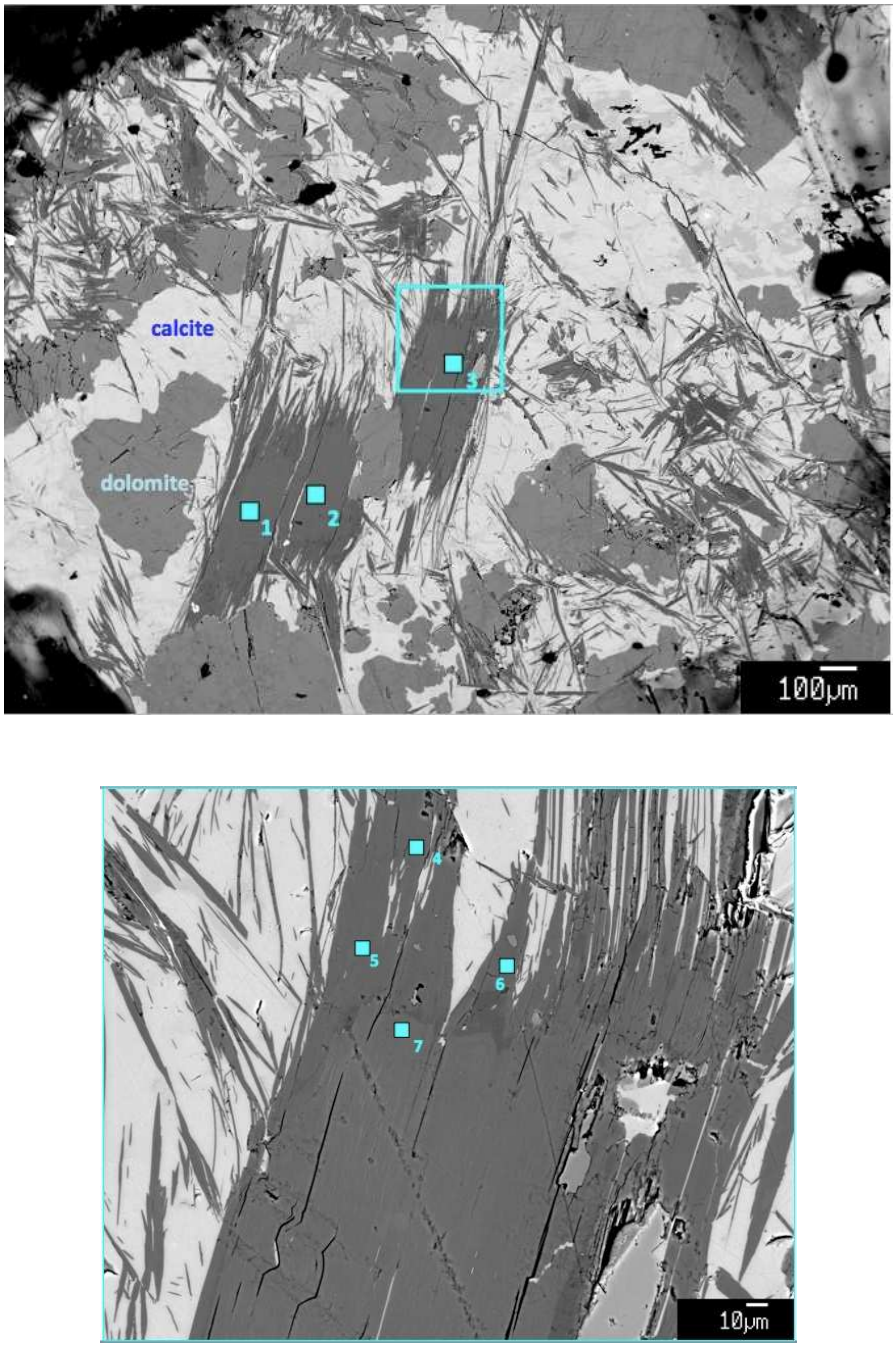

Figure 16: BSE image of chlorite/serpentine (blue boxes), calcite, and dolomite in sample WC_SF_N9A. This sample shows no signs of hydrothermal alteration. Bottom image is a BSE image of the blue box around point 3 at higher magnification.

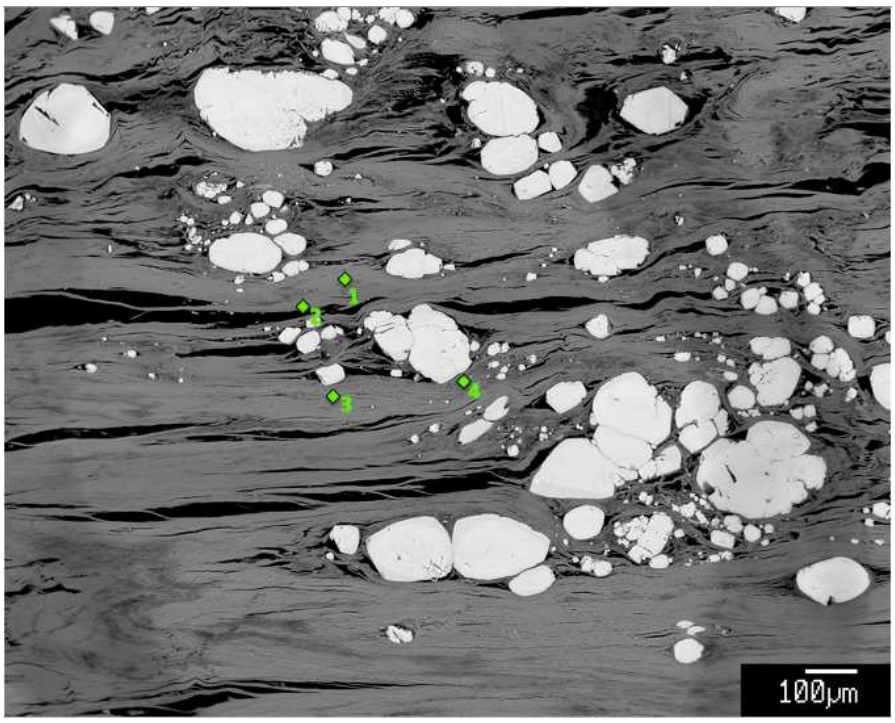

Figure 17: BSE image and analysis points for sepiolite (green diamonds) in sample WC_Sep. The white grains are calcite. Note the fibrous morphology of the sepiolite.

Table 1: Bulk XRF major and minor oxide concentrations (weight percent). Note the low concentrations of CaO, indicating that tremolite, calcite, or dolomite are not present in significant concentrations. The Al_2O_3 concentrations are related to the weight percent clinochlore in the sample. FeO^* concentrations represent the iron content in the mineral talc rather than in other phases.

Sample Name	SO3 >/=	SiO2	TiO2	Al2O3	FeO*	MnO	MgO	CaO	Na2O	K2O	P2O5	Sum	LOI (%)
Ideal	0.00	63.37	0.00	0.00	0.00	0.00	31.88	0.00	0.00	0.00	0.00	95.25	4.75
WC_1A	0.00	56.28	0.01	3.53	2.79	0.02	29.83	0.01	0.01	0.01	0.00	92.50	8.12
WC_8	0.00	60.73	0.00	2.73	1.34	0.01	29.88	0.01	0.03	0.01	0.00	94.73	4.82
YE_high	0.00	62.03	0.02	1.20	1.26	0.00	30.54	0.01	0.02	0.00	0.00	95.09	4.70
YE_low	0.00	62.92	0.00	0.31	1.42	0.00	30.78	0.01	0.00	0.00	0.00	95.45	4.68
TR_float	0.00	61.47	0.011	1.17	2.79	0.09	29.51	0.02	0.05	0.01	0.006	95.13	4.92

Table 2: Bulk XRF trace element concentrations (ppm) showing consistency between talc samples across the three ranges.

Sample Name	Ni	Cr	Sc	V	Ba	Rb	Sr	Zr	Y	Nb	Ga	Cu	Zn	Pb	La	Ce	Th	Nd	U
WC_1A	25	18	2	11	24	0	1	6	3	3.1	5	5	21	6	2	2	0	0	0
WC_8	16	22	2	4	0	0	0	0	1	1.3	4	7	13	2	1	0	0	0	2
YE_high	19	10	2	3	4	0	0	4	3	3.8	1	4	12	4	1	1	0	0	0
YE_low	9	4	1	4	1	0	0	0	1	1.1	1	1	12	3	0	0	0	0	0
Tr_float	12	10	2	5	3	0	0	2	4	2.7	2	3	15	5	0	5	0	0	0

Table 3: EPMA results reported in weight percent oxides, for talc ores/ore-quality samples shown in Figures 6-13

Sample Name	SiO_2	Al_2O_3	TiO_2	ZnO	Cr_2O_3	FeO	NiO	MnO	MgO	CaO	Na_2O	K_2O	P2O5	F	Total
Ideal talc	63.37	0.00	0.00	0.00	0.00	0.00	0.00	0.00	31.88	0.00	0.00	0.00	0.00	0.00	95.25
WC_1a	62.24(70)	0.06(4)	0.01(1)	-	-	1.63(64)	-	0.01(1)	30.83(48)	0.02(2)	0.02(2)	0.01(2)	0.00(1)	0.19(5)	94.8(1.2)
WC_8a	62.47(56)	0.05(8)	0.00(1)	-	-	1.88(51)	-	0.01(1)	30.82(41)	0.01(1)	0.02(1)	0.01(1)	0.00(1)	0.15(2)	95.3(1.0)
YE_high	62.13(77)	0.14(1)	0.00(2)	-	-	1.09(3)	-	0.00(1)	30.93(50)	0.03(1)	0.03(1)	0.00(0)	0.01(1)	0.29(2)	94.4(1.3)
YE_low	62.66(54)	0.07(1)	0.01(1)	-	-	1.36(2)	-	bdl	31.08(32)	0.04(2)	0.00(0)	0.00(1)	0.00(1)	0.31(2)	95.20(84)
TR_float	61.87(36)	0.19(7)	0.01(1)	-	-	2.70(54)	-	0.05(4)	30.34(22)	0.03(2)	0.03(1)	0.01(1)	0.00(1)	0.20(6)	95.23(98)
TR_G1	62.06(45)	0.10(4)	0.00(0)	0.01(1)	0.00(1)	0.79(95)	0.00(0)	0.00(0)	30.32(68)	0.01(0)	0.02(1)	0.00(0)	-	0.16(8)	93.32(46)
RE	62.07(63)	0.21(5)	0.01(0)	0.00(1)	0.00(1)	0.52(13)	0.00(0)	0.00(1)	30.44(41)	0.02(1)	0.06(1)	0.00(0)	-	0.10(1)	93.33(72)
BH	62.18(53)	0.15(10)	0.00(0)	0.00(1)	0.00(0)	0.52(38)	0.00(1)	0.00(1)	30.36(31)	0.01(1)	0.02(1)	0.00(0)	-	0.11(2)	93.25(46)
Ideal chlorite	35.23	17.59	0.00	0.00	0.00	0.00	0.00	0.00	34.76	0.00	0.00	0.00	0.00	0.00	87.58
*BH	34.3(1.4)	12.19(21)	0.01(0)	0.00(1)	0.02(0)	2.19(16)	0.00(0)	0.03(0)	33.85(50)	0.07(3)	0.02(1)	0.00(0)	-	0.10(2)	82.7(1.1)

Table 4: EPMA results, converted to APFU values, for talc ores/ore-quality samples shown in Figures 6-13.

Sample Name	Si4+	Al3+	Ti4+	Zn2+	Cr3+	Fe2+	Ni2+	Mn2+	Mg2+	Ca2+	Na+	K+	P	F-	OH-	O	T
Ideal talc	4.00	0.00	0.00	0.00	0.00	0.00	0.00	0.00	3.00	0.00	0.00	0.00	0.00	0.00	2.00	3.00	4.00
WC_1a	3.98(0)	0.00(0)	0.00(0)	-	-	0.09(3)	-	0.00(0)	2.94(3)	0.00(0)	0.00(0)	0.00(0)	0.00(0)	0.04(1)	1.96(1)	3.03(1)	3.99(1)
WC_8a	3.98(1)	0.00(1)	0.00(0)	-	-	0.10(3)	-	0.00(0)	2.93(2)	0.00(0)	0.00(0)	0.00(0)	0.00(0)	0.03(0)	1.97(0)	3.03(2)	3.99(1)
YE_high	3.98(1)	0.01(0)	0.00(0)	-	-	0.06(0)	-	0.00(0)	2.96(1)	0.00(0)	0.00(0)	0.00(0)	0.00(0)	0.06(0)	1.94(0)	3.01(1)	3.99(0)
YE_low	3.99(0)	0.00(0)	0.00(0)	-	-	0.07(0)	-	0.00(0)	2.95(1)	0.00(0)	0.00(0)	0.00(0)	0.00(0)	0.06(0)	1.94(0)	3.02(1)	3.99(1)
TR_float	3.96(1)	0.01(0)	0.00(0)	-	-	0.14(3)	-	0.00(0)	2.90(1)	0.00(0)	0.00(0)	0.00(0)	0.00(0)	0.04(1)	1.96(1)	3.05(2)	3.98(1)
TR_G1	4.01(1)	0.01(0)	0.00(0)	0.00(0)	0.00(0)	0.04(5)	0.00(0)	0.00(0)	2.92(6)	0.00(0)	0.00(0)	0.00(0)	-	0.03(2)	1.97(2)	2.97(3)	4.01(1)
RE	4.01(2)	0.02(0)	0.00(0)	0.00(0)	0.00(0)	0.03(1)	0.00(0)	0.00(0)	2.93(3)	0.00(0)	0.01(0)	0.00(0)	-	0.02(0)	1.98(0)	2.97(3)	4.01(1)
BH	4.02(2)	0.01(1)	0.00(0)	0.00(0)	0.00(0)	0.03(2)	0.00(0)	0.00(0)	2.92(3)	0.00(0)	0.00(0)	0.00(0)	-	0.02(0)	1.98(0)	2.96(4)	4.02(2)
Ideal chlorite	3.00	2.00	0.00	0.00	0.00	0.00	0.00	0.00	5.00	0.00	0.00	0.00	0.00	0.00	2.00	6.00	4.00
*BH	3.36(8)	1.41(4)	0.00(0)	0.00(0)	0.00(0)	0.18(1)	0.00(0)	0.00(0)	4.96(11)	0.01(0)	0.00(0)	0.00(0)	-	0.03(0)	7.97(0)	5.93(7)	4.00(0)

Table 5a: EPMA results reported as weight percent oxides for talc and tremolite in sample SF_WC_N9A, shown in Figure 14

Mineral	SiO2/MgO	SiO2	Al2O3	TiO2	ZnO	Cr2O3	FeO	NiO	MnO	MgO	CaO	Na2O	K2O	P2O5	SO3	Oxide Sum	Cl wt%	F wt%
Ideal	2.38	59.17								24.81	13.81					97.79		
Tremolite_1	2.59	57.82	0.39	0.03	bdl	bdl	2.42	bdl	0.84	22.33	13.42	0.13	0.02	-	bdl	97.38	bdl	0.14
Tremolite_2	2.57	57.60	0.39	0.02	0.01	0.01	2.27	bdl	0.82	22.39	13.44	0.13	0.01	-	bdl	97.10	0.01	0.11
Tremolite_3	2.56	57.38	0.41	0.02	bdl	0.01	2.39	bdl	0.89	22.38	13.32	0.12	0.01	-	bdl	96.90	0.01	0.08
Tremolite_4	2.56	57.07	0.47	0.02	0.00	bdl	2.43	0.01	0.92	22.32	13.24	0.12	0.01	-	bdl	96.59	bdl	0.09
Mineral		SiO2	Al2O3	TiO2	ZnO	Cr2O3	FeO	NiO	MnO	MgO	CaO	Na2O	K2O	P2O5	SO3	Oxide Sum	Cl wt%	F wt%
Ideal	1.99	63.37								31.88						95.25		
Talc_1	2.26	63.18	0.03	bdl	bdl	bdl	2.67	bdl	0.05	28.00	0.11	0.05	0.02	-	bdl	94.12	0.02	0.04
Talc_2	2.23	62.87	0.14	0.01	bdl	bdl	2.57	bdl	0.05	28.23	0.31	0.13	0.02	-	bdl	94.34	0.06	0.06
Talc_3	2.04	60.73	0.07	0.01	0.00	bdl	2.43	bdl	0.06	29.73	0.52	0.05	0.01	-	0.01	93.63	0.00	0.02

Table 5b. EPMA results, converted to APFU values for talc and tremolite shown in Figure 14

Sample #	Si4+	Al3+	Ti4+	Zn2+	Cr3+	Fe2+	Ni2+	Mn2+	Mg2+	Ca2+	Na+	K+	P2O5	S6+	F-	OH-	A	B	C	T
Ideal	8.00								5.00	2.00						2.00		2.00	5.00	8.00
Tremolite_1	7.97	0.06	0.00	0.00	0.00	0.28	0.00	0.10	4.59	1.98	0.04	0.00	-	0.00	0.06	1.94	0.00	2.00	5.00	8.00
Tremolite_2	7.96	0.06	0.00	0.00	0.00	0.26	0.00	0.10	4.61	1.99	0.04	0.00	-	0.00	0.05	1.95	0.00	2.00	5.00	8.00
Tremolite_3	7.95	0.07	0.00	0.00	0.00	0.28	0.00	0.10	4.62	1.98	0.03	0.00	-	0.00	0.03	1.97	0.00	2.00	5.00	8.00
Tremolite_4	7.94	0.08	0.00	0.00	0.00	0.28	0.00	0.11	4.63	1.97	0.03	0.00	-	0.00	0.04	1.96	0.00	2.00	5.00	8.00
	Si4+	Al3+	Ti4+	Zn2+	Cr3+	Fe2+	Ni2+	Mn2+	Mg2+	Ca2+	Na+	K+	P2O5	S6+	F-	OH-	Tet	Oct		
Ideal	4.00								3.00							2.00	4.00	3.00		
Talc_1	4.07	0.00	0.00	0.00	0.00	0.14	0.00	0.00	2.69	0.01	0.01	0.00	-	0.00	0.01	1.99	4.07	2.86		
Talc_2	4.05	0.01	0.00	0.00	0.00	0.14	0.00	0.00	2.71	0.02	0.02	0.00	-	0.00	0.01	1.99	4.05	2.90		
Talc_3	3.96	0.01	0.00	0.00	0.00	0.13	0.00	0.00	2.89	0.04	0.01	0.00	-	0.00	0.00	2.00	3.97	3.07		

Table 6a: EPMA results reported as weight percent oxides for chlorite and serpentine in sample WC_SF_N9A, shown in Figure 16. The data for serpentine analyses are shaded green

Mineral		SiO2	Al2O3	TiO2	ZnO	Cr2O3	FeO	NiO	MnO	MgO	CaO	Na2O	K2O	P2O5	SO3	Oxide Sum	Cl wt%	F wt%
Ideal clinochlore	0.89	32.43	18.35							36.26								
Ideal Mg-serpentine	0.99	43.36								43.63								
Chlor-serp_1	1.11	33.96	13.54	0.06	0.01	0.01	6.23	0.01	0.17	30.69	0.04	0.01	0.34	-	bdl	85.06	bdl	0.00
Chlor-serp_2	1.11	33.79	13.72	0.06	0.01	bdl	6.31	bdl	0.18	30.54	0.03	0.02	0.33	-	bdl	84.98	bdl	0.01
Chlor-serp_3	1.09	33.73	13.47	0.04	0.01	0.02	6.05	bdl	0.16	30.92	0.03	bdl	0.36	-	bdl	84.77	bdl	0.01
Chlor-serp_4	1.18	43.14	0.74	bdl	bdl	bdl	4.25	0.00	0.60	36.60	0.16	bdl	bdl	-	bdl	85.48	0.02	0.04
Chlor-serp_5	1.17	42.94	1.03	bdl	bdl	bdl	4.08	bdl	0.58	36.70	0.10	bdl	bdl	-	bdl	85.39	0.02	0.03
Chlor-serp_6	1.17	42.83	1.05	bdl	bdl	bdl	3.95	bdl	0.62	36.70	0.20	bdl	bdl	-	bdl	85.37	0.02	0.04
Chlor-serp_7	1.05	31.62	16.15	0.02	bdl	bdl	6.44	0.01	0.20	30.10	0.05	bdl	0.07	-	bdl	84.65	0.00	0.04

Table 6b: EPMA results converted to APFU values for chlorite and serpentine in sample WC_SF_N9A, shown in Figure 16

	Si4+	Al3+	Ti4+	Zn2+	Cr3+	Fe2+	Ni2+	Mn2+	Mg2+	Ca2+	Na+	K+	P2O5	S6+	F-	OH-	Tet	Oct
Ideal clinochlore	3.00	3.00							5.00							8.00	4.00	6.00
Ideal Mg-serpentine	2.00	0.00							3.00							4.00	2.00	3.00
Chlor-serp_1	3.32	1.56	0.00	0.00	0.00	0.51	0.00	0.01	4.47	0.00	0.00	0.04	-	0.00	0.00	8.00	4.00	5.87
Chlor-serp_2	3.30	1.58	0.00	0.00	0.00	0.52	0.00	0.01	4.45	0.00	0.00	0.04	-	0.00	0.00	8.00	4.00	5.88
Chlor-serp_3	3.30	1.56	0.00	0.00	0.00	0.50	0.00	0.01	4.52	0.00	0.00	0.05	-	0.00	0.00	8.00	4.00	5.89
Chlor-serp_4	2.06	0.04	0.00	0.00	0.00	0.17	0.00	0.02	2.61	0.01	0.00	0.00	-	0.00	0.01	3.99	2.06	2.85
Chlor-serp_5	2.05	0.06	0.00	0.00	0.00	0.16	0.00	0.02	2.62	0.01	0.00	0.00	-	0.00	0.01	3.99	2.05	2.86
Chlor-serp_6	2.05	0.06	0.00	0.00	0.00	0.16	0.00	0.03	2.62	0.01	0.00	0.00	-	0.00	0.01	3.99	2.05	2.86
Chlor-serp_7	3.11	1.87	0.00	0.00	0.00	0.53	0.00	0.02	4.41	0.00	0.00	0.01	-	0.00	0.01	7.99	4.00	5.94

Table 7a: EPMA results reported as weight percent oxides for sepiolite in sample WC_Sep

Mineral		SiO2	Al2O3	TiO2	ZnO	Cr2O3	FeO	NiO	MnO	MgO	CaO	Na2O	K2O	P2O5	SO3	Oxide Sum	Cl wt%	F wt%
Ideal	2.24	55.65								24.89						80.53		
Sepiolite_1	2.58	53.39	0.30	bdl	bdl	0.01	3.82	0.01	0.08	20.68	0.07	bdl	0.01	-	bdl	78.37	0.03	0.36
Sepiolite_2	2.76	48.11	0.25	bdl	bdl	bdl	3.66	0.01	0.08	17.42	0.07	0.01	bdl	-	bdl	69.60	0.02	0.39
Sepiolite_3	2.82	46.15	0.23	bdl	bdl	0.01	3.83	bdl	0.07	16.36	0.16	0.02	0.01	-	0.01	66.84	0.02	0.35
Sepiolite_4	2.68	46.33	0.29	0.01	bdl	bdl	3.67	0.01	0.08	17.28	0.22	0.01	0.01	-	bdl	67.91	0.02	0.46

Table 7b: EPMA results, converted to APFU values for sepiolite in sample WC_Sep

	Si4+	Al3+	Ti4+	Zn2+	Cr3+	Fe2+	Ni2+	Mn2+	Mg2+	Ca2+	Na+	K+	P2O5	S6+	F-	OH-	Tet	Oct
Ideal Sepiolite	6.00								4.00							2.00	6.00	4.00
Sepiolite_1	6.04	0.04	0.00	0.00	0.00	0.36	0.00	0.01	3.49	0.01	0.00	0.00	-	0.00	0.13	1.87	6.04	3.90
Sepiolite_2	6.12	0.04	0.00	0.00	0.00	0.39	0.00	0.01	3.30	0.01	0.00	0.00	-	0.00	0.16	1.84	6.12	3.73
Sepiolite_3	6.13	0.04	0.00	0.00	0.00	0.42	0.00	0.01	3.24	0.02	0.00	0.00	-	0.00	0.15	1.85	6.13	3.70
Sepiolite_4	6.06	0.04	0.00	0.00	0.00	0.40	0.00	0.01	3.37	0.03	0.00	0.00	-	0.00	0.19	1.81	6.06	3.82

Chapter 3: Stable O and H isotope analyses of talc; constraining environments of formation and compositionally distinguishing ores

Abstract

We conducted a suite of analytical methods on talc samples from locations worldwide in order to compositionally characterize both current and past economic talc deposits. Ores from multiple deposits have very similar compositions from major element to trace element concentrations, and we are currently exploring the possibility that ores may be distinguished based on stable isotope ratios. The talc samples in this study are from the Murphy marble belt in North Carolina, southwest Montana, northwest Death Valley region in California, Vermont, the Van Horn deposits in west Texas, and Chisone Valley in northern Italy. These deposits have formed under different processes, including regional metamorphism, contact metamorphism and metasomatism but altering fluids have been involved in varying degrees in all cases. It is expected that the paired H and O isotope ratios for these talcs are related to the composition of the altering fluids in each of these geologic environments. We present new data and revisit other researchers' data to better constrain the environment of talc formation in these economically important deposits and to determine whether these ores can be distinguished based on stable isotope ratios. Generally talc H and O isotope ratios cluster based on location although our assumptions of homogeneity were not appropriate for all locations.

Introduction

The O and H isotope ratios into geologic materials are largely dependent on temperature and the origin of those materials. Stable isotope studies are useful in tracing sediments and minerals, and understanding isotope fractionation as a function of environmental conditions. Although talc can form in many geologic environments, mineable talc deposits form after carbonate or ultramafic-derived rocks at temperatures generally in excess of 190°C (Gammons and Matt ,2002; Tornos and Spiro, 2000) but not exceeding 600°C (metamorphic facies diagram). These two protoliths, especially those of carbonate origin undergo extensive compositional changes in order for pure talc deposits to form, a process

that is aided by the addition of mostly Si-, Mg- and H_2O-rich fluid. In many cases these talc deposits have long histories of alteration and deformation but we expect the isotope ratios in talc to be constant throughout a deposit and to be a record of the fluid, rather than the protolith, composition. Therefore, we expect to see a record of those differing histories in the stable O and H isotope ratios preserved in talc.

The samples for this study were chosen from a larger set of commercial talcs that have been analyzed via powder x-ray diffraction, electron microprobe, and x-ray fluorescence spectroscopy. The initial goal of this project is to compositionally characterize these samples based on accessory mineral content, the composition of talc determined by microprobe data, and bulk trace element concentrations. Although moderately successful, there are still samples that are difficult to distinguish based solely on talc compositions. Table 1 includes the EPMA data converted to atoms per formula unit (APFU) for each of the samples, along with Ni and Cr trace element concentrations from bulk XRF analyses. These samples were chosen because they all are relatively pure of accessory phases (especially carbonates), and are not all that compositionally distinguishable with the exception of samples from Vermont and their high Ni concentrations. These have been purposefully ordered based on Fe content, showing how samples of different origins compositionally group with other samples. The selected samples are important from an economic standpoint because Montana, Texas, and Vermont are the largest domestic sources of talc in the U.S., and stock piles in California still provide enough ore to be considered a domestic source despite no current mining. (Flanagan, 2016). The talc from the Willow Creek Mine in Montana, Murphy Marble belt in North Carolina, and Chisone Valley in northern Italy are all known sources for Cashmere Bouquet Body Talc, a product that has been the focus of recent asbestos litigation. We are addressing several questions in this project; are isotope ratios in talc constant over a single talc-mining region, can talc from different mining regions be distinguished based on O and H isotope ratios, and what types of fluids were involved with creating these talc deposits? This last question can only be answered by approximations but is a motivation for more research on how hydrogen fractionates between minerals and fluids.

Most economic talc deposits are formed from altered carbonate rocks, as opposed to rocks of ultramafic origin, and those that have been metasomatically altered produce the most pure talc ores (Van Gosen et al., 2004). Metasomatism differs from isochemical metamorphism in that ions or ionic groups are perfectly mobile in solution, instead of H_2O or CO_2 being the only mobile components. This type of reaction generally produces rocks that have fewer phases than those created by replacement metamorphism, and results in rocks with different compositions than the protoliths. The number of phases tends to increase in the altered rock with distance from the fluid source, as alteration is less extensive (Zharikov et al., 2007). This would also result in a variation in stable oxygen and hydrogen isotope ratios over distance, with the most pervasively altered rocks having isotopic compositions more influenced by the fluid. In the case of hydrothermally altered talc deposits, aqueous fluids have transported silica, which interacted with dolomitic marbles. The silica has often been transported from a nearby SiO_2-rich lithology, and the fluids were introduced to the system through pre-existing faults or fractures. Regardless of the source of the fluids, which includes but is not limited to meteoric waters, connate brines, seawater, or a combination of sources, these deposits form in environments where there were high volumetric fluid-to-rock ratios, on the order of several hundred to 1000 (Moine et al., 1989; Anderson et al., 1990). Heat from igneous activity and hydrostatic pressure are the driving forces behind circulating the talc-forming fluids. This general process has occurred in the Van Horn (or Allamoore) mining district in west Texas, northwest of Death Valley in California, southwest Montana, as well as in a number of other locations worldwide (Van Gosen et al., 2004, Tornos and Spiro, 2000; Moine et al., 1989). Another common trait among these deposits is that they have polymetamorphic histories, at least requiring for dolomitization to have occurred before talc crystallization. Our samples from Italy and North Carolina are also carbonate-derived but the talc-forming process involved extensive regional metamorphism. Two of our samples are from the ultramafic-hosted talc deposits in Vermont. These deposits are associated with regional metamorphism and metasomatism, but have not experienced as much chemical exchange as the carbonate-hosted talcs as MgO, SiO_2, H and O were already abundant in the protolith.

Isotope Background

The concentrations of individual isotopes in most materials are so low that is it common practice to report isotopes as a ratio of the abundance of a heavy isotope and a more abundant, light isotope ($R=\frac{^{18}O}{^{16}O}$ for oxygen and $\frac{D}{H}$ for hydrogen). These ratios will be used in following calculations The $\delta^{18}O$ (said "delta O 18") in a sample is determined relative to a standard using Equation 1:

$$\delta^{18}O=\left[\frac{R_{sample}-R_{standard}}{R_{standard}}\right]*1000$$

The same type of equation is used for hydrogen isotopes using D and H, the ratio is expressed as δD. All isotope ratios in this paper are presented relative to the Vienna Standard Mean Ocean Water (VSMOW) in units of per mil (‰). Craig (1961) determined that δD ratios in precipitation and fresh surface waters were approximately eight times those of $\delta^{18}O$ ratios ($\delta D= 8\delta^{18}O + 10$). This relationship is often graphically shown as the meteoric water line (MWL). Waters from other environments have since been characterized based on isotope ratios in relation to meteoric waters making it possible to approximate the origins of waters in geologic environments. Atomic mass and bond energies determine how isotopes will fractionate between materials in equilibrium, described by the equilibrium fractionation factor (α). We are primarily concerned with the equilibrium fractionation of isotopes between talc and altering fluids (assumed to be H_2O) which is expressed for oxygen in Equation 2:

$$\propto^{Ox}_{talc\text{-}H2O}=\frac{(R_{talc})}{R_{H2O}}=\frac{1000\delta^{18}O_{talc}}{1000\delta^{18}O_{H2O}}$$

Oxygen equilibrium fractionation decreases with increasing temperature. When temperature increases, the rigidity of bonds in a phase decreases, allowing for both heavy and lighter isotopes to be more mobile. Heavier isotopes will preferentially occupy sites with the strongest and stiffest bonds, which are more of a factor at lower temperatures. Generally the equilibrium fractionation factor between a mineral and H_2O is expressed in the following form, Equation 3:

$$1000\ln\alpha_{mineral\text{-}H2O}=\left(\frac{a}{T^2}\right)+b$$

where a and b are constants unique for each of the two phases involved in fractionation, and T is in K. Equation 3 is approximately equal to $\delta^{18} O_{mineral}$-$\delta^{18} O_{H2O}$, referred to as Δ ("big delta"). Therefore, in hydrothermally altered rocks, if the temperature at which equilibrium between the fluids and a specific mineral was established is known, the measured $\delta^{18}O$ of a mineral can be measured and used to determine the composition of the altering fluids.

Equilibrium Fractionation factors

Zheng (1993) determined theoretical fractionation factors for oxygen isotopes between hydroxylated sheet silicates and water, quartz and calcite at temperatures of 0-1200° C. The calculations are based on the ability of a mineral's structure to contain ^{18}O, determined by the type of bonding and the mass of the cations surrounding the potential site for the heavy isotope. Because fractionation factors between hydrous silicates and water, hydrous silicates and quartz, and hydrous silicates and calcite were calculated, the fractionation factors between talc and other minerals have the potential to be determined if all phases are in equilibrium within in a rock. Due to the intended lack of carbonates, and purity of our samples we will only be concerned with the fractionation between water and talc. Zheng's equilibrium fractionation factor for talc and H_2O is:

$$1000\ln\alpha_{talc\text{-}H2O} = \left(\frac{4.2*10^6}{T^2}\right) + \left(\frac{-7.04*10^3}{T}\right) + 2.14$$

Savin and Lee (1998) empirically determined an oxygen equilibrium fractionation factor for talc and H_2O based on bond types only in which oxygen is bonded. This method does not consider the overall structure of a mineral. Their oxygen equilibrium fractionation factor approximation is:

$$1000\ln\alpha_{talc\text{-}H2O} = \left(\frac{0.084*10^{12}}{T^4}\right) + \left(\frac{-0.934*10^9}{T^3}\right) + \left(\frac{5.86*10^6}{T^2}\right) + \left(\frac{-3.94*10^3}{T}\right) - 4.27$$

These empirical equilibrium fractionation factors compare well at temperatures below 300° C. Fractionation of oxygen between talc and H_2O according to Zheng's calculation is not as affected by temperature as Savin and Lee's calculation, which becomes increasingly negative at higher temperatures, approaching -2.0 ‰ for an approximation of $1000\ln\alpha_{talc\text{-}H2O}$ at 550° C.

Both of these equations with T=273.15-823.15 K are plotted in Figure 2. The temperature in the figure is converted to Celsius.

Hydrogen equilibrium fractionation factors have not been as widely studied but Lee (2001) determined a hydrogen talc-H_2O equilibrium fractionation factor from 360-480°C. Generally H fractionates to a greater extent than oxygen and any other isotopes because the mass difference between H and D is nearly 100%, making it very important for us to have a better understanding for low temperature hydrogen fractionation. As this was not a main focus of our project we will be using the fractionation factor determined by Lee (2001) and extrapolate it for lower temperatures, but we recognize that our results should not be accepted as a final determination of the composition of altering fluids. The fractionation factor plotted versus temperature in Figure 3 determined by Lee is:

$$1000\ln\propto_{\text{talc-H2O}}=\frac{-16.9*10^{6}}{T^{2}}+28.90.$$

Isotopic studies on talc

Tornos and Spiro (2000), Yalcin and Bozkaya (2006) and Brady et al. (1998) used oxygen and hydrogen isotope ratio pairs to determine the origin and environments of formation of talcs. Although only one of our sample locations overlap with these locations, a summary of their findings and results are included for comparison. Due to the lack of research on hydrogen fractionation none of these sources confirmed fluid composition based on hydrogen fractionation factors.

Brady et al. did thermochronometry and stable isotope analyses on talc and associated minerals from the Ruby Range, the western-most range in the talc-mining region in Montana. The talc was formed from the hydrothermal alteration of Archean marbles, and talc bodies occur as lenses in the altered dolomitic marble (Berg, 1979). The unaltered carbonates and altered carbonates in this study were analyzed for C and O isotopes, while talc samples were analyzed for O and H isotopes. It was concluded that the hydrothermal fluid that altered the marble was CO_2-poor, however, the O isotopes between unaltered and altered carbonate samples varied, indicating that the altering fluid had an influence on the O isotope composition of the altered carbonates. The authors assumed the altering fluid was seawater ($\delta^{18}O=0$) and used the theoretical fractionation factors from Zheng (1993) to

calculate an equilibrium temperature range of 200-300°C. However, Gammons and Matt (2002) conducted a fluid inclusion study and determined the hydrothermal fluids infiltrating the dolomitic marbles were 190-250 °C and that they were highly saline brines rather than ocean water. Although we will be referencing the isotopic compositions from Brady et al. (1998), we will use the temperature range suggested by Gammons and Matt (2002) in discussing our results for all the samples from southwest Montana.

Tornos and Spiro (2000) analyzed talc from two mines in northern central Spain in the Cantabrian Zone. These deposits were predominantly formed by the hydrothermal alteration of carbonates, however, smaller sections of the deposits are derived from shale and quartz sandstone (now slate and quartzite). Talc from altered dolomite had $\delta^{18}O$ ratios of 10.7-12.7‰ and δD ratios of -62- -64‰. It is also worth noting that this area underwent at least three stages of alteration, including regional metamorphism and hydrothermal alteration. An earlier component of this study analyzed fluid inclusions in the dolomite, and concluded that the fluids that altered this deposit had peak temperatures from 280-405° C. This temperature estimate was then used to calculate the delta O^{18} value of the hydrothermal talc-forming fluids with the equation established by Zheng (1993). They concluded that the fluid O and H composition indicated a connate, metamorphic or igneous origin. The talc from different protoliths had slightly different oxygen isotope ratios suggesting an influence of protolith composition on isotope compositions.

Yalcin and Bozkaya (2006) characterized talcs from siliclastic and ultramafic deposits in north-central Turkey that have been diagenetically altered. The oxygen isotope ratio of the altering fluids in their publication were assumed to be 0‰ (seawater), resulting in equilibrium talc-water temperatures <100 °C. The $\delta^{18}O$ ratios and δD ratios were 13.8-17.5‰ and -60- -36‰ respectively. These values span a much wider range than those observed by Tornos and Spiro (2000), and Brady et al (1998) which may be a result of different degrees of alteration since two of the three samples have the same protolith.

The general grouping of samples based on location in this, albeit limited, collection of data makes us believe that data for talcs from the same region will cluster based on isotope ratios.

Methods and results

Monomineralic talc samples were crushed with a porcelain mortar and pestle and sieved so that portions of 20-48 mesh grains were selected for analyses. Samples were washed in 20% acetic acid for 8 hours to ensure no carbonates were present. The residual powder from sieving was tested with 5% HCl as well. Samples were rinsed in Millipore/deionized water three times and left to dry in a fume hood. Both methods required 2± 0.3mg of sample.

The O isotope analyses followed the procedure in Sharp (1990) using the laboratory space provided by Peter Larson at Washington State University. During analyses, oxygen was liberated from the sample when heated by a 20W CO_2 laser and was replaced in the sample by F from the BrF_5 reagent. The gases passed through a series of cold traps isolating the O_2 from any reagent gas, and then through molecular sieves to ensure O was the only element to reach the mass spectrometer. The O_2 was analyzed in the Finnigan MAT Mass Spectrometer with Delta S software (Takeuchi and Larson, 2005). We ran two rose quartz reference standards (RQS) before analyses to clear ambient O from the line. The Gore Mountain garnet (UWG-2) was used as a working standard between every three to four samples and sample ratios were corrected according to the accepted ratio 5.8‰ (Valley et al. 1995). We applied a linear correction to the sample ratios based on the standards run before and after each group of samples.

Hydrogen analyses were done in Peter Larson's isotope laboratory using the Thermo Finnigan Delta V mass spectrometer. Sample ratios were corrected relative to the Mica Mountain Muscovite standard (tentative accepted value δD=-67.4‰). Sample weights, results and notes for both analyses are included in Table 2 and plotted versus each other in Figures 4 and 5. Hydrogen and oxygen isotope ratios for samples from the aforementioned publications are also included in Figures 4 and 5. Samples are listed in the order that they were run for O analyses.

Discussion

Distinguishing talc samples based on mining region

The isotopic ratios for our talc samples fall within a small field below the MWL. There is a greater range in the δD ratios than in the $\delta^{18}O$ ratios. All of the carbonate-hosted samples have oxygen isotope compositions much lower than the range commonly seen in sedimentary carbonates (20 ‰), which was expected. Our data for the samples from Montana overlap with data published by Brady et al. (1998) for samples from talc mines in the Ruby Range. Our samples are from the Ruby, Greenhorn, and Gravelley Ranges, which span an area of 60 miles from west to east. We do not observe any trends in the data that suggest a relationship between sample location and the degree of alteration/composition of fluids, and feel comfortable concluding that these samples have a relatively small isotopic compositional range, despite the variability among major element concentrations shown in Table 1.

The two samples from Talc City Mine northwest of Death Valley have very similar oxygen and hydrogen isotope ratios (8.6‰ and 8.1‰, and 59.0‰ and 59.1‰ respectively). Although one sample from the Regal Mine in Montana (data from Brady et al., 1998) has isotope values very similar to the Talc City samples, we think the samples could be distinguished based on isotope ratios if we had more data for the Talc City samples.

The data for the three samples from the Chisone Valley in Italy create a tight cluster with δD ratios approximately 10‰ higher than the rest of the samples we analyzed (-29.4- -34.5‰), and $\delta^{18}O$ values somewhat overlapping with those of the samples from Montana (5.0-7.0‰) but the high hydrogen ratios make it much easier to distinguish these samples compared to the microprobe and XRF data that were indistinguishable from some samples from North Carolina.

The isotope data for the samples from Texas, Vermont, and North Carolina do not appear to cluster as well, but this also may be a result of not analyzing enough samples to. The oxygen and hydrogen isotope ratios for the two samples from western Texas are different by 3.7‰ and 10.9‰, respectively. Initially this discrepancy was thought to be from analytical drift while obtaining oxygen ratios, as these two were the last two samples to be

analyzed and the standard's ratio had climbed to 2.41‰ above the accepted value. However, the hydrogen ratios are also quite different from each other and the pink sample was analyzed twice with repeatable values. Therefore, the isotopic differences among these two samples are representative of differing isotope compositions despite being from the same mining region. Possible reasons for the difference between oxygen ratios in these two samples could be analyst error (for oxygen) or different degrees of alteration experienced by these two samples coupled with different protolith compositions. The talc from Van Horn, Texas is associated with sedimentary and metasedimentary rocks of the Precambrian Allamoore formation. The dark color of the talc, observed in our gray sample is thought to be a result of the carbonaceous material in the original sediments. These two samples however, are compositionally indistinguishable based on microprobe and XRF data despite their very different appearances. Even if the protolith compositions were different regarding carbon content, this should not affect oxygen or hydrogen isotope ratios in hydrothermally altered rocks, which these are thought to be. Therefore it is probable that the large difference in hydrogen isotopes is a result of different fluids interacting with the two samples.

The samples from the Johnson and Argonaut Mines in Vermont have δD ratios of -42.5 and -51.1‰ respectively. Although these two locations are >200 miles apart, they share a similar history in that they both formed after ultramafic protoliths. It is also worth noting that isotope ratios of these samples overlap with the rest of the samples, showing no influence of the ultramafic origin on the isotopic composition, despite how high the trace element concentrations are in these samples compared to carbonate-derived talcs. We have little confidence that the isotope ratios collected for this project would be helpful in distinguishing these ores from others. Trace element data remain sufficient to distinguish between ultramafic- and carbonate-hosted talcs.

Our isotope ratios for the two samples from North Carolina have very similar $\delta^{18}O$ ratios (8.2‰ and 7.8‰) but the δD values were different from each other by 6.6‰ (-44.3 and 50.9‰). Again, this apparent difference may be a result of not analyzing enough samples. The difference between the hydrogen isotope values in these two samples is no greater than the

difference observed between the samples from Montana, the data points for which are relatively contained in Figures 4 and 5.

What types of fluids were involved with creating these talc deposits?

The talc-H_2O oxygen equilibrium fractionation factors for all of these samples cannot be determined because we do not know the temperature at which talc and the fluids equilibrated for all the samples, but we do know some limitations. Additionally we are only considering temperature in determining the composition of the fluids, but other factors affect this. The talc from Montana, west Texas, and Talc City in California likely equilibrated at temperatures between 190-400° C based on the data from Gammons and Matt (2002) and Van Gosen (2004). This is a wide temperature range so we will focus mostly on the samples from Montana. The composition of the fluids in this talc-forming environment has been researched in great detail, but no work has been done to constrain the hydrogen isotope composition.

Our data combined with those from Brady et al. (1998) indicate that the final hydrothermal alteration of the dolomitic marble in southwest Montana involved fluids of roughly the same composition. The hydrogen isotope composition of fluids in this area have not been determined, but if we extrapolate using use Lee's (2001) and Zheng's (1993) approximations, at 190° C ($1000\ln\alpha_{talc\text{-}H2O}$= -47.5‰) the fluid composition has a δD value of -10.6- 3.3‰ (converted from δD_{talc} of -57.6‰ - -44.2‰) . The $\delta^{18}O$ composition of the altering fluid, when using an equilibrium temperature of 190° C, is -2.3‰- 2.3‰. These values are very close to the isotopic composition of ocean water. If we use the higher temperature of 250° C, suggested by Gammons and Matt, δD= -26.6- -13.2‰, and $\delta^{18}O$ = 0.2-4.8‰. Fluids with these isotope ratios would be categorized as brines or water that has been buffered by metamorphic rock (Sharp, 2007). Similar values for oxygen isotope composition of the fluid are determined when using the empirical approximation by Savin and Lee (1988). This calculation matches relatively well with what Gammons and Matt determined. However, we should still be cautious in extrapolating Lee's (2001) equilibrium fractionation factor because brines can have a range of isotopic compositions and our results could be off by 10‰ for both

oxygen and hydrogen and the fluid would still be characterized as a brine. These values are plotted in Figure 6.

Brady et al., (2006) and references within provide a pressure-temperature-time path of the talc-rich rocks near Proctorsville, VT (about 6 miles east of Ludlow Vermont) with a peak temperature of 450-550° C. This is based on an antigorite+talc assemblage and may not be accurate since these samples are pure. However, these temperatures, which are in a realistic range produce an oxygen talc-H_2O equilibrium fractionation factor of 0.44- -0.21‰ based on Zheng (1993), or -0.67- -1.90‰ based on Savin and Lee's empirical fractionation factor; these values result in H_2O oxygen isotope ratios of approximately 7.5-8.1‰ or 8.6-9.8‰ respectively for the talc from the Johnson and Argonaut Mines. This same temperature range when used with Lee's equilibrium fractionation factor corresponds to a fluid of igneous origin, or metamorphic waters (δD= -55.8- -40.1‰). Lower temperature estimates, down to approximately 180° C, still relate to isotope compositions for igneous or metamorphic fluids. It is unlikely that the deposits in Vermont formed by the influence of brines like many of the carbonate-hosted deposits have formed.

Seawater

Some past researchers (Brady et al, 1998; Yalcin and Bozkaya, 2006) have determined the temperature at which talc and water equilibrated by assuming the fluids had the isotopic composition of modern seawater. If we apply this assumption to the samples for which we do not have equilibrium temperatures we can simply use the measured isotope ratios as an approximation of $1000\ln\alpha_{talc\text{-}H2O}$. The temperature approximations for oxygen based on Zheng (1993), Savin and Lee (1988), and for hydrogen based on Lee (2001) are listed in Table 3. The hydrogen equilibrium temperatures do not always match well with the two oxygen isotope temperatures (which agree quite well with each other). This may be a result of extrapolating the equilibrium fractionation factor beyond its theoretical limits. However, the H and O isotope ratios in samples from Montana, one sample from North Carolina, Talc City, California, and one from Van Horn, Texas do result in narrow temperature ranges. The large temperature ranges for H and O isotope equilibrium between talc and the fluids for the rest

of the samples may indicate disequilibrium between hydrothermal fluids and the talc. In this case the isotope ratios in talc would be related to the protolith. We do recognize that our assumption and applying two unrelated talc-H_2O equilibrium fractionation may result in inaccurate values.

Conclusions

Our findings were significantly limited by our intentional selection of pure samples. Many of these samples did not include separable accessory phases that could be analyzed by these methods. However, if calcite or quartz grains were analyzed, and were known to be in equilibrium with the talc, it would have been much easier to constrain the isotopic compositions of the fluids. Generally the samples from Montana have hydrogen and oxygen isotope ratios in a limited range, suggesting a common alteration history. The same preliminary statement could be said for the talc samples from Talc City, California, Chisone Valley in Italy and North Carolina. There does not appear to be a relationship between protolith, trace element concentrations, or major element concentrations and stable isotope ratios. This confirms that all of these rocks have been pervasively altered by fluids. The hydrogen equilibrium fractionation factor approximated by Lee (2001) for relatively high temperatures was used to identify fluid compositions for much lower temperatures and resulted in reasonable values.

Acknowledgements

We would like to thank Peter Larson for his assistance and providing his lab space, and Gilbert Ching for running the H isotope analyses.

References

Berg, R. (1979) Talc and chlorite deposits in Montana. Montana Bureau of Mines and Geology Memoir 45.

Brady, J. B., Cheny, J. T., Rhodes, A., Vasquez, A., Green, C., Duvall, M., Kogut, A., Kaufman, L., Kovaric,D. (1998) Isotope geochemistry of Proterozoic talc occurrences in Archean arbles of the Ruby Mountains, southwest Montana, U.S.A. Geological Materials Research, 1,2,1-41.

Craig, H. (1961) Isotopic variations in meteoric waters, Science, 133, 1702-1703.

Greene, R.C. (1995) Talc resources of the conterminous United States. Open-File Report OF 95-586. U.S. Geological Survey, Menlo Park, CA.

Flanagan, Daniel M. (2016) Talc and Pyrophyllite. In U.S. Department of the Interior and U.S. Geological Survey Mineral Commodity Summaries 2016, p.164-165. U.S. Geological Survey, Reston, Virginia.

Lee, I. (2001) Evaluation of hydrogen isotope fractionation in the system talc-carbonate water: empirical consideration based on the model at the Dongyang talc deposit, Korea. Geosciences Journal, 5, 85.

Moine, B., Fortune, J., Moreau, P., and Viguier, F. (1989) Comparative mineralogy, geochemistry, and conditions of formation of two metasomatic talc and chlorite deposits: Trimouns (Pyrenees, France) and Rabenwald (Eastern Alps, Austria). Economic Geology, 84, 1398-1416.

Robinson, G.R., Van Gosen, B.S., and Foley, N.K. (2006) Ultramafic-hosted talc-magnesite deposits (presentation). 42nd Forum on the Geology of Industrial Minerals, Asheville, N.C.

Savin, S.M. and Lee, M. (1988) Isotopic studies of phyllosilicates. In S.W. Bailey, Eds., Hydrous phyllosilicates (excusive of micas), 19,p. 189-223. Reviews in Mineralogy and Geochemistry, Mineralogical Society of America, Chantilly, Virginia.

Sharp, Z.D., Atudorei, V., Durakiewicz, T. (2001) A rapid method for determination of hydrogen and oxygen ratios from water and hydrous minerals. Chemical Geology, 178, 197-210.

Sharp, Z. (2007) Chapter 12: Metamorphic geology, section 12.3 Fluid sources and fluid-rock interaction. Principles of stable isotope geochemistry, Pearson Prentice Hall, Upper Saddle River, N.J..

Takeuchi, A. and Larson, P.B. (2005) Oxygen isotope evidence for the late Cenezoic development of an orographic rain shadow in eastern Washington, USA. Geology, 4, 313-316.

Tornos, F., and Spiro, B. F.(2000) The Geology and Isotope Geochemistry of the Talc Deposits of Puebla de Lillo(Cantabrian Zone, Northern Spain). Economic Geology, 95, 1277-1296.

Van Gosen, B.S., Lowers, H.A., Sutley, S.J., and Gent, C.A. (2004) Using the geologic setting of talc deposits as an indicator of amphibole asbestos content. Environmental Geology, 45, 920-939.

Virta, R. (2004) Talc and pyrophyllite. U.S. Geological Survey Minerals Yearbook, 75.1-75.8.

Yalcin, H. and Bozkaya, O. (2006) Mineralogy and Geochemistry of Paleocene ultramafic- and sedimentary-hosted talc deposits in the southern part of the Sivas Basin, Turkey. Clays and Clay Minerals, 54, 3, 333-350.

Zheng, Y. (1993) Calculation of oxygen isotope fractionation in hydroxyl-bearing silicates. Earth and Planetary Science Letters, 120, 247-263.

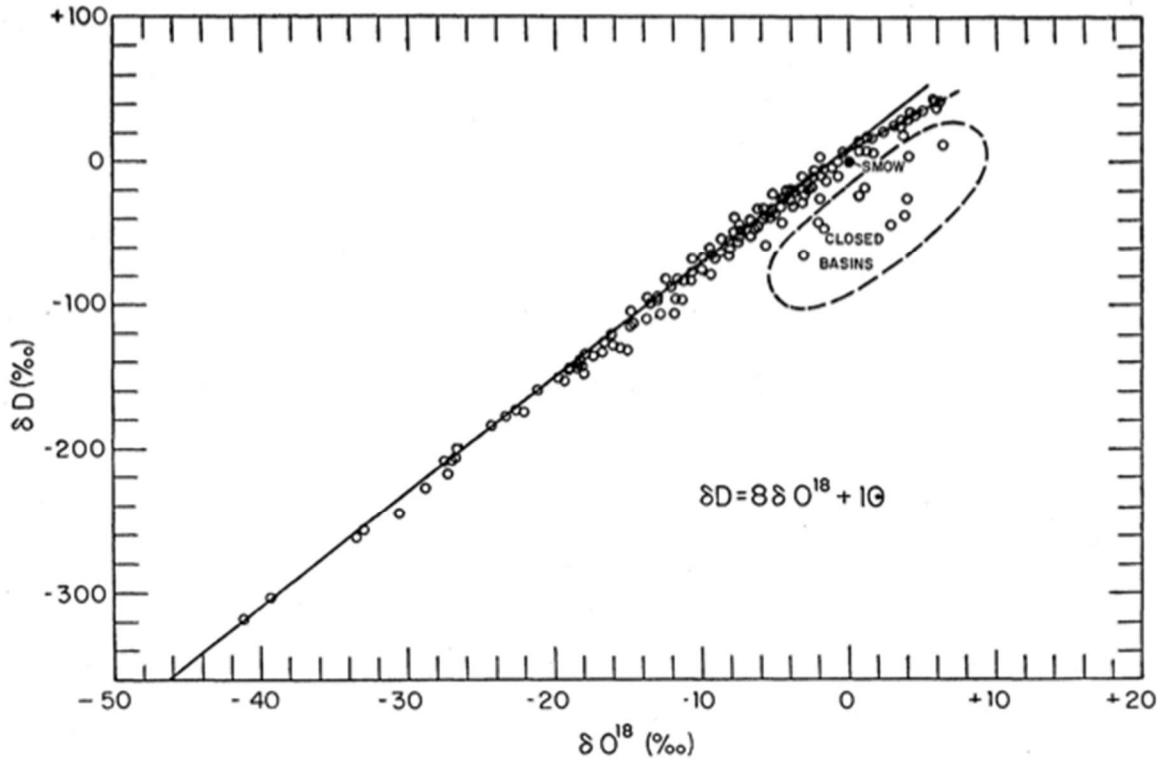

Figure 1: (From Craig, 1961) δD and $\delta^{18}O$ ratios relative to SMOW are plotted for meteoric waters, showing δD variations are roughly 8 times those of δO^{18}

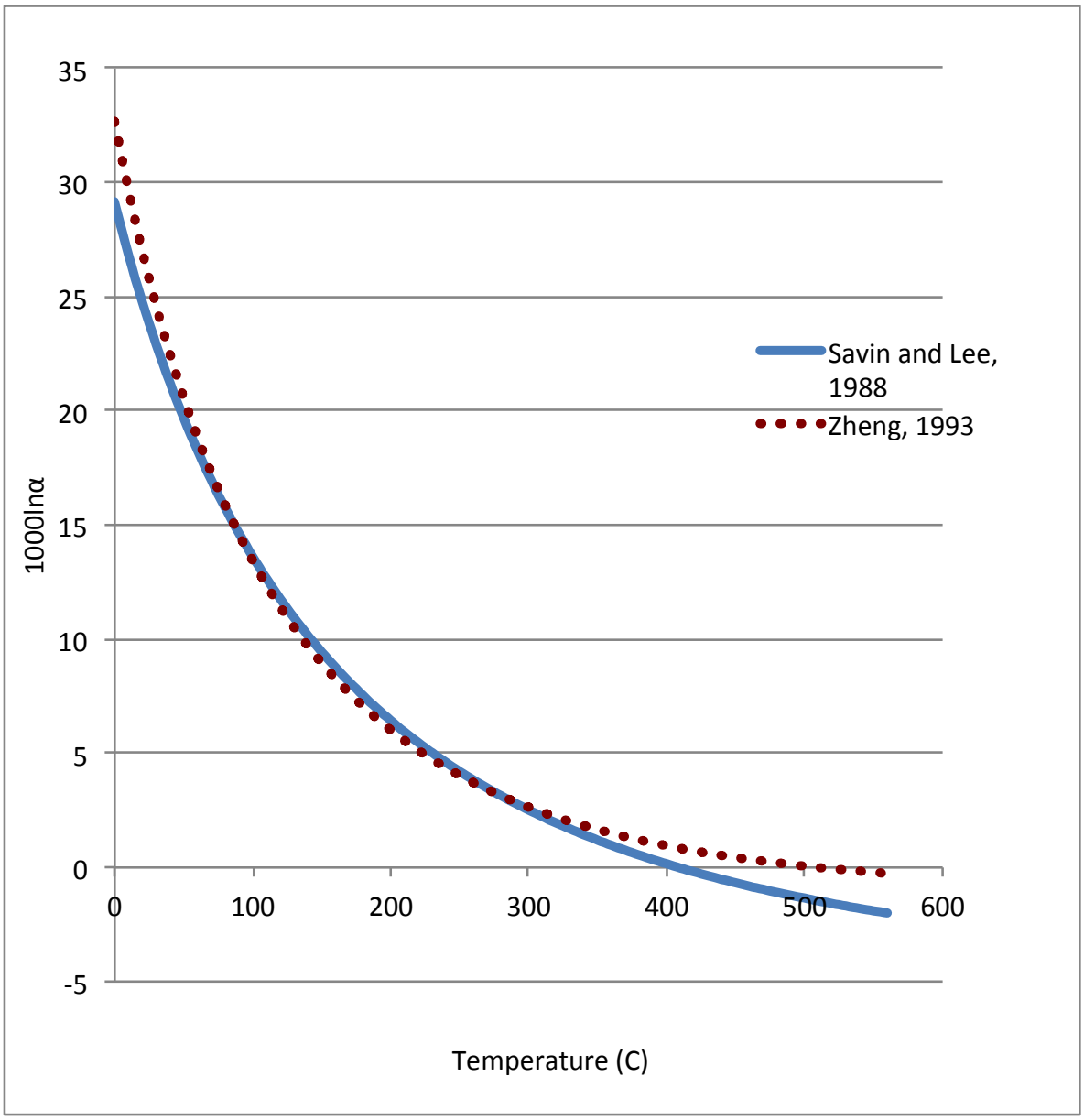

Figure 2: Theoretical equilibrium fractionation factors for talc-water determined by Zheng (1993), and Savin and Lee (1988)

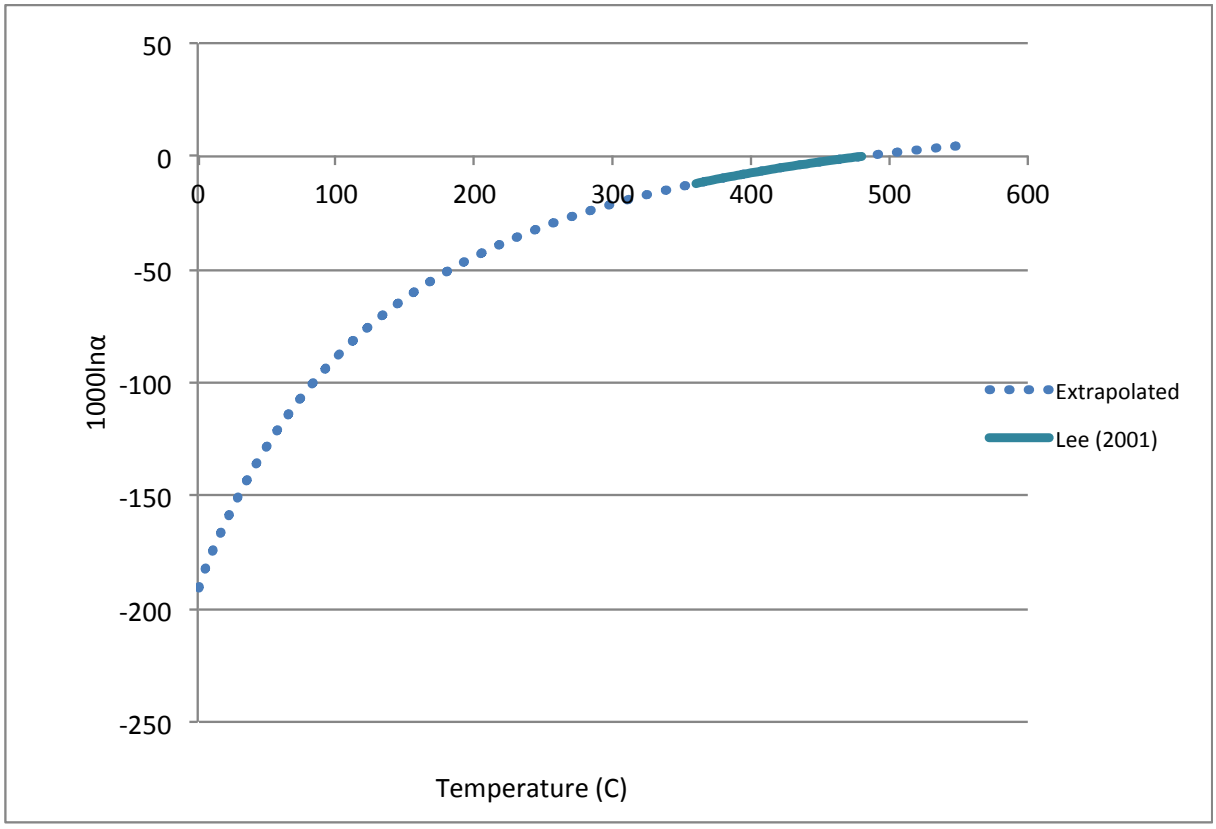

Figure 3: Hydrogen talc-H_2O equilibrium fractionation factor from Lee (2001)

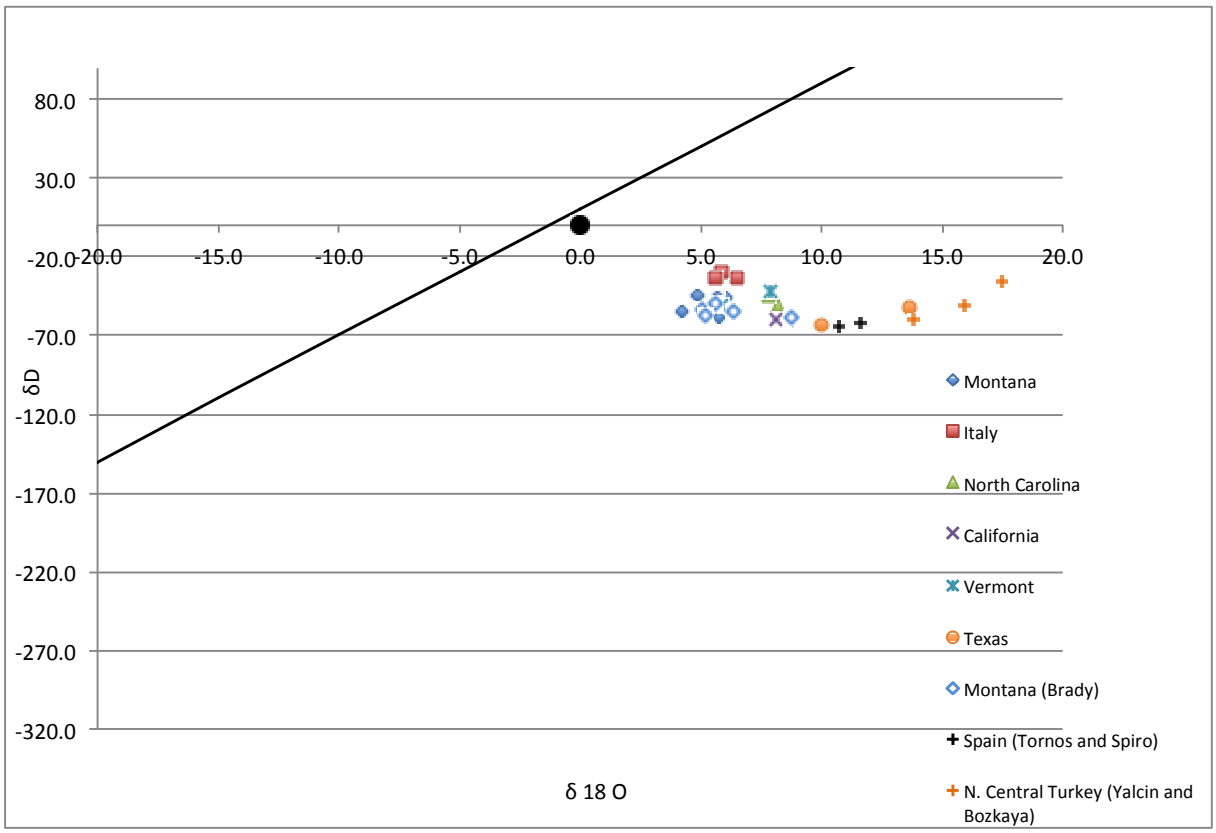

Figure 4: Oxygen and hydrogen isotope ratios for our samples and those from other studies for comparison, plotted relative to the MWL and modern seawater

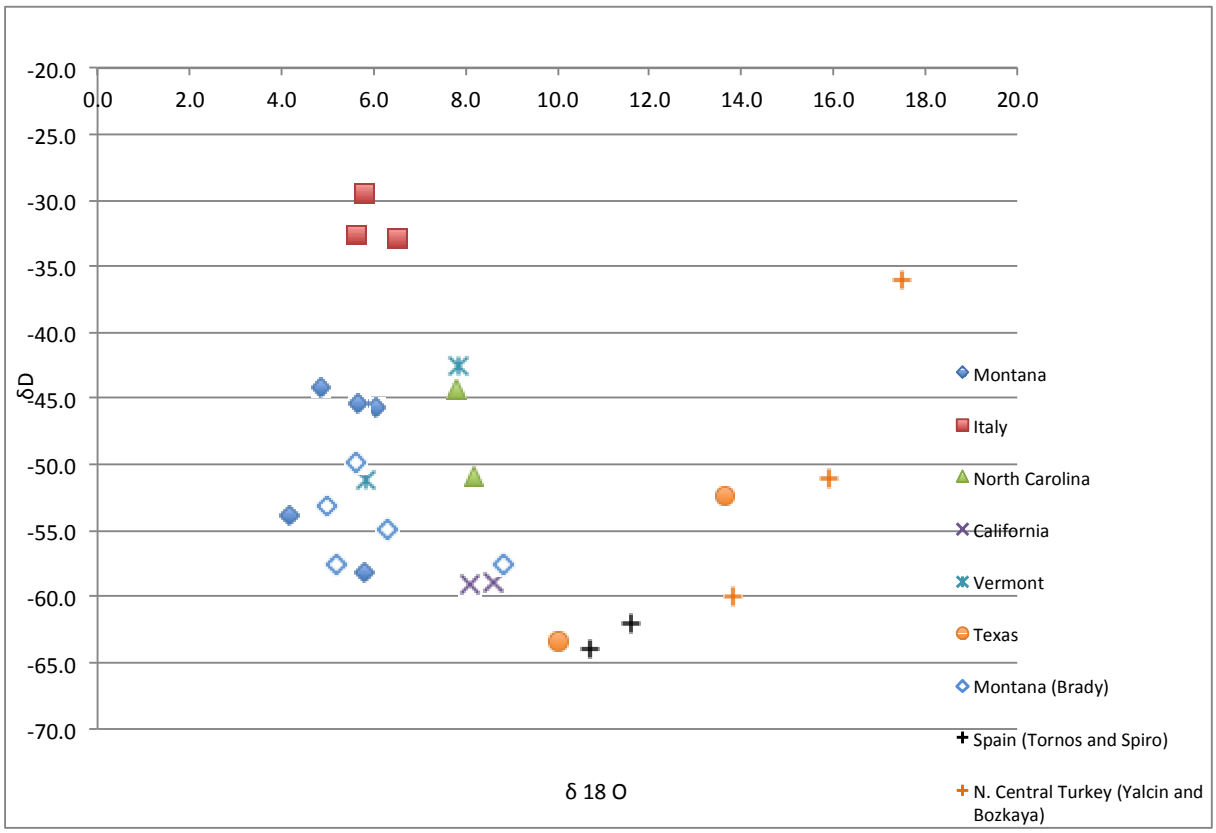

Figure 5: A zoomed in view of the oxygen and hydrogen isotope ratios for our samples and those from other studies to show variation among samples from different locations

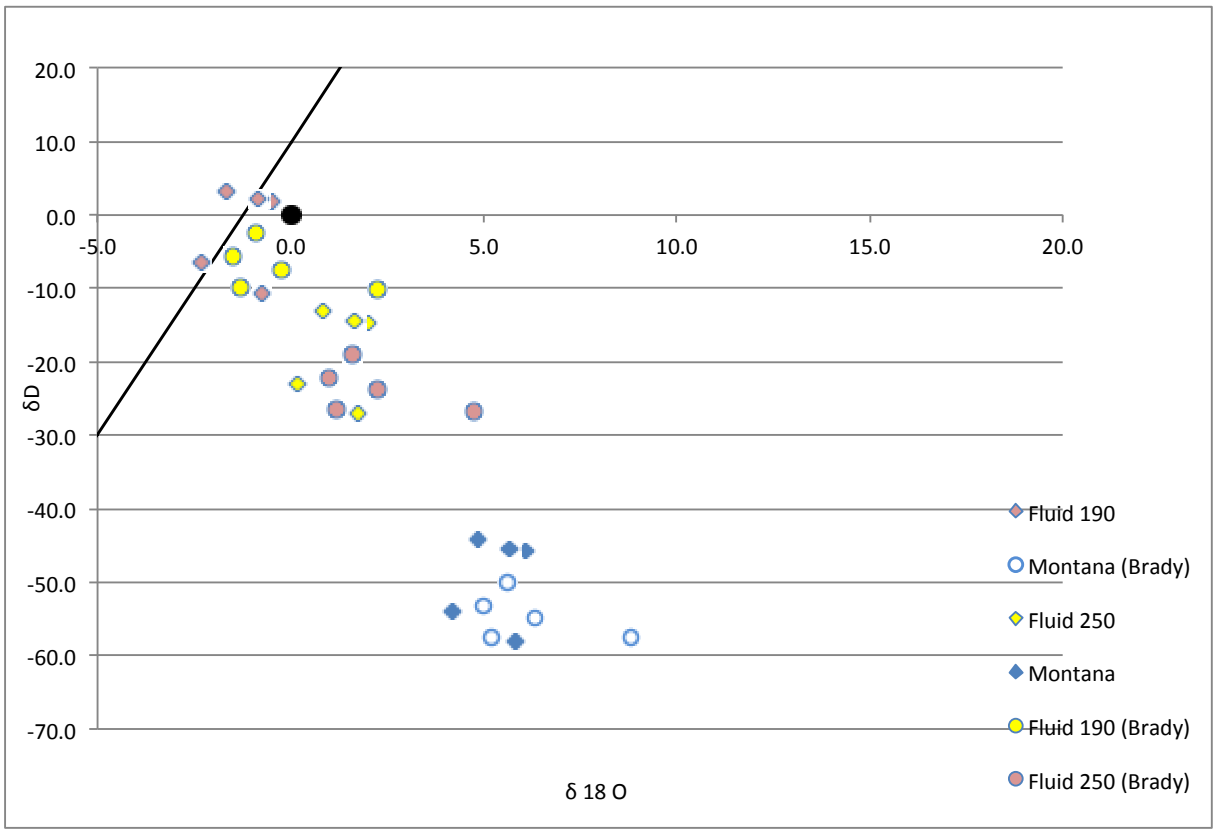

Figure 6: A plot showing the hydrogen and oxygen isotope compositions of the talc-forming fluid based on Lee's (2001) and Zheng's (1993) talc-H_2O equilibrium fractionation factors. The temperature range of 190-250° C is from Gammons and Matt (2002).

Table 1: Compositional EPMA and XRF data for talc samples
Atoms per formula unit (APFU) values are calculated based on weight percent oxide EPMA data.
Trace element concentrations are in parts per million (ppm), (-) indicates not analyzed for.
Samples are ordered based on Fe content, which is often helpful in distinguishing ultramafic- from carbonate-hosted talcs. The two samples from Vermont at the only ones with ultramafic origin, yet they are compositionally similar to some samples from Montana, excluding the Ni and Cr content. Samples from carbonate-hosted talc ores are not easy to distinguish based on composition.

	APFU values from EPMA										Trace elements from XRF	
Sample Name	Si4+	Al3+	Fe2+	Mg2+	Ca2+	Na+	F-	OH-	Tet	Oct	Ni	Cr
USA_TX_VanHorn_gray	4.01	0.01	0.00	2.95	0.01	0.01	0.07	1.93	4.01	2.97	1.40	2.66
USA_TX_VanHorn_pink	4.00	0.00	0.00	2.99	0.00	0.01	0.04	1.96	4.00	3.00	1.68	2.38
USA_MT_Treasure_G1_lo Fe	4.01	0.01	0.01	2.95	0.00	0.00	0.02	1.98	4.01	2.98	27.86	2.24
USA_MT_Regal_HG	4.01	0.02	0.03	2.93	0.00	0.01	0.02	1.98	4.01	2.98	20.37	25.78
ITA_Gianna_C	4.02	0.01	0.04	2.91	0.00	0.00	0.05	1.95	4.02	2.96	10.18	7.64
ITA_Paola_A	4.01	0.01	0.04	2.91	0.00	0.00	0.05	1.95	4.01	2.97	18.06	15.12
USA_CA_TalcCity_6_dark	4.04	0.03	0.04	2.83	0.00	0.01	0.04	1.96	4.04	2.91	-	-
USA_NC_Foote	3.99	0.01	0.05	2.96	0.00	0.00	0.10	1.90	3.99	3.01	10.00	91.00
USA_CA_TalcCity_6_light	4.02	0.02	0.05	2.87	0.00	0.01	0.05	1.95	4.02	2.96	-	-
USA_NC_HC_light rock	3.97	0.03	0.06	2.95	0.00	0.00	0.08	1.92	4.00	3.02	7.00	9.00
USA_MT_Yellowstone_HG	3.98	0.01	0.06	2.96	0.00	0.00	0.06	1.94	3.99	3.02	18.89	9.60
ITA_Gianna_A	4.02	0.01	0.07	2.87	0.00	0.00	0.06	1.94	4.02	2.96	8.06	11.17
USA_MT_Yellowstone_LG	3.99	0.00	0.07	2.95	0.00	0.00	0.06	1.94	3.99	3.02	4.68	8.69
USA_VT_Argonaut_flake	3.99	0.00	0.10	2.92	0.00	0.00	0.01	1.99	3.99	3.02	2421.00	54.00
USA_MT_Treasure_pseudo	4.01	0.01	0.10	2.85	0.00	0.01	0.03	1.97	4.01	2.98	-	-
USA_MT_Willow Creek_8	3.98	0.00	0.10	2.93	0.00	0.00	0.03	1.97	3.99	3.03	16.26	22.12
USA_MT_Treasure_G1_hi Fe	4.02	0.00	0.12	2.83	0.00	0.00	0.06	1.94	4.02	2.96	27.86	2.24
USA_VT_Johnson_black	3.99	0.00	0.18	2.84	0.00	0.00	0.02	1.98	3.99	3.02	621.00	1043.00

Table 2: Oxygen and hydrogen isotope ratios for talc samples, our results and previously published.

Sample	Location	δ18O	δ18O repeat	δ18O repeat	Average O	H	Repeat H	Average
USA_MT_WillowCr 8	Greenhorn Range, MT	6.1			6.1	-45.6		-45.6
USA_MT_Yellowstone_ HG	Gravelly Range, MT	4.2			4.2	-53.9		-53.9
USA_MT_Treasure_G1	Ruby Range, MT	5.7			5.7	-45.4		-45.4
USA_MT_Yellowstone_LG	Gravelly Range, MT	5.8			5.8	-58.1		-58.1
USA_MT Regal_HG	Ruby Range, MT	4.9			4.9	-44.2		-44.2
USA_MT_ Treasure_pseudo	Ruby Range, MT	5.7			5.7	-45.4		-45.4
ITA_Paola_A	Chisone Valley, Italy	6.7	6.3		6.5	-32.9		-32.9
ITA_Gianna_A	Chisone Valley, Italy	5.8			5.8	-29.4		-29.4
ITA_Gianna_C	Chisone, Valley, Italy	5.0	7.0	5.0	5.6	-30.8	-34.5	-32.7
USA_NC_HC_rx-light	Hitchcock County, North Carolina	8.2			8.2	-50.9		-50.9
USA_ NC_Foote	Hitchcock County, North Carolina	8.3	7.3		7.8	-44.3		-44.3
USA_CA_TalcCity_6-light	Talc City, California	8.6			8.6	-58.3	-59.6	-59.0
USA_CA_TalcCity_6-dark	Talc City, California	8.1			8.1	-59.1		-59.1
USA_VT_Johnson_black	Johnson, Vermont	7.9			7.9	-41.8	-43.2	-42.5
USA_VT_Argonaut_xst	Ludlow, Vermont	5.8			5.8	-51.1		-51.1
USA_TX_VanHorn_gray	Van Horn, Texas	13.7			13.7	-52.4		-52.4
USA_TX_VanHorn_pink	Van Horn, Texas	10.0			10.0	-63.1	-63.5	-63.3
Publication	Location, Mine							
Tornos & Spiro	N Central Spain (Cantabria)				10.7			-64.0
Tornos & Spiro	N Central Spain (Cantabria)				11.6			-62.0
Brady et al. (1998)	MT, Regal Keystone				8.8			-57.6
Brady et al. (1998)	MT, Regal Keystone				6.3			-54.9
Brady et al. (1998)	MT, American Chemet				5.0			-53.1
Brady et al. (1998)	MT, American Chemet				5.6			-49.9
Brady et al. (1998)	MT, Treasure Chest				5.2			-57.5
Yalcin & Bozkaya	N Central Turkey (sed)				17.5			-36.0
Yalcin & Bozkaya	N Central Turkey (um)				13.8			-60.0
Yalcin & Bozkaya	N Central Turkey (um)				15.9			-51.0

Table 3: Results and previously published isotope ratios and corresponding equilibrium temperatures if we assume fluids had modern seawater composition. The approximations based on Zheng (1993) and Savin and Lee (1988) are in agreement. The approximations based on Lee (2001) are not always in agreement but produce reasonable values.

		Measured	Zheng	Savin & Lee	Measured	Lee
Sample	Location	δ18 O	T(C)	T(C)	δD	T (C)
USA_MT_WillowCr 8	Greenhorn Range, MT	6.1	198.0	206.0	-45.6	196.0
USA_MT_Yellowstone_ HG	Gravelly Range, MT	4.2	245.0	250.0	-53.9	172.0
USA_MT_Treasure_G1	Ruby Range, MT	5.7	207.0	215.0	-45.4	197.0
USA_MT_Yellowstone_LG	Gravelly Range, MT	5.8	205.0	213.0	-58.1	161.0
USA_MT Regal_HG	Ruby Range, MT	4.9	226.0	233.0	-44.2	200.0
USA_MT_ Treasure_pseudo	Ruby Range, MT	5.7	207.0	215.0	-45.4	197.0
ITA_Paola_A	Chisone Valley, Italy	6.5	190.0	199.0	-32.9	242.0
ITA_Gianna_A	Chisone Valley, Italy	5.8	205.0	213.0	-29.4	257.0
ITA_Gianna_C	Chisone, Valley, Italy	5.6	209.0	217.0	-32.7	243.0
USA_NC_HC_rx-light	Hitchcock County, North Carolina	8.2	161.0	169.0	-50.9	180.0
USA_ NC_Foote	Hitchcock County, North Carolina	7.8	168.0	176.0	-44.3	200.0
USA_CA_TalcCity_6-light	Talc City, California	8.6	155.0	163.0	-59.0	159.0
USA_CA_TalcCity_6-dark	Talc City, California	8.1	163.0	171.0	-59.1	159.0
USA_VT_Johnson_black	Johnson, Vermont	7.9	166.0	174.0	-42.5	206.0
USA_VT_Argonaut_xst	Ludlow, Vermont	5.8	205.0	213.0	-51.1	179.0
USA_TX_VanHorn_gray	Van Horn, Texas	13.7	98.0	99.0	-52.4	176.0
USA_TX_VanHorn_pink	Van Horn, Texas	10.0	136.0	142.0	-63.3	148.0
Publication	Location, Mine	Published			Published	
Tornos & Spiro	N Central Spain (Cantabria)	10.7	128.0	133.0	-64.0	147.0
Tornos & Spiro	N Central Spain (Cantabria)	11.6	118.0	122.0	-62.0	152.0
Brady et al. (1998)	MT, Regal Keystone	8.8	152.0	159.0	-57.6	162.0
Brady et al. (1998)	MT, Regal Keystone	6.3	193.0	205.0	-54.9	158.0
Brady et al. (1998)	MT, American Chemet	5.0	224.0	231.0	-53.1	174.0
Brady et al. (1998)	MT, American Chemet	5.6	209.0	217.0	-49.9	183.0
Brady et al. (1998)	MT, Treasure Chest	5.2	219.0	226.0	-57.5	163.0
Yalcin & Bozkaya	N Central Turkey (sed)	17.5	69.0	67.0	-36.0	229.0
Yalcin & Bozkaya	N Central Turkey (um)	13.8	97.0	98.0	-60.0	156.0
Yalcin & Bozkaya	N Central Turkey (um)	15.9	80.0	79.0	-51.0	179.0

Appendix A: Powder X-ray Diffractograms

This appendix includes the unlabeled diffractograms for all samples discussed in this dissertation. The samples are organized in alphabetical order by location. The first three diffractograms are labeled examples to reference prominent peaks for commonly found phases.

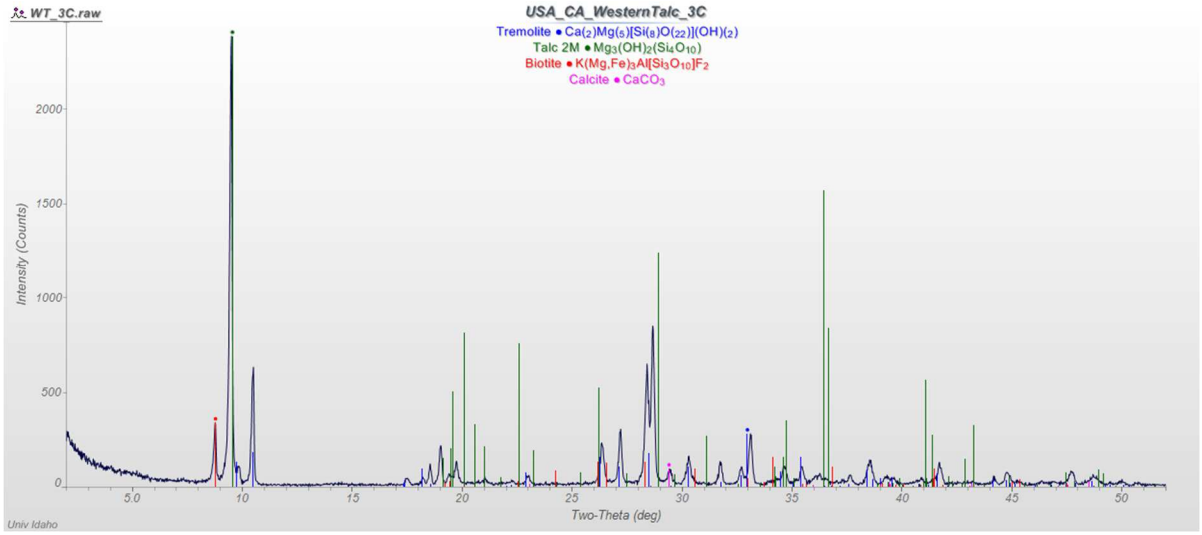

In a mixture such as this we can only confirm that an amphibole species is present, not necessarily tremolite.

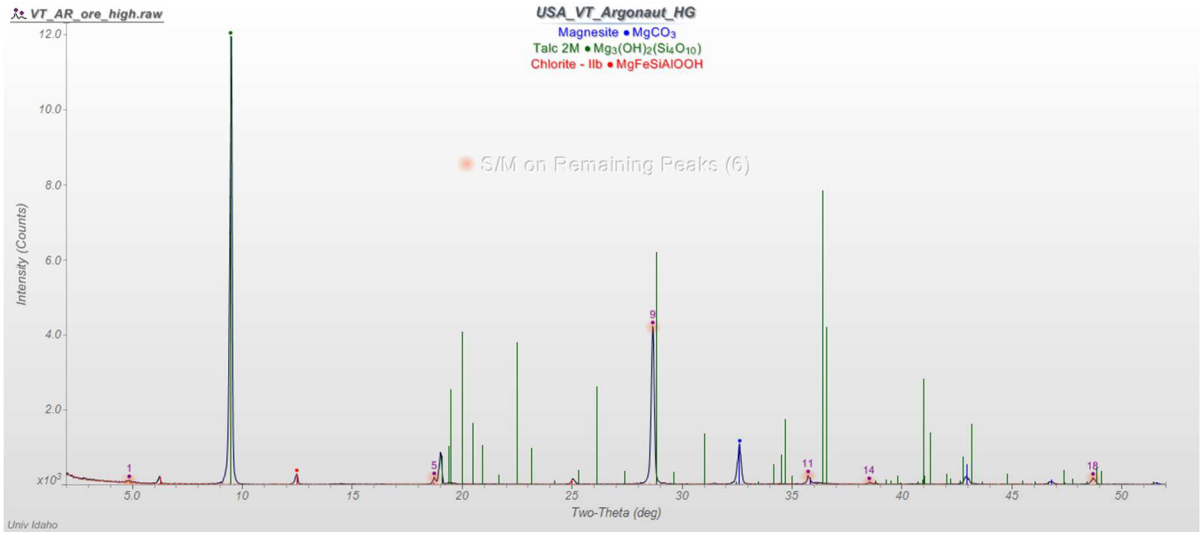

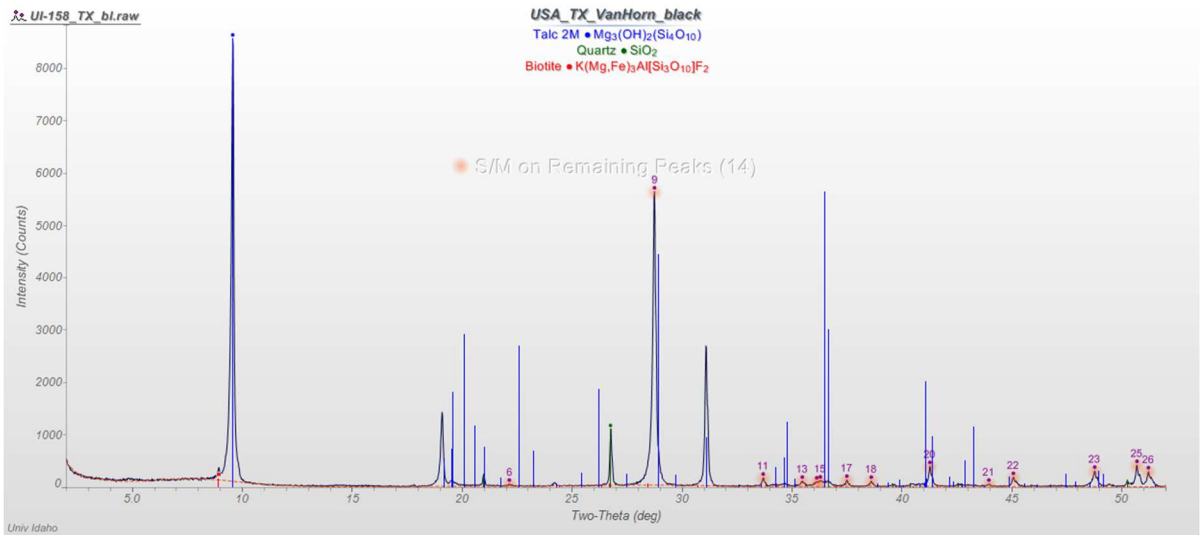
UI-158_TX_bl.raw
USA_TX_VanHorn_black
Talc 2M • $Mg_3(OH)_2(Si_4O_{10})$
Quartz • SiO_2
Biotite • $K(Mg,Fe)_3Al[Si_3O_{10}]F_2$
S/M on Remaining Peaks (14)
Intensity (Counts)
Two-Theta (deg)
Univ Idaho

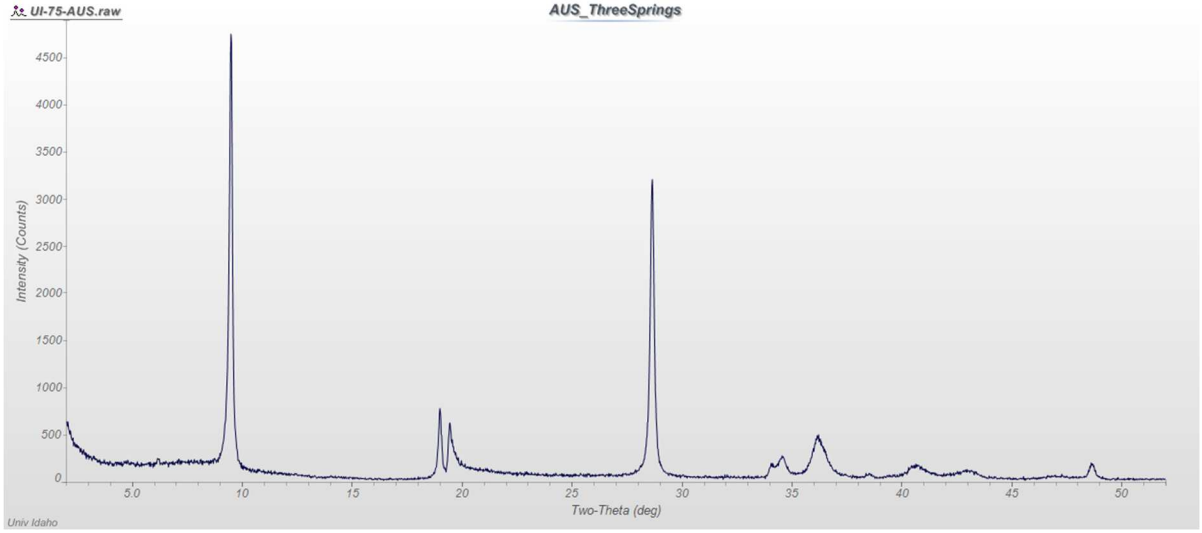
UI-75-AUS.raw
AUS_ThreeSprings
Intensity (Counts)
Two-Theta (deg)
Univ Idaho

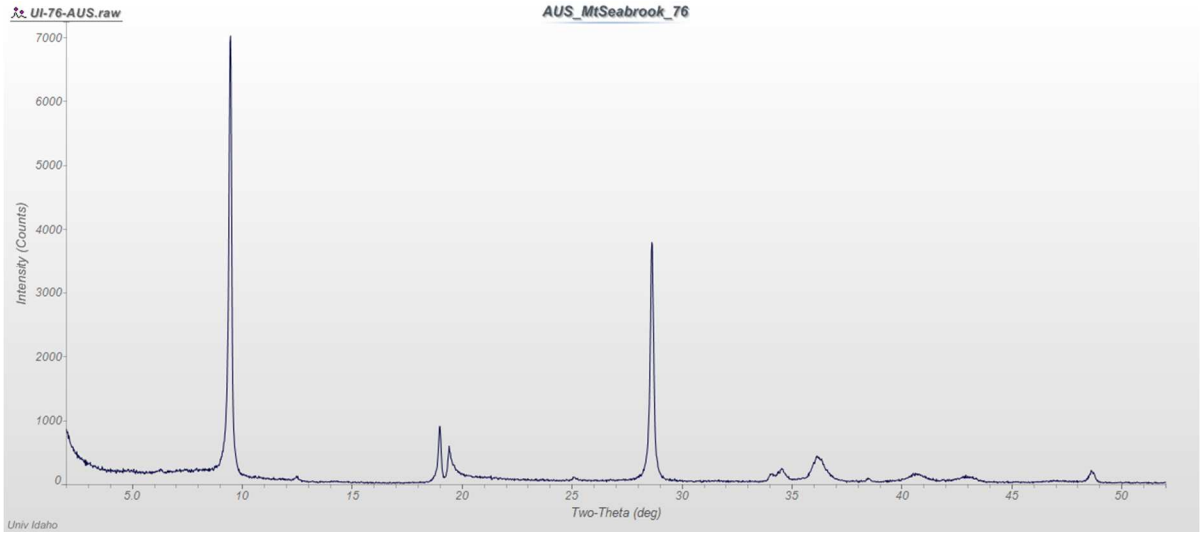
UI-76-AUS.raw
AUS_MtSeabrook_76
Intensity (Counts)
Two-Theta (deg)
Univ Idaho

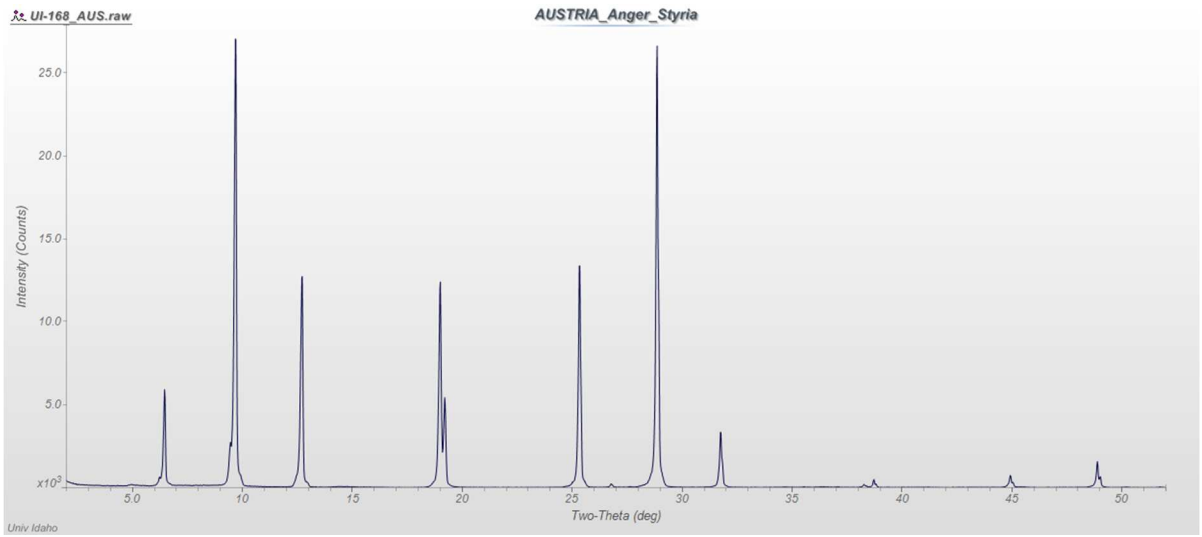
UI-168_AUS.raw
AUSTRIA_Anger_Styria
Intensity (Counts)
x10^3
Two-Theta (deg)
Univ Idaho

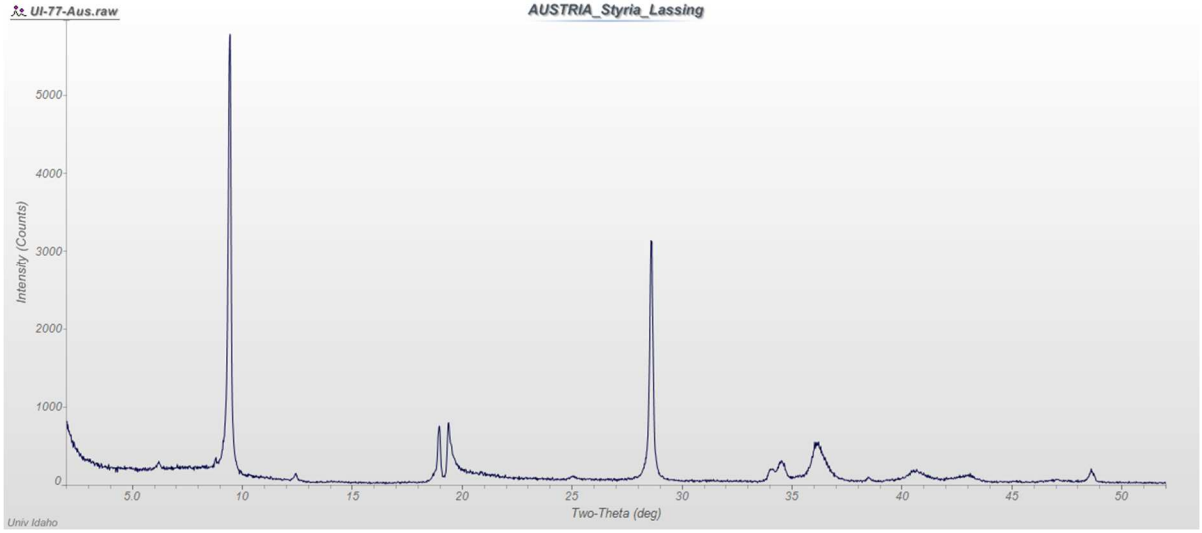
UI-77-Aus.raw
AUSTRIA_Styria_Lassing
Intensity (Counts)
Two-Theta (deg)
Univ Idaho

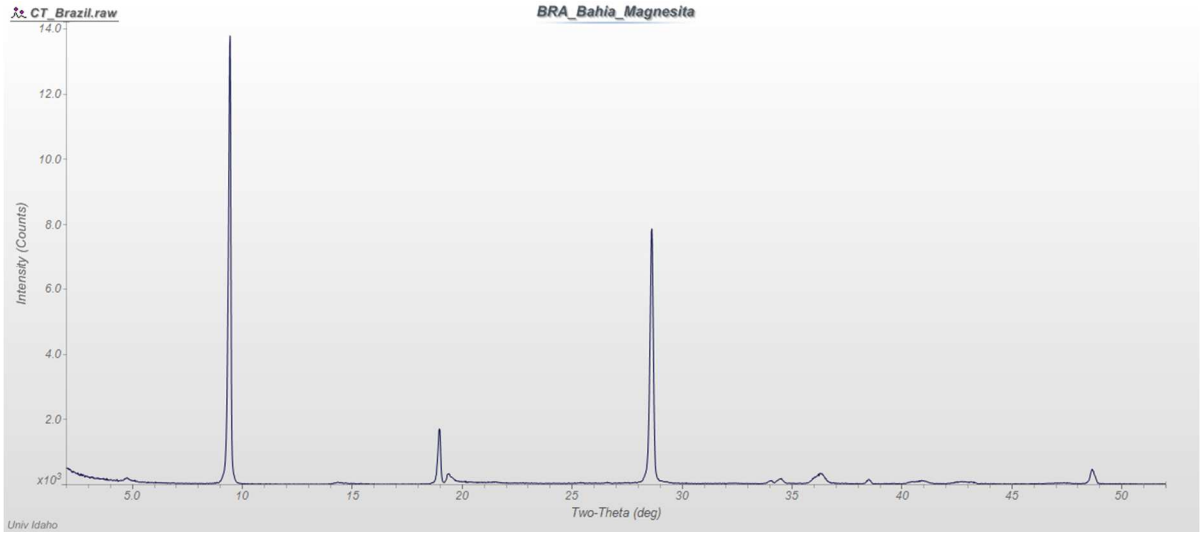
CT_Brazil.raw
BRA_Bahia_Magnesita
Intensity (Counts)
x10^3
Two-Theta (deg)
Univ Idaho

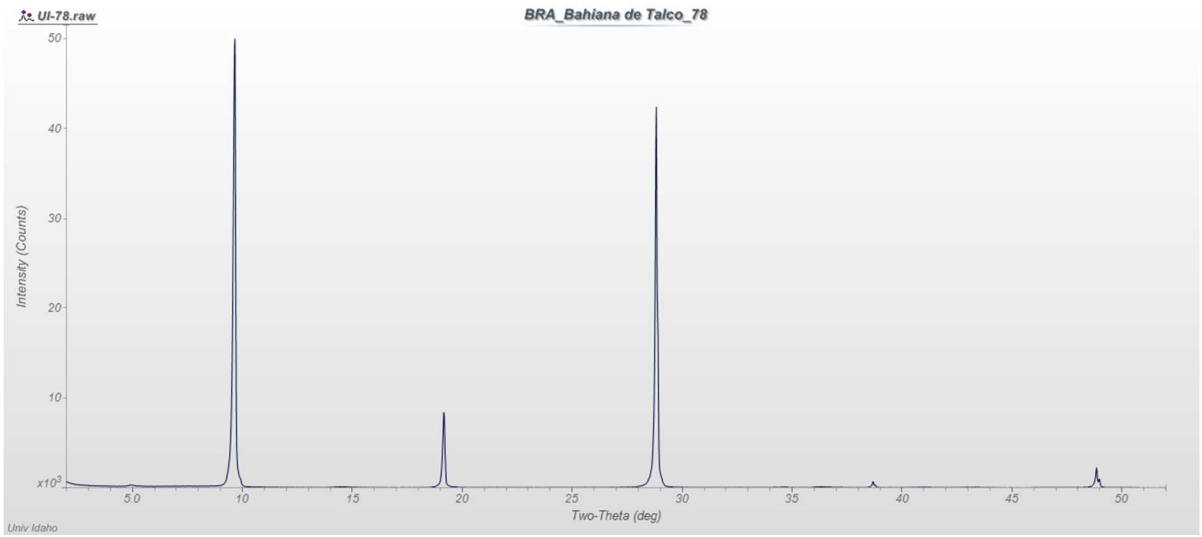
UI-78.raw
BRA_Bahiana de Talco_78
Intensity (Counts)
x10^3
Two-Theta (deg)
Univ Idaho

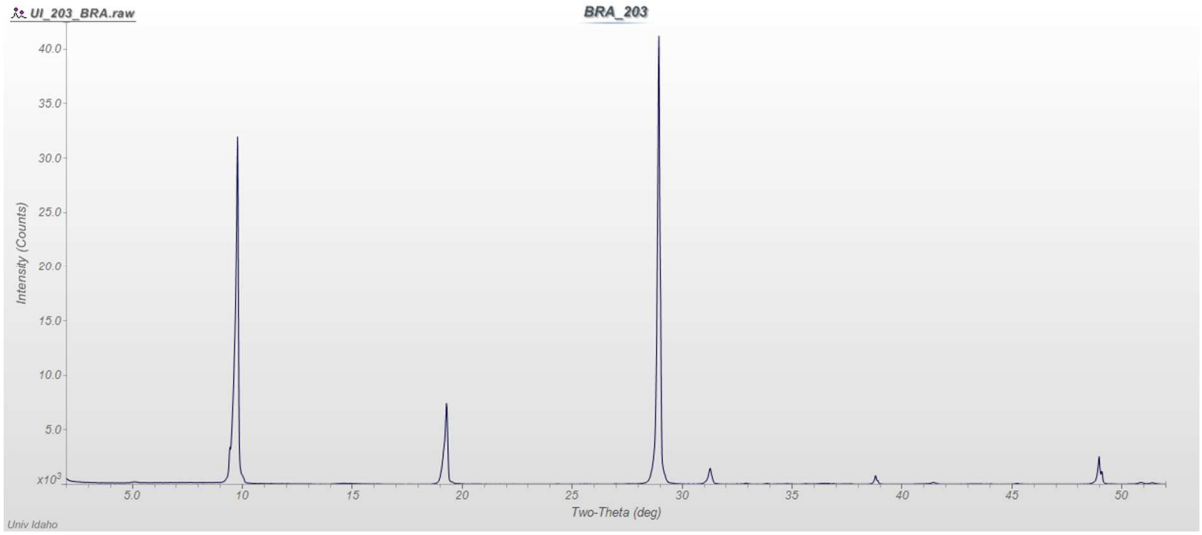
UI_203_BRA.raw
BRA_203
Intensity (Counts)
x10^3
Two-Theta (deg)
Univ Idaho

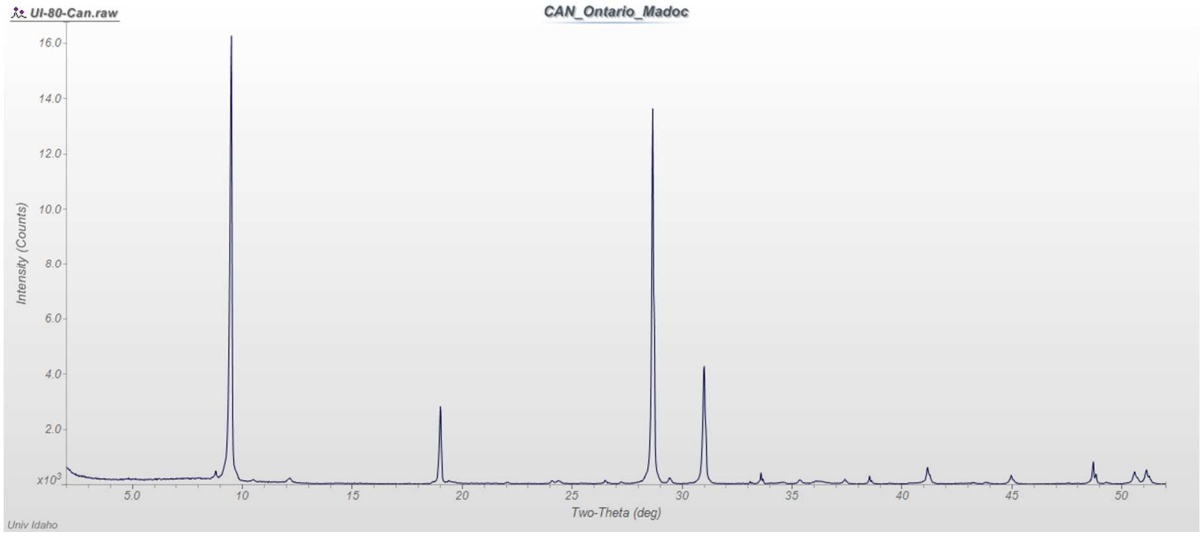
UI-80-Can.raw
CAN_Ontario_Madoc
Intensity (Counts)
x10^3
Two-Theta (deg)
Univ Idaho

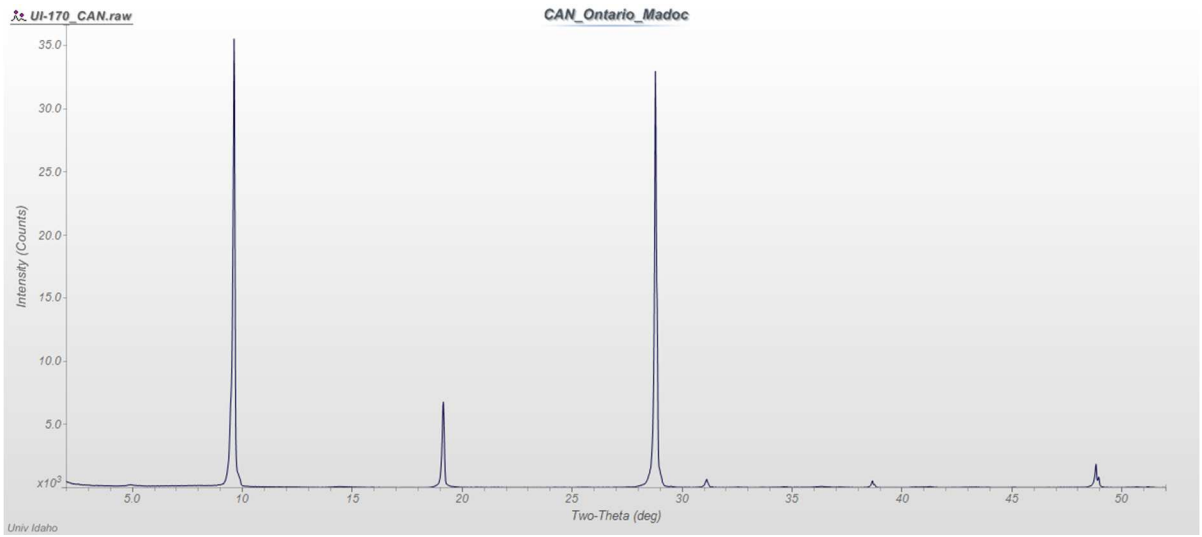
UI-170_CAN.raw
CAN_Ontario_Madoc
Intensity (Counts)
x10^3
Two-Theta (deg)
Univ Idaho

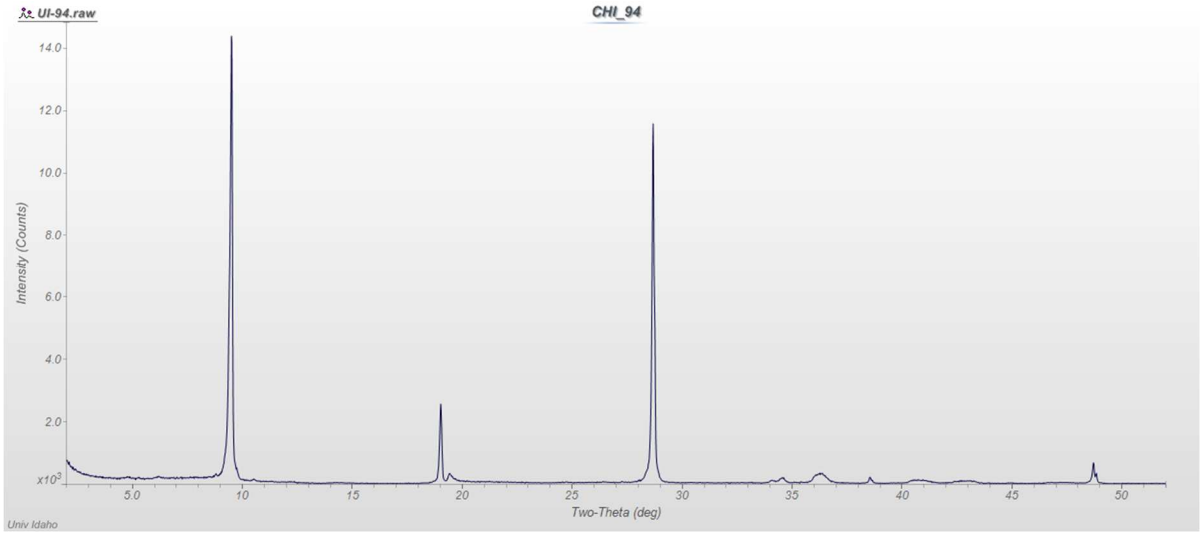
UI-94.raw
CHI_94
Intensity (Counts)
x10^3
Two-Theta (deg)
Univ Idaho

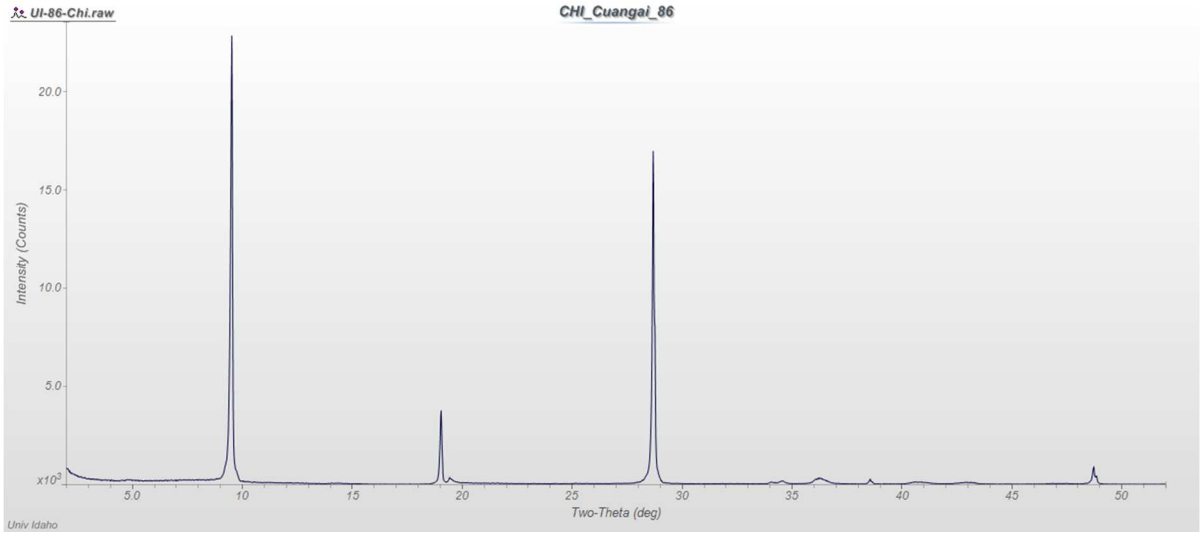
UI-86-Chi.raw
CHI_Cuangai_86
Intensity (Counts)
x10^3
Two-Theta (deg)
Univ Idaho

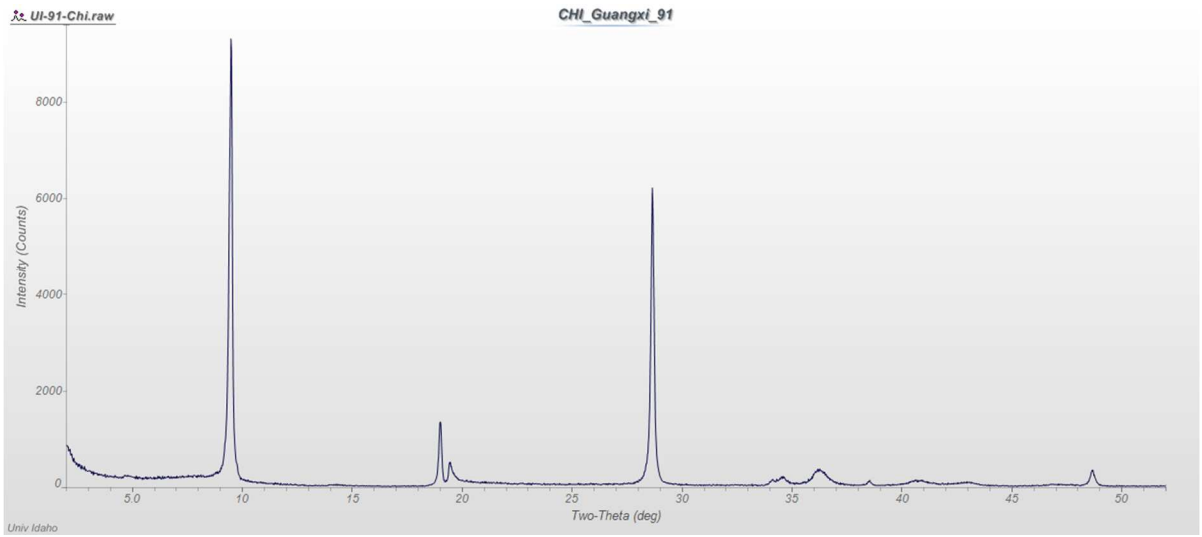
UI-91-Chi.raw
CHI_Guangxi_91
Intensity (Counts)
8000
6000
4000
2000
0
5.0
10
15
20
25
30
35
40
45
50
Two-Theta (deg)
Univ Idaho

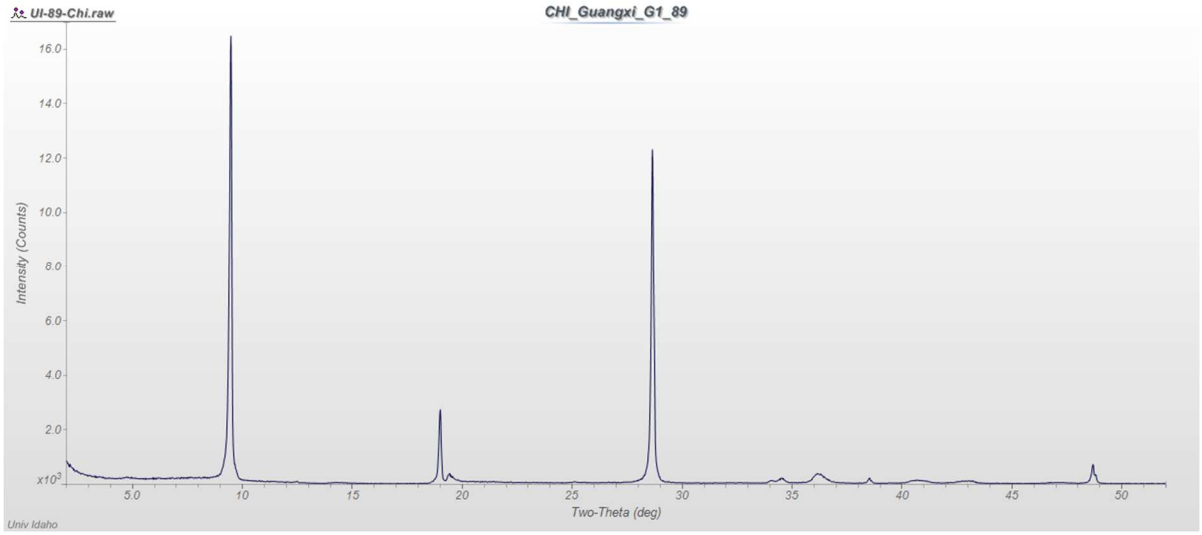
UI-89-Chi.raw
CHI_Guangxi_G1_89
Intensity (Counts)
16.0
14.0
12.0
10.0
8.0
6.0
4.0
2.0
x10^3
5.0
10
15
20
25
30
35
40
45
50
Two-Theta (deg)
Univ Idaho

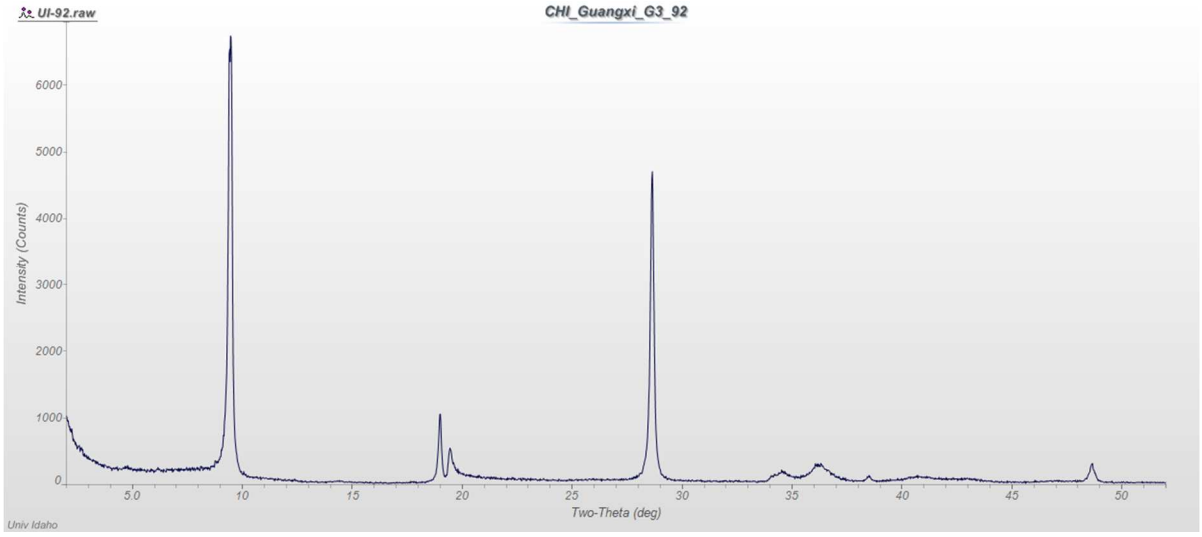
UI-92.raw
CHI_Guangxi_G3_92
Intensity (Counts)
6000
5000
4000
3000
2000
1000
0
5.0
10
15
20
25
30
35
40
45
50
Two-Theta (deg)
Univ Idaho

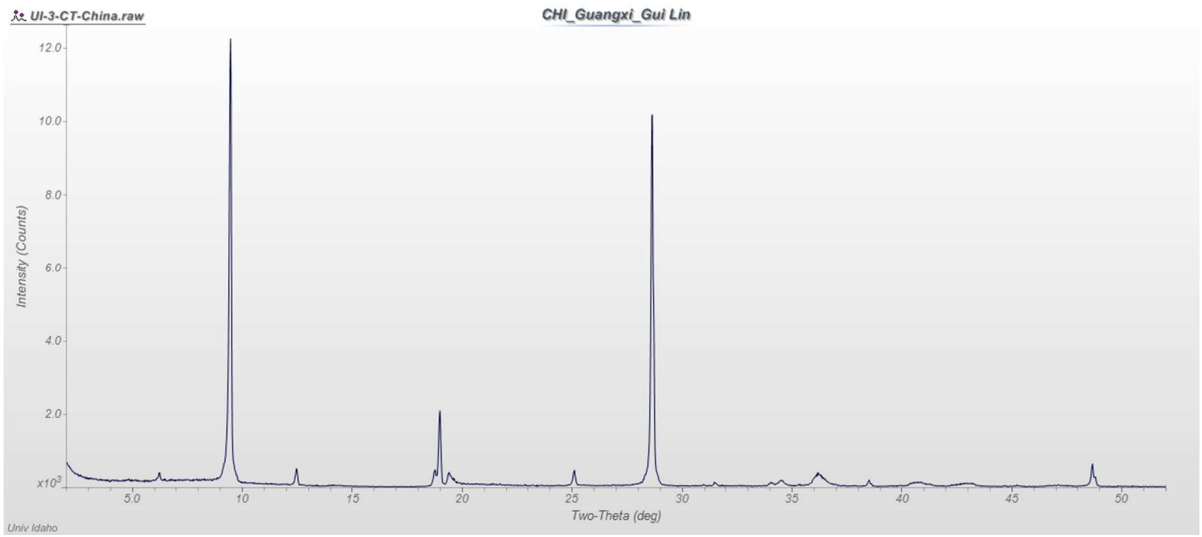
UI-3-CT-China.raw
CHI_Guangxi_Gui Lin
Intensity (Counts)
x10^3
Two-Theta (deg)
Univ Idaho

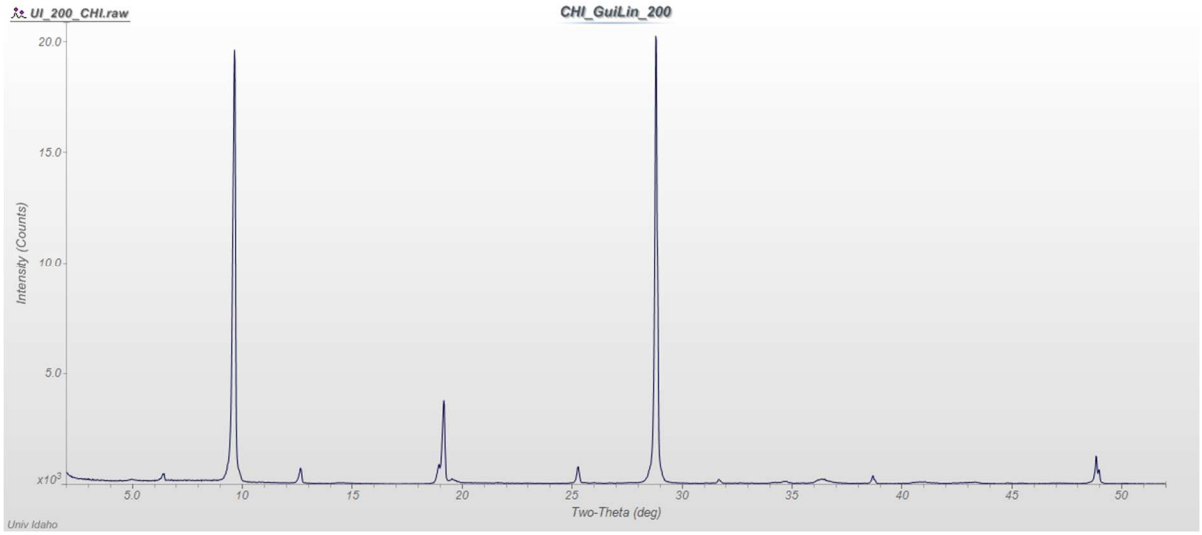
UI_200_CHI.raw
CHI_GuiLin_200
Intensity (Counts)
x10^3
Two-Theta (deg)
Univ Idaho

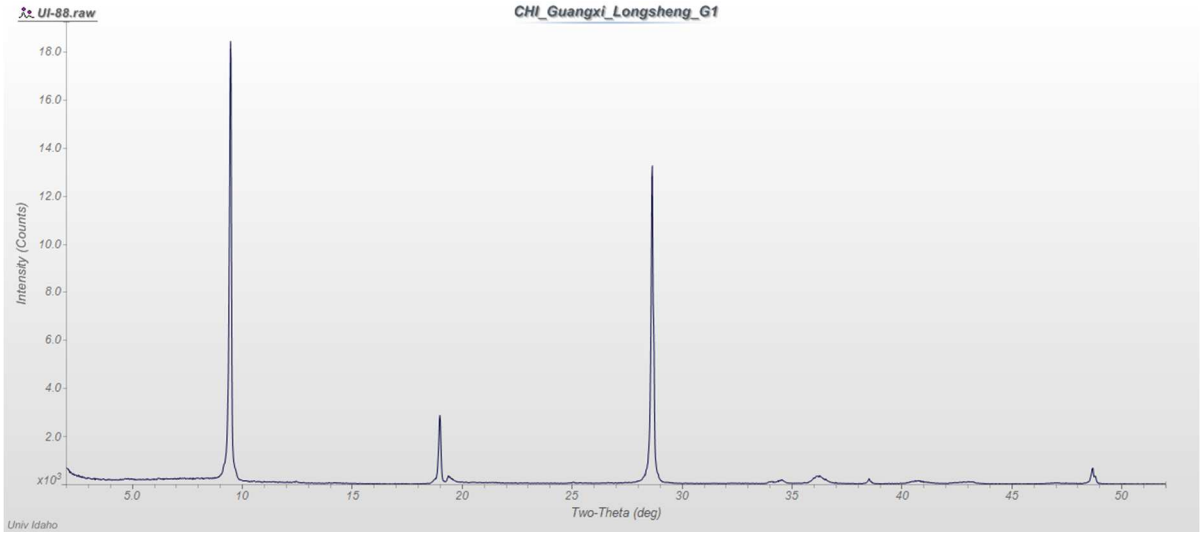
UI-88.raw
CHI_Guangxi_Longsheng_G1
Intensity (Counts)
x10^3
Two-Theta (deg)
Univ Idaho

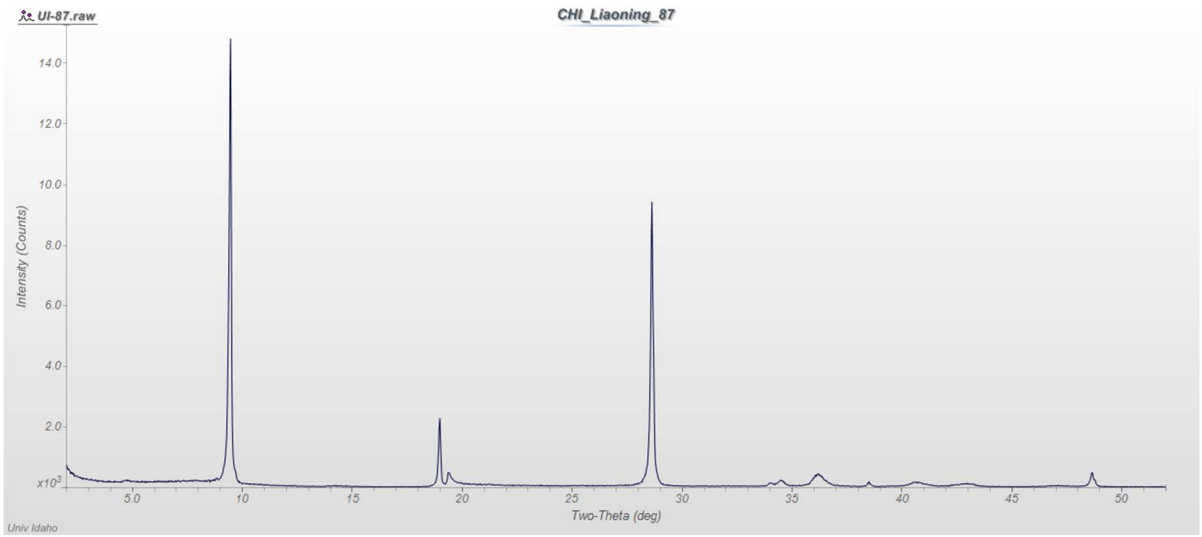
UI-87.raw
CHI_Liaoning_87
Intensity (Counts)
x10^3
Two-Theta (deg)
Univ Idaho

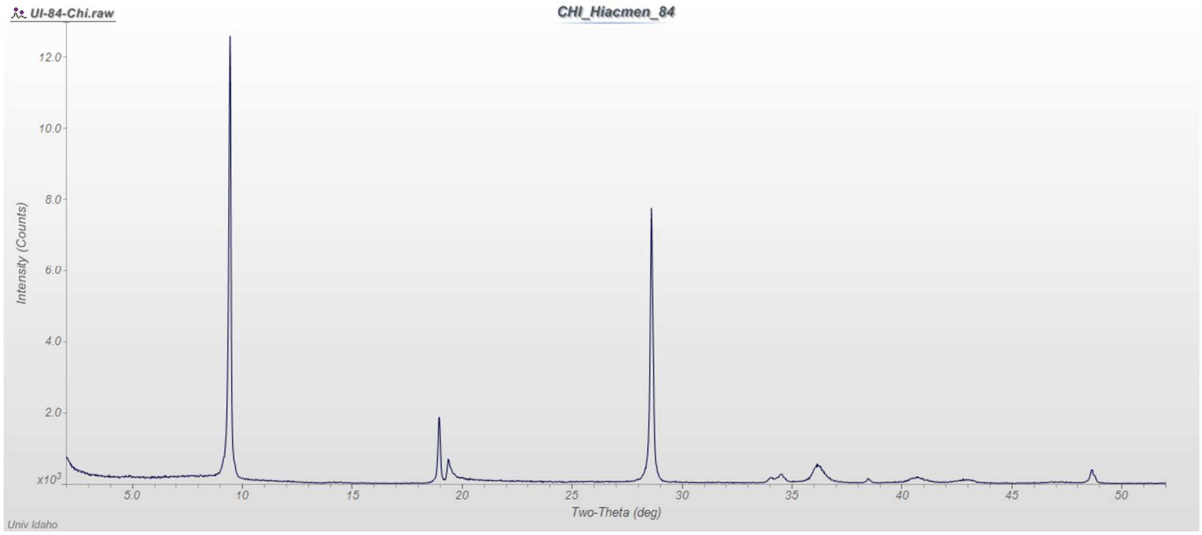
UI-84-Chi.raw
CHI_Hiacmen_84
Intensity (Counts)
x10^3
Two-Theta (deg)
Univ Idaho

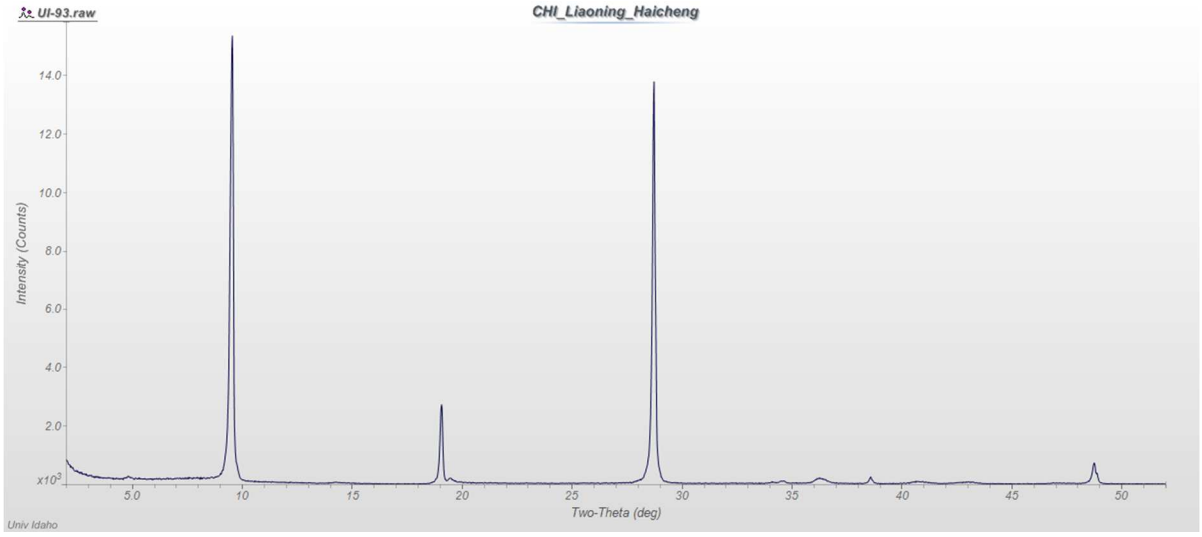
UI-93.raw
CHI_Liaoning_Haicheng
Intensity (Counts)
x10^3
Two-Theta (deg)
Univ Idaho

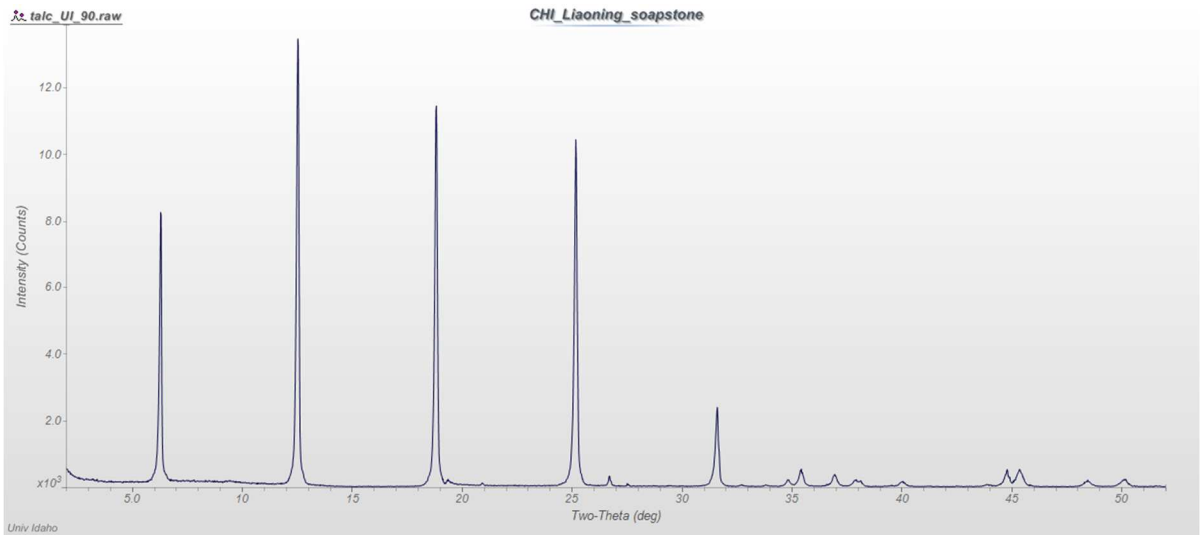
talc_UI_90.raw
CHI_Liaoning_soapstone
Intensity (Counts)
x10^3
Two-Theta (deg)
Univ Idaho

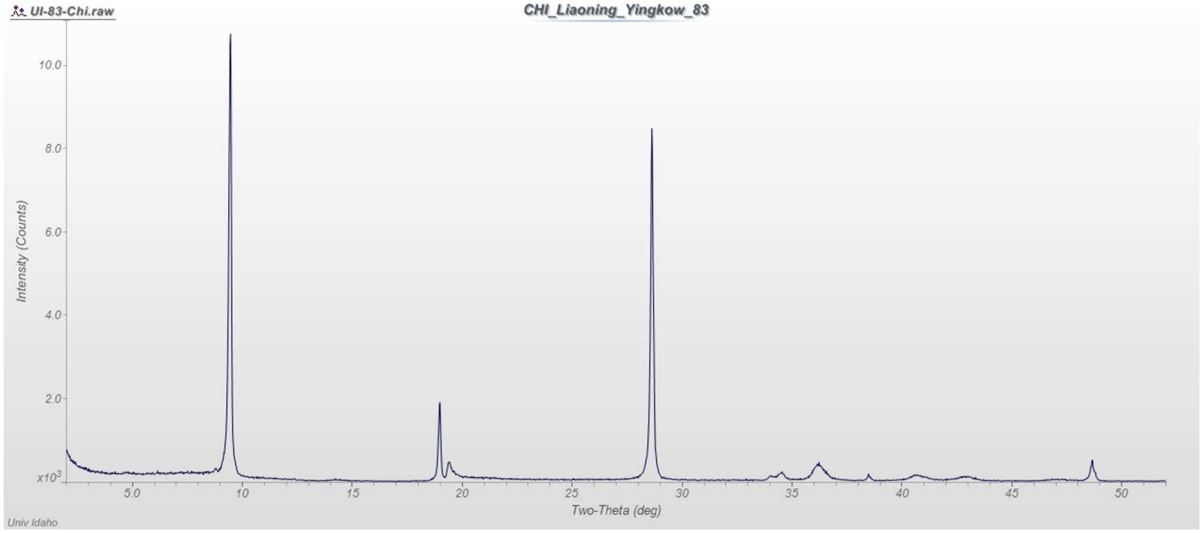
UI-83-Chi.raw
CHI_Liaoning_Yingkow_83
Intensity (Counts)
x10^3
Two-Theta (deg)
Univ Idaho

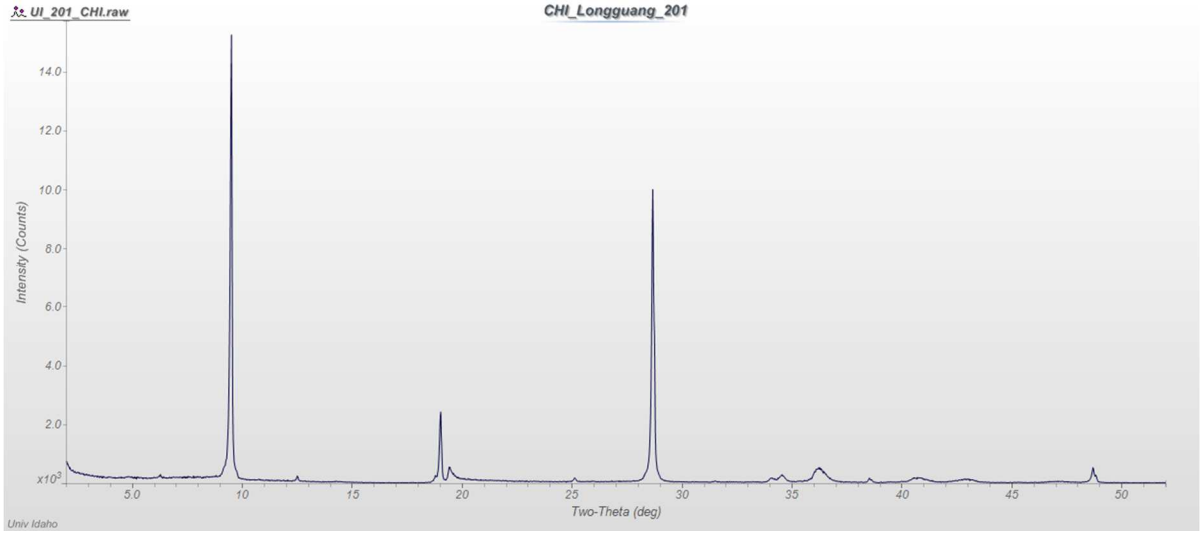
UI_201_CHI.raw
CHI_Longguang_201
Intensity (Counts)
x10^3
Two-Theta (deg)
Univ Idaho

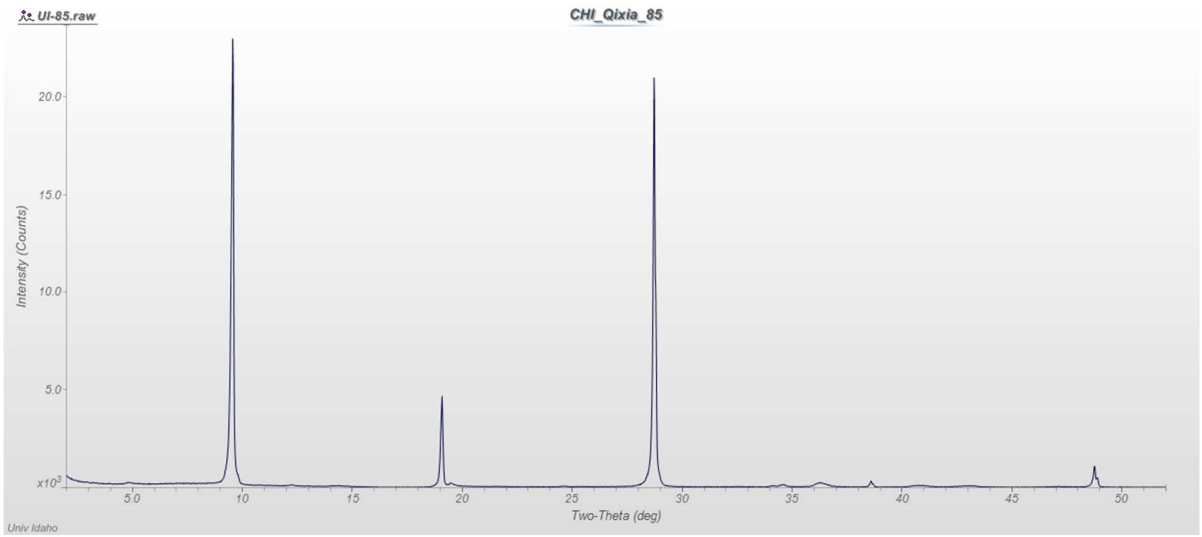
UI-85.raw
CHI_Qixia_85
Intensity (Counts)
x10^3
Two-Theta (deg)
Univ Idaho

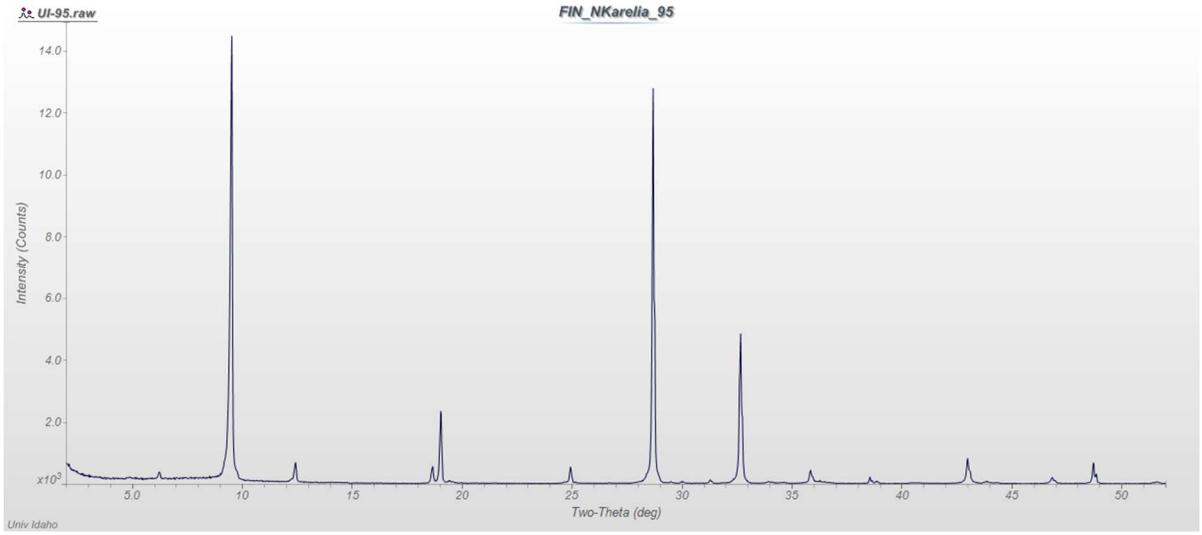
UI-95.raw
FIN_NKarelia_95
Intensity (Counts)
x10^3
Two-Theta (deg)
Univ Idaho

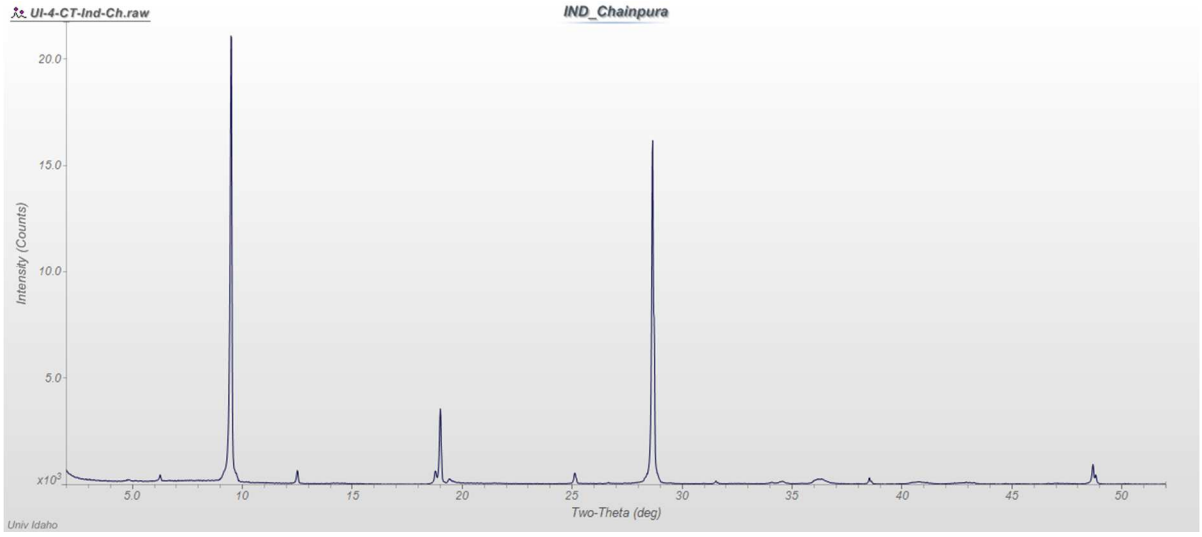
UI-4-CT-Ind-Ch.raw
IND_Chainpura
Intensity (Counts)
x10^3
Two-Theta (deg)
Univ Idaho

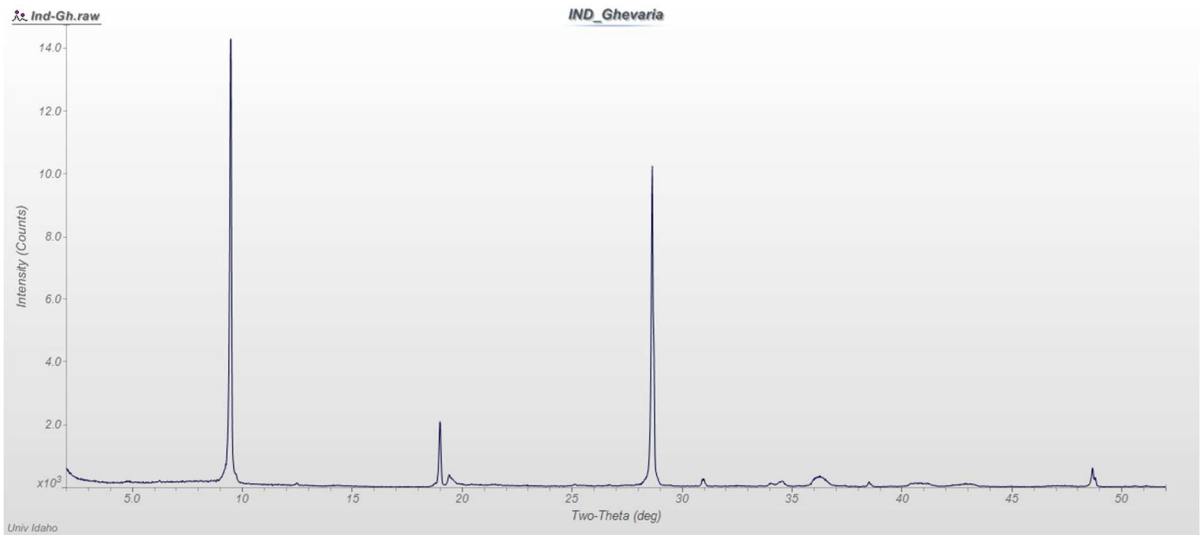
Ind-Gh.raw
IND_Ghevaria
Intensity (Counts)
x10^3
Two-Theta (deg)
Univ Idaho

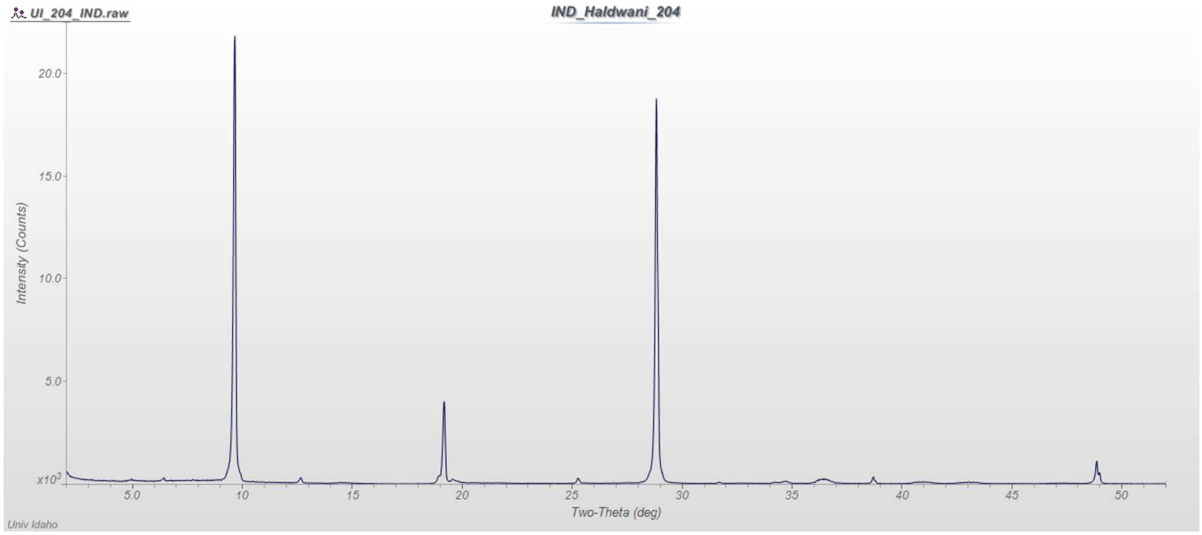
UI_204_IND.raw
IND_Haldwani_204
Intensity (Counts)
x10^3
Two-Theta (deg)
Univ Idaho

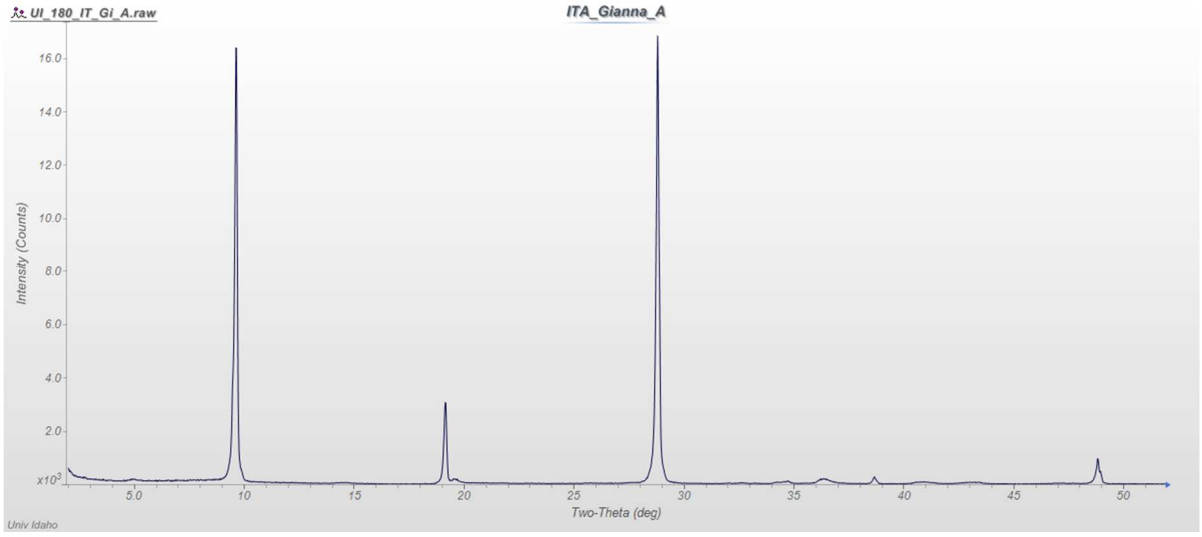
UI_180_IT_Gi_A.raw
ITA_Gianna_A
Intensity (Counts)
x10^3
Two-Theta (deg)
Univ Idaho

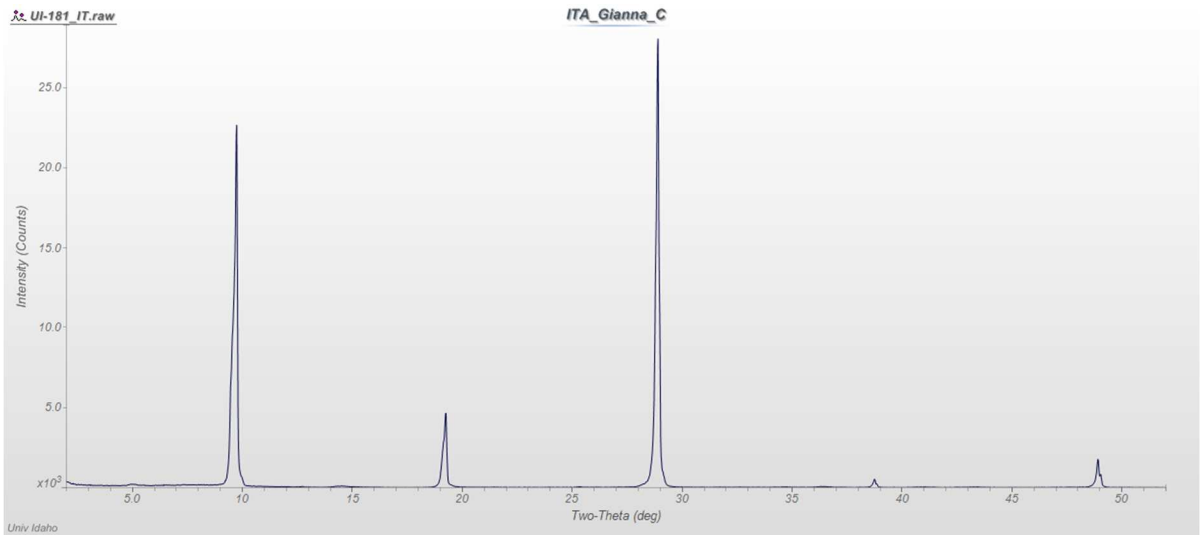
UI-181_IT.raw
ITA_Gianna_C
Intensity (Counts)
x10^3
25.0
20.0
15.0
10.0
5.0
5.0
10
15
20
25
30
35
40
45
50
Two-Theta (deg)
Univ Idaho

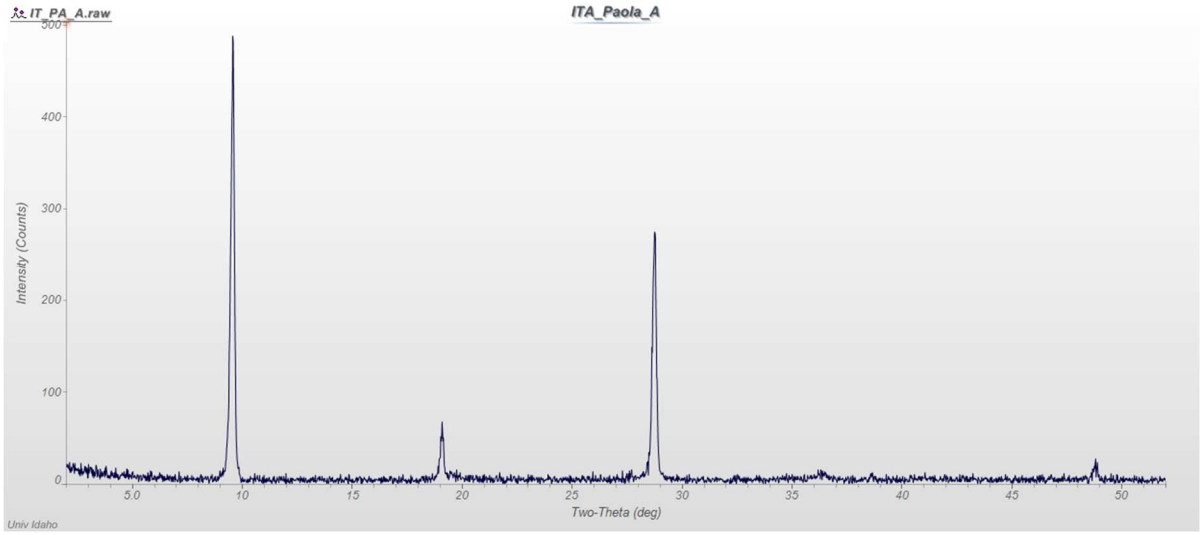
IT_PA_A.raw
ITA_Paola_A
Intensity (Counts)
500
400
300
200
100
0
5.0
10
15
20
25
30
35
40
45
50
Two-Theta (deg)
Univ Idaho

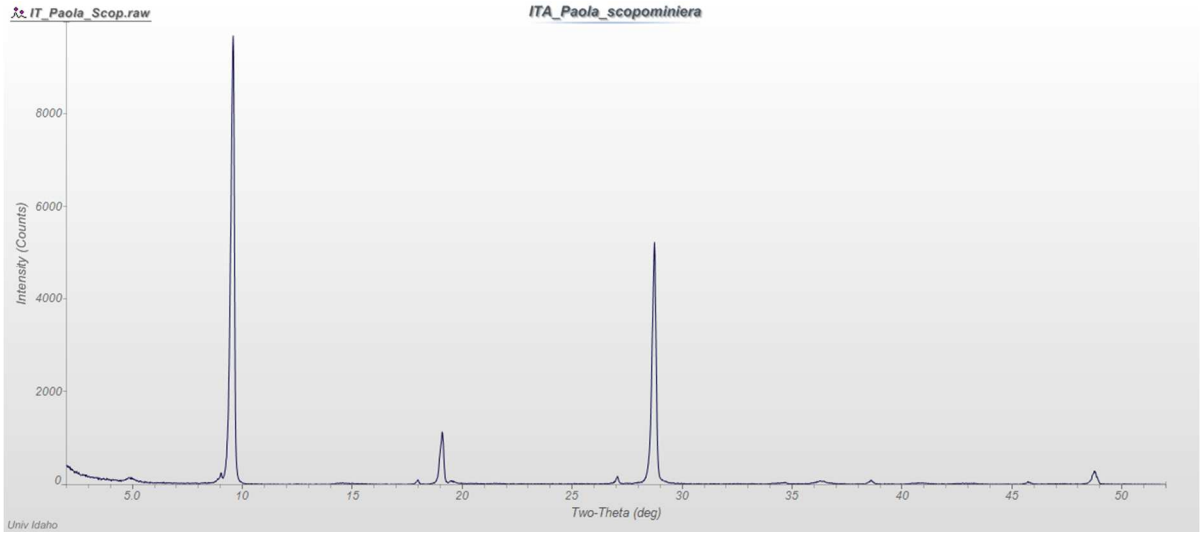
IT_Paola_Scop.raw
ITA_Paola_scopominiera
Intensity (Counts)
8000
6000
4000
2000
0
5.0
10
15
20
25
30
35
40
45
50
Two-Theta (deg)
Univ Idaho

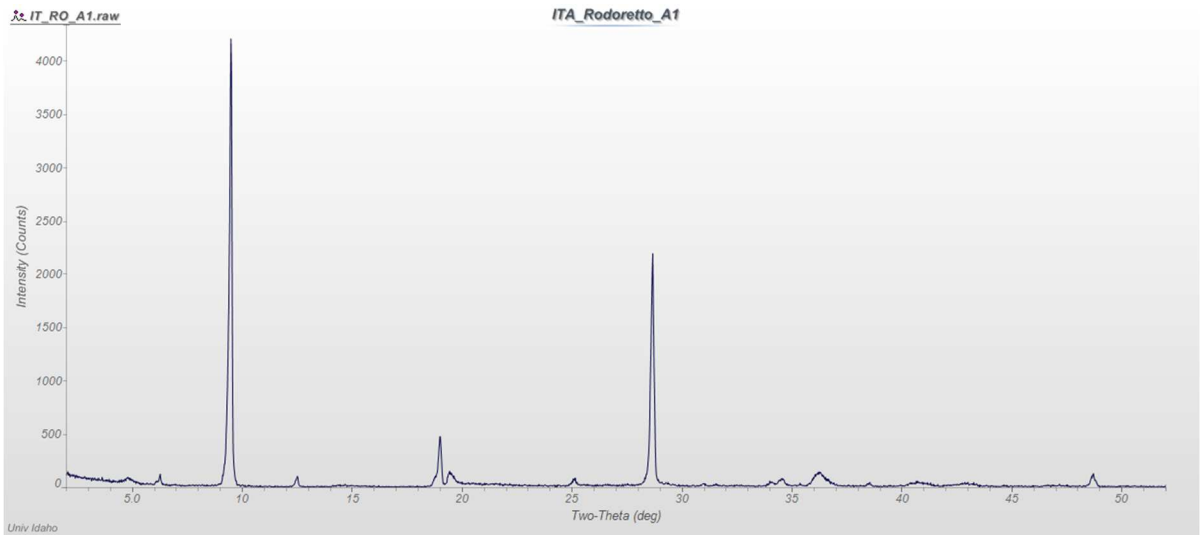
IT_RO_A1.raw
ITA_Rodoretto_A1
Intensity (Counts)
Two-Theta (deg)
Univ Idaho

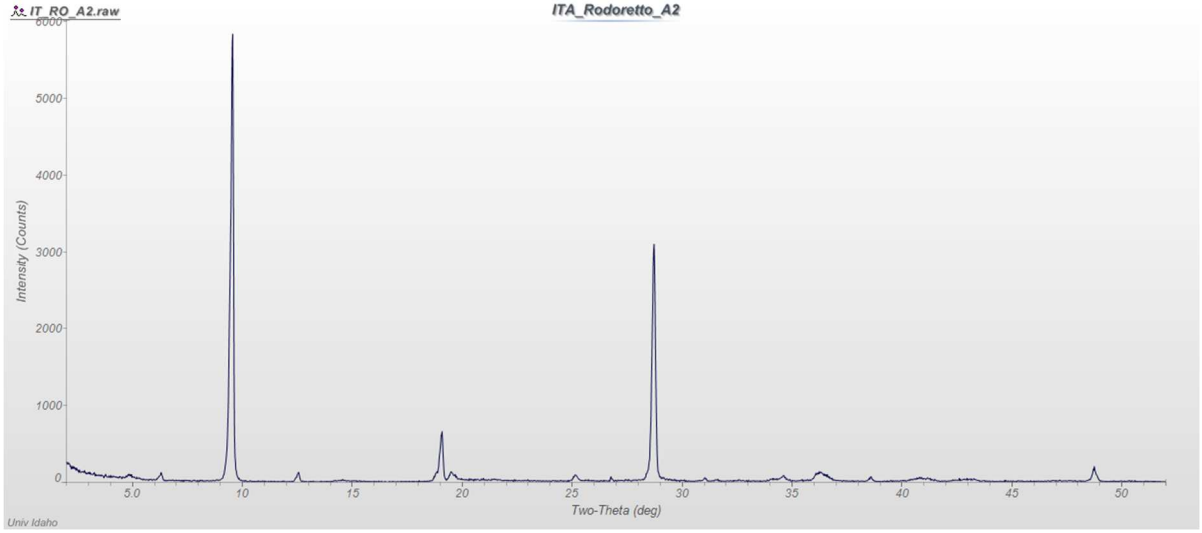
IT_RO_A2.raw
ITA_Rodoretto_A2
Intensity (Counts)
Two-Theta (deg)
Univ Idaho

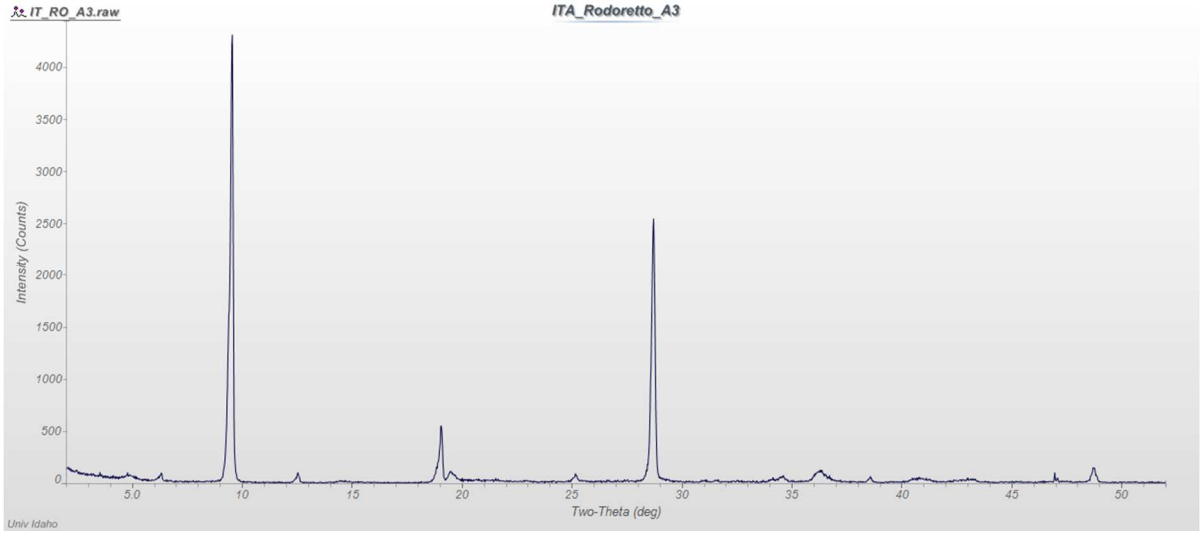
IT_RO_A3.raw
ITA_Rodoretto_A3
Intensity (Counts)
Two-Theta (deg)
Univ Idaho

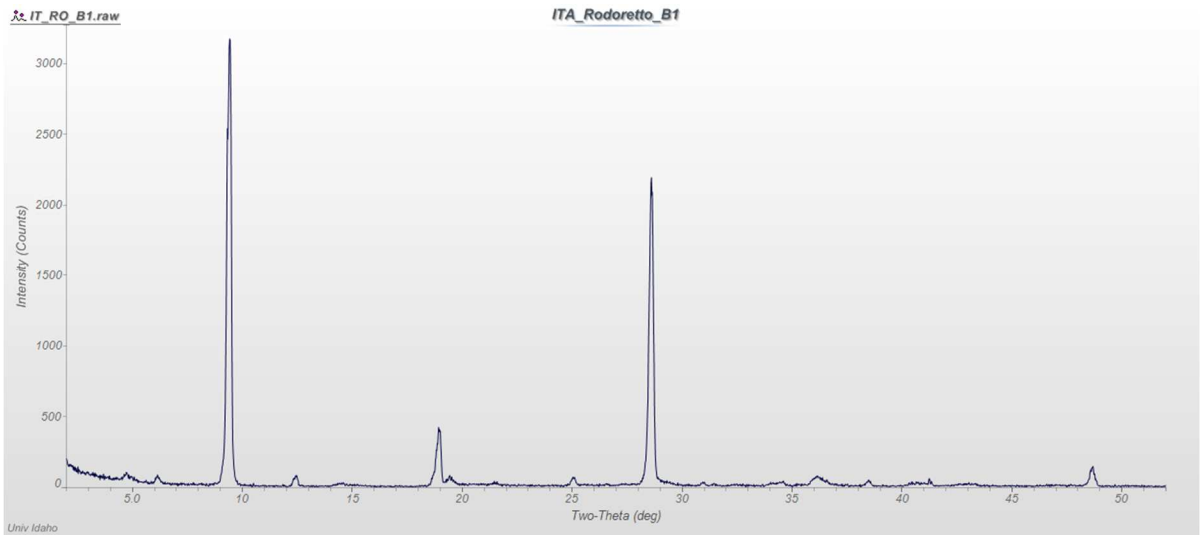
IT_RO_B1.raw
ITA_Rodoretto_B1
Intensity (Counts)
Two-Theta (deg)
Univ Idaho

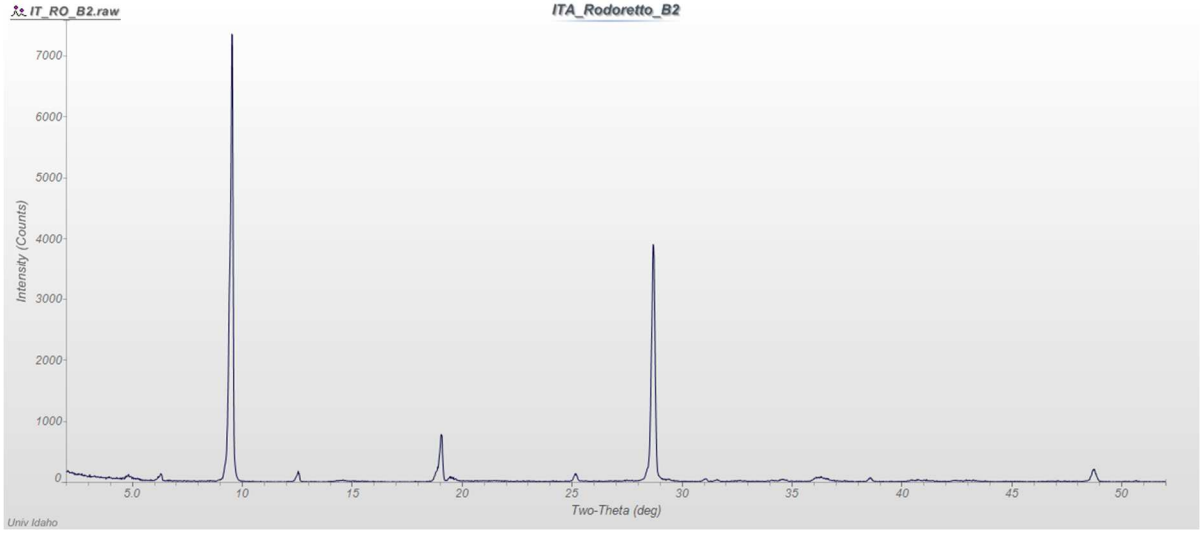
IT_RO_B2.raw
ITA_Rodoretto_B2
Intensity (Counts)
Two-Theta (deg)
Univ Idaho

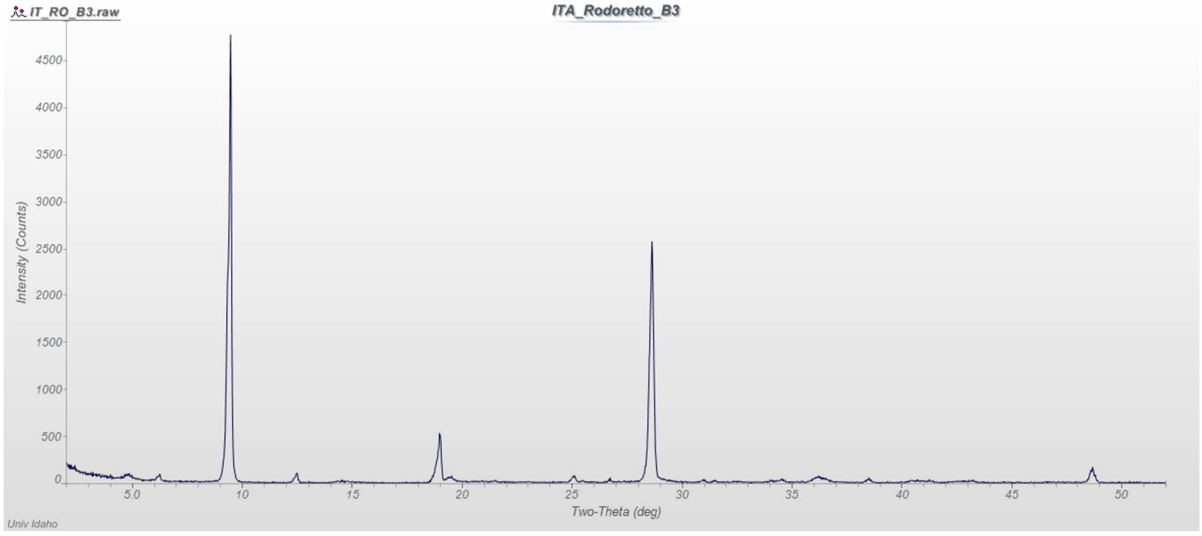
IT_RO_B3.raw
ITA_Rodoretto_B3
Intensity (Counts)
Two-Theta (deg)
Univ Idaho

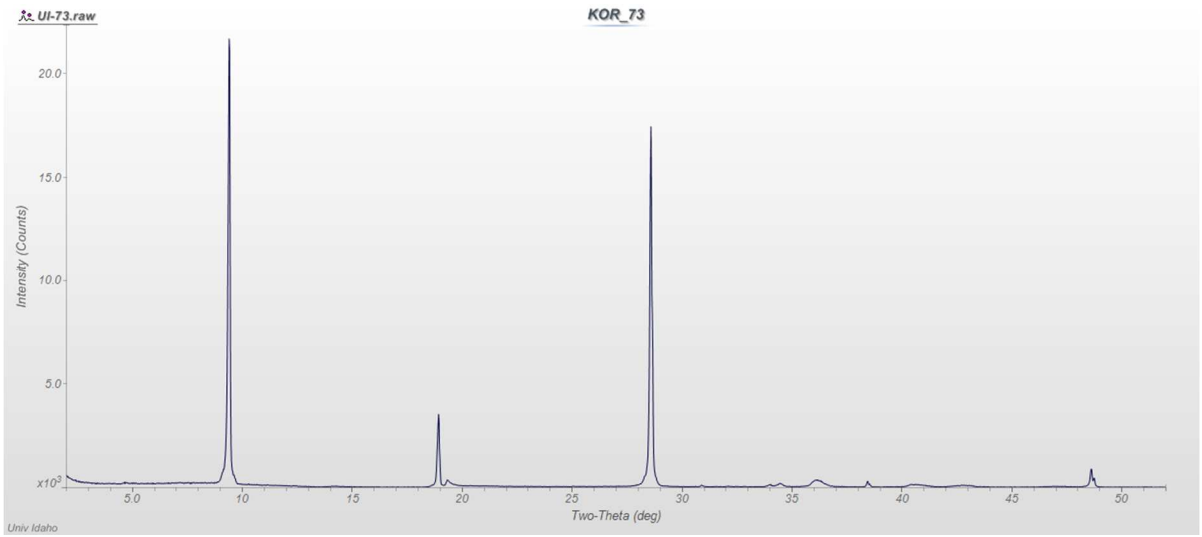
UI-73.raw
KOR_73
Intensity (Counts)
x10^3
Two-Theta (deg)
Univ Idaho

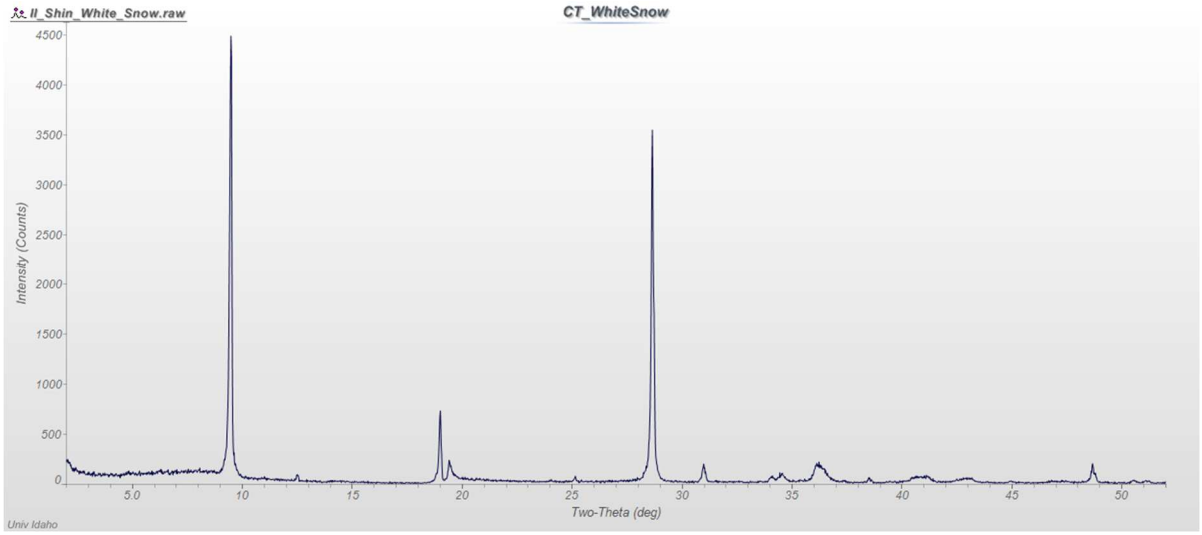
Il_Shin_White_Snow.raw
CT_WhiteSnow
Intensity (Counts)
Two-Theta (deg)
Univ Idaho

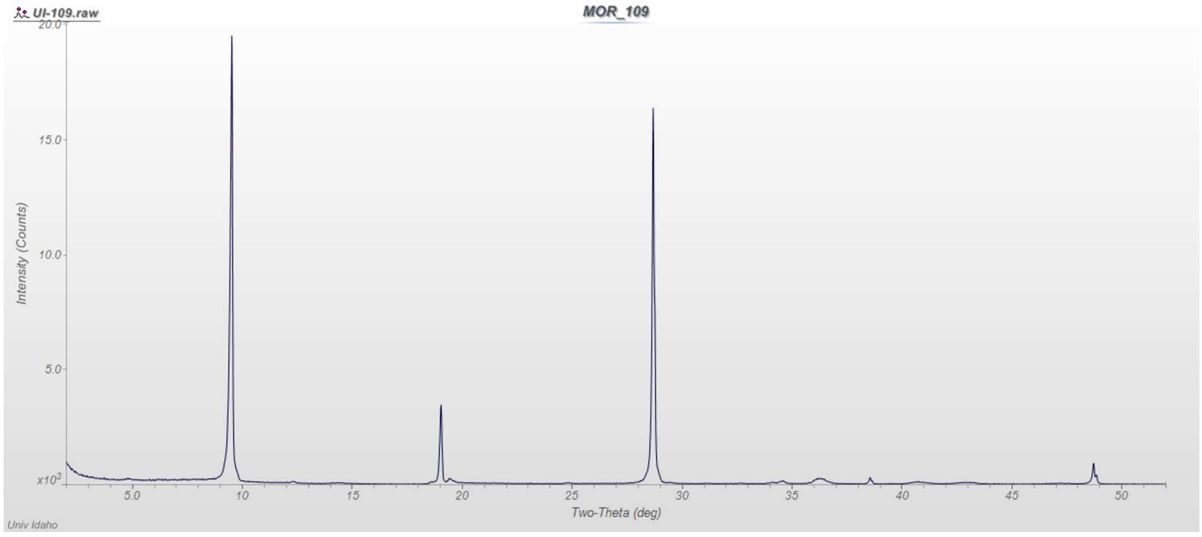
UI-109.raw
MOR_109
Intensity (Counts)
x10^3
Two-Theta (deg)
Univ Idaho

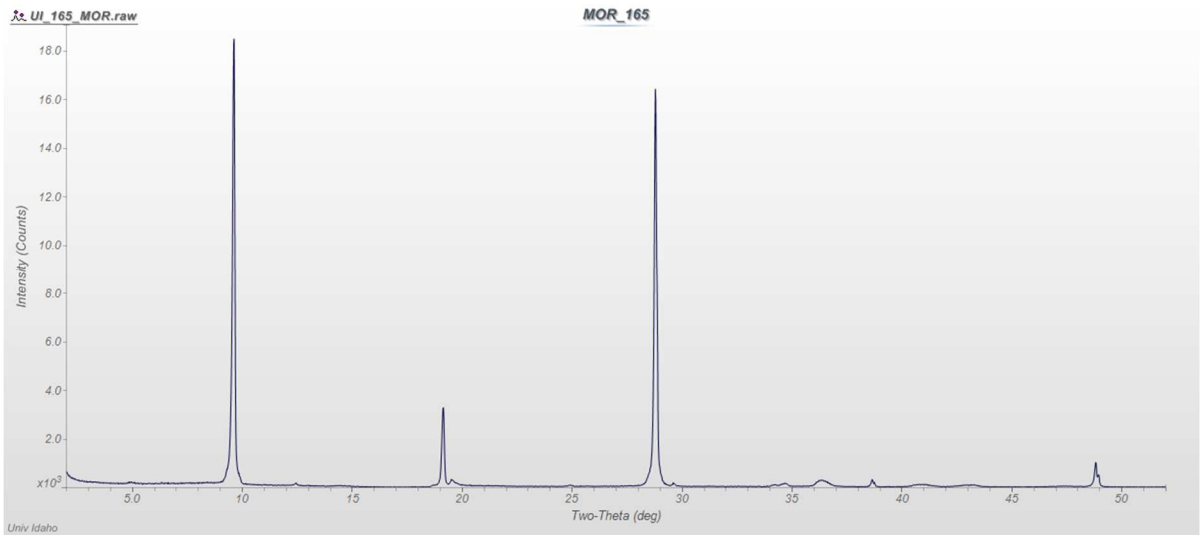
UI_165_MOR.raw
MOR_165
Intensity (Counts)
x10^3
Two-Theta (deg)
Univ Idaho

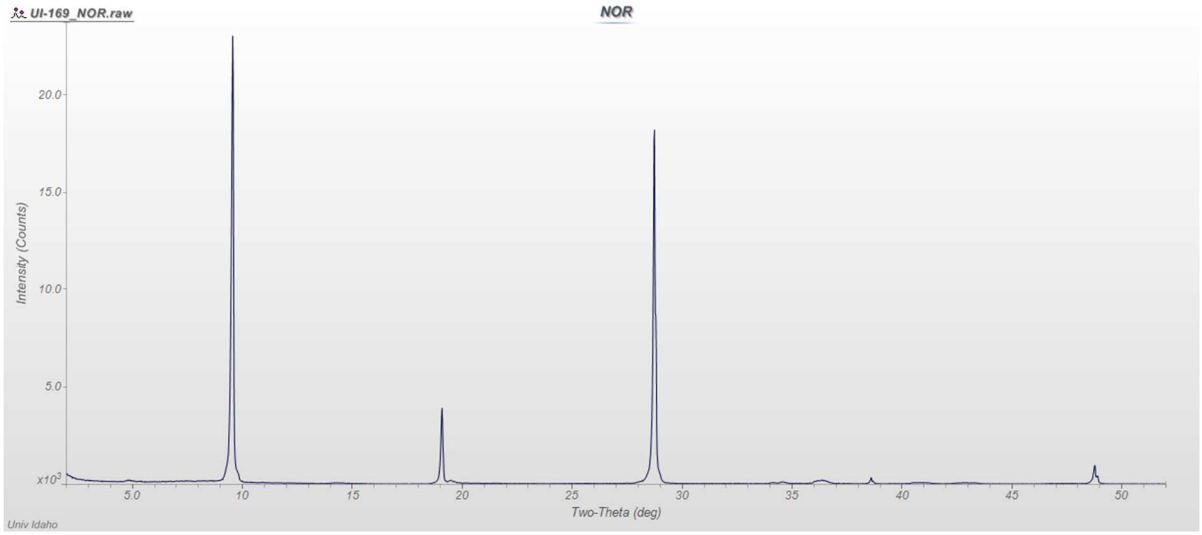
UI-169_NOR.raw
NOR
Intensity (Counts)
x10^3
Two-Theta (deg)
Univ Idaho

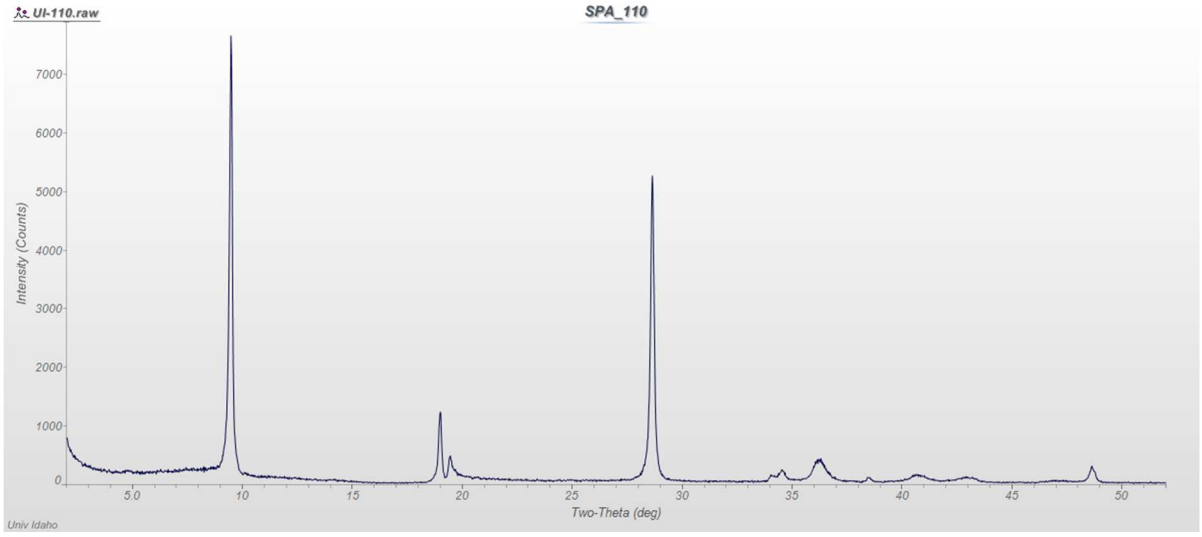
UI-110.raw
SPA_110
Intensity (Counts)
Two-Theta (deg)
Univ Idaho

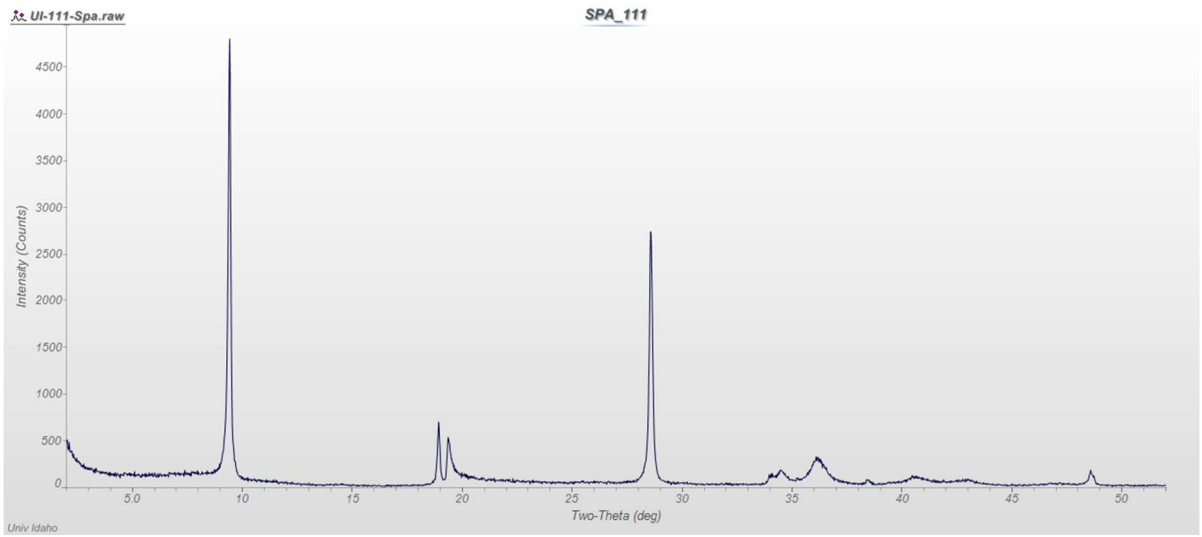
UI-111-Spa.raw
SPA_111
Intensity (Counts)
Two-Theta (deg)
Univ Idaho

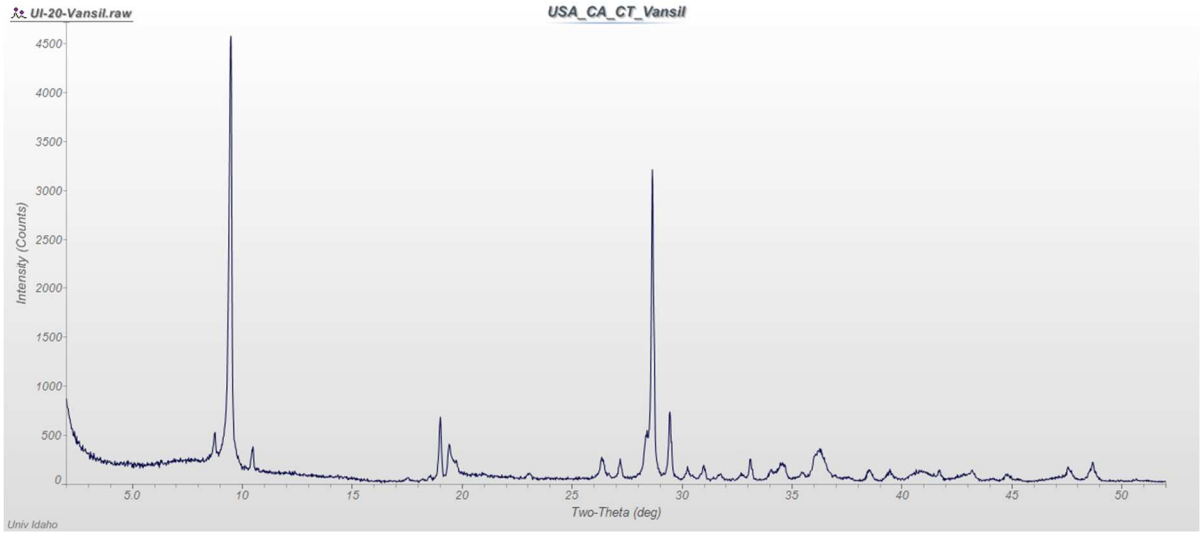
UI-20-Vansil.raw
USA_CA_CT_Vansil
Intensity (Counts)
Two-Theta (deg)
Univ Idaho

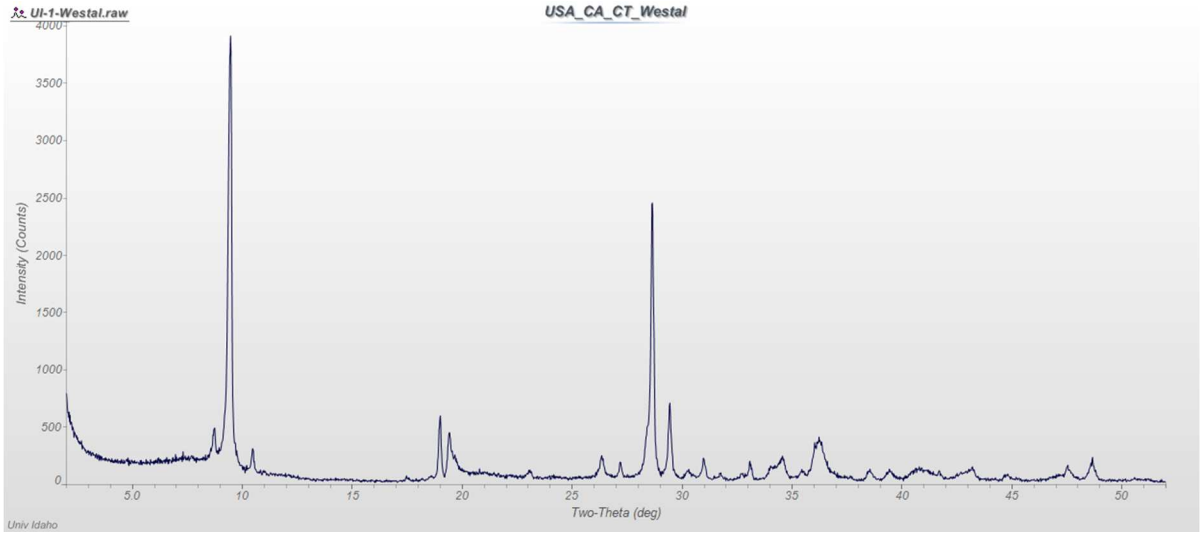
UI-1-Westal.raw
USA_CA_CT_Westal
Intensity (Counts)
Two-Theta (deg)
Univ Idaho

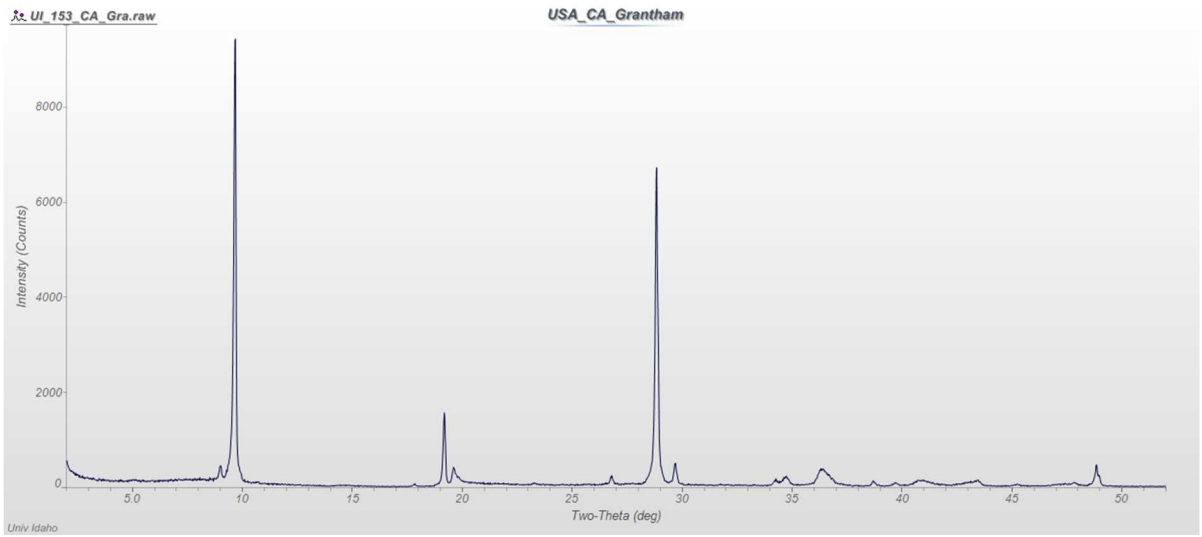
UI_153_CA_Gra.raw
USA_CA_Grantham
Intensity (Counts)
Two-Theta (deg)
Univ Idaho

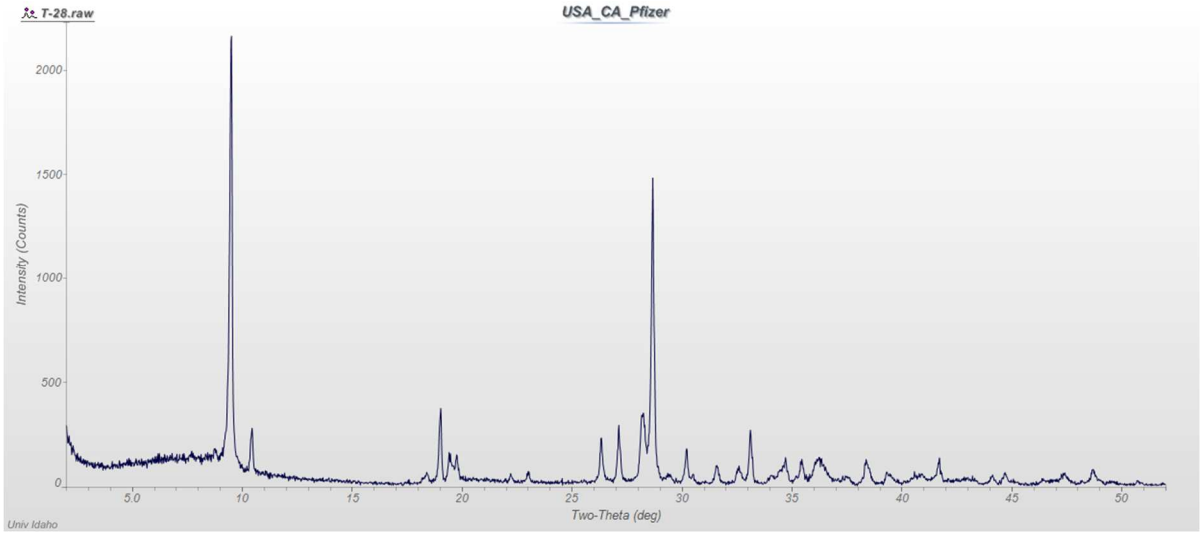
T-28.raw
USA_CA_Pfizer
Intensity (Counts)
Two-Theta (deg)
Univ Idaho

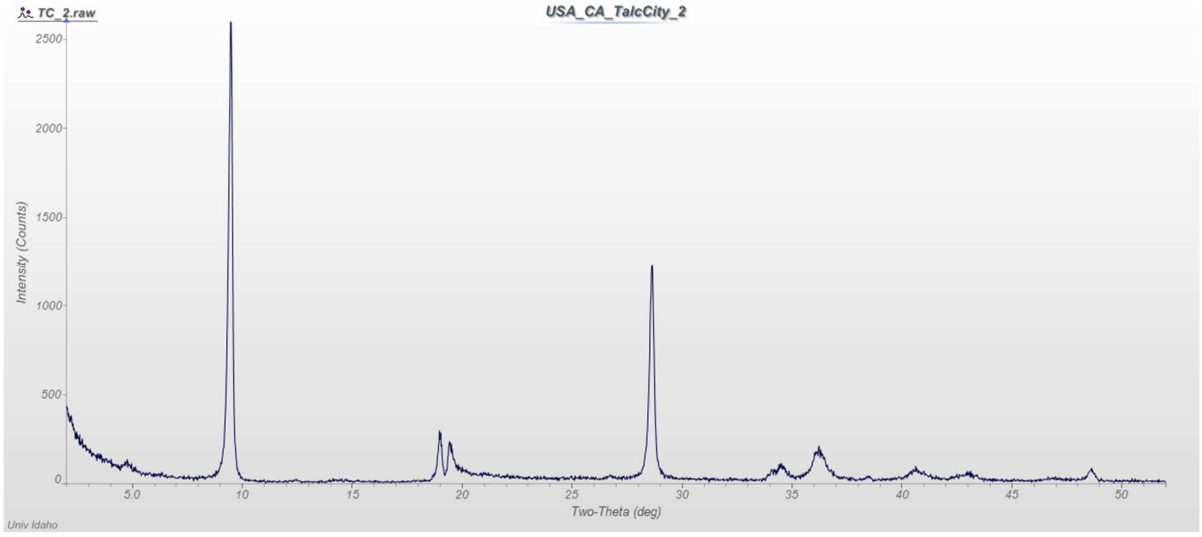
TC_2.raw
USA_CA_TalcCity_2
Intensity (Counts)
Two-Theta (deg)
Univ Idaho

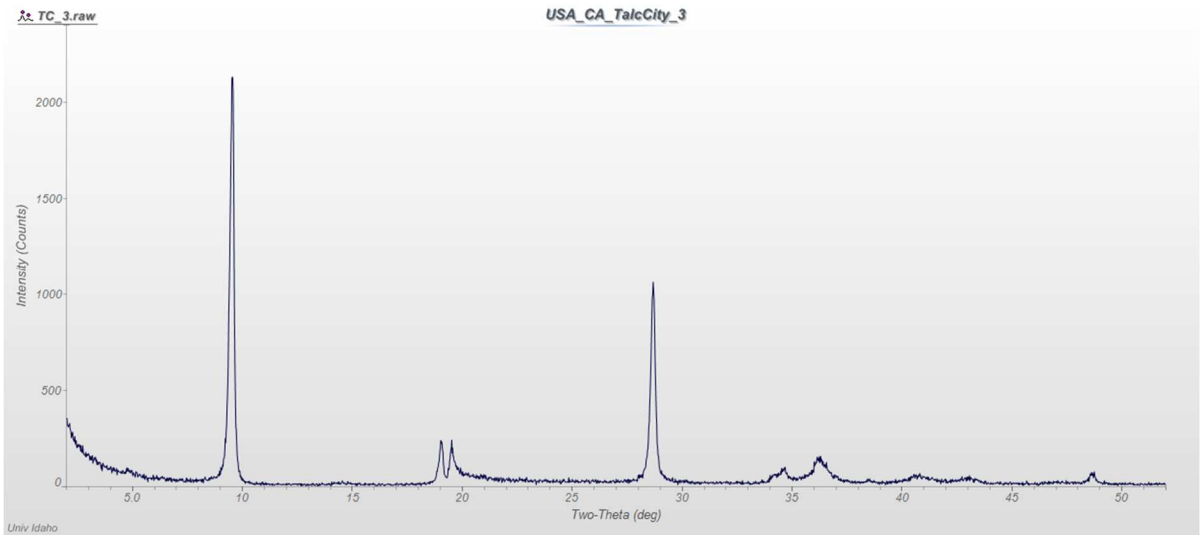
TC_3.raw
USA_CA_TalcCity_3
Intensity (Counts)
Two-Theta (deg)
Univ Idaho

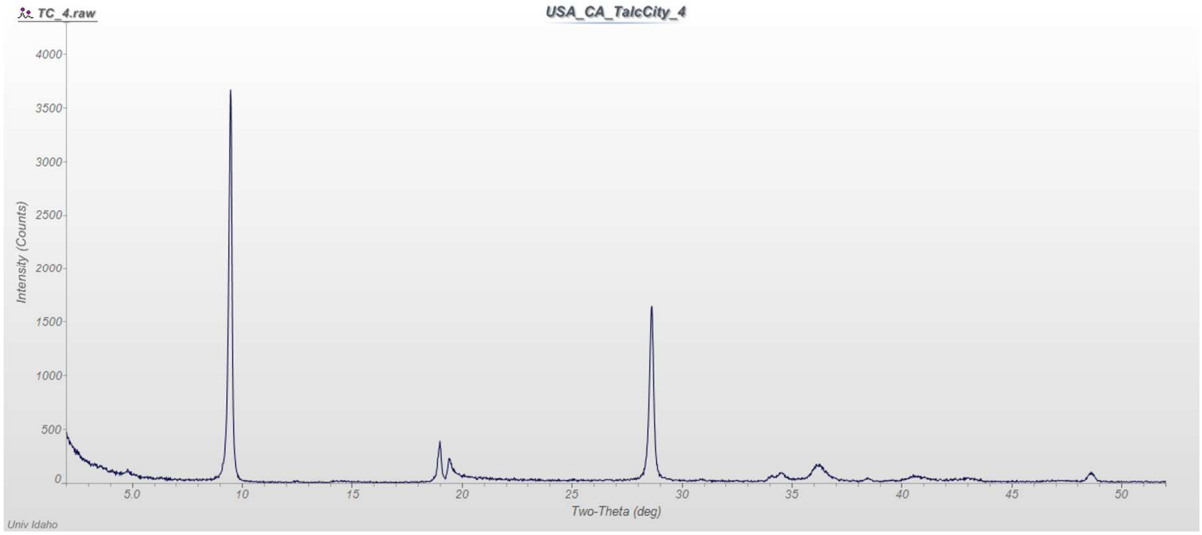
TC_4.raw
USA_CA_TalcCity_4
Intensity (Counts)
Two-Theta (deg)
Univ Idaho

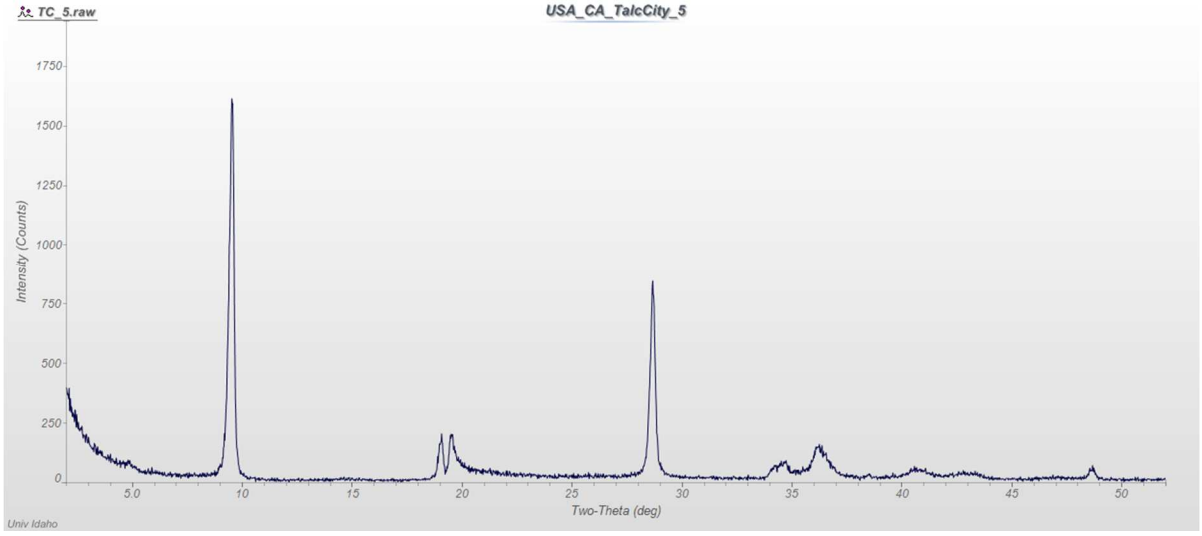
TC_5.raw
USA_CA_TalcCity_5
Intensity (Counts)
Two-Theta (deg)
Univ Idaho

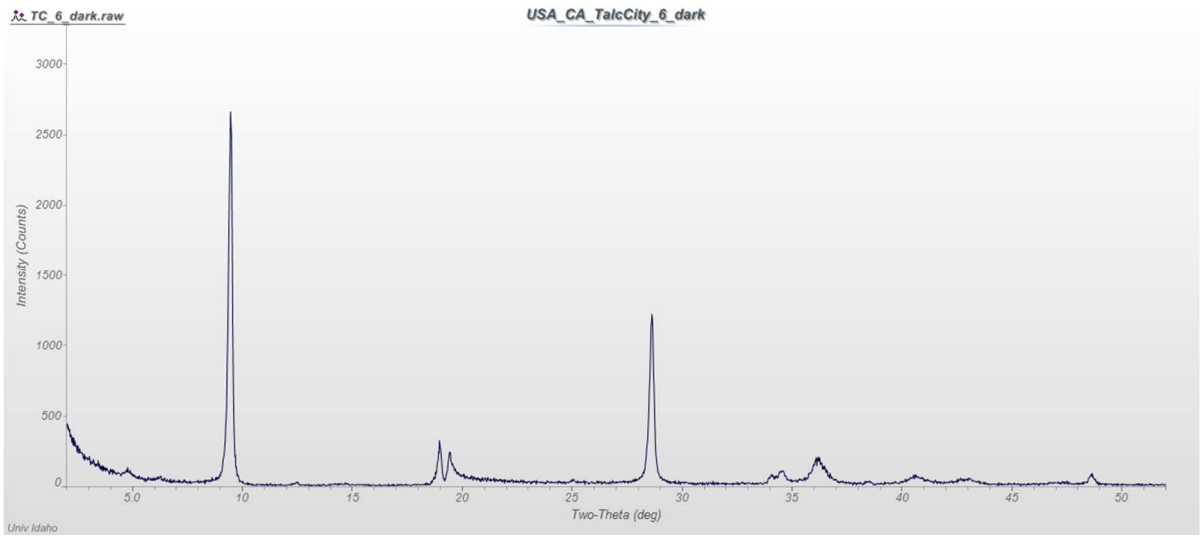
TC_6_dark.raw
USA_CA_TalcCity_6_dark
Intensity (Counts)
Two-Theta (deg)
Univ Idaho

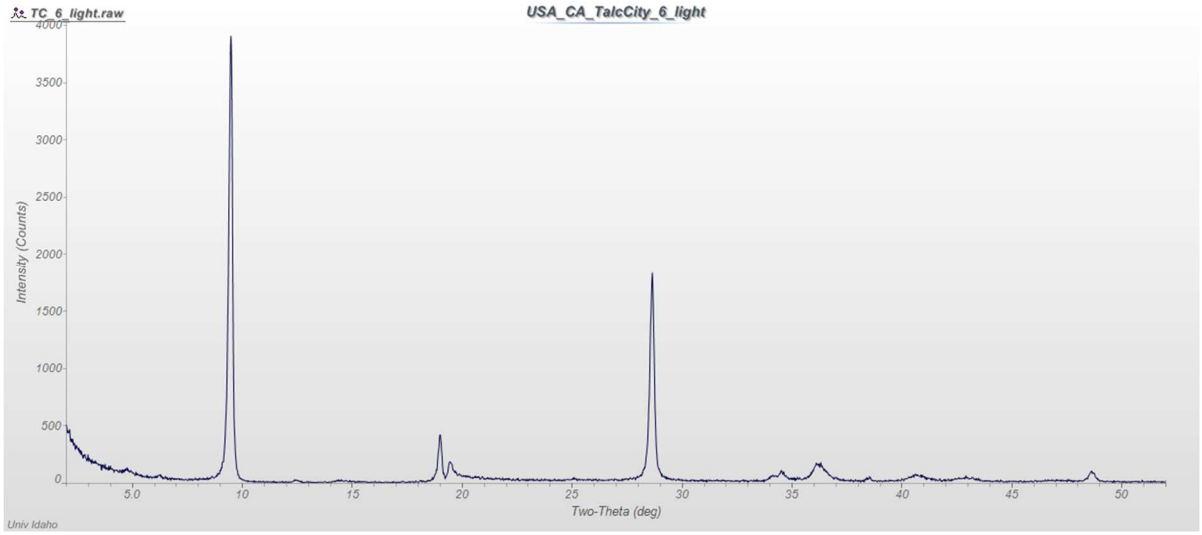
TC_6_light.raw
USA_CA_TalcCity_6_light
Intensity (Counts)
Two-Theta (deg)
Univ Idaho

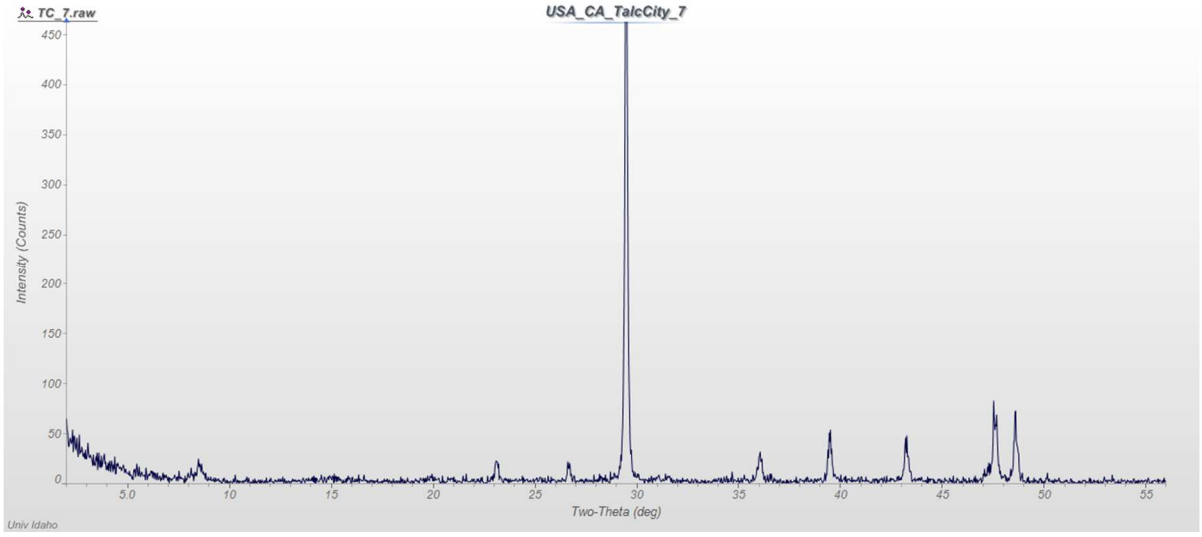
TC_7.raw
USA_CA_TalcCity_7
Intensity (Counts)
Two-Theta (deg)
Univ Idaho

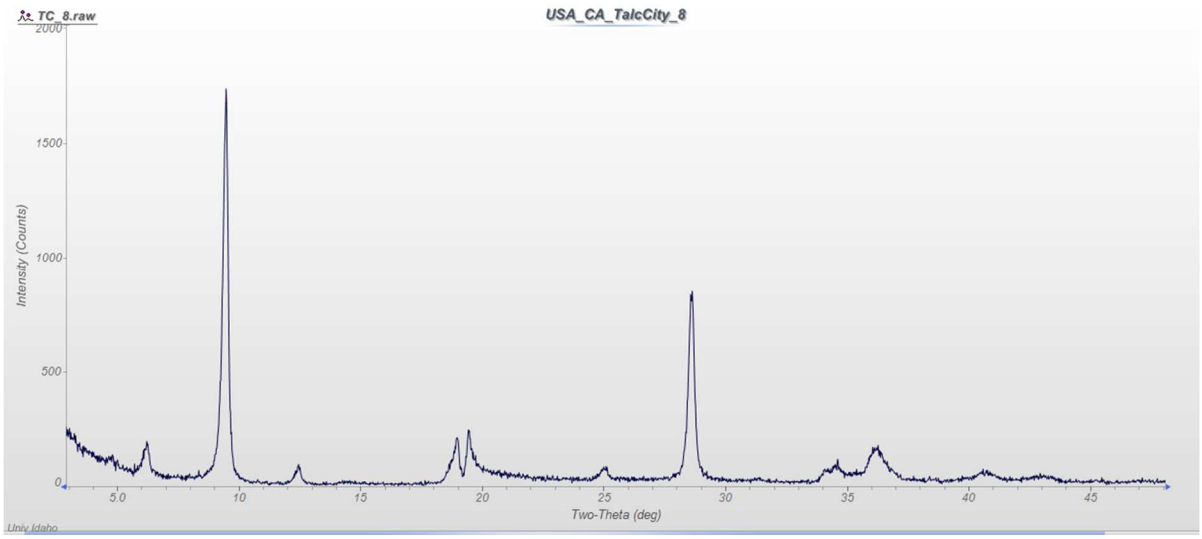
TC_8.raw
USA_CA_TalcCity_8
Intensity (Counts)
Two-Theta (deg)
Univ Idaho

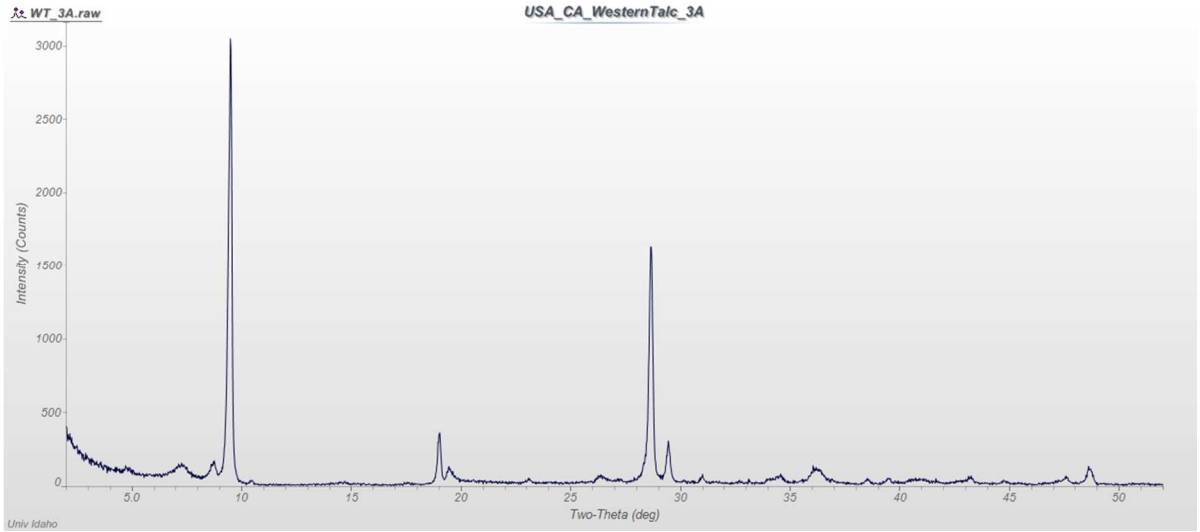
WT_3A.raw
USA_CA_WesternTalc_3A
Intensity (Counts)
Two-Theta (deg)
Univ Idaho

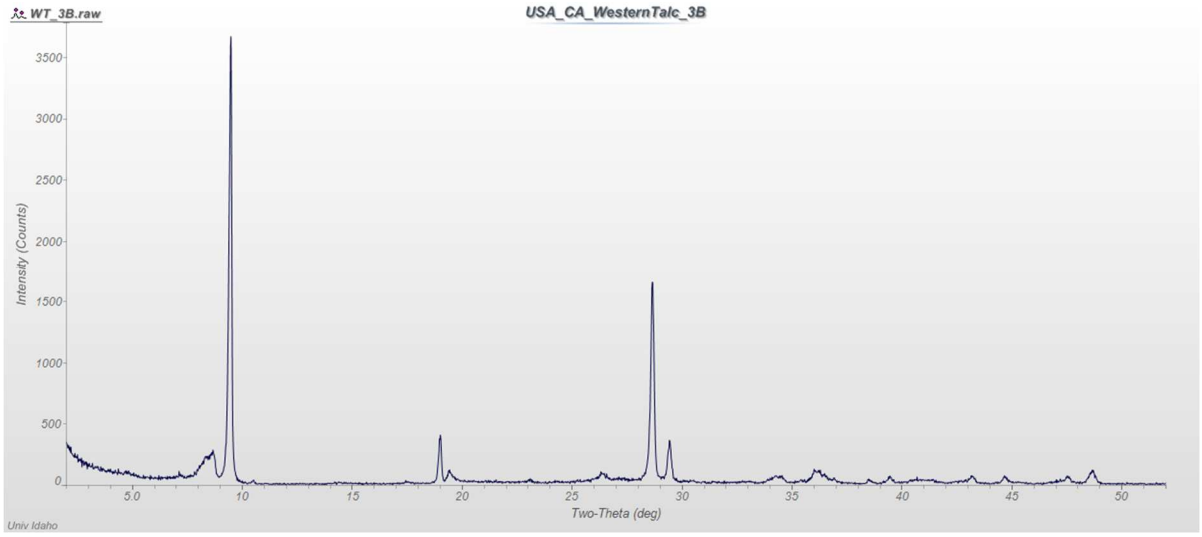
WT_3B.raw
USA_CA_WesternTalc_3B
Intensity (Counts)
Two-Theta (deg)
Univ Idaho

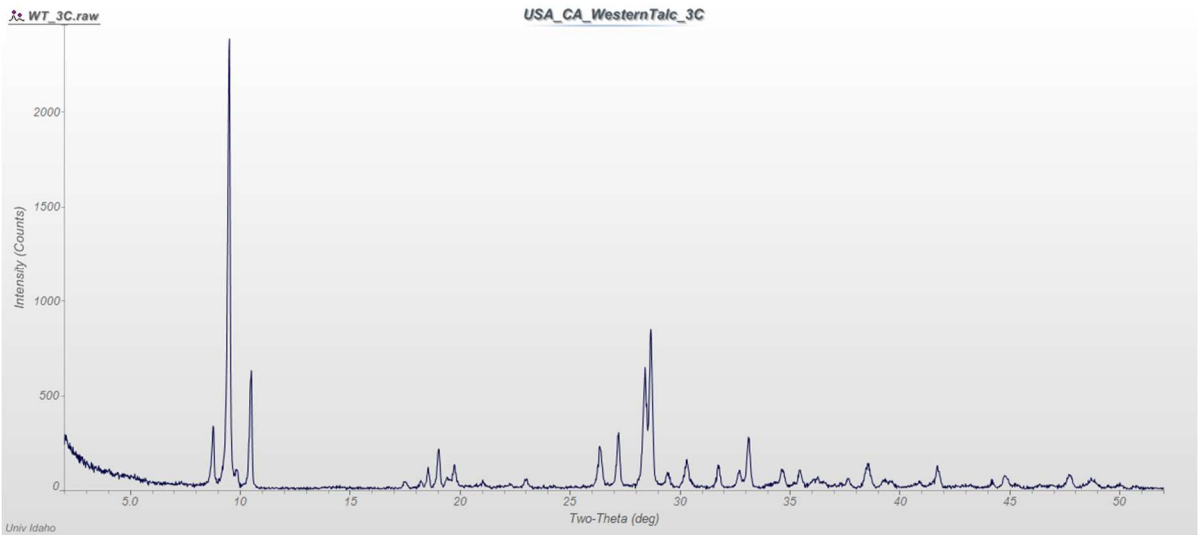
WT_3C.raw
USA_CA_WesternTalc_3C
Intensity (Counts)
Two-Theta (deg)
Univ Idaho

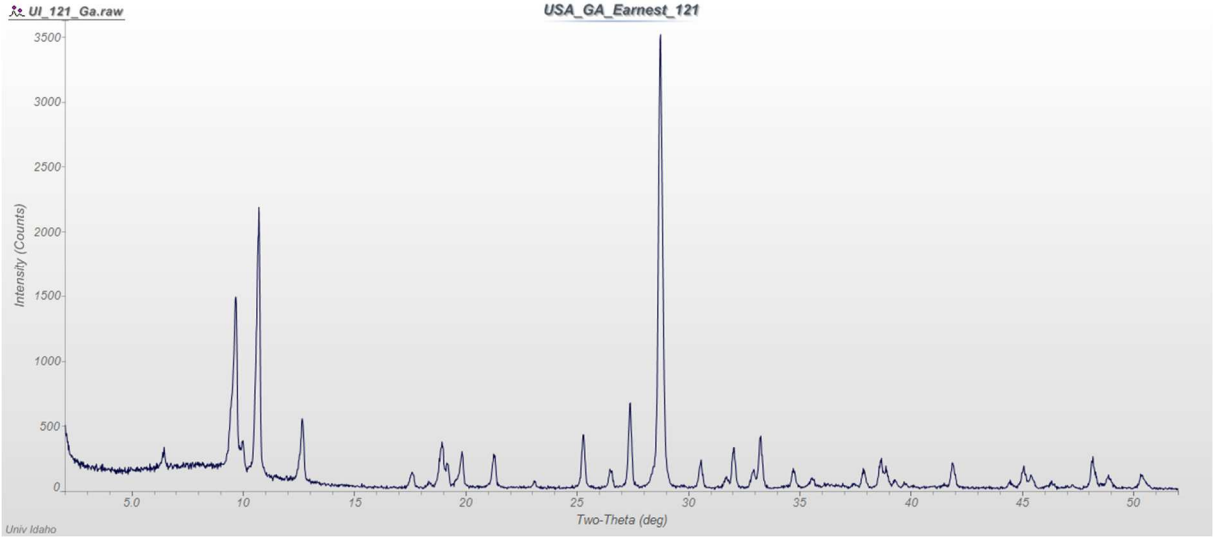
UI_121_Ga.raw
USA_GA_Earnest_121
Intensity (Counts)
Two-Theta (deg)
Univ Idaho

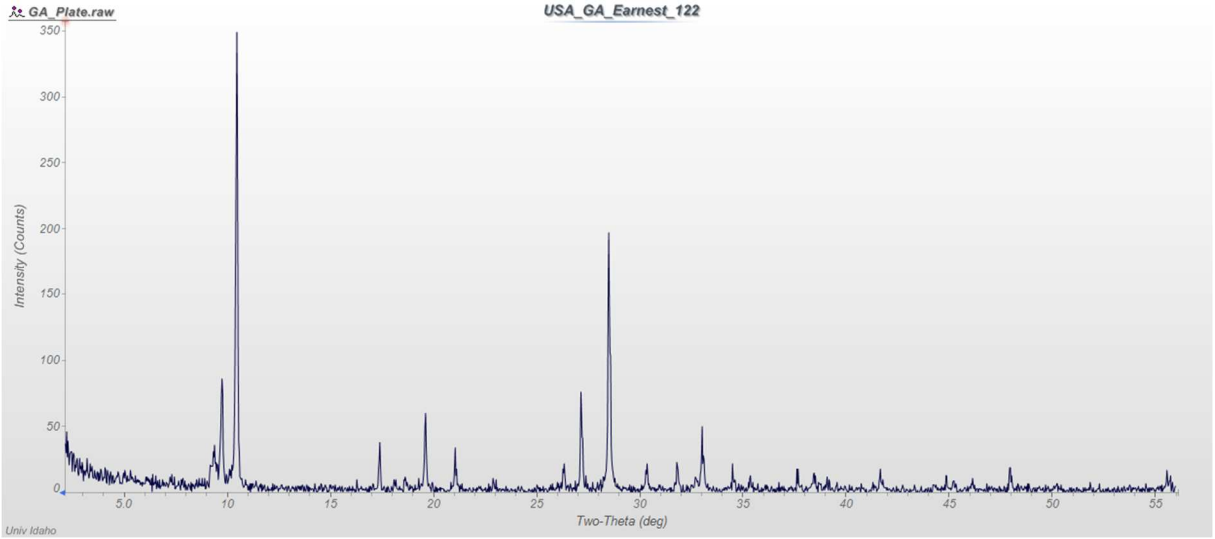
GA_Plate.raw
USA_GA_Earnest_122
Intensity (Counts)
Two-Theta (deg)
Univ Idaho

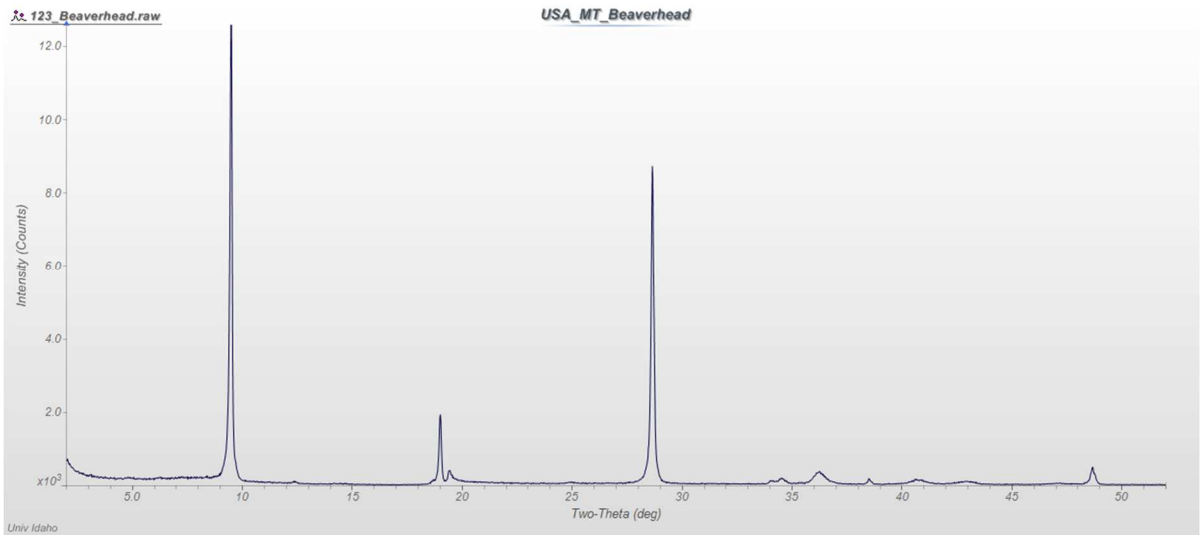
123_Beaverhead.raw
USA_MT_Beaverhead
Intensity (Counts)
x10^3
12.0
10.0
8.0
6.0
4.0
2.0
5.0
10
15
20
25
30
35
40
45
50
Two-Theta (deg)
Univ Idaho

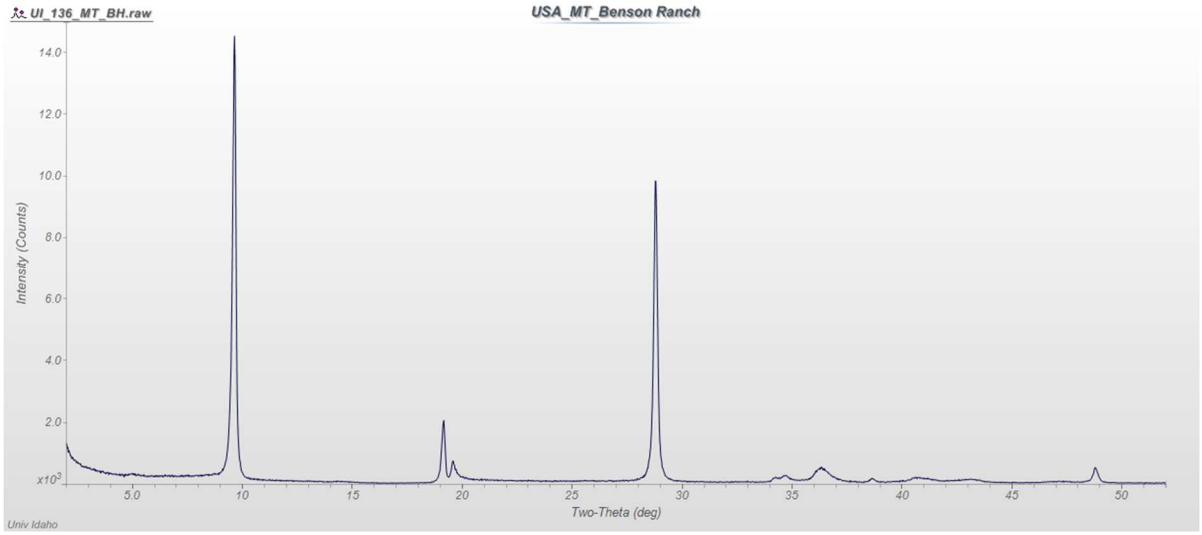
UI_136_MT_BH.raw
USA_MT_Benson Ranch
Intensity (Counts)
x10^3
14.0
12.0
10.0
8.0
6.0
4.0
2.0
5.0
10
15
20
25
30
35
40
45
50
Two-Theta (deg)
Univ Idaho

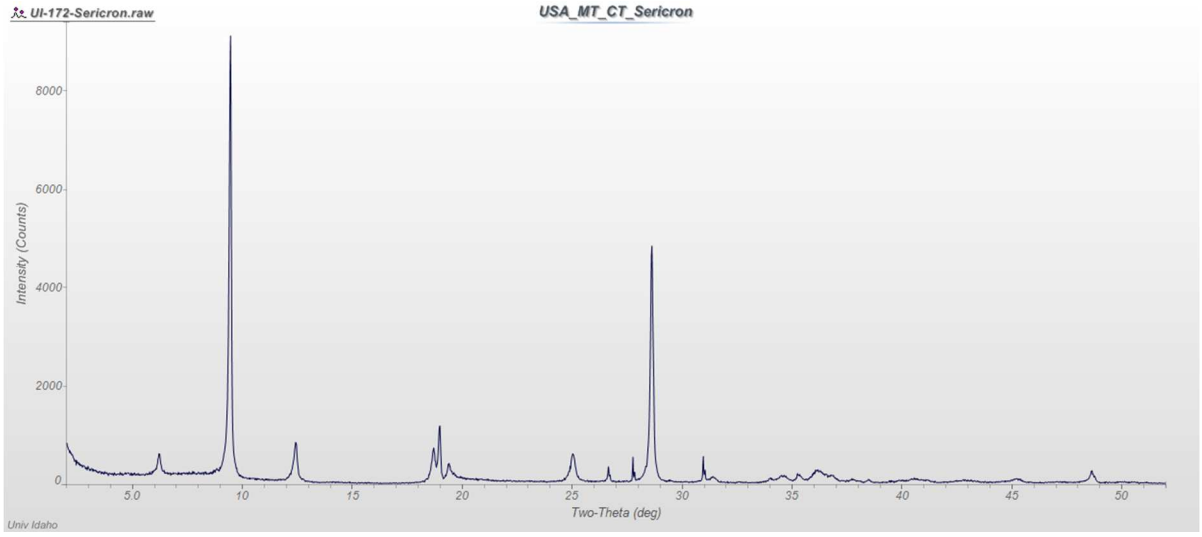
UI-172-Sericron.raw
USA_MT_CT_Sericron
Intensity (Counts)
8000
6000
4000
2000
0
5.0
10
15
20
25
30
35
40
45
50
Two-Theta (deg)
Univ Idaho

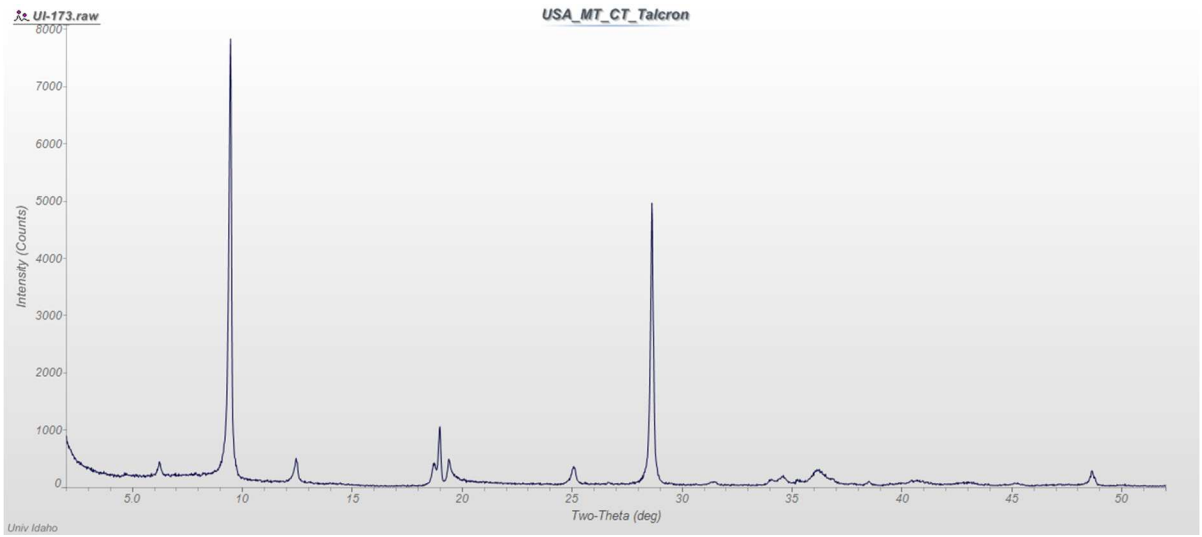
UI-173.raw
USA_MT_CT_Talcron
Intensity (Counts)
Two-Theta (deg)
Univ Idaho

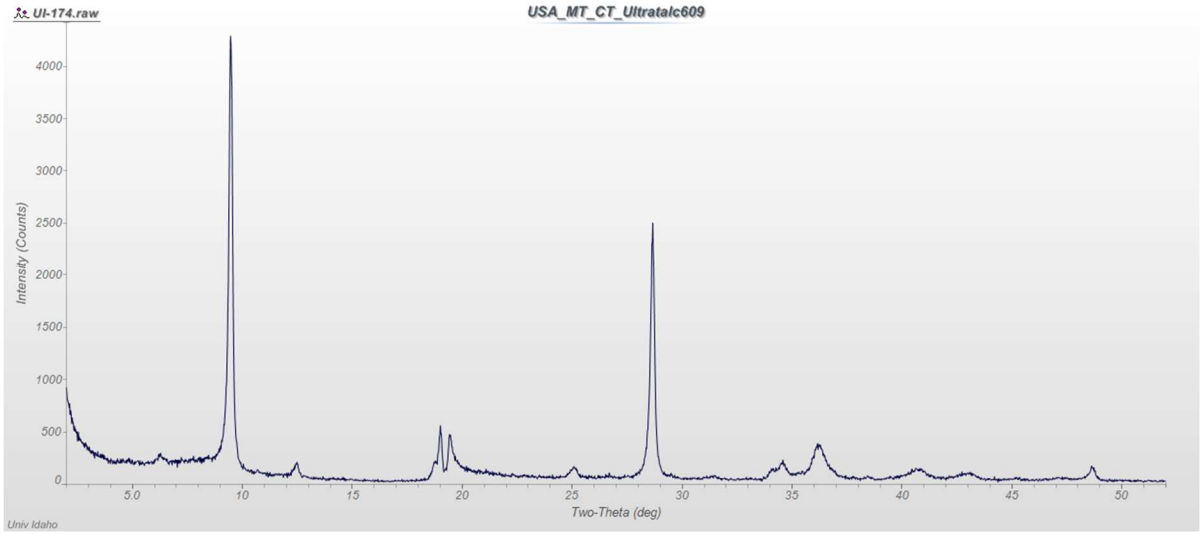
UI-174.raw
USA_MT_CT_Ultratalc609
Intensity (Counts)
Two-Theta (deg)
Univ Idaho

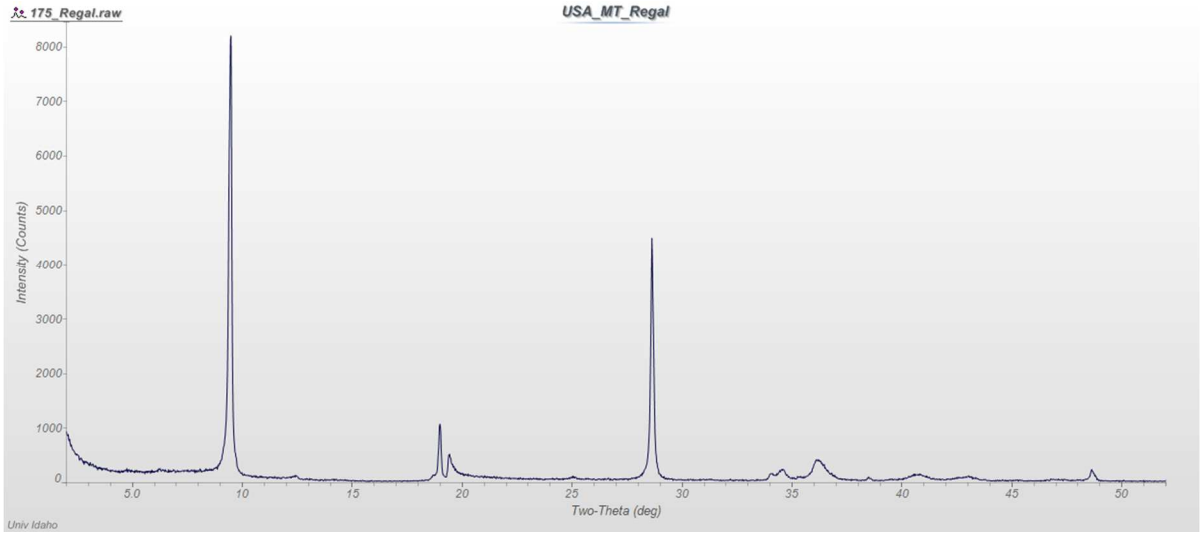
175_Regal.raw
USA_MT_Regal
Intensity (Counts)
Two-Theta (deg)
Univ Idaho

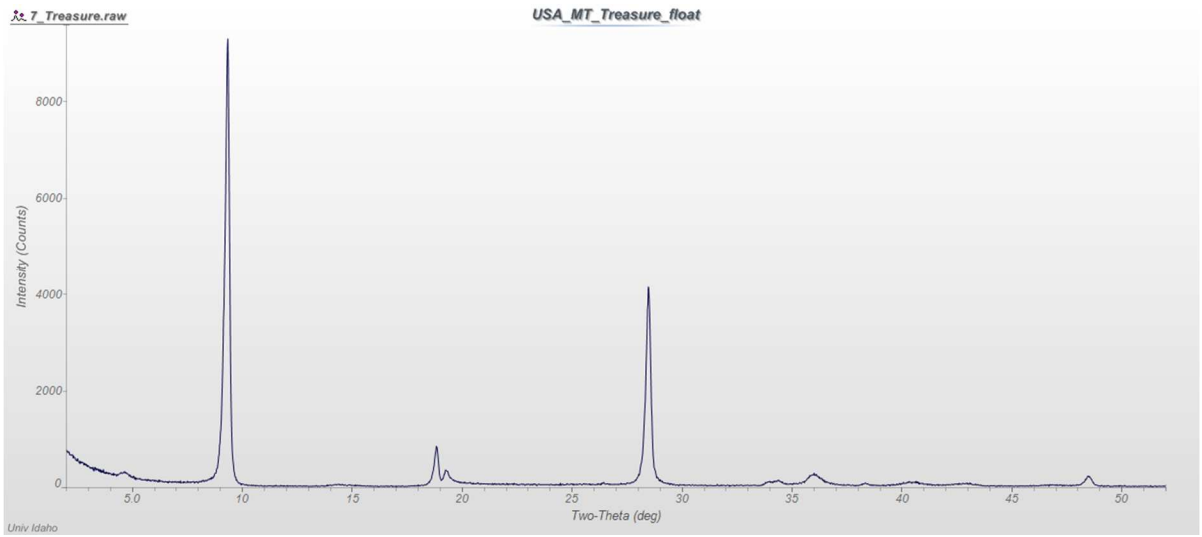
7_Treasure.raw
USA_MT_Treasure_float
Intensity (Counts)
8000
6000
4000
2000
0
5.0
10
15
20
25
30
35
40
45
50
Two-Theta (deg)
Univ Idaho

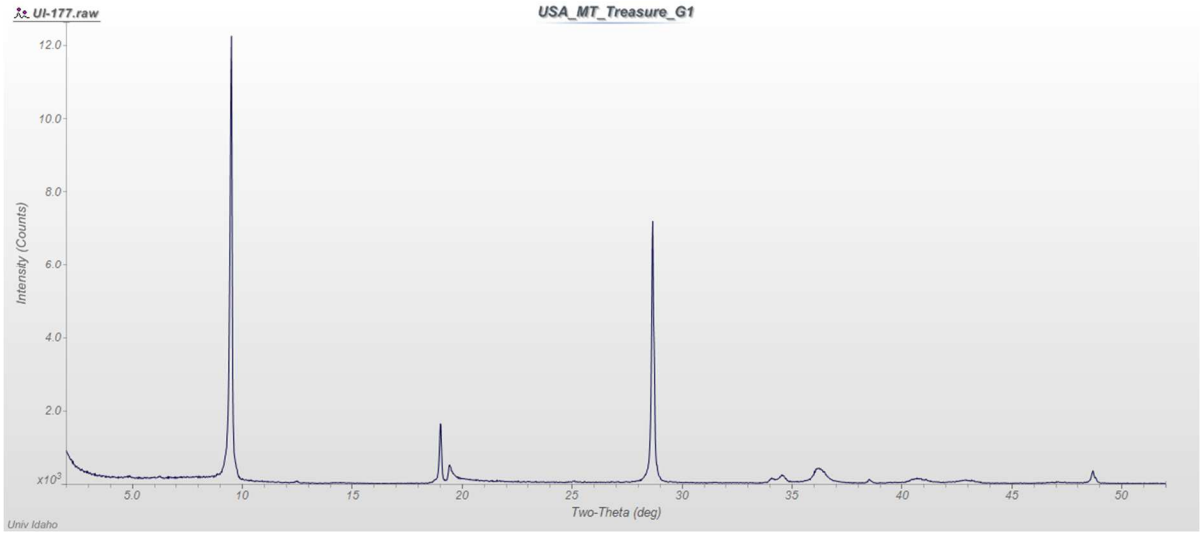
UI-177.raw
USA_MT_Treasure_G1
Intensity (Counts)
12.0
10.0
8.0
6.0
4.0
2.0
x10^3
5.0
10
15
20
25
30
35
40
45
50
Two-Theta (deg)
Univ Idaho

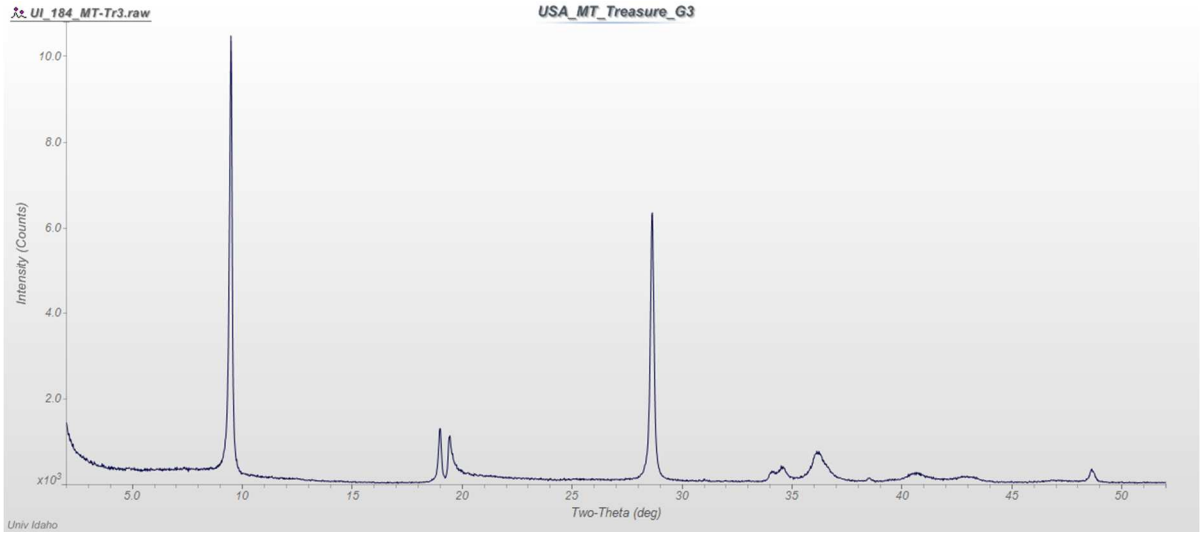
UI_184_MT-Tr3.raw
USA_MT_Treasure_G3
Intensity (Counts)
10.0
8.0
6.0
4.0
2.0
x10^3
5.0
10
15
20
25
30
35
40
45
50
Two-Theta (deg)
Univ Idaho

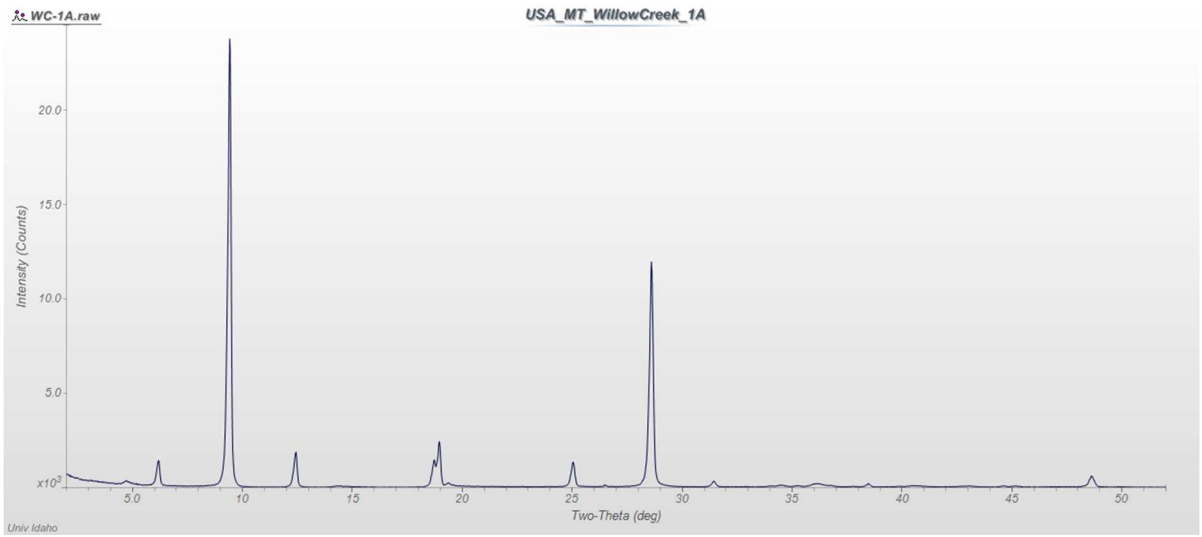
WC-1A.raw
USA_MT_WillowCreek_1A
Intensity (Counts)
x10^3
Two-Theta (deg)
Univ Idaho

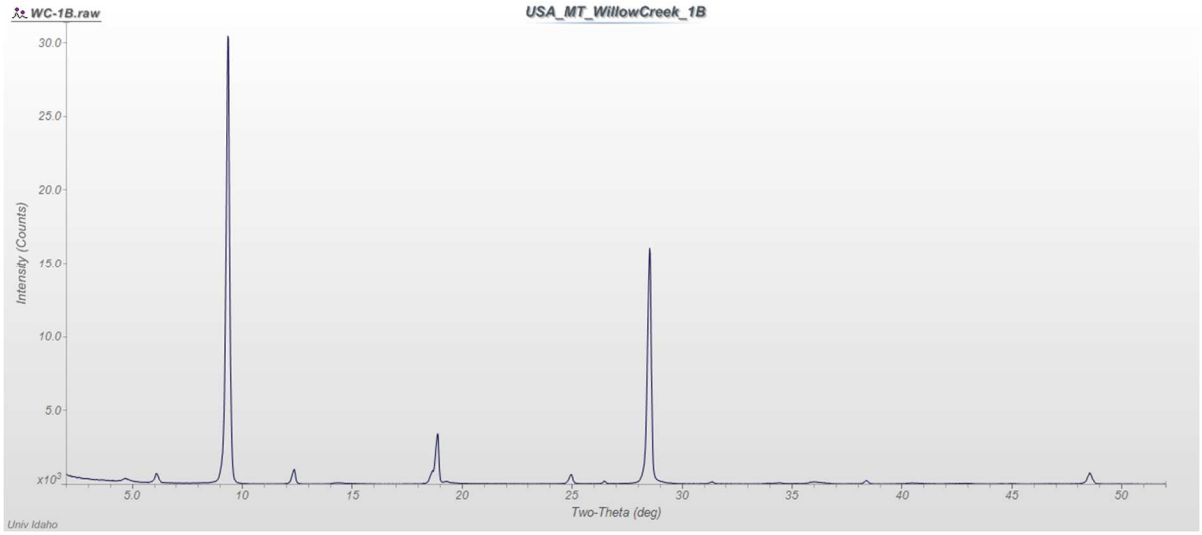
WC-1B.raw
USA_MT_WillowCreek_1B
Intensity (Counts)
x10^3
Two-Theta (deg)
Univ Idaho

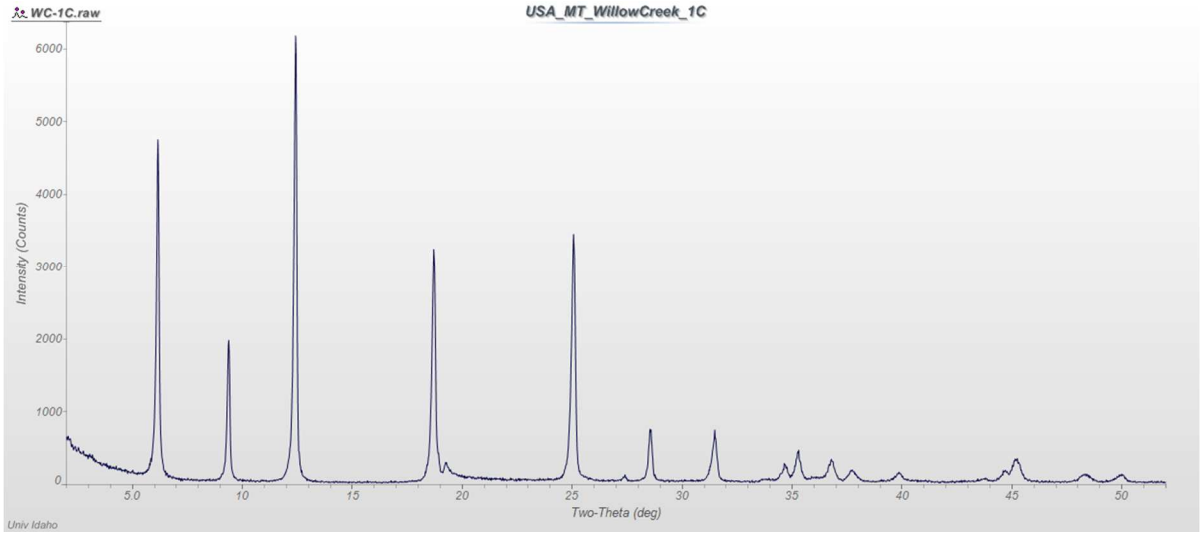
WC-1C.raw
USA_MT_WillowCreek_1C
Intensity (Counts)
Two-Theta (deg)
Univ Idaho

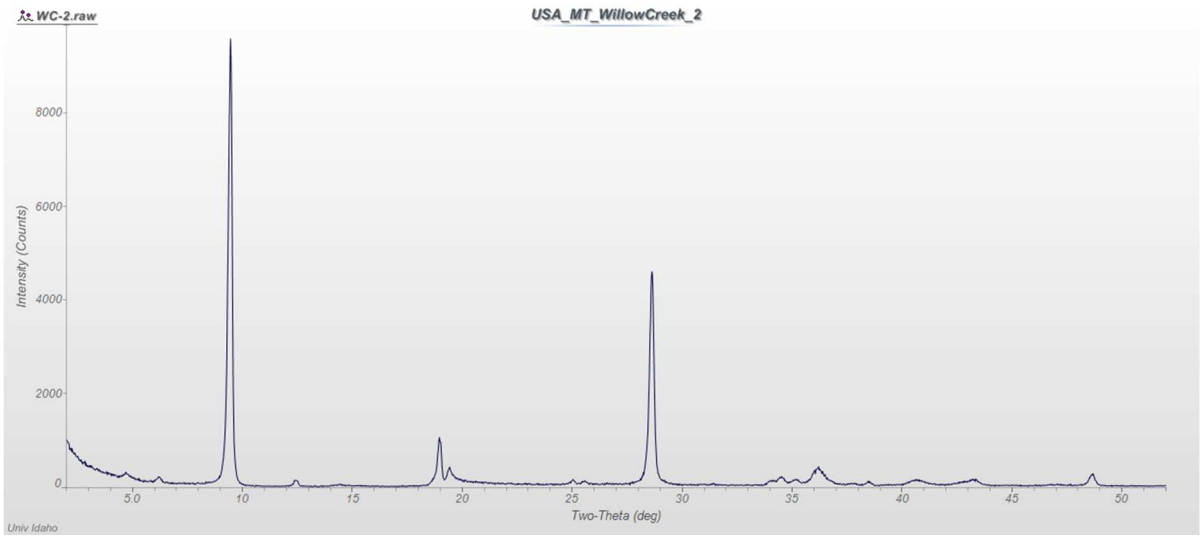
WC-2.raw
USA_MT_WillowCreek_2
Intensity (Counts)
Two-Theta (deg)
Univ Idaho

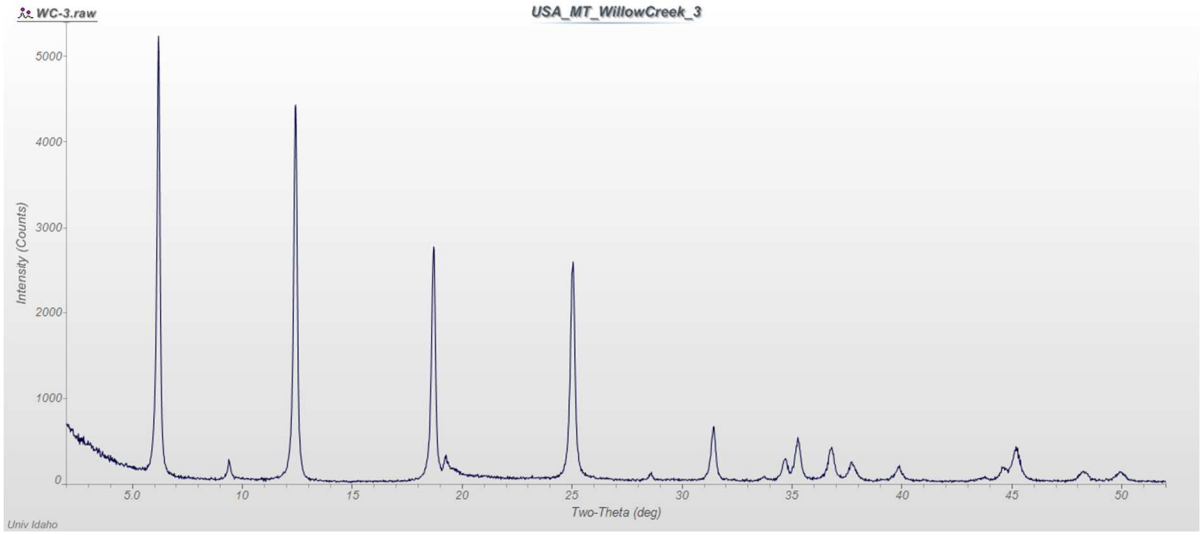
WC-3.raw
USA_MT_WillowCreek_3
Intensity (Counts)
Two-Theta (deg)
Univ Idaho

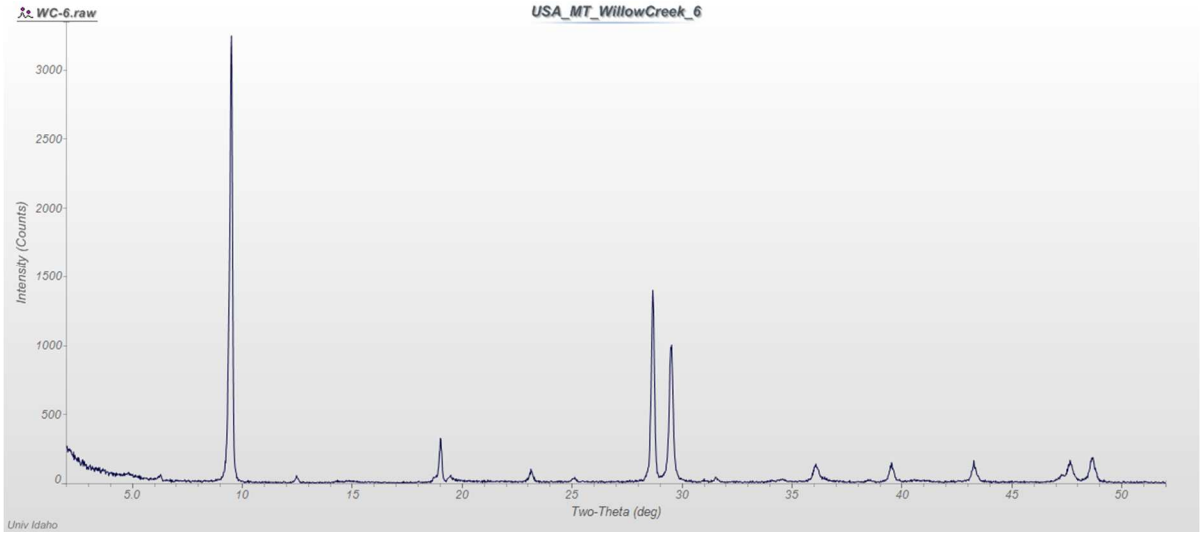
WC-6.raw
USA_MT_WillowCreek_6
Intensity (Counts)
Two-Theta (deg)
Univ Idaho

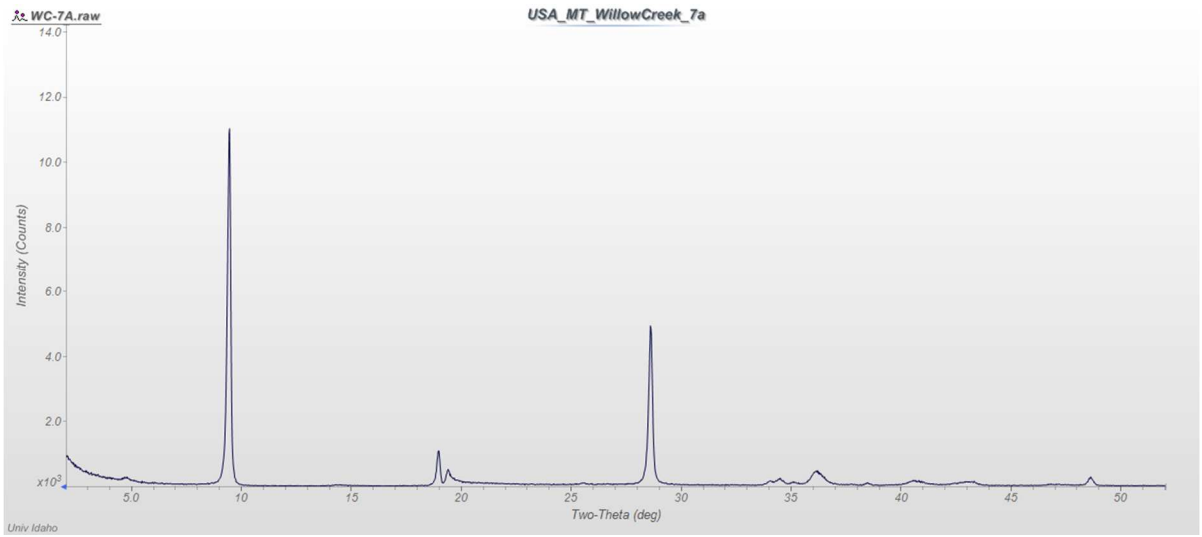
WC-7A.raw
USA_MT_WillowCreek_7a
Intensity (Counts)
x10^3
Two-Theta (deg)
Univ Idaho

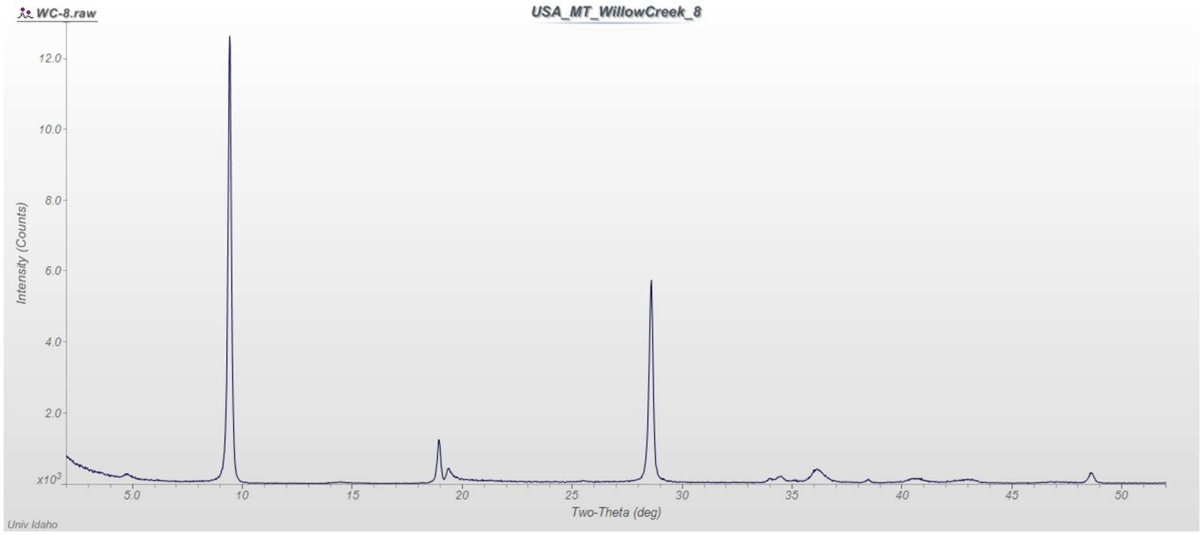
WC-8.raw
USA_MT_WillowCreek_8
Intensity (Counts)
x10^3
Two-Theta (deg)
Univ Idaho

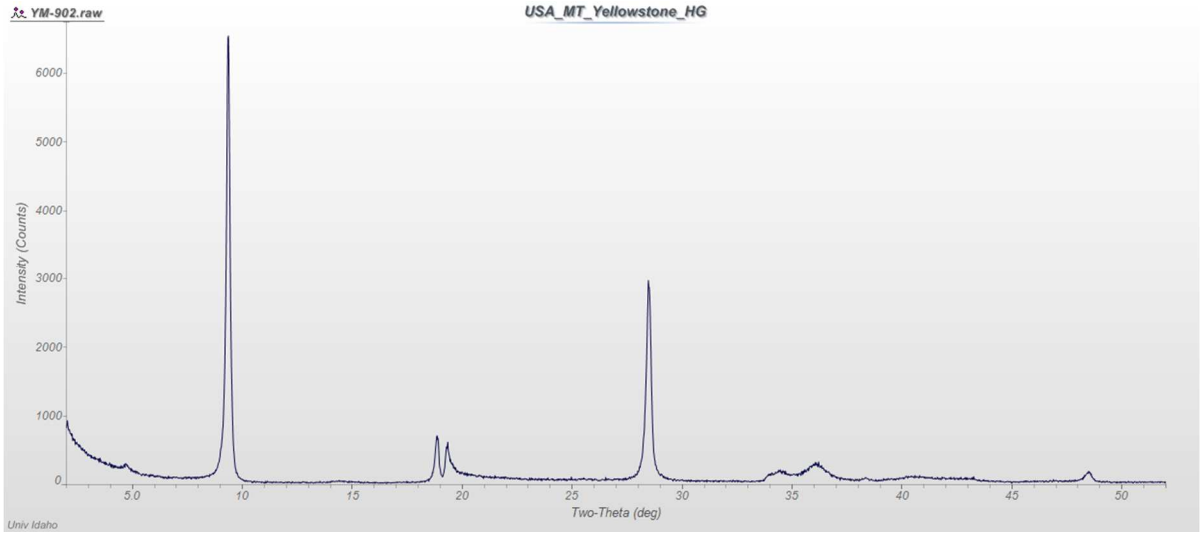
YM-902.raw
USA_MT_Yellowstone_HG
Intensity (Counts)
Two-Theta (deg)
Univ Idaho

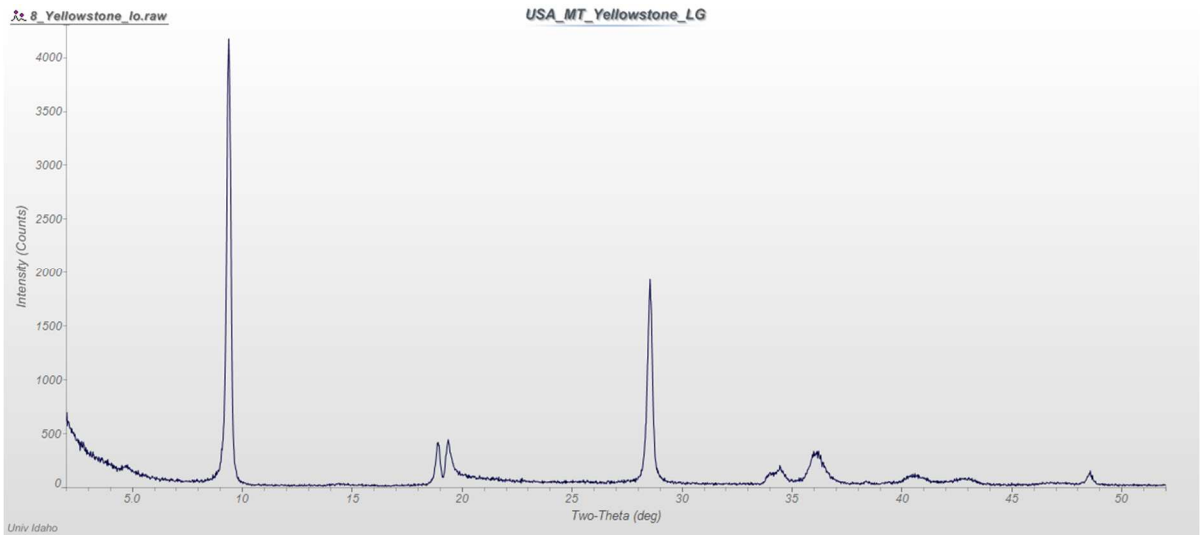
8_Yellowstone_lo.raw
USA_MT_Yellowstone_LG
Intensity (Counts)
Two-Theta (deg)
Univ Idaho

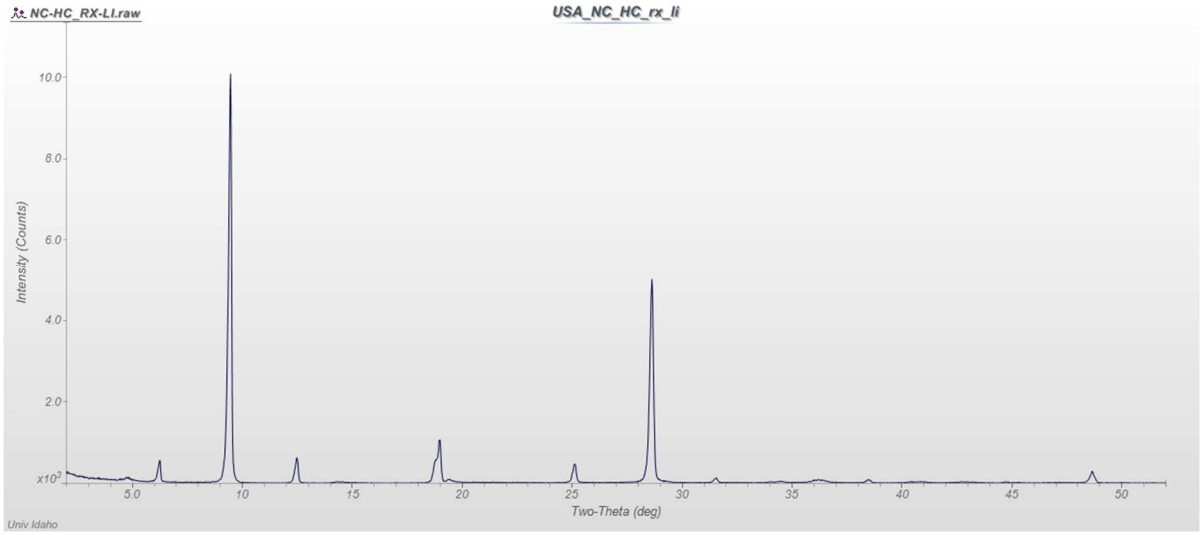
NC-HC_RX-LI.raw
USA_NC_HC_rx_li
Intensity (Counts)
x10^3
Two-Theta (deg)
Univ Idaho

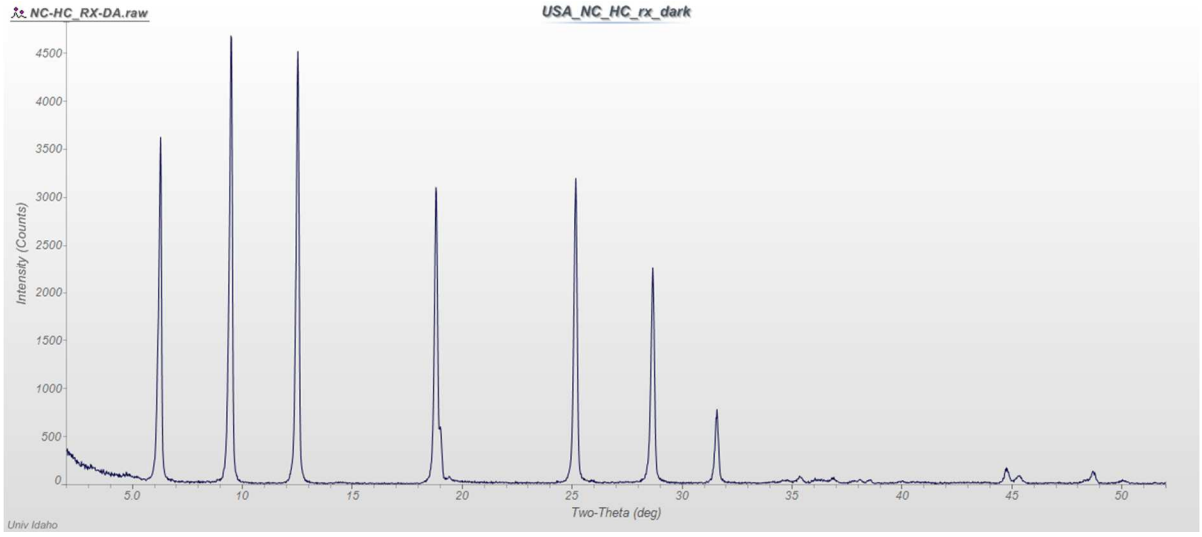
NC-HC_RX-DA.raw
USA_NC_HC_rx_dark
Intensity (Counts)
Two-Theta (deg)
Univ Idaho

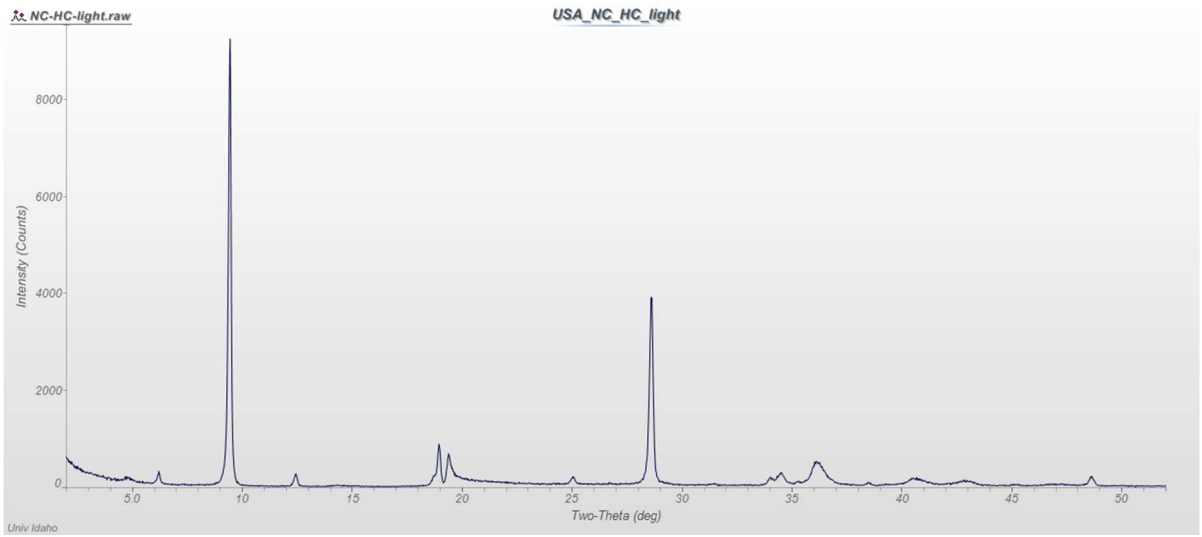
NC-HC-light.raw
USA_NC_HC_light
Intensity (Counts)
8000
6000
4000
2000
0
5.0
10
15
20
25
30
35
40
45
50
Two-Theta (deg)
Univ Idaho

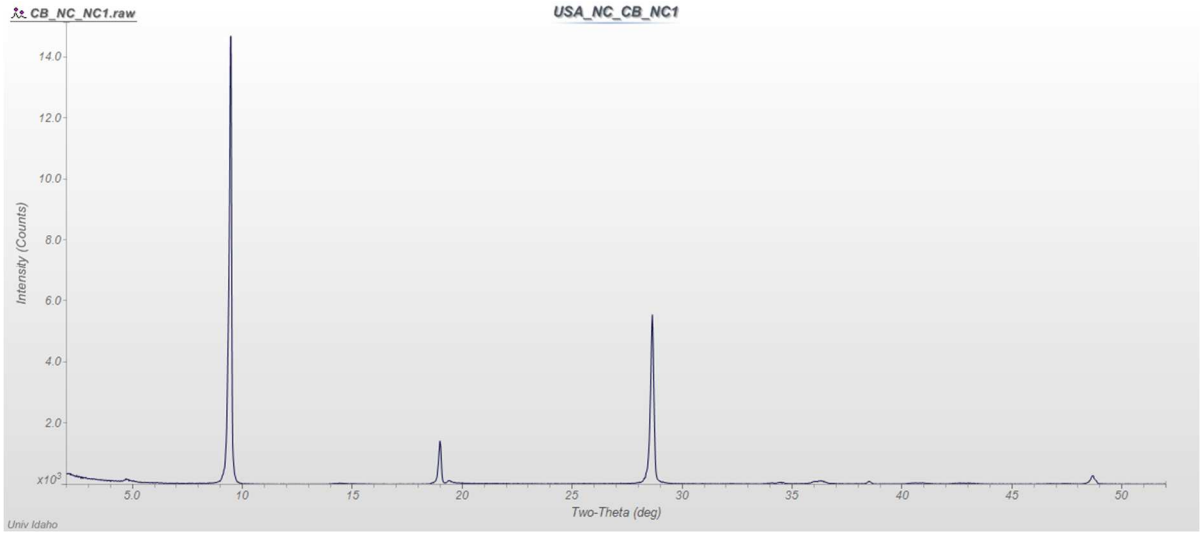
CB_NC_NC1.raw
USA_NC_CB_NC1
Intensity (Counts)
14.0
12.0
10.0
8.0
6.0
4.0
2.0
x10^3
5.0
10
15
20
25
30
35
40
45
50
Two-Theta (deg)
Univ Idaho

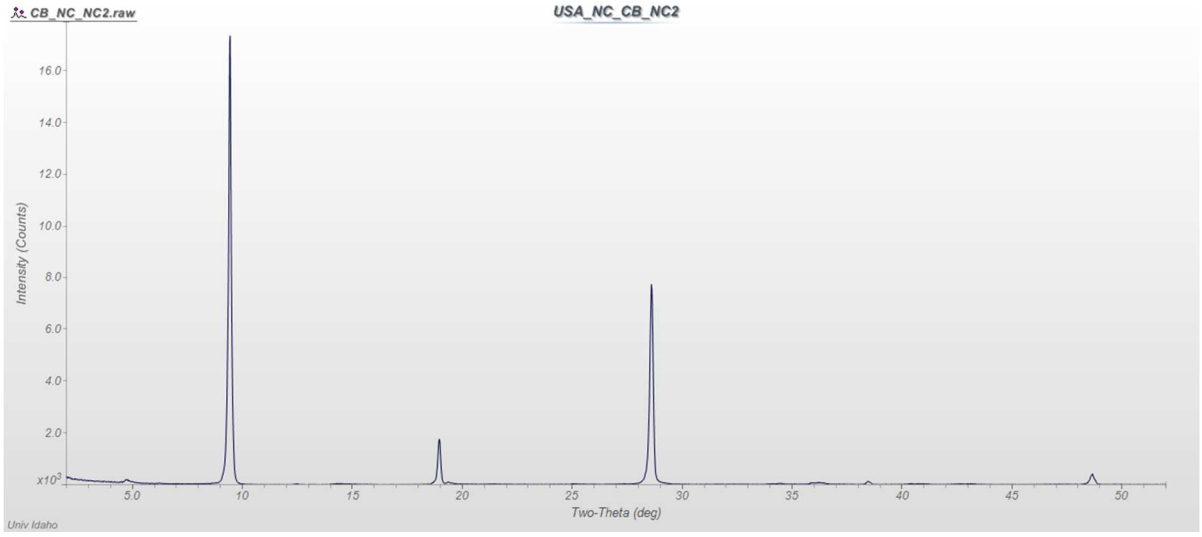
CB_NC_NC2.raw
USA_NC_CB_NC2
Intensity (Counts)
16.0
14.0
12.0
10.0
8.0
6.0
4.0
2.0
x10^3
5.0
10
15
20
25
30
35
40
45
50
Two-Theta (deg)
Univ Idaho

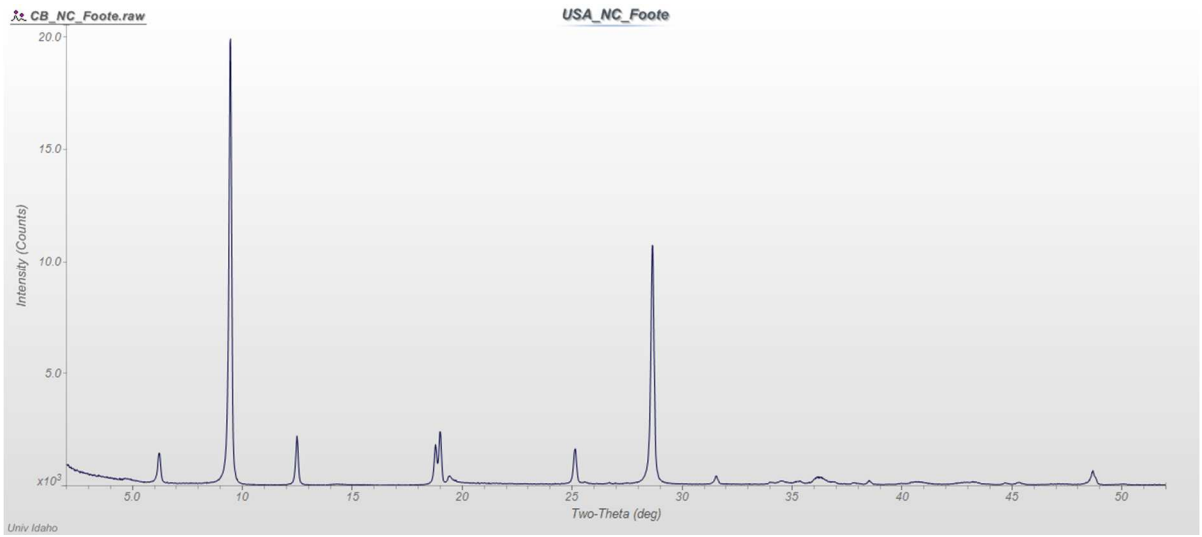
CB_NC_Foote.raw
USA_NC_Foote
Intensity (Counts)
x10^3
Two-Theta (deg)
Univ Idaho

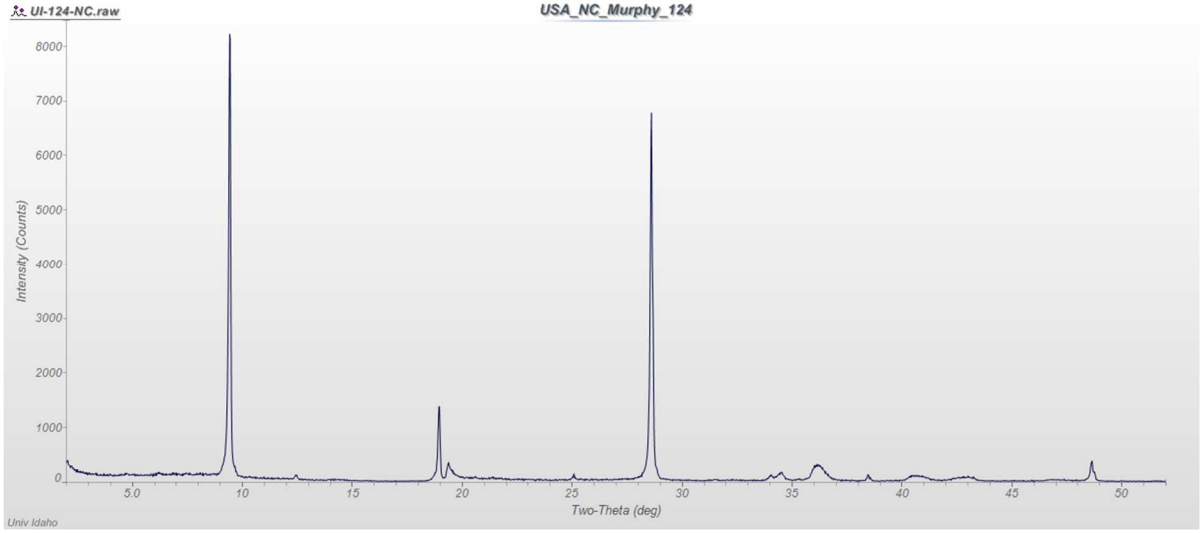
UI-124-NC.raw
USA_NC_Murphy_124
Intensity (Counts)
Two-Theta (deg)
Univ Idaho

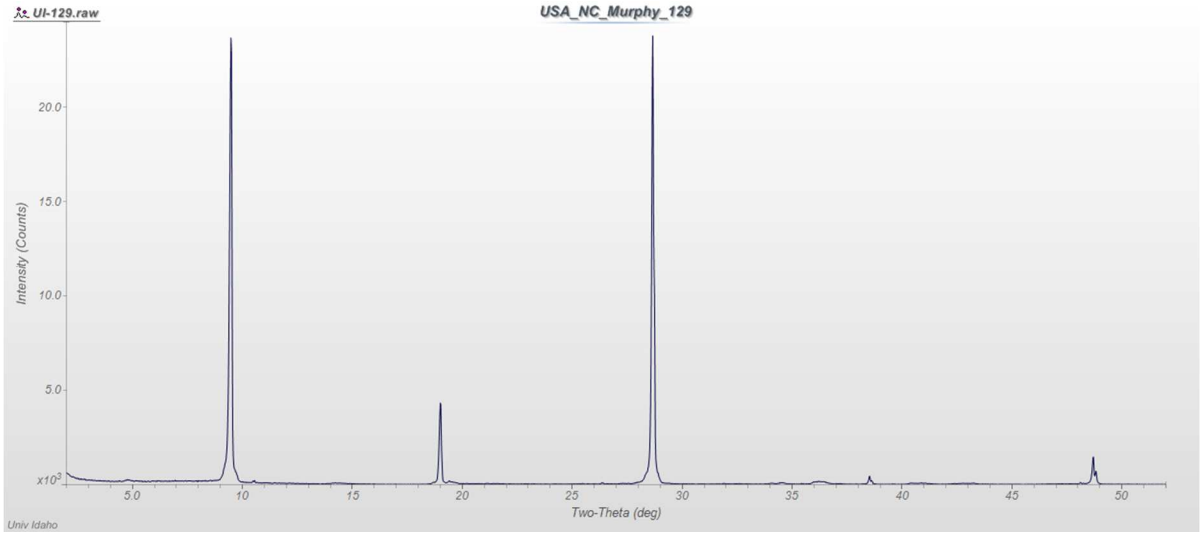
UI-129.raw
USA_NC_Murphy_129
Intensity (Counts)
x10^3
Two-Theta (deg)
Univ Idaho

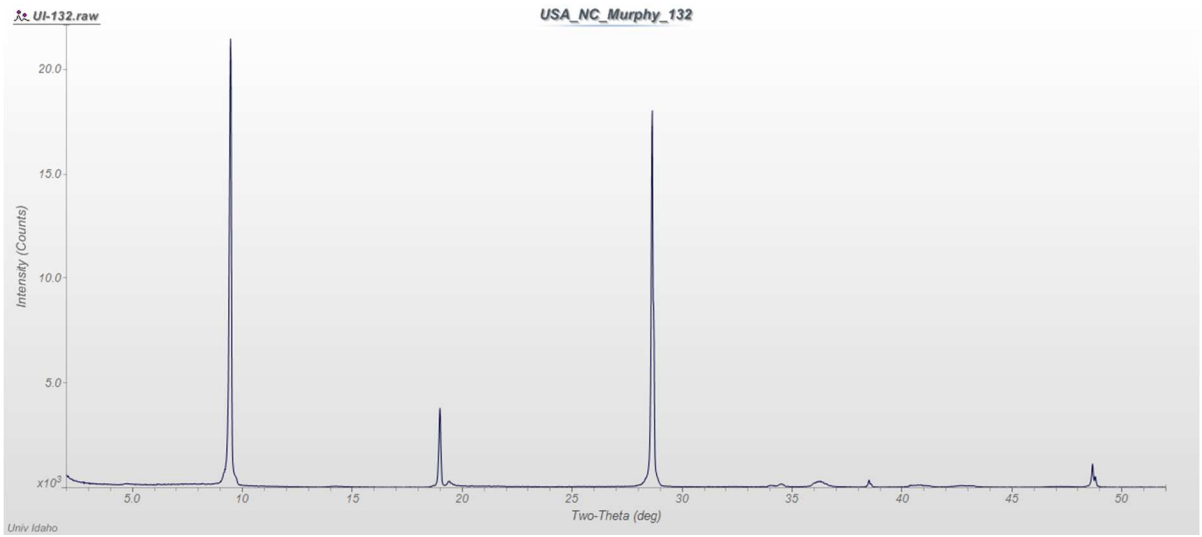
UI-132.raw
USA_NC_Murphy_132
Intensity (Counts)
x10^3
Two-Theta (deg)
Univ Idaho

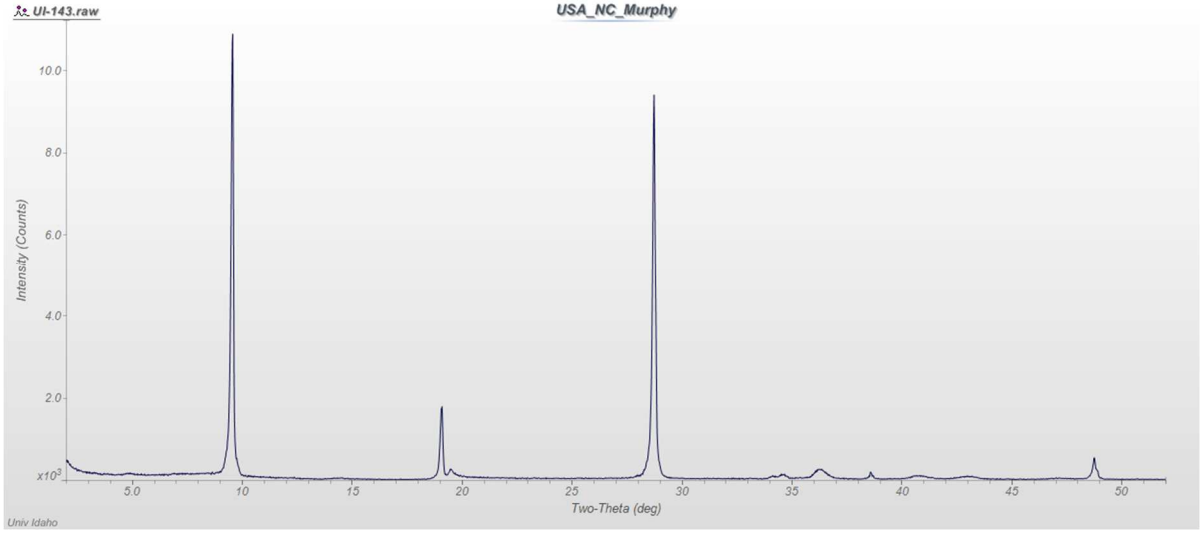
UI-143.raw
USA_NC_Murphy
Intensity (Counts)
x10^3
Two-Theta (deg)
Univ Idaho

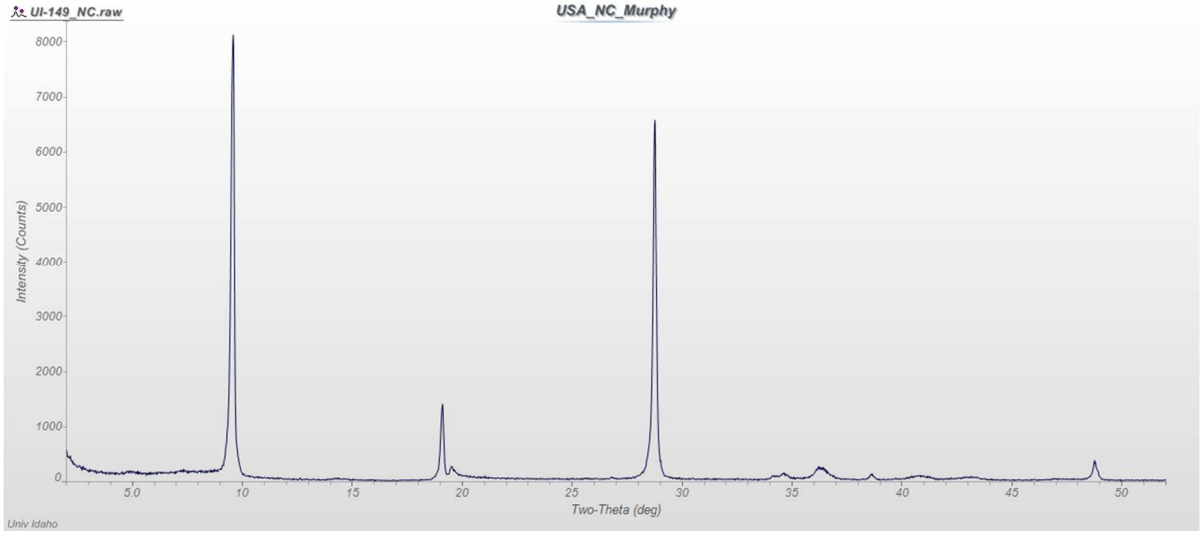
UI-149_NC.raw
USA_NC_Murphy
Intensity (Counts)
Two-Theta (deg)
Univ Idaho

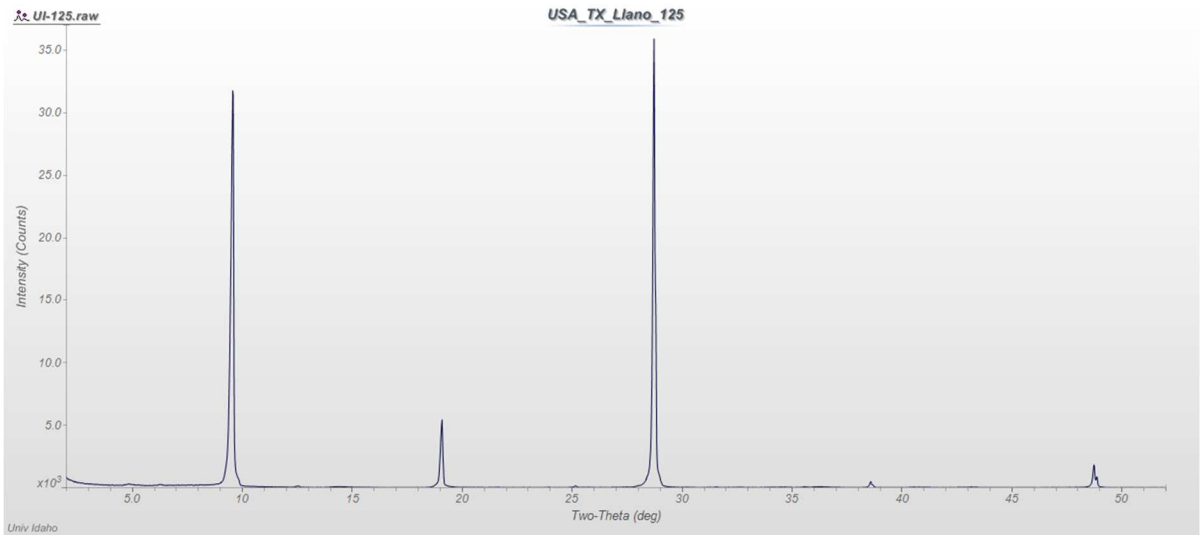
UI-125.raw
USA_TX_Llano_125
Intensity (Counts)
x10^3
Two-Theta (deg)
Univ Idaho

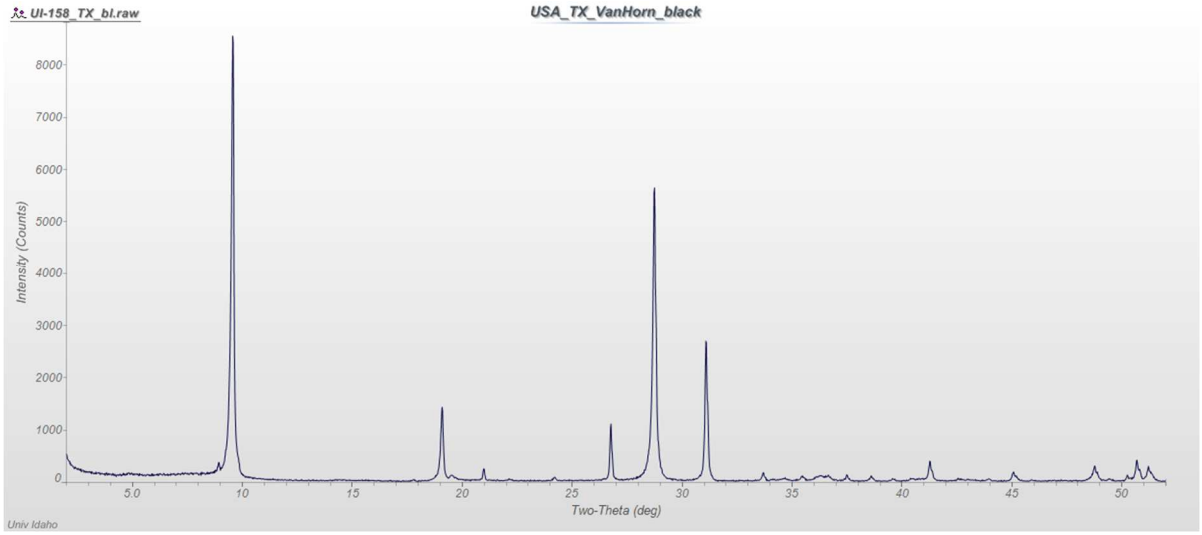
UI-158_TX_bl.raw
USA_TX_VanHorn_black
Intensity (Counts)
Two-Theta (deg)
Univ Idaho

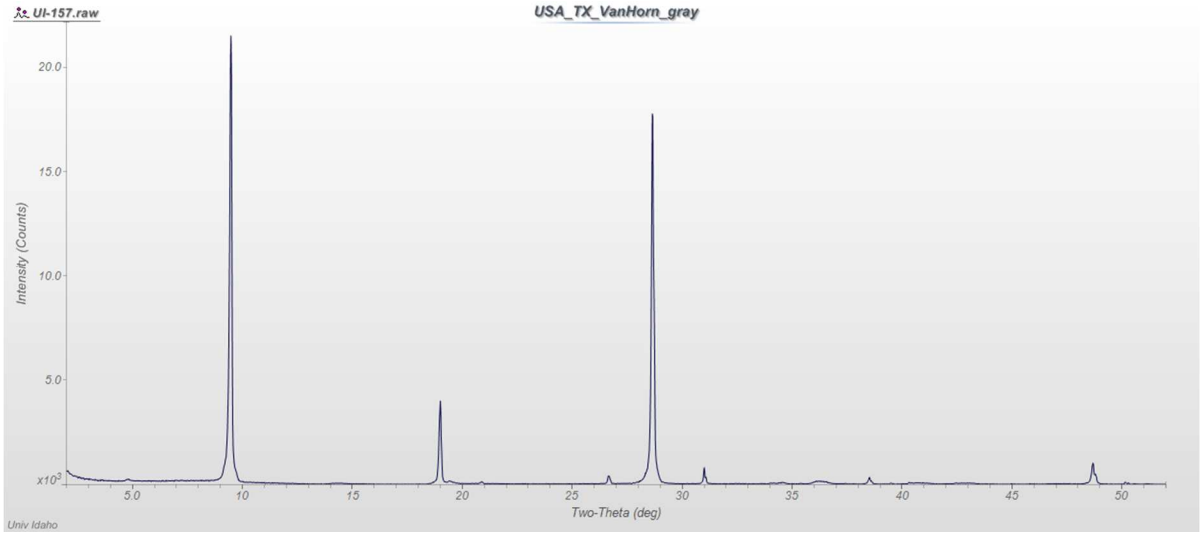
UI-157.raw
USA_TX_VanHorn_gray
Intensity (Counts)
x10^3
Two-Theta (deg)
Univ Idaho

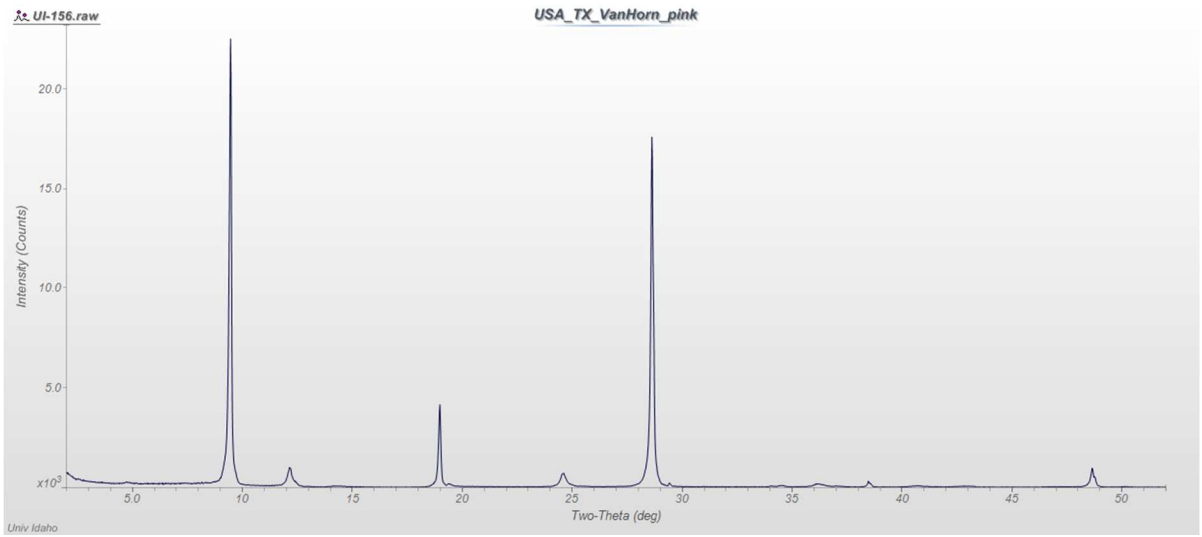
UI-156.raw
USA_TX_VanHorn_pink
Intensity (Counts)
x10^3
Two-Theta (deg)
Univ Idaho

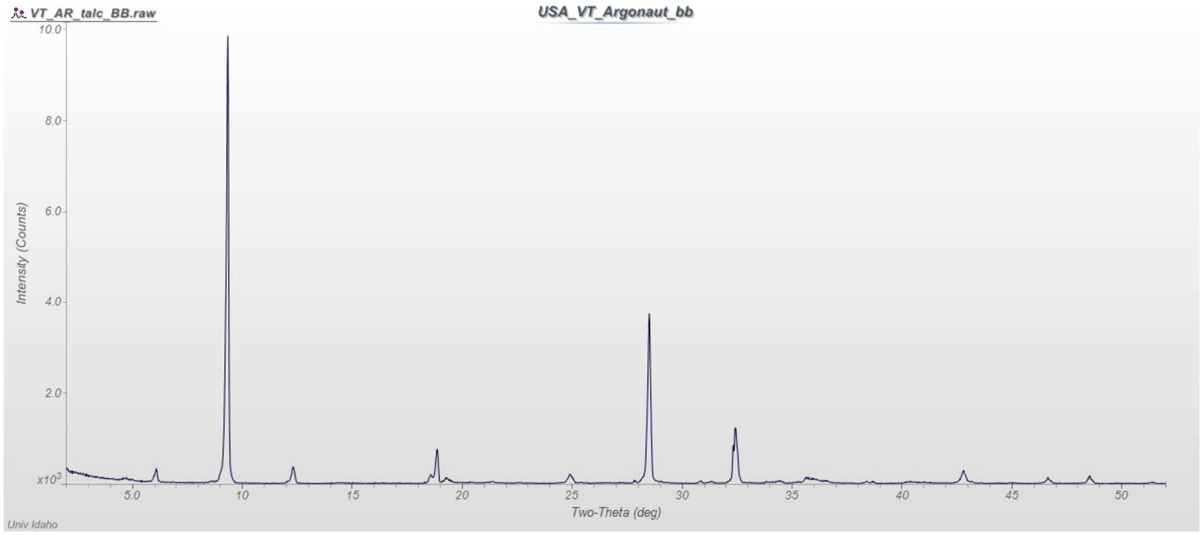
VT_AR_talc_BB.raw
USA_VT_Argonaut_bb
Intensity (Counts)
x10^3
Two-Theta (deg)
Univ Idaho

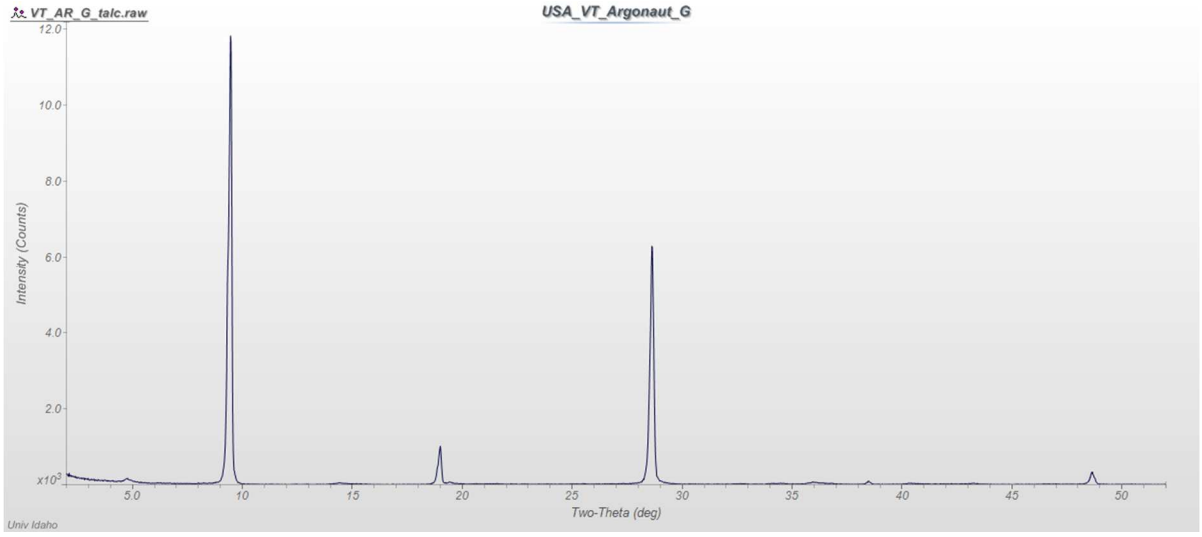
VT_AR_G_talc.raw
USA_VT_Argonaut_G
Intensity (Counts)
x10^3
Two-Theta (deg)
Univ Idaho

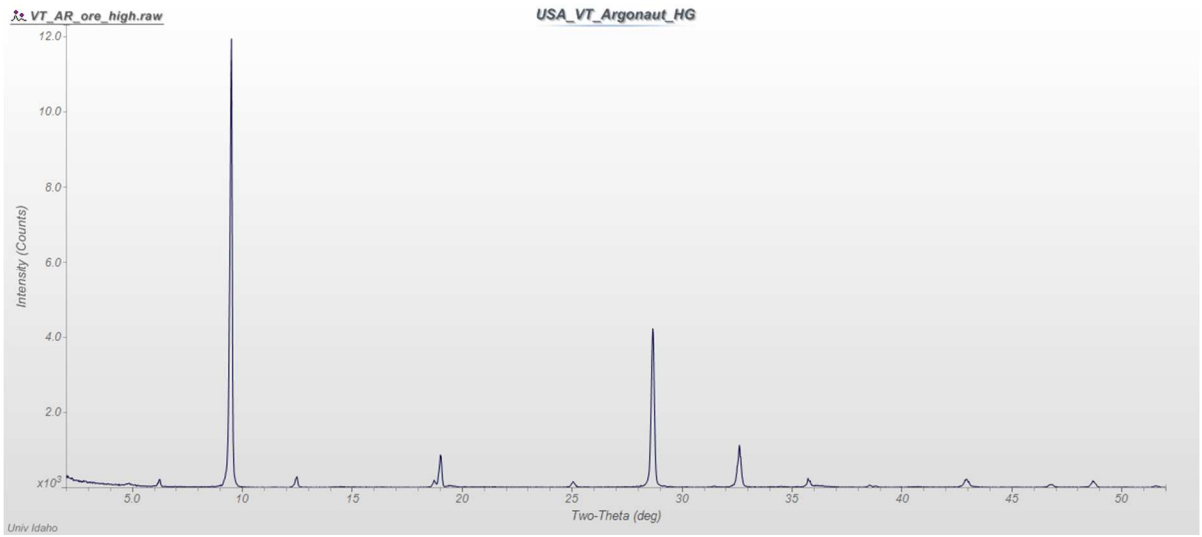
VT_AR_ore_high.raw
USA_VT_Argonaut_HG
Intensity (Counts)
x10^3
Two-Theta (deg)
Univ Idaho

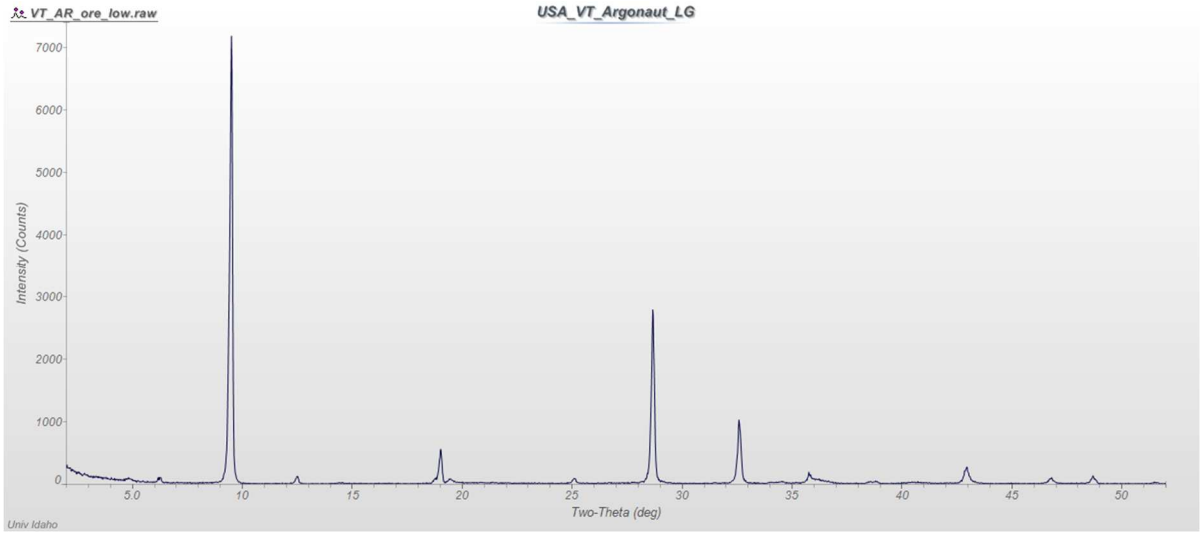
VT_AR_ore_low.raw
USA_VT_Argonaut_LG
Intensity (Counts)
Two-Theta (deg)
Univ Idaho

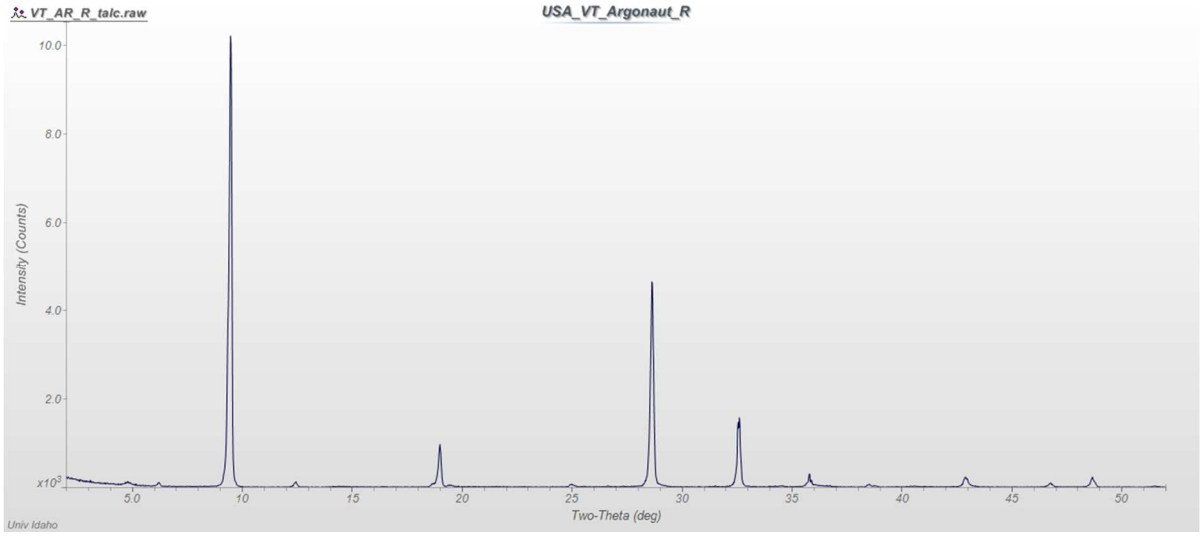
VT_AR_R_talc.raw
USA_VT_Argonaut_R
Intensity (Counts)
x10^3
Two-Theta (deg)
Univ Idaho

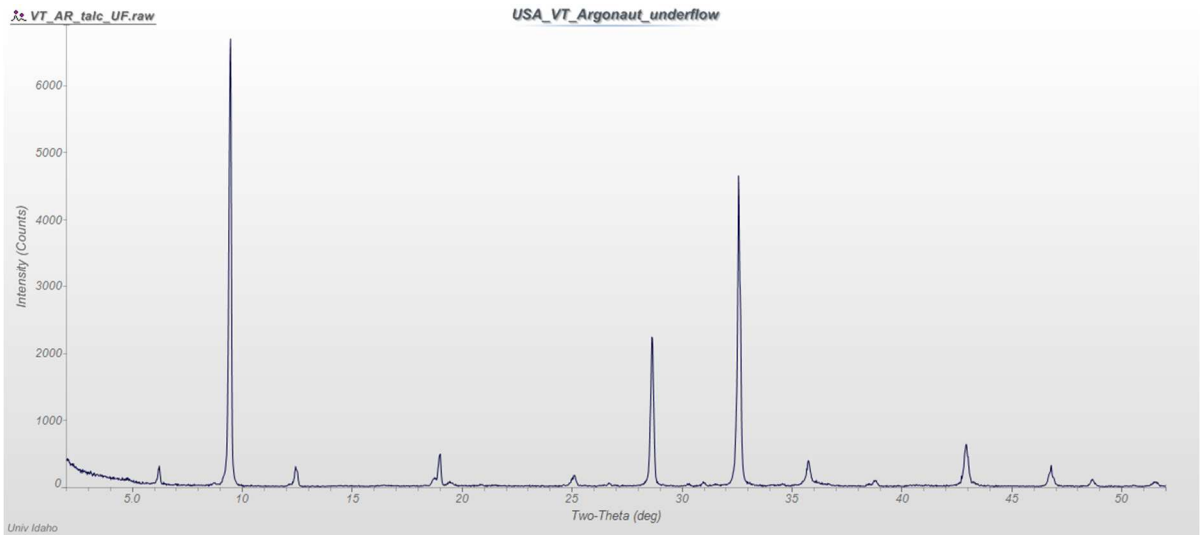
VT_AR_talc_UF.raw
USA_VT_Argonaut_underflow
Intensity (Counts)
Two-Theta (deg)
Univ Idaho

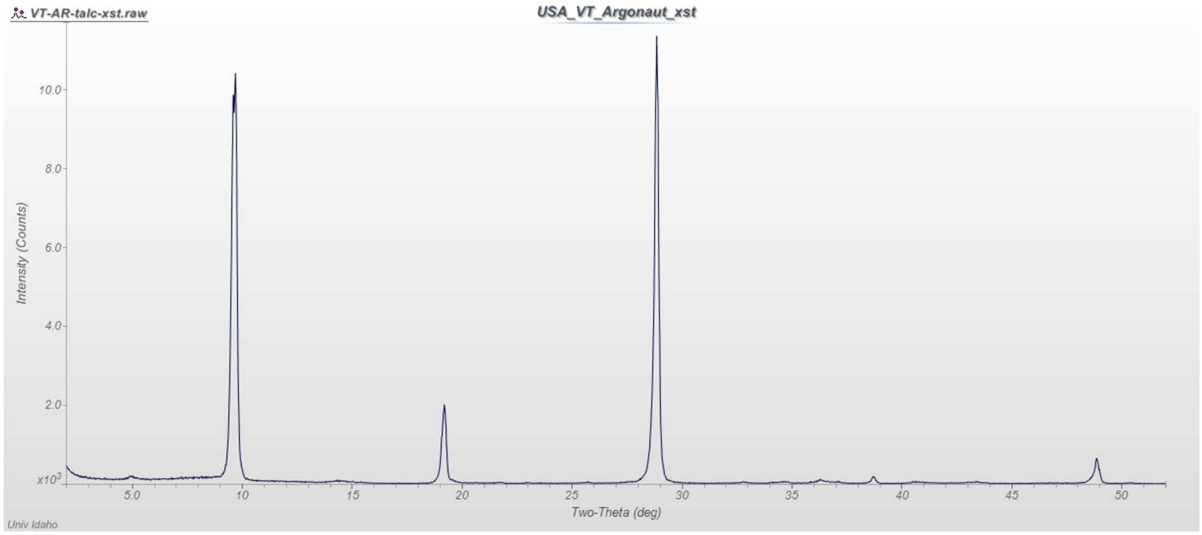
VT-AR-talc-xst.raw
USA_VT_Argonaut_xst
Intensity (Counts)
x10^3
Two-Theta (deg)
Univ Idaho

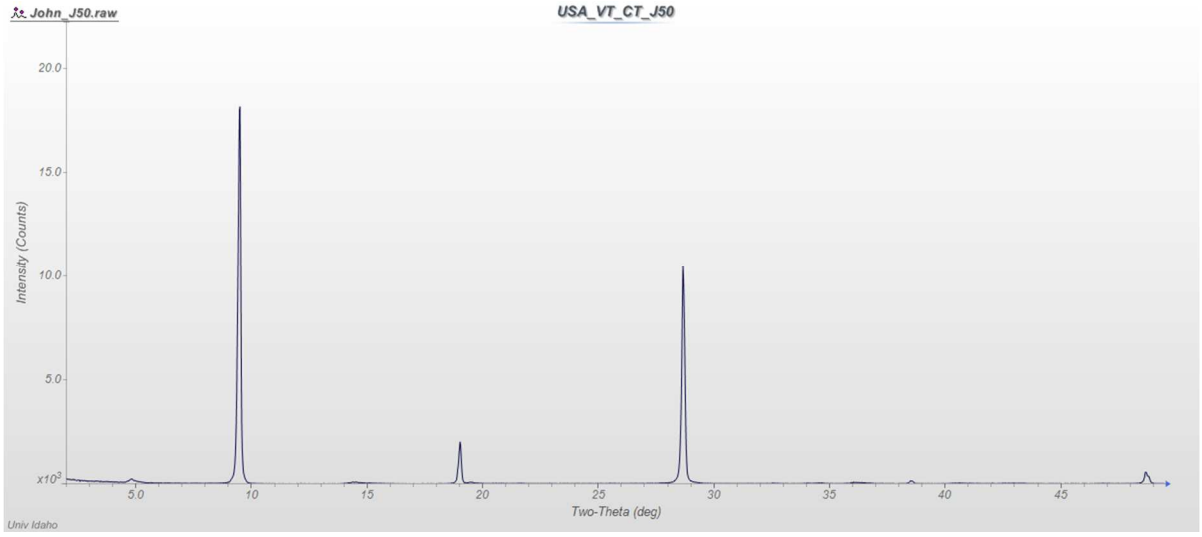
John_J50.raw
USA_VT_CT_J50
Intensity (Counts)
x10^3
Two-Theta (deg)
Univ Idaho

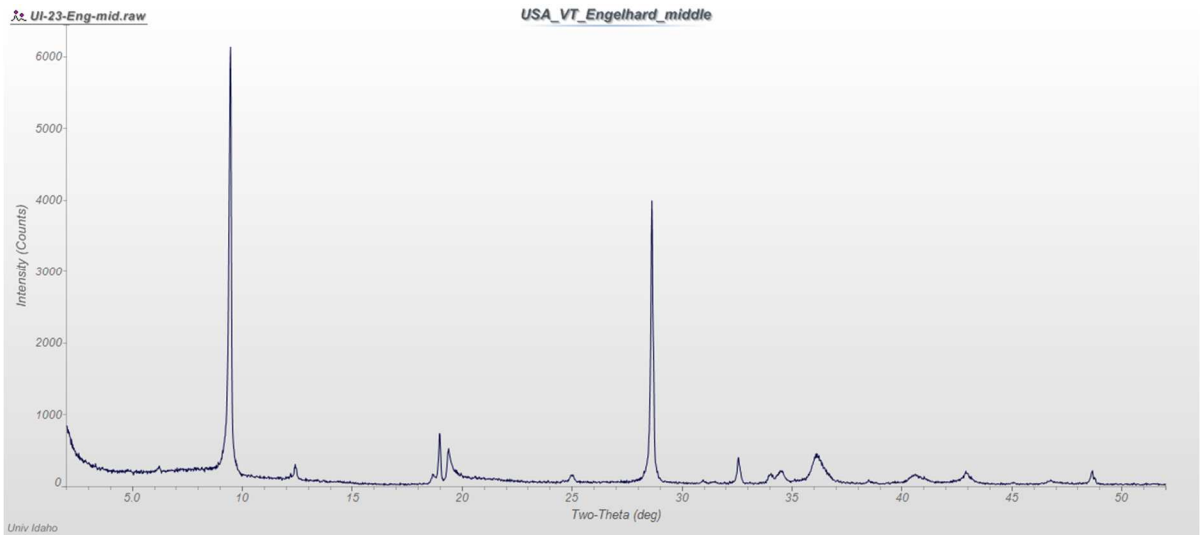
UI-23-Eng-mid.raw
USA_VT_Engelhard_middle
Intensity (Counts)
Two-Theta (deg)
Univ Idaho

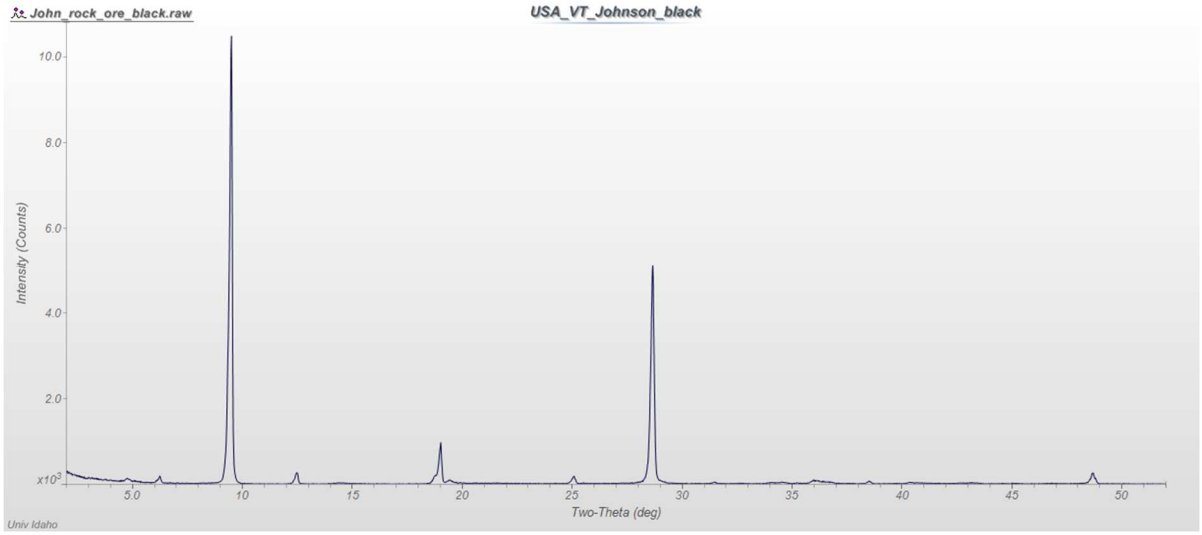
John_rock_ore_black.raw
USA_VT_Johnson_black
Intensity (Counts)
x10^3
Two-Theta (deg)
Univ Idaho

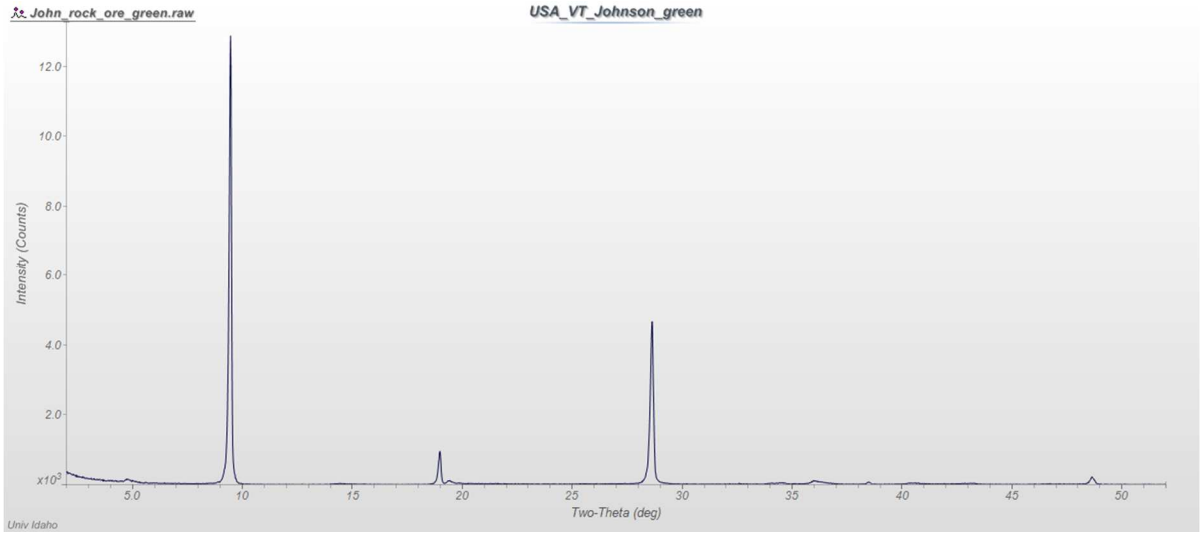
John_rock_ore_green.raw
USA_VT_Johnson_green
Intensity (Counts)
x10^3
Two-Theta (deg)
Univ Idaho

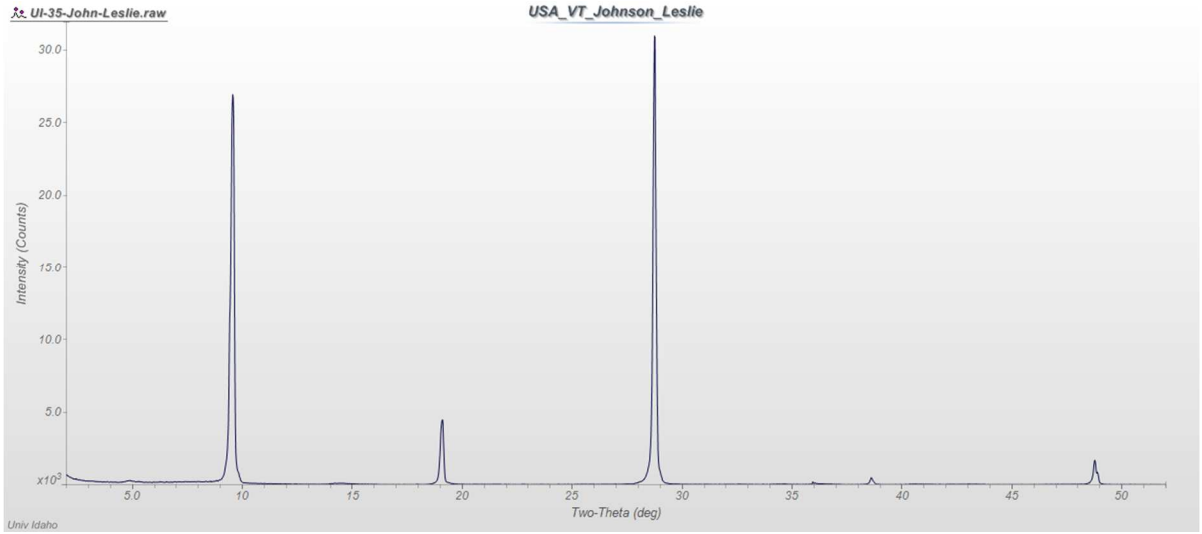
UI-35-John-Leslie.raw
USA_VT_Johnson_Leslie
Intensity (Counts)
x10^3
Two-Theta (deg)
Univ Idaho

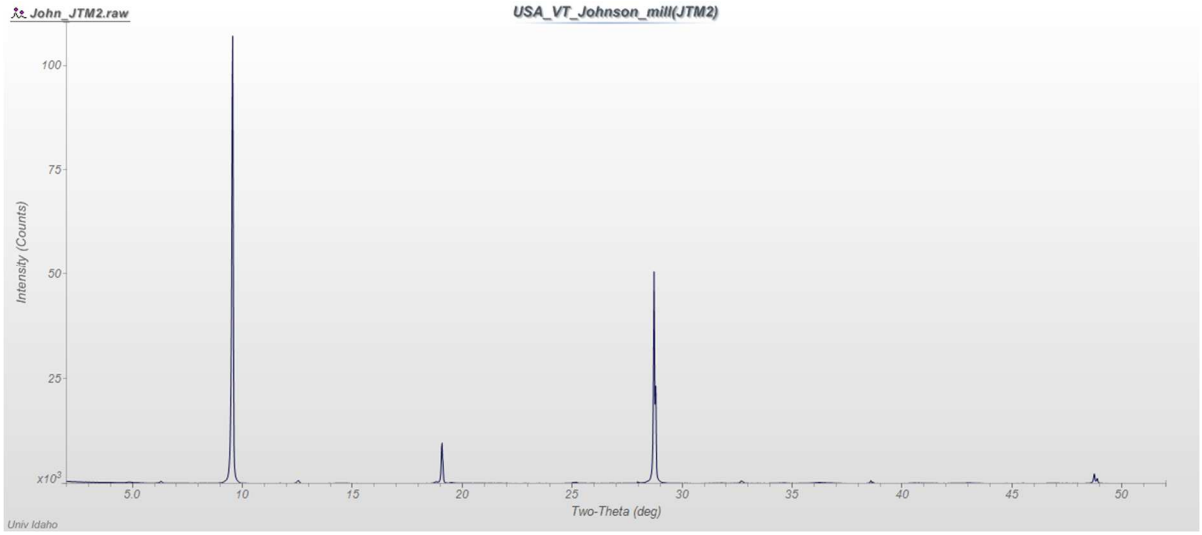
John_JTM2.raw
USA_VT_Johnson_mill(JTM2)
Intensity (Counts)
x10^3
Two-Theta (deg)
Univ Idaho

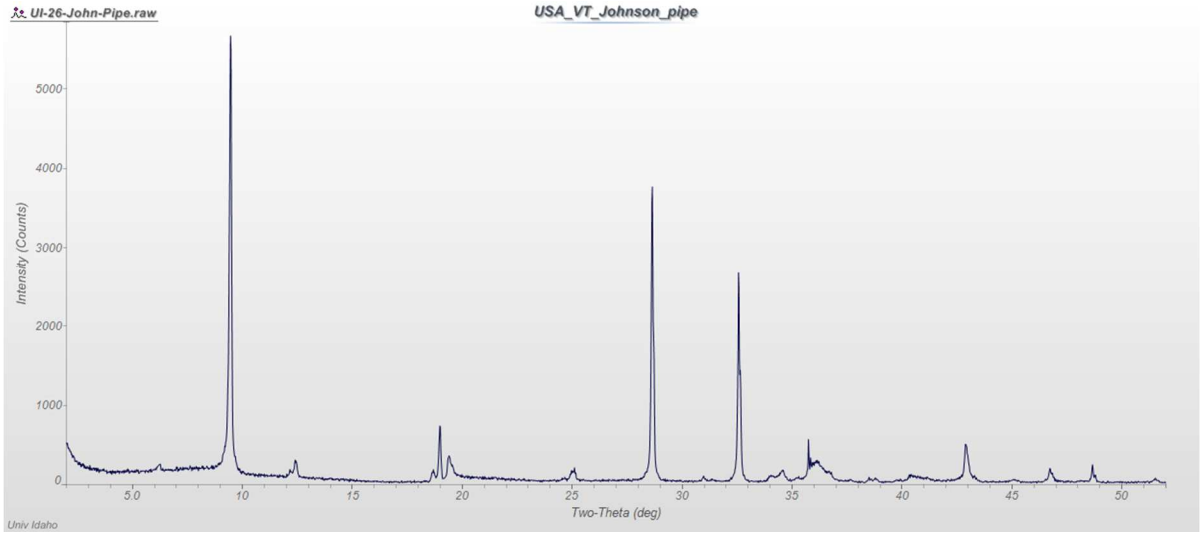
UI-26-John-Pipe.raw
USA_VT_Johnson_pipe
Intensity (Counts)
Two-Theta (deg)
Univ Idaho

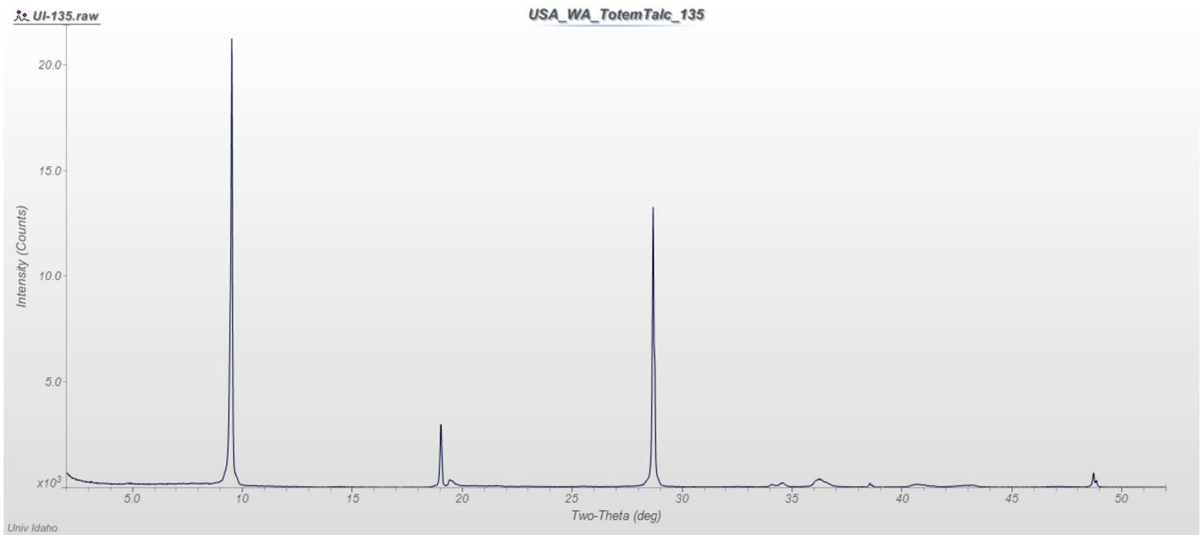
UI-135.raw
USA_WA_TotemTalc_135
Intensity (Counts)
x10^3
Two-Theta (deg)
Univ Idaho

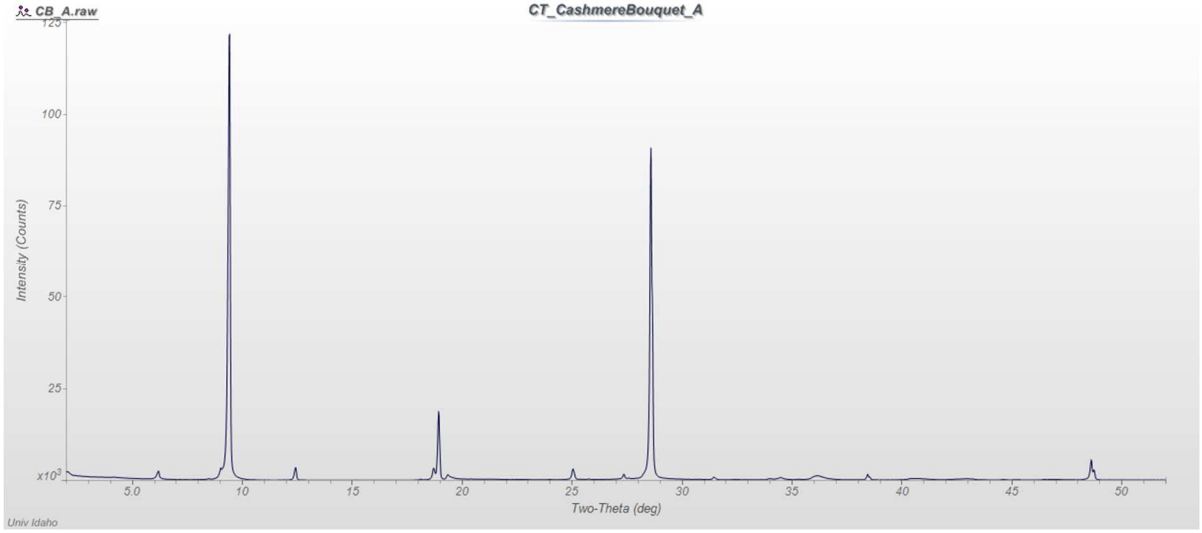
CB_A.raw
CT_CashmereBouquet_A
Intensity (Counts)
x10^3
Two-Theta (deg)
Univ Idaho

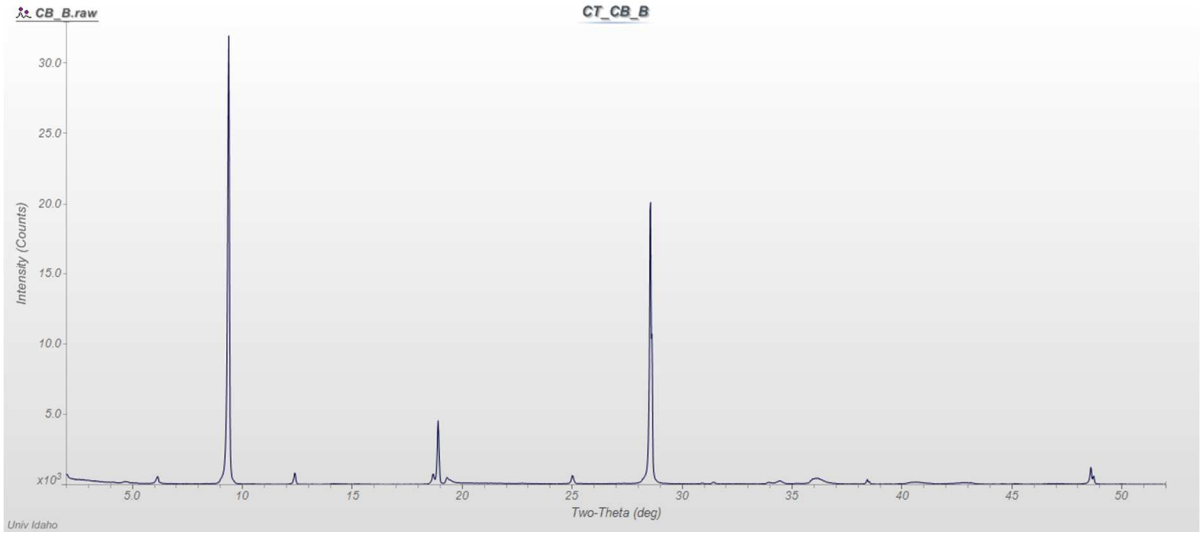
CB_B.raw
CT_CB_B
Intensity (Counts)
x10^3
Two-Theta (deg)
Univ Idaho

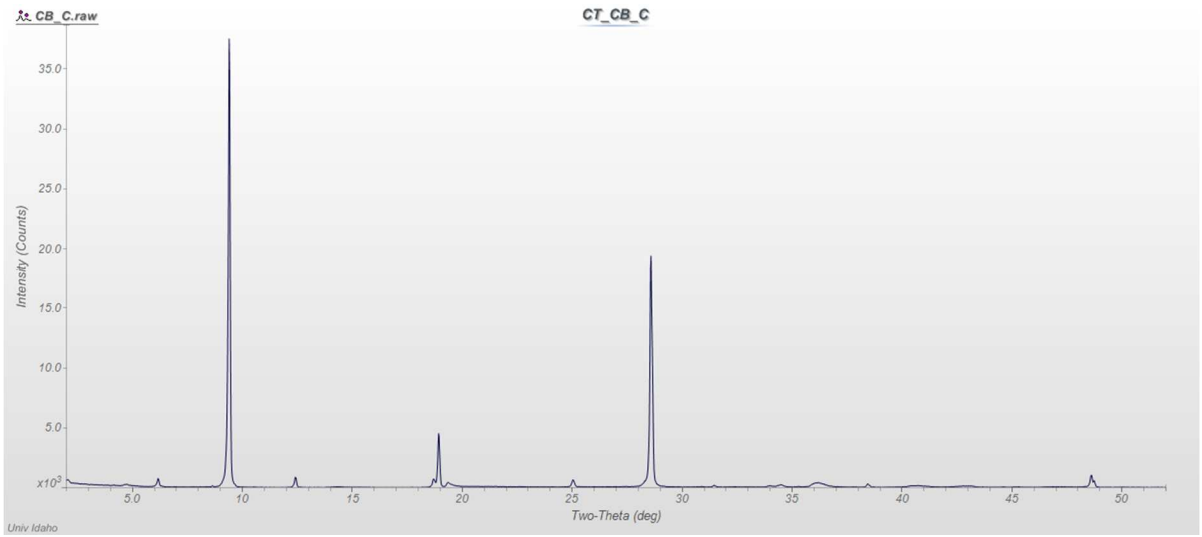
CB_C.raw
CT_CB_C
Intensity (Counts)
x10^3
Two-Theta (deg)
Univ Idaho

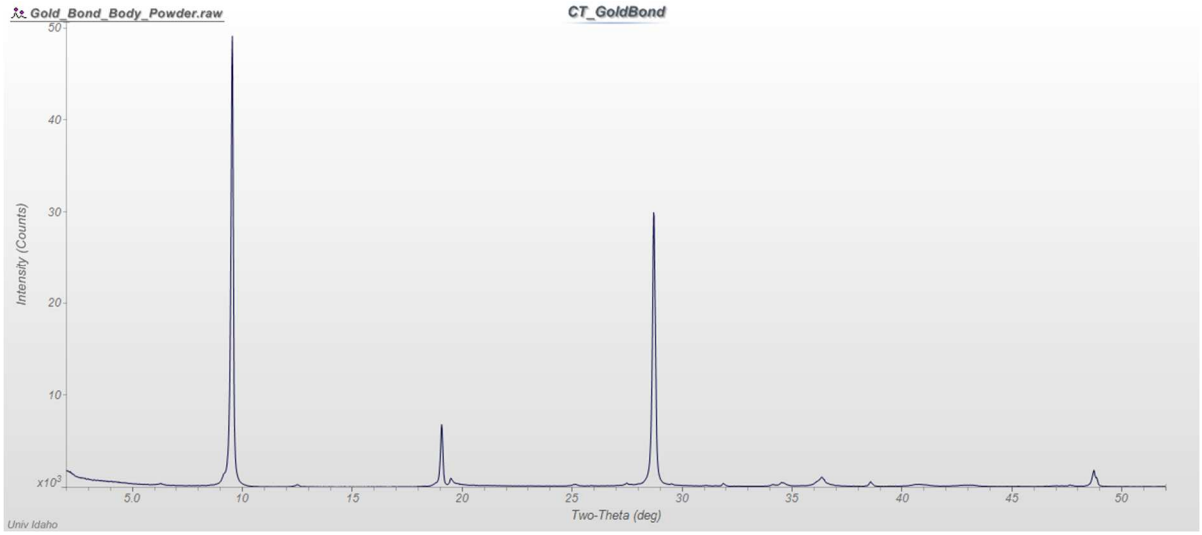
Gold_Bond_Body_Powder.raw
CT_GoldBond
Intensity (Counts)
x10^3
Two-Theta (deg)
Univ Idaho

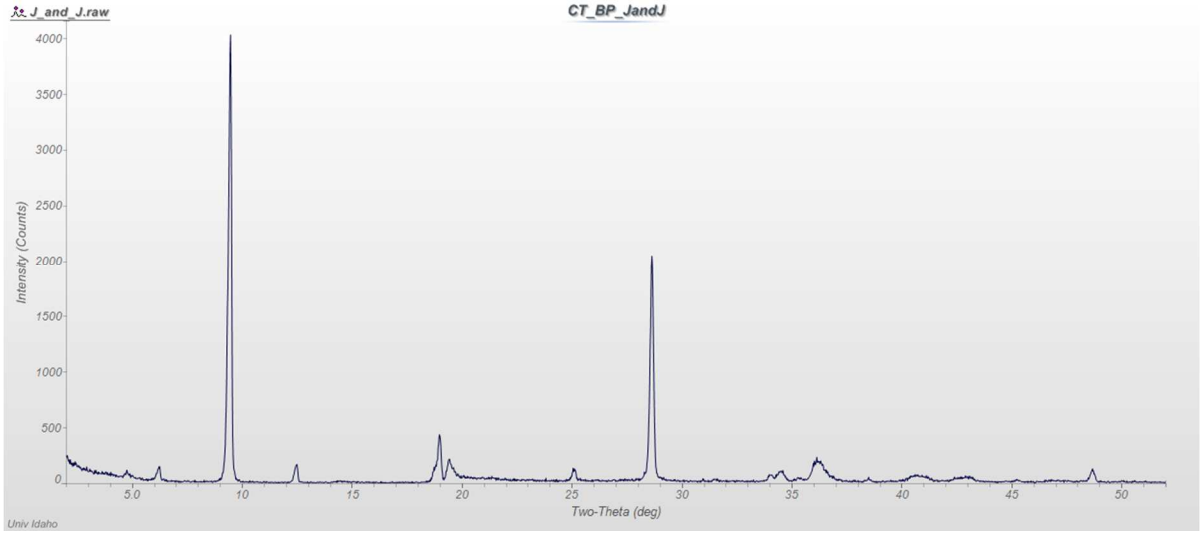
J_and_J.raw
CT_BP_JandJ
Intensity (Counts)
Two-Theta (deg)
Univ Idaho

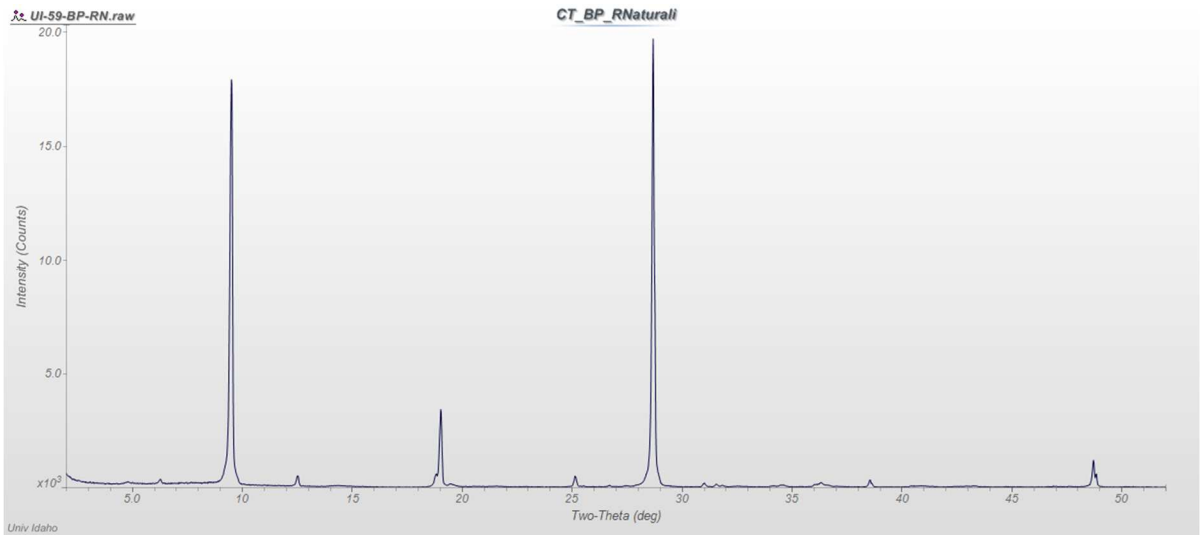
UI-59-BP-RN.raw
CT_BP_RNaturali
Intensity (Counts)
x10^3
Two-Theta (deg)
Univ Idaho

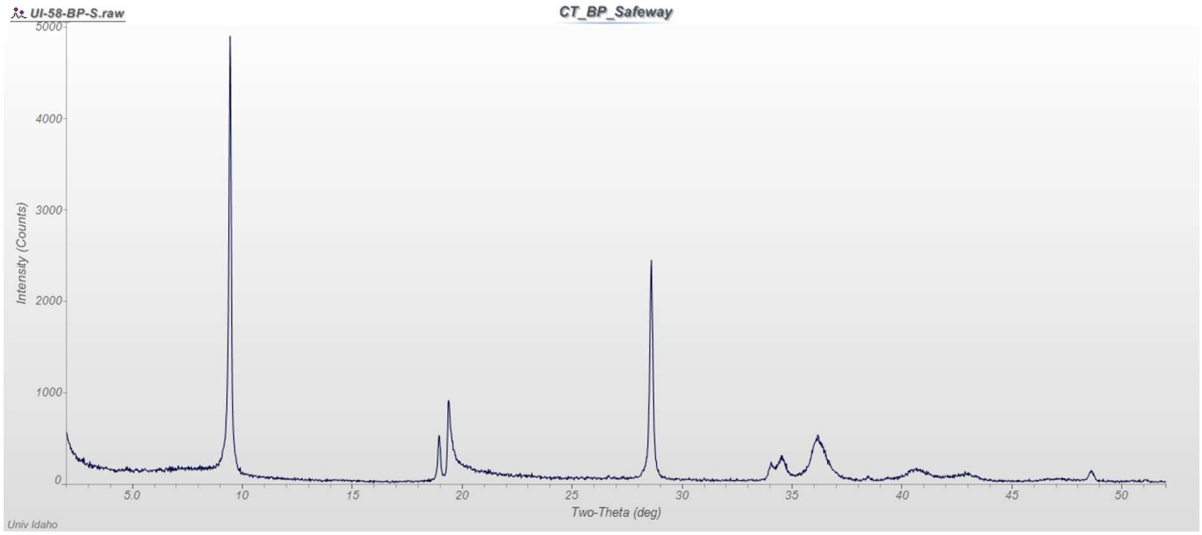
UI-58-BP-S.raw
CT_BP_Safeway
Intensity (Counts)
Two-Theta (deg)
Univ Idaho

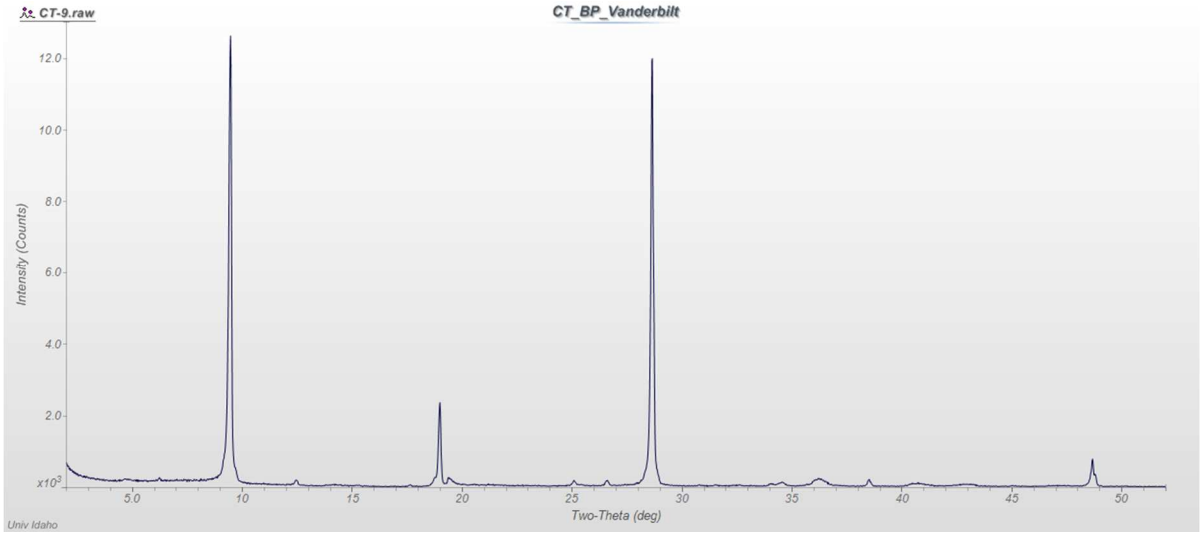
CT-9.raw
CT_BP_Vanderbilt
Intensity (Counts)
x10^3
Two-Theta (deg)
Univ Idaho

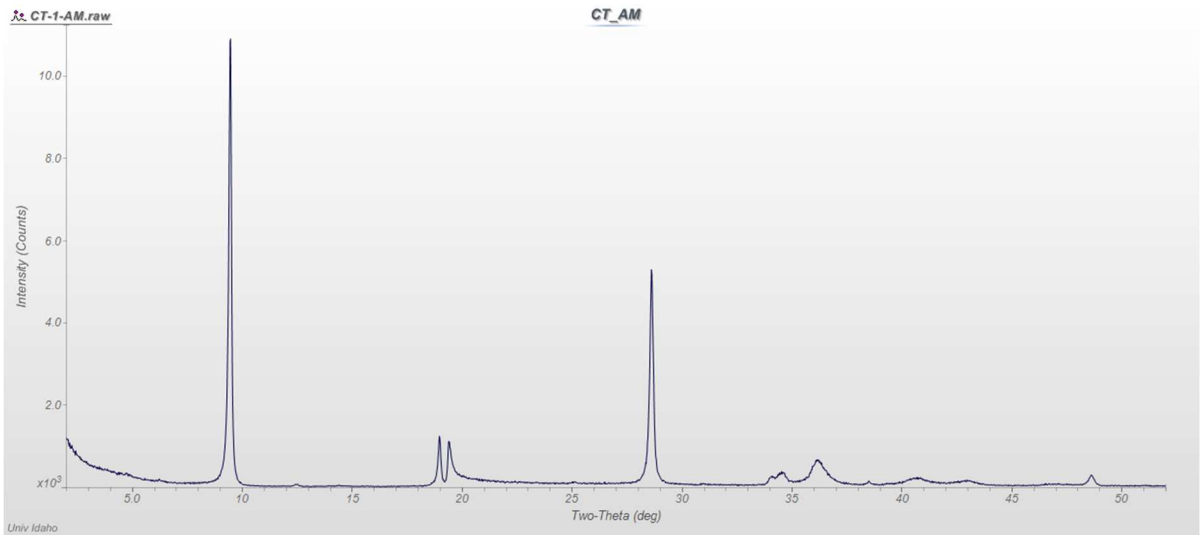
CT-1-AM.raw
CT_AM
Intensity (Counts)
x10^3
Two-Theta (deg)
Univ Idaho

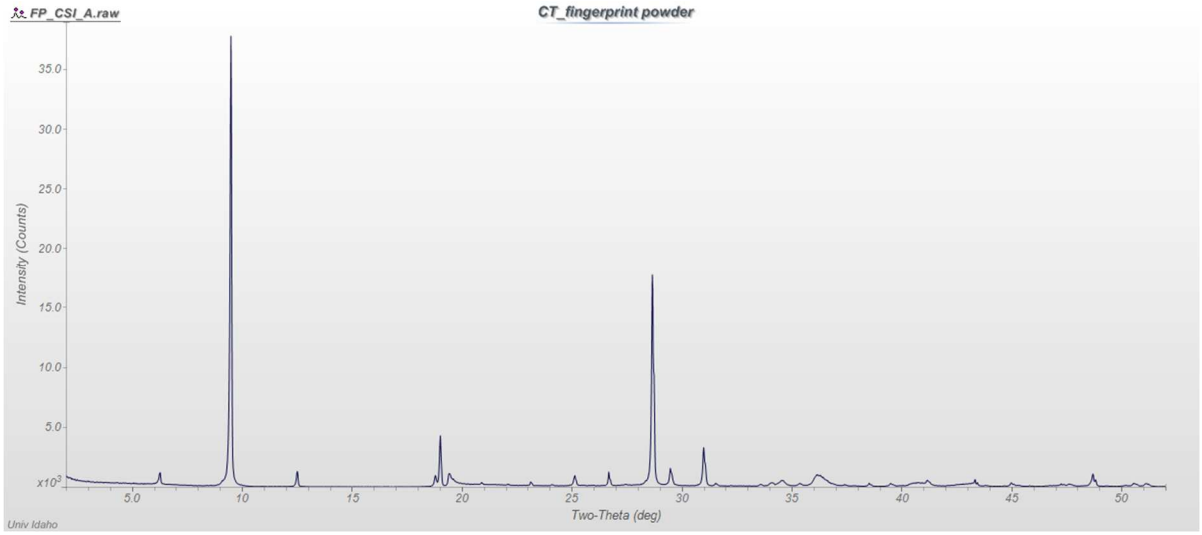
FP_CSI_A.raw
CT_fingerprint powder
Intensity (Counts)
x10^3
Two-Theta (deg)
Univ Idaho

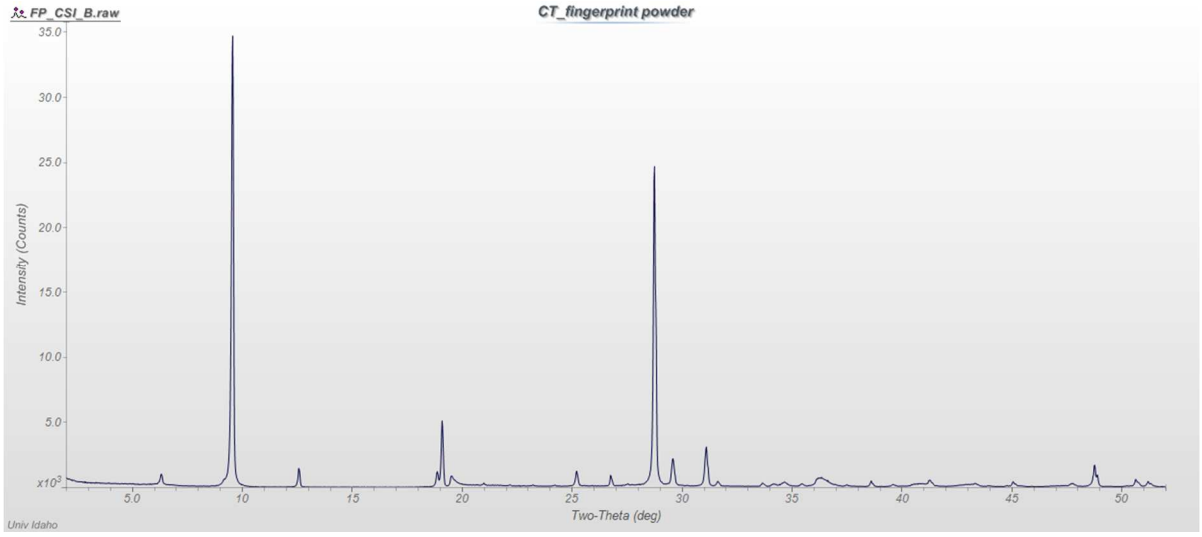
FP_CSI_B.raw
CT_fingerprint powder
Intensity (Counts)
x10^3
Two-Theta (deg)
Univ Idaho

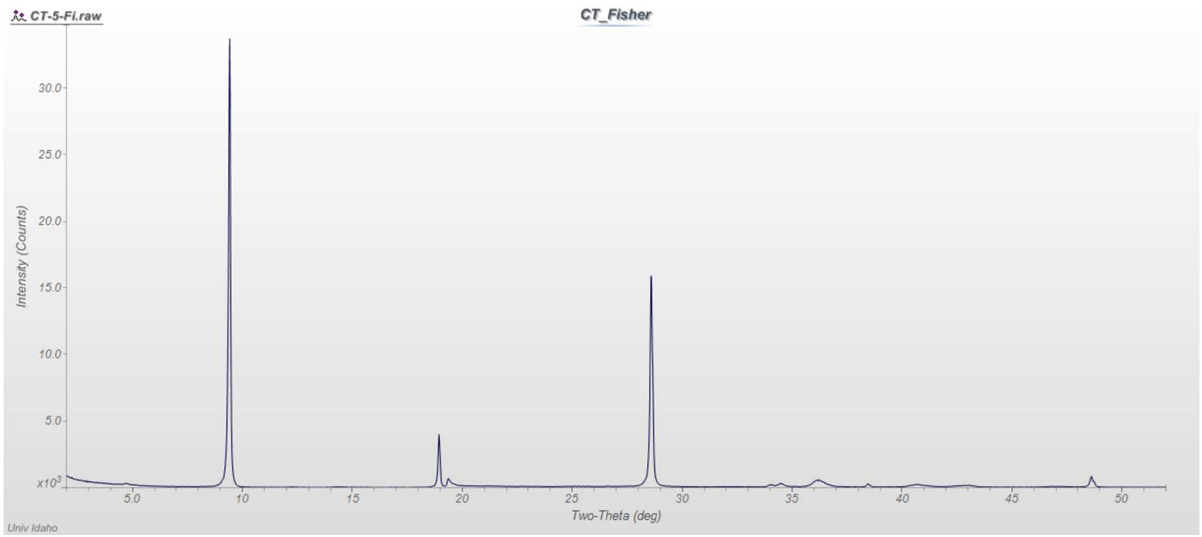
CT-5-Fi.raw
CT_Fisher
Intensity (Counts)
x10^3
Two-Theta (deg)
Univ Idaho

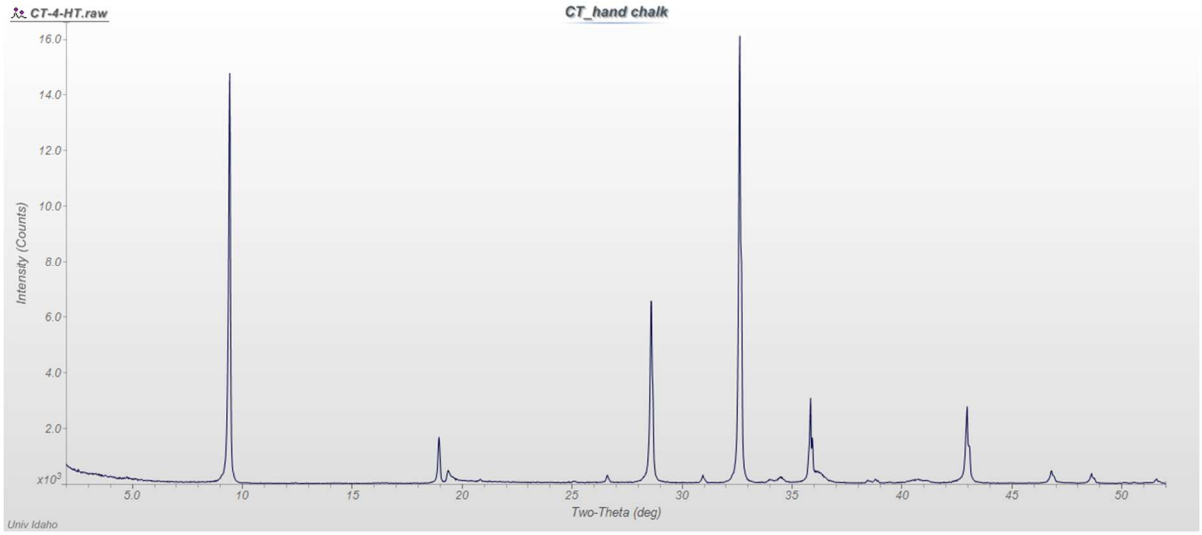
CT-4-HT.raw
CT_hand chalk
Intensity (Counts)
x10^3
Two-Theta (deg)
Univ Idaho

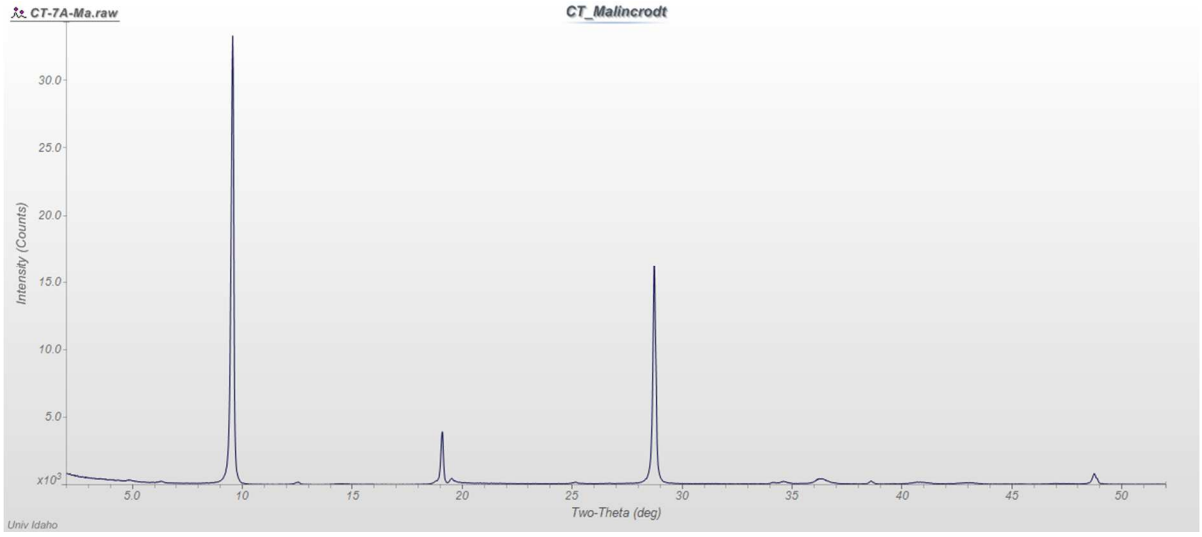
CT-7A-Ma.raw
CT_Malincrodt
Intensity (Counts)
x10^3
Two-Theta (deg)
Univ Idaho

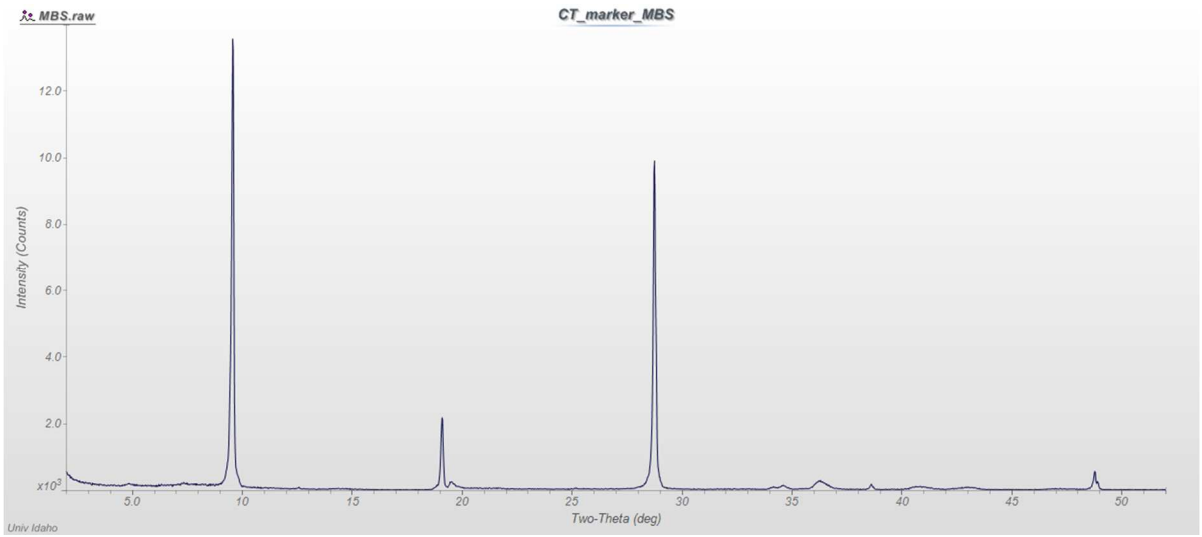
MBS.raw
CT_marker_MBS
Intensity (Counts)
x10^3
Two-Theta (deg)
Univ Idaho

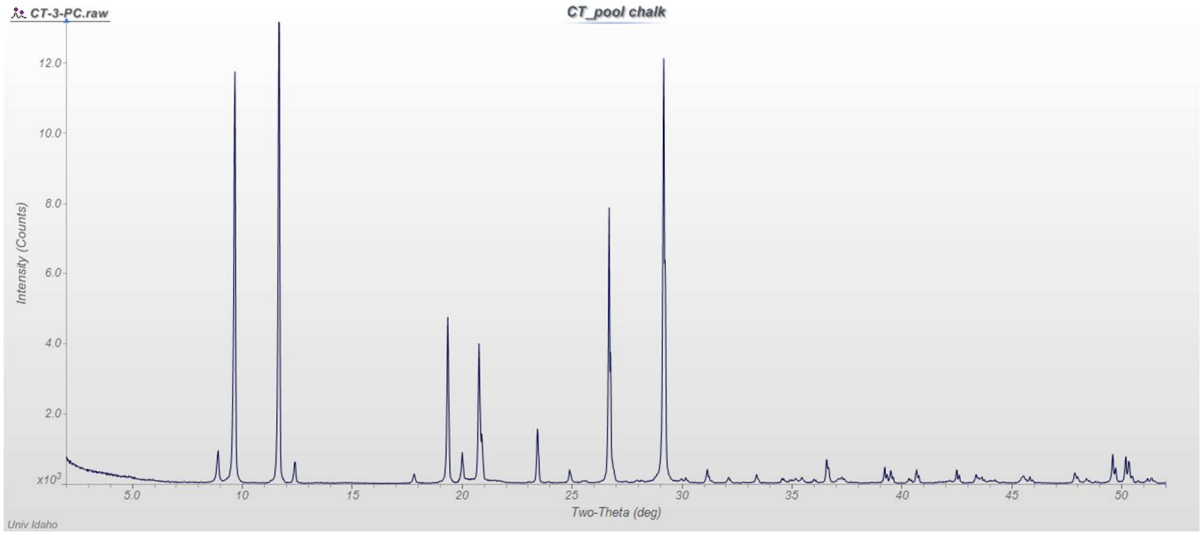
CT-3-PC.raw
CT_pool chalk
Intensity (Counts)
x10^3
Two-Theta (deg)
Univ Idaho

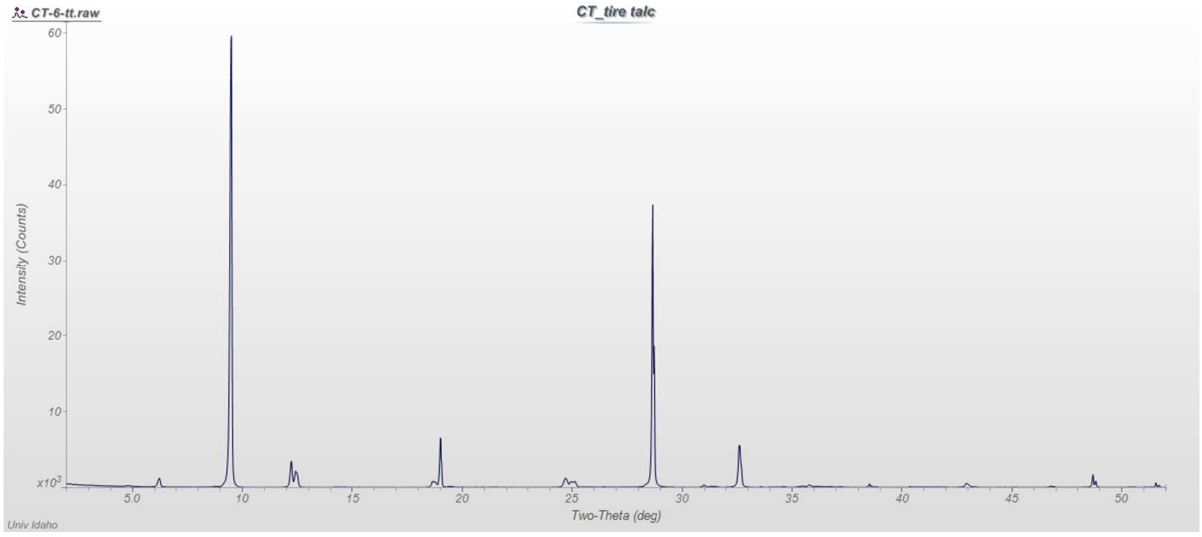
CT-6-tt.raw
CT_tire talc
Intensity (Counts)
x10^3
Two-Theta (deg)
Univ Idaho

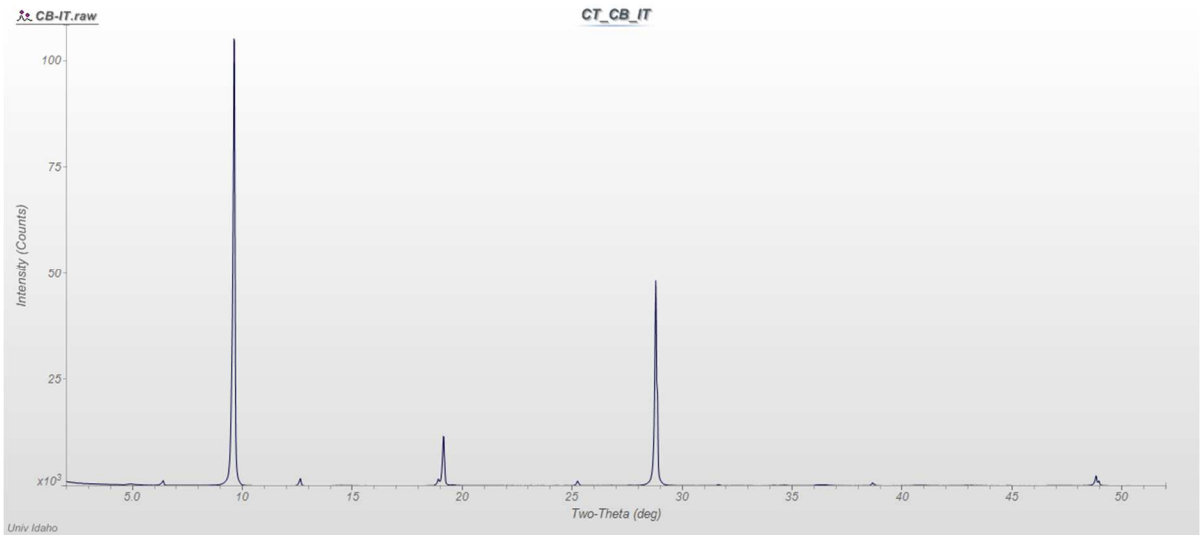
CB-IT.raw
CT_CB_IT
Intensity (Counts)
x10^3
Two-Theta (deg)
Univ Idaho

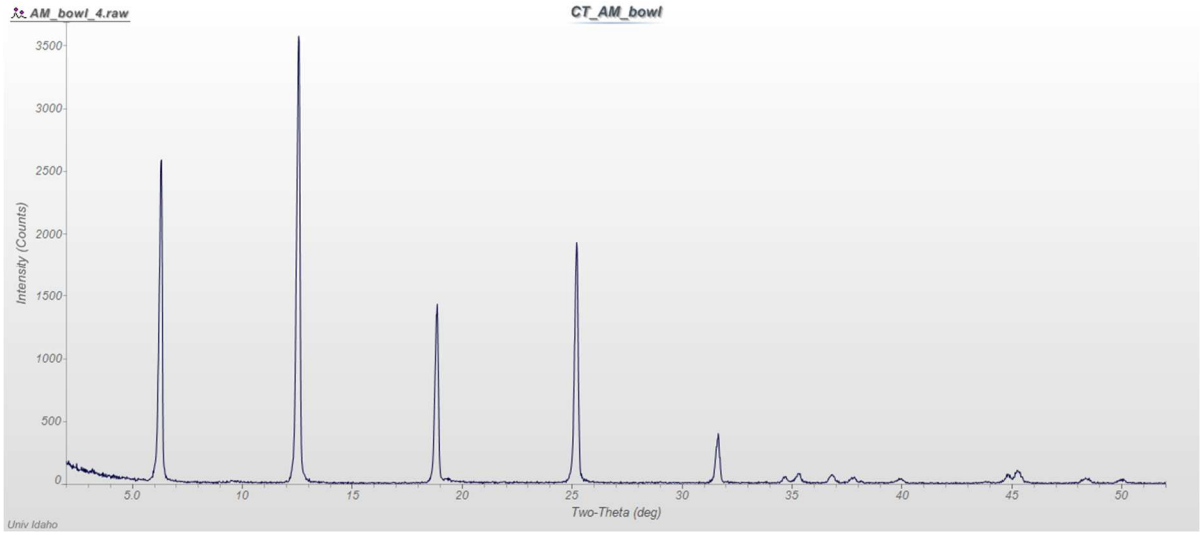
AM_bowl_4.raw
CT_AM_bowl
Intensity (Counts)
Two-Theta (deg)
Univ Idaho

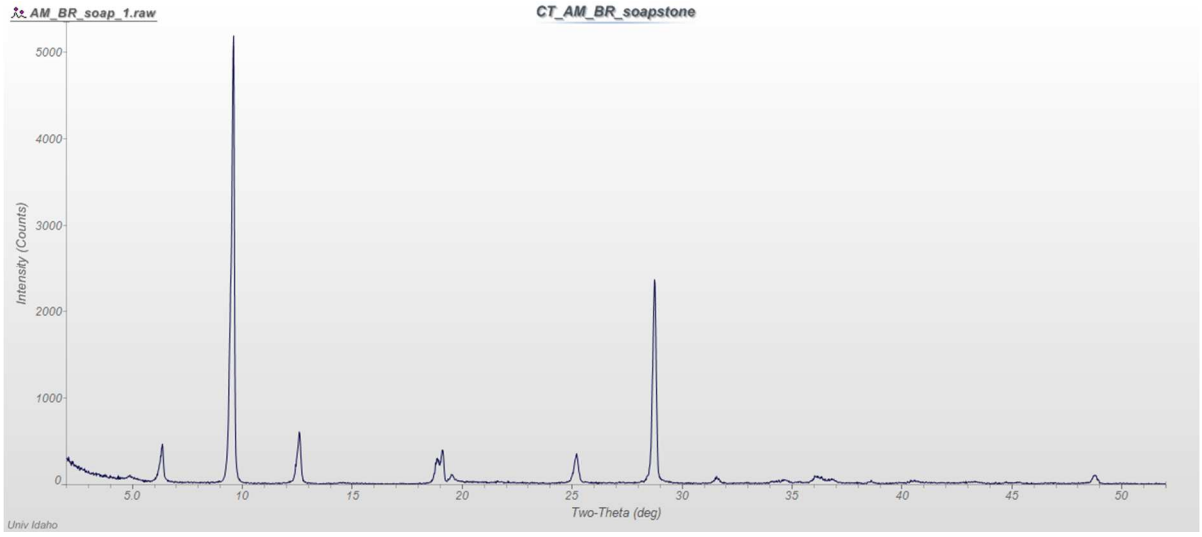
AM_BR_soap_1.raw
CT_AM_BR_soapstone
Intensity (Counts)
Two-Theta (deg)
Univ Idaho

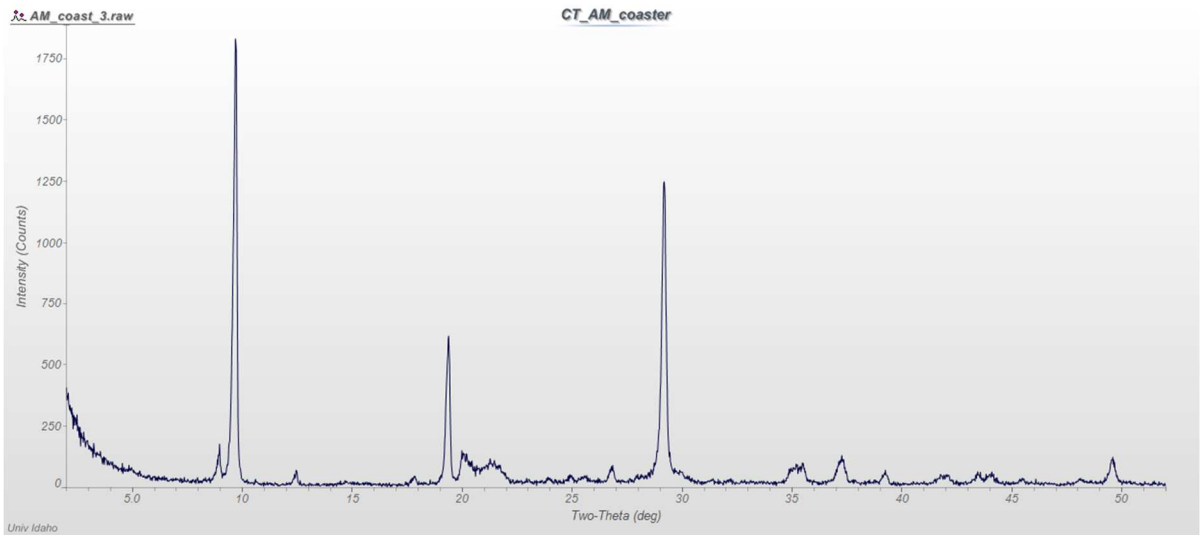
AM_coast_3.raw
CT_AM_coaster
Intensity (Counts)
Two-Theta (deg)
Univ Idaho

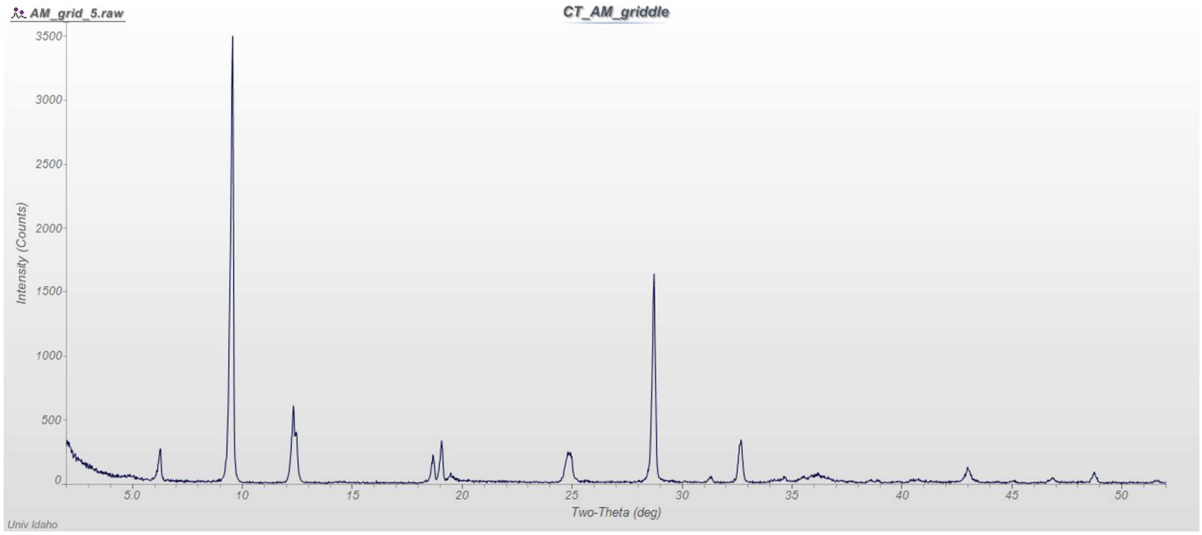
AM_grid_5.raw
CT_AM_griddle
Intensity (Counts)
Two-Theta (deg)
Univ Idaho

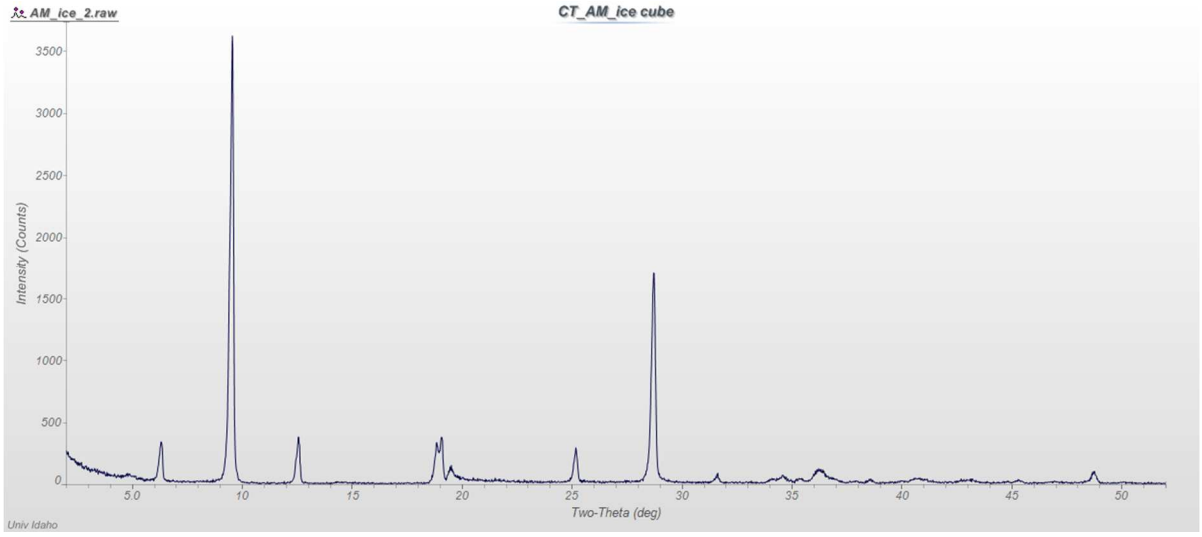
AM_ice_2.raw
CT_AM_ice cube
Intensity (Counts)
Two-Theta (deg)
Univ Idaho

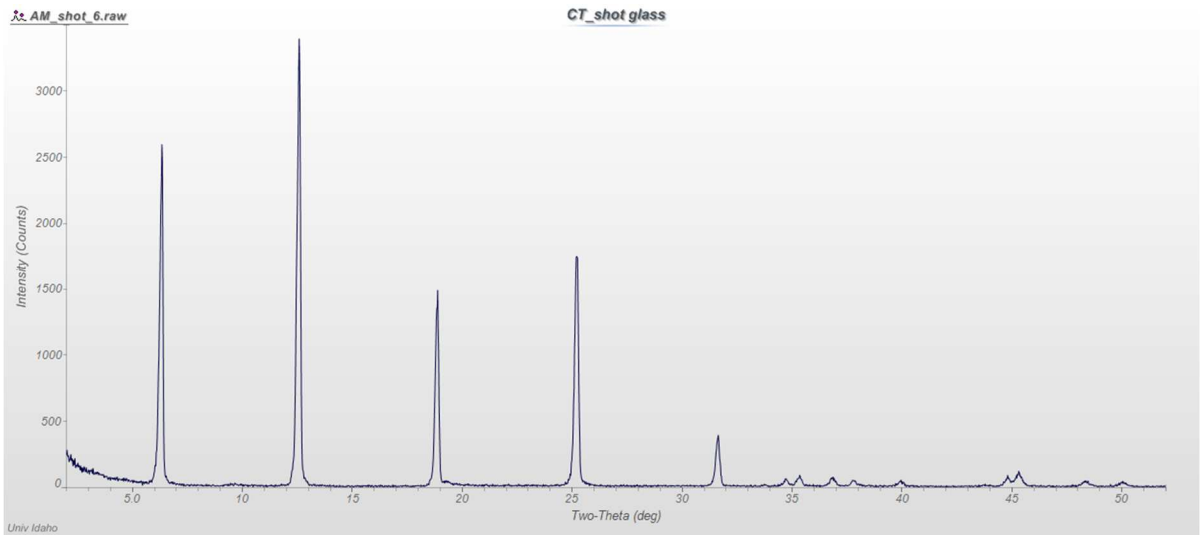
AM_shot_6.raw
CT_shot glass
Intensity (Counts)
Two-Theta (deg)
Univ Idaho

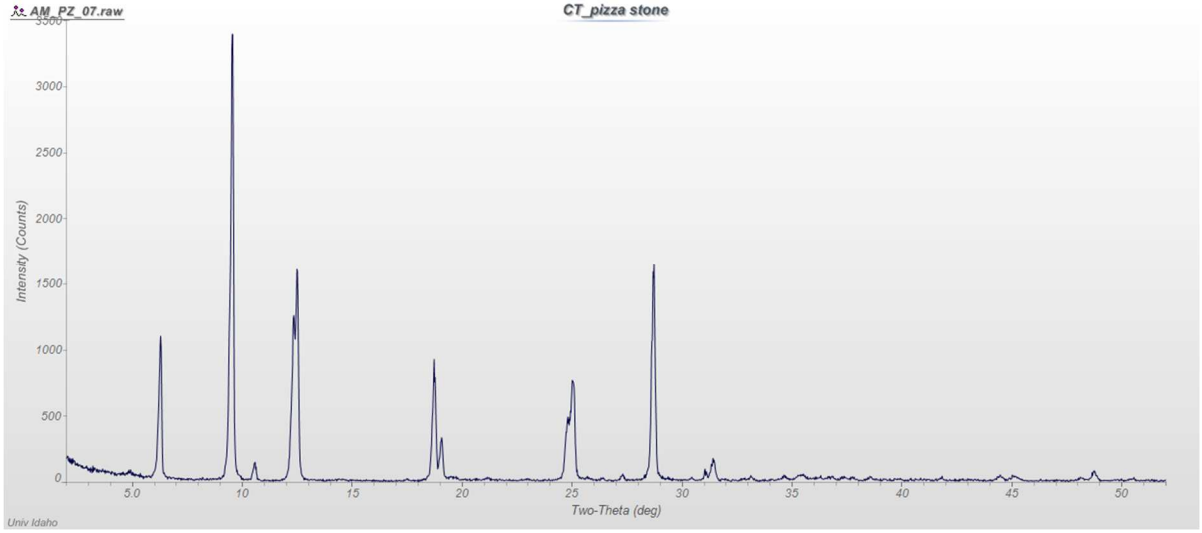
AM_PZ_07.raw
CT_pizza stone
Intensity (Counts)
Two-Theta (deg)
Univ Idaho

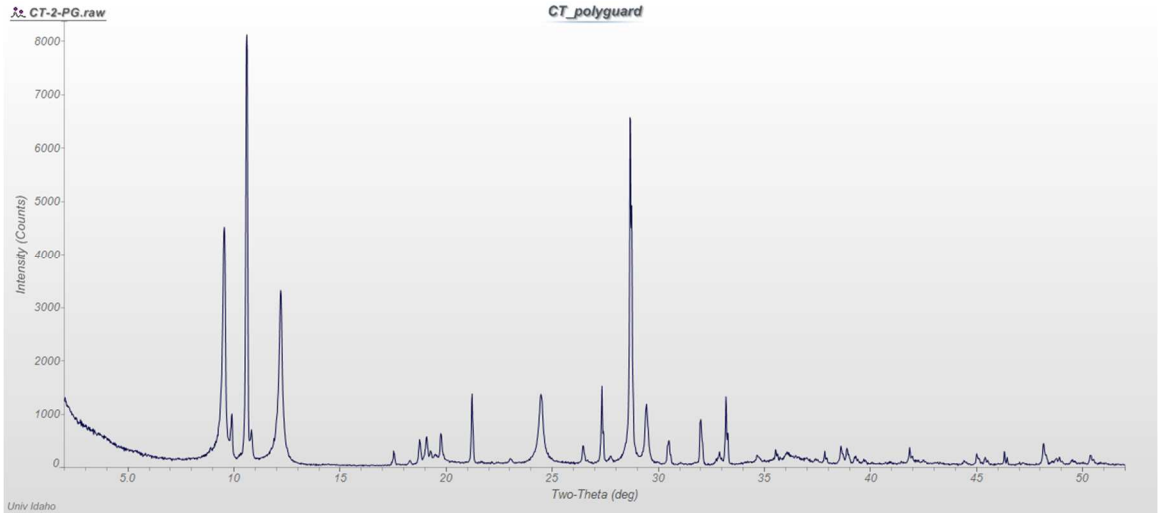
CT-2-PG.raw
CT_polyguard
Intensity (Counts)
Two-Theta (deg)
Univ Idaho

Appendix B: Bulk X-ray Fluorescence Spectroscopy

Weight percent oxides of major and minor elements are included in Part 1. Trace element concentrations (in ppm) are listed in Part 2.

Part 1:

	SiO2/MgO	SiO2	TiO2	Al2O3	FeO*	MnO	MgO	CaO	Na2O	K2O	P2O5	Sum	LOI (%)
AUS_MtSeabrook	2.00	61.22	0.01	1.18	0.85	0.00	30.62	0.07	0.04	0.00	0.02	94.02	4.76
AUS_ThreeSprings	2.04	62.47	0.01	0.39	1.08	0.00	30.69	0.17	0.01	0.00	0.07	94.89	4.77
AUSTRIA_Styria_Anger	1.57	49.42	0.32	9.13	1.21	0.01	31.57	0.20	0.00	0.00	0.13	92.00	0.00
AUSTRIA_Lassing_Styria	2.00	61.84	0.01	0.65	1.08	0.01	30.88	0.17	0.03	0.00	0.03	94.69	5.00
BRA_Bahia_78	2.02	61.70	0.01	0.49	1.01	0.02	30.49	0.06	0.00	0.00	0.01	93.79	5.30
BRA_Bahia_78®	2.03	61.48	0.01	0.49	1.01	0.02	30.34	0.06	0.00	0.00	0.01	93.42	5.30
BRA_Bahia_mill	2.02	62.93	0.01	0.58	0.23	0.00	31.11	0.00	0.01	0.00	0.00	94.85	4.72
BRA_Bahia_Tabua	2.03	62.22	0.02	0.41	0.70	0.00	30.62	0.02	0.06	0.00	0.00	94.05	4.75
BRA_Bahia_core	1.76	52.59	0.03	0.23	0.26	0.01	29.85	4.74	0.00	0.00	0.01	87.70	11.62
CAN_Ontario_Madoc_80	1.29	33.94	0.01	0.44	0.21	0.05	26.27	14.59	0.06	0.09	0.00	75.66	23.48
CAN_Ontario_Madoc_170	2.02	62.75	0.01	0.95	0.52	0.00	31.11	0.05	0.16	0.00	0.01	95.56	0.00
CHI_94	2.00	62.58	0.00	0.48	0.28	0.00	31.25	0.25	0.00	0.02	0.03	94.89	4.70
CHI_Cuangai_86	2.02	63.26	0.00	0.15	0.48	0.00	31.36	0.07	0.00	0.00	0.04	95.37	4.63
CHI_Guangxi_GuiLin_mill	1.97	60.63	0.03	1.07	0.94	0.00	30.79	0.14	0.00	0.00	0.02	93.62	5.24
CHI_Guangxi_GuiLin_200	1.97	60.20	0.04	1.27	0.82	0.00	30.62	0.24	0.00	0.00	0.12	93.31	5.11
CHI_Guangxi_G1_89	2.00	62.52	0.00	0.47	0.46	0.00	31.20	0.03	0.00	0.00	0.01	94.70	4.72
CHI_Guangxi_G3_91	1.99	62.16	0.00	0.23	0.03	0.00	31.28	0.04	0.00	0.00	0.00	93.75	3.51
CHI_ Guangxi_92	1.98	62.19	0.00	0.42	0.00	0.00	31.37	0.03	0.32	0.01	0.02	94.37	2.74
CHI_ Guangxi_Longsheng_G1_88	2.03	61.52	0.00	0.31	0.60	0.00	30.38	0.10	0.00	0.00	0.00	92.92	6.41
CHI_Haicmen_84	2.01	63.44	0.00	0.06	0.21	0.00	31.62	0.02	0.00	0.00	0.00	95.36	4.55
CHI_Liaoning_87	1.99	62.32	0.00	0.13	0.26	0.00	31.32	0.04	0.00	0.00	0.02	94.08	4.46
CHI_ Liaoning_Haicheng_93	2.00	62.23	0.00	0.38	0.03	0.00	31.12	0.17	0.00	0.00	0.11	94.05	4.84
CHI_Liaoning_Yingkow_83	2.01	62.81	0.00	0.46	0.32	0.00	31.23	0.09	0.00	0.00	0.01	94.92	4.74
CHI_Longguang_201	2.00	62.05	0.01	0.49	0.43	0.00	30.99	0.07	0.00	0.00	0.02	94.06	4.91
CHI_Shadong_Qixia_85	2.00	62.91	0.00	0.35	0.12	0.00	31.47	0.16	0.00	0.00	0.08	95.10	4.63
FIN_NKarelia_95	0.83	29.58	0.01	0.59	6.23	0.09	35.55	0.09	0.00	0.00	0.01	72.15	26.66
IND_Chainpura_mill	1.96	61.01	0.13	0.91	0.51	0.00	31.14	0.27	0.00	0.00	0.01	93.98	5.19
IND_Ghevaria_mill	1.96	60.94	0.01	0.16	0.51	0.00	31.11	1.11	0.00	0.00	0.01	93.84	5.90

	SiO2/MgO	SiO2	TiO2	Al2O3	FeO*	MnO	MgO	CaO	Na2O	K2O	P2O5	Sum	LOI (%)
IND_Haldwani	1.99	62.62	0.01	0.60	0.23	0.00	31.44	0.06	0.00	0.00	0.04	95.00	4.89
IND_Udaipur_A	2.02	61.61	0.03	0.88	1.23	0.02	30.55	0.14	0.00	0.00	0.08	94.55	4.84
IND_Udaipur_B	2.09	61.90	0.01	0.59	2.52	0.01	29.63	0.02	0.00	0.00	0.00	94.68	4.56
ITA_Gianna_A	2.02	61.91	0.01	0.87	0.96	0.00	30.67	0.29	0.00	0.01	0.21	94.93	4.64
ITA_Gianna_C	2.03	62.88	0.01	0.56	0.72	0.00	31.05	0.09	0.00	0.00	0.06	95.36	4.65
ITA_Paola_A	2.02	62.04	0.01	0.71	0.84	0.00	30.69	0.09	0.00	0.00	0.05	94.44	4.80
IT_Paola_Scop	2.06	62.03	0.06	1.17	0.82	0.00	30.11	0.13	0.00	0.28	0.08	94.69	4.68
ITA_Rodoretto_A1	1.99	60.88	0.02	0.93	0.79	0.00	30.64	0.47	0.01	0.01	0.04	93.80	5.38
ITA_Rodoretto_A2	1.98	60.49	0.02	0.90	0.78	0.00	30.55	0.47	0.02	0.01	0.04	93.29	5.55
ITA_Rodoretto_A3	1.98	61.09	0.02	0.94	0.79	0.00	30.79	0.48	0.12	0.02	0.04	94.28	5.46
ITA_Rodoretto_B1	1.99	59.69	0.04	0.97	1.17	0.01	30.04	0.71	0.03	0.02	0.05	92.73	5.59
ITA_Rodoretto_B2	2.00	60.29	0.03	0.95	1.18	0.01	30.20	0.72	0.00	0.02	0.05	93.46	5.55
ITA_Rodoretto_B3	1.99	60.15	0.03	0.98	1.18	0.01	30.25	0.72	0.04	0.02	0.05	93.44	5.75
KOR_73	2.02	62.56	0.01	0.32	1.05	0.00	30.96	0.09	0.13	0.01	0.01	95.14	3.95
MOR_109	2.00	62.33	0.03	0.30	0.40	0.00	31.15	0.27	0.09	0.00	0.01	94.59	5.04
MOR_165	2.00	62.55	0.03	0.36	0.38	0.00	31.25	0.26	0.00	0.00	0.01	94.84	4.92
NOR_169	2.02	62.59	0.01	0.98	0.52	0.00	31.05	0.06	0.02	0.00	0.01	95.24	0.00
SPA_110	1.98	61.78	0.00	0.84	0.16	0.00	31.19	0.13	0.10	0.00	0.06	94.27	4.74
SPA_111	1.99	62.81	0.00	0.09	0.19	0.00	31.51	0.03	0.04	0.00	0.00	94.68	4.55
USA_CA_CT_Vansil	2.02	55.77	0.02	0.72	0.25	0.01	27.63	6.02	0.91	0.89	0.01	92.23	8.18
USA_CA_CT_Westal	1.99	55.16	0.02	0.81	0.26	0.01	27.77	6.55	0.64	0.87	0.01	92.10	8.97
USA_CA_CT_Westal R	1.98	54.50	0.02	0.82	0.26	0.01	27.59	6.47	0.64	0.86	0.01	91.18	8.97
USA_CA_Grantham	2.00	58.82	0.04	0.76	0.20	0.01	29.44	2.95	0.02	0.46	0.01	92.72	6.57
USA_CA_SnowWhite_RX	1.66	54.22	0.04	1.76	0.45	0.02	32.76	3.16	0.13	0.13	0.01	92.67	
USA_CA_TalcCity_3	2.03	61.25	0.01	1.16	1.06	0.01	30.18	0.29	0.09	0.02	0.02	94.09	4.95
USA_CA_TalcCity_5	2.04	62.10	0.01	1.37	1.06	0.01	30.43	0.21	0.19	0.02	0.01	95.40	4.51
USA_CA_Victorville	2.17	59.28	0.02	0.93	0.18	0.00	27.29	3.21	2.33	1.41	0.00	94.65	4.61
USA_CA_WesternTalc_3a	1.96	53.08	0.03	1.47	0.30	0.02	27.03	6.40	0.41	0.86	0.01	89.59	9.96
USA_CA_WesternTalc_3c	2.00	55.05	0.04	1.37	0.38	0.02	27.49	4.95	0.55	0.96	0.02	90.82	8.61
USA_GA_Earnest_fibrous	2.55	54.77	0.02	1.52	6.81	0.19	21.50	9.69	0.18	0.04	0.00	94.73	5.05
USA_GA__Earnest_platy	2.73	55.14	0.02	0.53	6.25	0.22	20.21	12.16	0.06	0.07	0.00	94.67	4.98
USA_MT_Beaverhead Co.	2.05	61.93	0.00	0.26	2.08	0.07	30.20	0.04	0.00	0.00	0.00	94.58	4.67
USA_MT_Beaverhead	1.99	62.47	0.01	0.42	0.37	0.00	31.38	0.09	0.16	0.00	0.05	94.95	1.98
USA_MT_CT_Sericron	1.92	58.06	0.02	2.51	2.23	0.01	30.21	0.35	0.00	0.00	0.02	93.41	6.07
USA_MT_CT_Talcron	1.96	60.06	0.04	1.65	1.68	0.01	30.61	0.34	0.00	0.00	0.01	94.41	5.78

	SiO2/MgO	SiO2	TiO2	Al2O3	FeO*	MnO	MgO	CaO	Na2O	K2O	P2O5	Sum	LOI (%)
USA_MT_CT_Ultratalc609	1.97	61.81	0.03	1.01	0.62	0.01	31.35	0.09	0.00	0.01	0.02	94.95	5.18
USA_MT_Regal_HG	1.73	52.48	0.11	5.38	1.84	0.03	30.30	1.02	0.00	0.04	0.04	91.24	8.27
USA_MT_Treasure_float	2.08	61.47	0.01	1.17	2.79	0.09	29.51	0.02	0.05	0.01	0.01	95.13	4.92
USA_MT_Treasure_G1	2.01	63.23	0.01	0.21	0.50	0.00	31.53	0.08	0.00	0.00	0.03	95.58	4.16
USA_MT_Treasure_G3	2.05	61.57	0.02	0.44	2.43	0.01	30.03	0.09	0.02	0.00	0.03	94.62	4.88
USA_MT_WillowCr_1A	1.89	56.28	0.01	3.53	2.79	0.02	29.83	0.01	0.01	0.01	0.00	92.50	8.12
USA_MT_WillowCr_6	1.94	27.69	0.04	0.91	1.11	0.29	14.25	29.12	0.00	0.00	0.01	73.42	25.83
USA_MT_WillowCr_8	2.03	60.73	0.00	2.73	1.34	0.01	29.88	0.01	0.03	0.01	0.00	94.73	4.82
USA_MT_Yellowstone_HG	2.03	62.03	0.02	1.20	1.26	0.00	30.54	0.01	0.02	0.00	0.00	95.09	4.70
USA_MT_Yellowstone_LG	2.04	62.92	0.00	0.31	1.42	0.00	30.78	0.01	0.00	0.00	0.00	95.45	4.68
USA_NC_Kinsey	2.02	63.67	0.00	0.16	0.32	0.00	31.58	0.00	0.00	0.00	0.00	95.73	
USA_NC_Murphy_124	2.01	62.04	0.04	0.76	0.80	0.00	30.90	0.02	0.08	0.00	0.01	94.66	1.35
USA_NC_Murphy_129	2.03	62.38	0.01	0.33	0.88	0.00	30.68	0.56	0.04	0.00	0.03	94.92	4.86
USA_NC_Murphy_129®	2.02	62.23	0.01	0.30	0.88	0.00	30.81	0.61	0.00	0.00	0.03	94.87	4.86
USA_NC_Murphy_132	2.01	63.07	0.00	0.14	0.11	0.00	31.41	0.01	0.01	0.00	0.00	94.76	4.69
USA_NC_Murphy_143	2.03	62.55	0.00	0.96	0.64	0.00	30.88	0.02	0.00	0.00	0.01	95.05	4.69
USA_NC_Murphy_149	2.02	61.66	0.01	0.74	0.73	0.00	30.60	0.09	0.00	0.00	0.01	93.84	4.87
USA_NC_CCFoote	1.86	54.60	0.04	8.29	1.25	0.00	29.42	0.13	0.05	0.02	0.06	93.87	6.14
USA_NC_HC_CT_light	1.98	61.11	0.02	0.97	1.60	0.01	30.83	0.23	0.02	0.01	0.03	94.84	5.18
USA_NC_HC_CT_light R	1.99	61.41	0.02	0.97	1.61	0.01	30.82	0.24	0.02	0.01	0.03	95.16	5.18
USA_NC_HC_dark rock	1.54	47.59	0.19	10.93	2.14	0.00	30.96	0.06	0.01	0.01	0.04	91.92	8.21
USA_NC_HC_light rock	1.94	59.29	0.02	2.87	1.30	0.00	30.64	0.00	0.02	0.01	0.01	94.15	5.16
USA_TX_Llano	2.08	60.36	0.01	0.58	3.79	0.03	28.97	0.04	0.05	0.00	0.01	93.84	4.99
USA_TX_VanHorn_black	1.70	43.03	0.02	0.44	0.08	0.00	25.26	10.42	0.16	0.14	0.01	79.56	19.03
USA_TX_VanHorn_gray	2.07	62.32	0.00	0.04	0.01	0.00	30.14	0.99	0.00	0.00	0.00	93.50	5.93
USA_TX_VanHorn_pink	1.91	61.53	0.00	0.11	0.02	0.00	32.17	0.26	0.07	0.01	0.01	94.19	5.67
USA_VT_Argonaut_CT_brokenbag	1.03	34.86	0.03	0.98	6.30	0.10	33.90	0.56	0.03	0.05	0.01	76.83	22.34
USA_VT_Argonaut_G	2.16	61.37	0.00	0.48	4.63	0.06	28.43	0.00	0.00	0.01	0.00	94.97	4.57
USA_VT_Argonaut_HG	0.98	33.41	0.01	1.22	6.25	0.07	34.05	0.17	0.00	0.00	0.00	75.18	23.88
USA_VT_Argonaut_LG	0.97	33.64	0.01	1.00	6.08	0.10	34.60	0.14	0.04	0.03	0.00	75.64	23.84
USA_VT_Argonaut_R	1.00	34.15	0.02	0.80	5.78	0.09	34.16	0.15	0.00	0.00	0.00	75.16	23.58
USA_VT_Argonaut_underflow	0.29	11.05	0.06	1.30	9.11	0.18	38.26	0.61	0.02	0.02	0.01	60.63	35.20
USA_VT_Argonaut_xst	2.08	62.25	0.01	0.63	2.11	0.01	30.00	0.00	0.01	0.00	0.00	95.02	4.77
USA_VT_CT_Engelhard_bottom	1.86	57.07	0.01	0.51	3.45	0.02	30.67	0.14	0.01	0.01	0.00	91.89	8.20
USA_VT_CT_Engelhard_middle	1.87	56.81	0.01	0.49	3.44	0.02	30.46	0.14	0.00	0.00	0.00	91.36	8.21

	SiO2/MgO	SiO2	TiO2	Al2O3	FeO*	MnO	MgO	CaO	Na2O	K2O	P2O5	Sum	LOI (%)
USA_VT_CT_Engelhard_top	1.87	57.10	0.01	0.49	3.48	0.02	30.58	0.14	0.00	0.00	0.00	91.80	8.20
USA_Johnson_black	2.05	59.99	0.00	1.36	3.70	0.02	29.32	0.00	0.00	0.00	0.00	94.37	4.73
USA_Johnson__bl and gr	2.06	61.41	0.00	0.74	3.86	0.02	29.78	0.00	0.00	0.00	0.00	95.79	4.58
USA_VT_Johnson_green	2.06	61.10	0.00	0.49	3.45	0.02	29.69	0.00	0.00	0.00	0.00	94.73	5.97
USA_Johnson_Leslie	2.08	62.54	0.00	0.00	2.54	0.00	30.10	0.00	0.00	0.00	0.00	95.18	3.89
USA_Johnson_pipe	1.30	40.39	0.02	0.93	6.76	0.08	31.05	0.69	0.02	0.04	0.01	79.99	18.77
USA_VT_Johnson_JTM2	1.93	57.34	0.01	0.41	4.12	0.02	29.65	0.16	0.19	0.03	0.01	91.94	7.58
USA_VT_Johnson_UVM	2.09	60.37	0.00	0.88	4.52	0.04	28.89	0.00	0.00	0.00	0.00	94.69	4.59
USA_WA_TotemTalc135	2.02	63.05	0.00	0.04	0.47	0.00	31.24	0.03	0.00	0.00	0.02	94.85	4.27
CB_IT	2.00	60.96	0.22	1.92	0.56	0.00	30.49	0.21	0.02	0.05	0.10	94.53	5.38
CT_AM	2.01	62.72	0.00	0.24	1.27	0.01	31.16	0.15	0.01	0.00	0.02	95.57	4.95
CT_BP_CashmereBouquet_A	1.96	60.41	0.03	0.92	1.02	0.00	30.88	0.11	0.00	0.00	0.02	93.40	6.59
CT_BP_GoldBond	1.99	59.62	0.01	0.41	0.76	0.01	29.98	0.32	0.01	0.00	0.01	91.12	6.27
CT_BP_Johnson	1.94	60.07	0.05	1.44	1.00	0.00	30.93	0.38	0.00	0.00	0.02	93.89	5.68
CT_BP_RicetteNaturali	1.98	57.96	0.03	0.85	1.08	0.01	29.34	0.54	0.01	0.02	0.07	89.90	7.21
CT_BP_Safeway	2.03	61.74	0.00	0.03	1.28	0.01	30.45	0.08	0.00	0.00	0.01	93.60	4.87
CT_BP_Vanderbilt	1.94	59.02	0.20	0.82	0.66	0.00	30.35	0.07	0.02	0.10	0.04	91.28	7.94
CT_poolchalk	981.91	55.57	0.17	13.04	0.39	0.00	0.06	8.23	0.12	0.65	0.05	78.27	8.34
CT_handtalc	0.73	28.98	0.00	0.02	0.12	0.01	39.66	0.56	0.00	0.00	0.04	69.40	30.30
CT_handtalc R	0.74	28.93	0.00	0.03	0.14	0.01	39.25	0.56	0.00	0.01	0.04	68.96	30.30
CT_Fisher	2.03	63.15	0.01	0.46	0.39	0.00	31.17	0.03	0.01	0.02	0.00	95.24	4.51
CT_tiretalc	1.05	35.61	0.04	0.97	6.40	0.10	33.76	0.74	0.02	0.01	0.01	77.67	21.59
CT_FP_CSI	1.88	54.05	0.04	1.01	0.94	0.02	28.74	4.51	0.01	0.01	0.08	89.41	9.98
CT_Malincrodt	1.99	61.82	0.01	0.52	0.69	0.01	31.11	0.19	0.01	0.00	0.02	94.39	5.04
CT_Polyguard	1.74	53.62	0.02	0.34	0.13	0.12	30.80	6.35	0.17	0.11	0.04	91.71	6.59
CT_soap_BR	2.04	56.55	0.09	3.44	5.34	0.04	27.76	0.03	0.00	0.00	0.00	93.25	5.74
CT_soap_coaster	418.20	62.74	0.43	28.71	0.35	0.00	0.15	0.07	0.10	0.91	0.08	93.55	5.57
CT_soap_griddle	1.33	42.16	0.06	1.96	6.29	0.04	31.69	0.29	0.07	0.03	0.06	82.66	15.83
CT_soap_icecube	1.85	57.40	0.13	3.66	1.26	0.00	30.99	0.05	0.00	0.00	0.02	93.51	6.00
CT_soap_pizzastone	1.57	46.17	0.11	5.34	6.88	0.08	29.44	2.25	0.05	0.01	0.01	90.33	8.26
CT_tiretalc	1.06	35.67	0.04	0.97	6.46	0.10	33.68	0.73	0.01	0.01	0.01	77.70	21.59
CT_NYTAL_100	1.89	54.92	0.03	0.36	0.15	0.20	29.08	8.63	0.18	0.12	0.03	93.69	5.39
CT_NYTAL_200	1.75	53.74	0.02	0.25	0.11	0.14	30.69	7.23	0.12	0.11	0.03	92.45	6.17
CT_NYTAL_300	1.64	52.13	0.02	0.26	0.12	0.10	31.82	7.10	0.13	0.11	0.03	91.81	8.10

	SiO2/MgO	SiO2	TiO2	Al2O3	FeO*	MnO	MgO	CaO	Na2O	K2O	P2O5	Sum	LOI (%)
CT_NYTAL_400	1.74	53.64	0.03	0.30	0.13	0.11	30.78	7.06	0.13	0.11	0.03	92.33	7.14
CT_Mouldene	2.16	61.27	0.02	0.22	0.11	0.29	28.31	5.37	0.22	0.12	0.02	95.95	3.84
CT_Fibertal_1	2.21	61.35	0.02	0.21	0.09	0.25	27.72	5.28	0.21	0.12	0.02	95.28	3.71
CT_Fibertal_2	2.27	62.36	0.01	0.15	0.09	0.31	27.47	5.13	0.18	0.12	0.02	95.86	3.28
CT_Fibertal_6	2.12	59.27	0.03	0.38	0.14	0.30	27.91	6.73	0.23	0.12	0.03	95.13	4.00
IL_Shin_White_snow	1.97	58.68	0.04	0.55	1.60	0.01	29.77	1.64	0.00	0.00	0.01	92.31	7.01
IL_Shin_White_snow R	1.97	58.78	0.04	0.52	1.59	0.01	29.79	1.63	0.00	0.00	0.01	92.39	7.01

Part 2: Trace element concentrations

	Ni	Cr	Sc	V	Ba	Rb	Sr	Zr	Y	Nb	Ga	Cu	Zn	Pb	La	Ce	Th	Nd	U	sum tr.
AUS_MtSeabrook	5.04	8.40	1.54	8.82	7.56	0.00	0.14	9.56	2.38	0.00	1.82	13.30	29.82	3.50	2.66	0.00	0.70	1.96	0.00	97.20
AUS_ThreeSprings	10.50	6.86	1.12	7.70	7.14	0.70	8.96	7.73	1.54	0.98	0.98	14.84	31.50	3.08	0.00	1.82	0.00	1.54	0.00	106.99
AUSTRIA_Styria_Anger	26.02	44.68	3.82	42.28	10.89	0.00	0.71	136.16	8.63	12.02	13.01	26.58	36.34	15.84	0.28	3.25	0.00	1.70	0.00	382.20
AUSTRIA_Lassing_Styria	6.58	6.30	1.26	12.74	4.20	0.14	1.54	19.68	3.08	1.54	2.10	13.72	31.36	4.06	0.00	1.12	1.54	1.40	0.00	112.36
BRA_Bahia_78	35.63	4.52	2.12	6.50	9.62	0.28	1.13	5.11	2.26	0.99	0.85	15.41	21.21	49.07	1.70	0.00	0.00	1.70	0.00	158.11
BRA_Bahia_78®	36.48	4.38	2.40	6.36	6.93	0.28	1.41	3.98	1.56	1.27	1.56	11.74	19.23	48.36	0.00	0.00	0.00	0.99	0.00	146.93
BRA_Bahia_mill	8.48	6.97	0.30	5.76	0.00	0.00	0.30	0.61	1.82	0.71	0.61	0.20	2.32	2.22	0.00	0.00	0.00	0.91	0.00	31.21
BRA_Bahia_Tabua	23.10	3.64	1.26	26.04	3.92	0.70	0.56	5.06	8.82	0.56	0.98	3.92	7.98	2.66	0.98	0.00	1.96	2.38	0.00	94.52
BRA_Bahia_core	10.08	7.28	0.98	3.36	4.76	0.00	5.60	3.94	2.52	0.00	0.42	12.04	8.12	4.62	1.26	0.00	0.42	0.70	0.42	66.52
CAN_Ontario_Madoc_80	1.84	4.81	1.27	8.63	25.88	3.82	2121.28	7.67	3.68	0.00	1.98	13.29	48.08	17.53	2.26	5.80	0.28	3.11	1.84	2273.04
CAN_Ontario_Madoc_170	3.39	9.05	0.42	4.24	5.09	0.28	0.99	5.25	1.84	0.00	0.85	12.73	22.48	4.67	2.12	0.00	0.00	1.70	1.13	76.24
CHI_94	1.40	5.32	0.70	4.76	6.58	4.06	1.82	3.94	0.98	0.14	0.98	11.48	10.78	2.38	0.00	0.00	0.14	0.56	0.28	56.30
CHI_Cuangai_86	0.57	3.54	1.70	3.11	3.82	0.00	0.42	6.96	1.84	1.13	1.27	11.45	6.65	1.13	1.84	0.00	0.00	2.40	0.14	47.96
CHI_Guangxi_GuiLin_mill	4.95	5.25	2.12	11.72	3.84	0.00	0.30	13.23	3.23	2.12	1.31	0.00	11.82	2.12	1.21	4.24	0.71	1.31	0.30	69.79
CHI_Guangxi_GuiLin_200	4.76	9.38	1.12	18.62	0.84	0.84	1.68	15.33	2.38	0.84	2.10	2.38	9.94	2.94	0.00	0.00	0.56	1.96	1.12	76.79
CHI_Guangxi_G1_89	0.71	5.23	0.85	5.37	4.38	0.14	0.00	6.11	0.14	0.71	0.00	12.73	7.64	4.38	2.40	0.00	0.00	0.00	0.00	50.79
CHI_Guangxi_G3_91	1.27	6.93	0.28	8.48	4.81	0.99	0.00	7.10	3.11	0.14	1.41	16.12	9.05	75.08	0.00	0.00	0.00	1.41	0.57	136.76
CHI_ Guangxi_92	2.69	6.50	0.57	16.83	6.36	0.85	0.71	5.82	2.40	0.42	1.98	11.88	3.54	0.71	2.97	0.00	0.42	0.00	0.14	64.79
CHI_ Guangxi_Longsheng_G1_88	1.68	3.78	1.26	7.14	6.02	0.28	0.00	3.80	0.98	0.28	0.42	13.72	6.16	125.30	0.14	0.00	0.00	1.96	0.00	172.92
CHI_Haicmen_84	31.08	2.10	0.00	2.38	4.34	0.70	0.42	3.37	0.70	0.28	0.56	12.74	5.18	3.92	1.40	0.00	0.56	1.26	0.84	71.83
CHI_Liaoning_87	2.40	2.40	0.00	3.54	4.10	0.00	0.00	3.27	0.28	0.85	1.56	12.02	1.27	2.69	1.56	1.41	0.00	0.71	0.71	38.76
CHI_ Liaoning_Haicheng_93	1.40	6.16	0.00	2.80	3.78	0.00	1.12	4.50	1.12	0.00	0.84	12.46	1.82	3.08	0.00	0.00	0.00	0.14	4.48	43.70
CHI_Liaoning_Yingkow_83	2.94	5.18	0.28	3.92	3.64	1.12	6.72	3.66	0.00	0.56	3.22	11.20	3.50	1.26	0.00	0.00	0.00	1.12	0.56	48.88
CHI_Longguang_201	3.92	3.22	2.24	9.52	4.48	0.14	1.68	7.03	1.12	0.28	1.40	2.10	6.58	2.24	2.10	0.00	1.26	0.00	0.00	49.31
CHI_Shadong_Qixia_85	0.00	3.25	0.71	2.97	8.20	0.00	3.25	3.41	1.13	0.57	0.71	11.31	3.25	1.98	1.98	0.57	0.00	3.11	1.84	48.23
FIN_NKarelia_95	2216.76	904.26	3.92	13.16	5.04	0.84	1.26	7.31	0.28	0.00	1.54	14.98	37.94	9.24	0.00	0.00	1.40	0.00	0.70	3218.63
IND_Chainpura_mill	7.17	7.98	1.11	13.74	0.00	0.00	0.51	111.61	6.16	2.12	1.21	0.00	1.72	1.21	2.32	0.10	7.78	1.72	0.00	166.45
IND_Ghevaria_mill	6.46	3.13	1.01	4.65	0.10	0.00	0.61	7.68	1.82	1.01	0.61	0.00	0.71	0.71	2.42	1.52	0.51	0.00	0.00	32.93
IND_Haldwani	5.88	5.74	0.70	4.76	2.10	0.00	0.28	13.50	0.84	0.42	1.54	6.44	7.28	2.38	1.82	0.00	0.84	1.26	0.00	55.78
IND_Udaipur_A	7.64	8.20	1.98	8.34	4.24	0.57	0.00	30.81	6.79	0.71	1.98	4.38	10.18	1.84	2.40	0.00	1.98	0.00	0.00	92.04
IND_Udaipur_B	1314.03	28.00	0.00	3.39	0.85	0.00	0.00	4.12	0.57	0.00	1.41	5.09	36.91	2.83	0.71	0.00	0.00	1.84	0.00	1399.74
ITA_Gianna_A	8.06	11.17	0.00	5.23	6.65	1.41	3.82	5.11	6.22	0.28	0.57	11.59	18.24	2.83	0.85	0.00	0.00	0.85	1.41	84.30
ITA_Gianna_C	10.18	7.64	1.84	4.24	10.18	0.71	2.26	4.83	3.11	0.00	1.56	10.32	8.48	2.69	0.42	0.00	0.14	1.56	1.98	72.13
ITA_Paola_A	18.06	15.12	1.96	4.34	5.18	0.56	1.26	5.06	5.04	0.98	1.82	15.12	9.38	3.22	33.60	57.54	0.28	24.64	1.96	205.12
IT_Paola_Scop	16.94	25.20	1.82	8.96	21.00	15.12	3.22	14.62	24.36	2.52	3.78	25.76	10.92	3.36	12.88	30.24	0.00	13.86	4.62	239.18
ITA_Rodoretto_A1	4.34	4.20	1.68	8.82	5.60	0.84	1.54	10.12	3.36	0.70	1.82	8.12	7.56	2.24	0.98	0.00	0.00	4.34	1.40	67.66
ITA_Rodoretto_A2	5.74	4.06	1.82	7.84	6.72	0.84	1.26	9.56	3.64	0.56	2.10	6.44	7.00	2.52	1.26	0.00	0.00	2.80	1.40	65.56
ITA_Rodoretto_A3	5.32	7.00	0.84	8.54	4.62	1.26	1.54	9.42	3.64	0.42	2.66	6.86	6.02	2.80	3.64	0.00	0.00	0.00	1.82	66.40
ITA_Rodoretto_B1	9.52	8.82	2.52	6.30	6.16	1.12	4.76	12.65	9.66	2.24	3.64	7.84	10.22	3.08	2.80	5.46	0.00	5.04	2.80	104.63
ITA_Rodoretto_B2	10.22	8.40	2.24	5.60	6.44	1.40	4.20	13.50	9.38	1.54	3.36	9.10	9.24	1.82	3.50	0.42	0.70	2.24	3.92	97.22
ITA_Rodoretto_B3	10.92	10.92	1.54	8.68	9.80	1.96	3.92	12.65	10.22	1.26	4.34	8.12	10.36	1.54	3.78	4.06	1.26	5.04	3.92	114.29

	Ni	Cr	Sc	V	Ba	Rb	Sr	Zr	Y	Nb	Ga	Cu	Zn	Pb	La	Ce	Th	Nd	U	sum tr.
KOR_73	14.14	6.02	0.00	7.56	5.74	1.12	2.94	5.48	0.84	0.00	0.84	10.50	62.72	1.26	3.64	0.00	0.28	0.00	0.00	123.08
MOR_109	14.70	9.10	0.14	2.66	8.40	0.56	0.56	37.68	1.68	0.56	1.12	8.26	47.60	2.52	0.56	0.00	0.42	4.48	0.00	141.00
MOR_165	4.10	6.36	0.71	3.96	7.92	0.71	0.14	34.64	1.84	0.85	0.42	12.87	48.36	5.37	0.00	0.42	0.42	2.26	0.99	132.35
NOR_169	2.55	11.59	0.00	2.97	2.26	0.28	0.00	5.54	0.42	0.42	1.13	14.00	23.47	5.37	0.00	0.00	0.00	0.00	0.28	70.30
SPA_110	5.80	7.21	1.13	4.24	7.49	0.28	0.71	5.82	0.99	1.56	1.27	9.05	5.37	4.81	0.00	0.00	0.00	1.56	0.00	57.29
SPA_111	3.96	6.50	1.27	4.24	6.93	0.00	0.28	3.69	1.84	0.71	1.98	7.21	2.55	2.83	0.42	0.00	0.28	3.96	0.14	48.80
USA_CA_CT_Vansil	3.64	5.35	1.52	20.00	50.40	28.28	207.35	13.53	3.94	0.40	1.31	0.00	12.22	2.63	0.61	0.00	0.81	2.22	0.71	354.91
USA_CA_CT_Westal	4.24	5.76	1.82	20.40	52.12	32.12	292.70	14.95	4.24	1.41	1.92	0.40	12.02	3.13	1.62	0.30	0.81	1.72	1.41	453.09
USA_CA_CT_Westal R	5.86	8.38	3.13	19.39	50.60	31.41	289.67	14.65	5.45	0.51	1.82	1.82	8.79	3.23	0.40	1.62	0.00	1.62	0.81	449.15
USA_CA_Grantham	3.08	8.40	1.68	14.56	11.48	15.54	96.88	18.14	2.94	0.42	0.70	14.28	40.46	16.10	5.18	0.14	1.54	0.98	0.56	253.06
USA_CA_SnowWhite_RX	5.00	18.00	2.00	31.00	3.00	1.00	127.00	22.00	5.00	2.20	3.00	10.00	57.00	32.00	4.00	0.00	1.00	1.00	2.00	330.00
USA_CA_TalcCity_3	4.48	12.18	1.12	9.24	3.64	1.40	1.12	10.54	1.40	0.70	1.68	17.64	16.66	4.48	0.00	0.00	0.42	0.98	0.00	87.68
USA_CA_TalcCity_5	3.36	10.36	0.00	9.94	5.18	0.70	2.80	10.26	1.54	0.00	1.96	16.52	34.44	3.78	3.22	0.00	0.42	0.00	0.00	104.48
USA_CA_Victorville	3.70	11.39	2.33	18.25	18.38	15.09	66.82	16.95	1.92	1.10	0.96	8.64	23.87	7.27	0.00	0.41	0.82	5.35	1.92	205.19
USA_CA_WesternTalc_3a	2.52	14.70	0.14	14.84	84.70	37.66	268.38	21.23	5.04	0.00	3.36	11.62	19.60	6.86	1.96	0.98	0.84	4.62	0.00	499.05
USA_CA_WesternTalc_3c	2.08	10.95	3.05	18.43	80.25	37.84	217.46	30.91	4.57	1.11	3.60	9.15	14.55	6.93	1.94	2.08	0.69	3.60	0.55	449.75
USA_GA_Earnest_fibrous	757.17	1162.84	3.69	42.72	9.15	0.68	24.98	6.31	3.96	0.00	3.55	16.24	104.56	9.28	0.00	3.55	0.41	1.64	0.00	2150.72
USA_GA__Earnest_platy	728.64	228.64	4.50	30.44	10.24	3.00	35.90	23.59	8.05	0.41	1.50	10.92	69.48	15.42	0.00	0.00	0.82	3.55	0.00	1175.10
USA_MT_Beaverhead Co.	1.12	2.52	1.12	2.94	7.84	0.28	0.98	4.92	1.40	0.56	0.28	9.10	15.12	3.08	1.54	0.00	0.84	1.82	0.00	55.46
USA_MT_Beaverhead	32.62	5.04	0.84	6.58	6.16	1.40	0.00	5.76	15.68	0.28	0.70	7.28	4.34	1.40	0.00	0.00	0.14	0.00	0.84	89.06
USA_MT_CT_Sericron	22.12	9.10	0.98	10.08	6.58	0.42	1.40	9.70	8.96	2.94	5.18	8.12	12.60	1.12	1.68	0.00	0.84	1.40	0.70	103.92
USA_MT_CT_Talcron	24.78	16.52	2.24	13.30	12.88	1.26	1.40	9.84	5.32	1.82	1.96	8.12	11.62	2.52	3.64	0.00	0.00	2.38	1.96	121.56
USA_MT_CT_Ultratalc609	15.26	7.70	2.10	7.98	8.68	0.70	1.54	13.92	1.96	1.12	0.56	8.82	2.66	2.10	0.00	0.00	0.98	2.24	1.54	79.86
USA_MT_Regal_HG	20.37	25.78	4.16	17.60	15.38	1.39	6.10	26.87	13.17	7.21	9.42	8.73	8.87	2.36	3.74	7.35	3.47	5.82	1.25	189.03
USA_MT_Treasure_float	12.32	10.20	1.62	4.75	3.43	0.00	0.30	1.92	3.74	2.73	2.22	3.13	15.45	4.55	0.20	5.25	0.00	0.10	0.00	71.91
USA_MT_Treasure_G1	27.86	2.24	1.68	6.30	4.76	1.12	0.70	5.91	2.38	0.42	1.12	7.84	6.86	2.24	1.68	0.00	0.14	3.78	0.00	77.03
USA_MT_Treasure_G3	87.08	8.68	3.78	9.52	6.44	0.84	1.26	8.58	3.08	0.98	1.68	12.46	14.56	2.94	2.10	0.00	0.00	0.42	1.26	165.66
USA_MT_WillowCr_1A	24.70	17.90	1.70	10.80	23.50	0.00	1.20	5.80	2.50	3.10	5.10	4.50	21.10	6.00	1.60	1.70	0.00	0.00	0.00	131.20
USA_MT_WillowCr_6	5.04	46.62	1.68	7.28	12.74	1.12	70.98	31.21	10.92	0.56	1.26	33.74	15.68	8.82	3.08	5.32	1.12	2.94	1.96	262.07
USA_MT_WillowCr_8	16.26	22.12	1.82	4.34	0.00	0.00	0.00	0.20	1.01	1.31	3.64	6.57	13.23	2.12	0.51	0.00	0.00	0.40	1.82	75.35
USA_MT_Yellowstone_HG	18.89	9.60	1.52	3.23	3.94	0.00	0.10	4.24	2.53	3.84	1.21	4.34	12.42	4.14	1.41	0.91	0.00	0.00	0.00	72.32
USA_MT_Yellowstone_LG	8.69	3.74	0.91	3.74	0.71	0.00	0.00	0.10	0.91	1.11	1.21	0.61	12.42	2.93	0.00	0.00	0.00	0.00	0.00	37.07
USA_NC_Kinsey	11.00	8.00	0.00	3.00	0.00	0.00	0.00	0.00	1.00	0.70	0.00	0.00	14.00	1.00	0.00	0.00	0.00	0.00	0.00	40.00
USA_NC_Murphy_124	1.54	5.88	1.26	3.92	15.12	0.00	2.10	60.74	3.50	0.98	1.54	7.84	21.70	3.50	23.52	5.88	2.94	20.02	0.00	181.98
USA_NC_Murphy_129	18.20	4.48	0.28	5.32	4.06	0.70	0.28	6.61	1.40	0.56	0.70	7.14	33.04	1.82	0.42	0.00	0.28	0.00	0.00	85.29
USA_NC_Murphy_129®	16.32	4.92	0.84	5.07	4.50	0.00	0.00	6.50	2.39	0.00	1.41	8.02	32.08	2.25	0.00	0.00	0.00	0.00	0.00	84.31
USA_NC_Murphy_132	1.80	2.36	0.28	0.00	0.00	0.42	0.00	4.04	0.55	0.14	0.83	7.90	2.63	2.36	4.16	0.00	0.14	1.25	0.00	28.85
USA_NC_Murphy_143	8.54	11.76	0.00	3.50	5.32	0.00	2.80	3.51	1.26	0.00	0.70	9.94	22.82	2.66	1.82	0.00	0.00	0.70	0.00	75.33
USA_NC_Murphy_149	9.38	5.88	0.14	6.30	3.78	0.28	5.88	4.92	1.12	0.42	0.42	10.08	23.10	2.38	0.00	0.00	0.56	2.66	0.00	77.30
USA_NC_CCFoote	10.00	91.00	1.00	6.00	16.00	0.00	1.00	73.00	3.00	4.10	9.00	7.00	22.00	7.00	0.00	3.00	1.00	3.00	3.00	259.00
USA_NC_HC_CT_light	14.00	12.00	2.00	6.00	194.00	0.00	8.00	7.00	4.00	0.90	2.00	2.00	63.00	10.00	7.00	9.00	1.00	5.00	0.00	348.00
USA_NC_HC_CT_light R	13.00	10.00	2.00	7.00	188.00	1.00	8.00	7.00	5.00	0.90	1.00	2.00	66.00	10.00	5.00	12.00	0.00	5.00	1.00	345.00
USA_NC_HC_dark rock	11.00	49.00	5.00	60.00	4.00	0.00	0.00	132.00	5.00	7.90	15.00	8.00	34.00	4.00	3.00	7.00	6.00	5.00	2.00	356.00

	Ni	Cr	Sc	V	Ba	Rb	Sr	Zr	Y	Nb	Ga	Cu	Zn	Pb	La	Ce	Th	Nd	U	sum tr.
USA_NC_HC_light rock	7.00	9.00	1.00	5.00	2.00	0.00	0.00	57.00	3.00	2.50	5.00	4.00	23.00	4.00	0.00	3.00	0.00	1.00	0.00	126.00
USA_TX_Llano	1722.98	1261.12	2.52	17.36	13.58	0.00	0.98	3.80	2.38	0.56	1.54	9.80	81.06	1.40	0.84	0.00	0.00	1.82	0.00	3121.74
USA_TX_VanHorn_black	1.70	10.04	1.27	12.16	128.11	6.79	423.07	10.51	1.56	0.00	1.56	12.16	8.06	3.96	5.23	0.00	1.70	0.85	1.98	630.69
USA_TX_VanHorn_gray	1.40	2.66	0.00	4.20	0.00	0.00	28.70	3.94	0.98	0.00	0.70	6.58	7.84	2.66	3.08	0.00	0.98	2.38	0.28	66.38
USA_TX_VanHorn_pink	1.68	2.38	0.00	3.78	105.28	1.12	7.56	7.73	0.70	0.00	0.14	7.14	10.50	2.10	4.62	0.00	0.00	0.14	0.00	154.87
USA_VT_Argonaut_CT_brokenbag	1788.00	2715.00	6.00	24.00	10.00	2.00	14.00	4.00	1.00	0.80	2.00	12.00	36.00	2.00	1.00	4.00	1.00	3.00	0.00	4648.00
USA_VT_Argonaut_G	1607.00	1227.00	1.00	11.00	0.00	0.00	0.00	1.00	1.00	1.90	2.00	3.00	58.00	3.00	2.00	0.00	0.00	0.00	0.00	3087.00
USA_VT_Argonaut_HG	2117.22	2687.44	8.68	18.34	6.02	0.42	1.40	5.91	0.98	0.00	1.68	42.14	41.72	13.02	0.00	0.00	0.00	0.00	0.00	4944.97
USA_VT_Argonaut_LG	2009.00	2002.00	6.00	22.00	5.00	1.00	1.00	3.00	2.00	2.00	1.00	14.00	36.00	9.00	2.00	2.00	0.00	1.00	1.00	4133.00
USA_VT_Argonaut_R	1945.72	2444.26	4.20	12.04	9.38	1.40	0.56	7.03	0.28	0.42	1.12	15.12	45.92	8.96	0.00	3.22	0.84	2.80	0.70	4503.97
USA_VT_Argonaut_underflow	1373.00	6116.00	6.00	43.00	13.00	1.00	17.00	21.00	3.00	3.80	1.00	25.00	82.00	13.00	0.00	4.00	0.00	0.00	0.00	7746.00
USA_VT_Argonaut_xst	2421.00	54.00	1.00	2.00	1.00	0.00	0.00	3.00	2.00	1.80	1.00	13.00	17.00	2.00	3.00	0.00	0.00	2.00	0.00	2523.00
USA_VT_CT_Engelhard_bottom	1256.00	1471.00	3.00	19.00	5.00	0.00	16.00	0.00	1.00	0.90	2.00	2.00	34.00	1.00	1.00	3.00	0.00	1.00	0.00	2891.00
USA_VT_CT_Engelhard_middle	1243.00	1464.00	2.00	19.00	0.00	1.00	15.00	0.00	1.00	0.40	1.00	1.00	32.00	1.00	0.00	0.00	0.00	1.00	0.00	2859.00
USA_VT_CT_Engelhard_top	1237.00	1473.00	3.00	21.00	0.00	0.00	15.00	0.00	2.00	0.80	1.00	2.00	33.00	2.00	0.00	0.00	0.00	0.00	0.00	2857.00
USA_Johnson_black	621.00	1043.00	5.00	16.00	4.00	0.00	0.00	1.00	4.00	1.60	4.00	7.00	32.00	2.00	0.00	2.00	0.00	2.00	0.00	1748.00
USA_Johnson__bl and gr	712.00	815.00	4.00	12.00	0.00	0.00	0.00	0.00	1.00	0.30	2.00	5.00	31.00	0.00	0.00	2.00	0.00	2.00	0.00	1622.00
USA_VT_Johnson_green	407.00	59.00	0.00	1.00	0.00	0.00	0.00	1.00	2.00	2.00	0.00	4.00	31.00	2.00	5.00	8.00	0.00	3.00	0.00	527.00
USA_Johnson_Leslie	1049.00	19.00	0.00	0.00	0.00	0.00	1.00	0.00	0.00	0.20	0.00	0.00	21.00	1.00	0.00	0.00	0.00	0.00	1.00	1099.00
USA_Johnson_pipe	1618.00	1939.00	7.00	27.00	11.00	1.00	59.00	3.00	2.00	1.70	2.00	11.00	374.00	16.00	1.00	2.00	0.00	1.00	0.00	4278.00
USA_VT_Johnson_JTM2	2907.00	791.00	2.00	9.00	9.00	1.00	6.00	45.00	1.00	0.00	0.00	25.00	121.00	4.00	1.00	3.00	0.00	1.00	0.00	3936.00
USA_VT_Johnson_UVM	1512.00	2072.00	5.00	21.00	4.00	0.00	1.00	2.00	2.00	2.00	3.00	1.00	35.00	3.00	1.00	5.00	0.00	2.00	0.00	3824.00
USA_WA_TotemTalc135	2.38	2.80	1.96	6.44	2.66	0.00	0.14	2.95	1.26	0.56	1.68	7.70	4.48	2.24	7.56	0.00	0.00	1.12	0.42	46.35
CB_IT	15.00	26.00	3.00	15.00	5.00	0.00	3.00	17.00	5.00	6.10	4.00	9.00	11.00	12.00	2.00	8.00	0.00	4.00	0.00	144.00
CT_AM	9.60	5.35	1.11	5.96	0.00	0.00	1.01	3.64	1.62	1.41	0.61	0.20	22.12	2.93	1.52	0.00	0.00	1.52	0.00	58.58
CT_BP_CashmereBouquet_A	5.45	5.45	1.82	12.42	5.25	0.00	0.00	11.11	2.83	1.21	0.61	0.51	1073.93	1.31	2.93	4.34	0.00	2.42	0.51	1132.11
CT_BP_GoldBond	27.17	6.46	0.91	4.24	0.00	0.00	1.31	0.51	2.12	1.41	0.91	2.73	9024.05	0.61	1.01	2.93	0.10	0.00	0.20	9076.67
CT_BP_Johnson	5.45	6.77	1.92	13.23	22.83	0.00	2.22	17.98	3.54	2.53	2.12	0.00	14.14	1.52	2.42	5.86	0.40	2.42	0.40	105.75
CT_BP_RicetteNaturali	12.32	8.89	1.52	5.45	0.00	0.00	3.33	7.88	9.19	2.02	4.34	1.52	4051.72	2.32	5.96	5.15	0.71	3.74	3.64	4129.69
CT_BP_Safeway	12.63	3.84	0.61	4.55	0.00	0.30	0.91	0.00	1.11	1.31	1.41	0.20	20.81	1.31	0.00	0.00	0.00	0.00	0.40	49.39
CT_BP_Vanderbilt	14.14	8.28	1.52	5.76	0.00	5.56	0.51	5.15	3.23	2.32	2.12	1.41	8.18	2.93	2.63	0.00	0.00	1.31	0.20	65.25
CT_poolchalk	1.82	4.55	5.66	6.16	44.24	23.23	318.66	161.10	21.21	6.87	14.95	5.56	15.35	13.33	21.72	43.33	5.76	18.69	1.11	733.26
CT_handtalc	1.62	5.66	0.61	2.83	0.00	0.00	1.62	0.00	1.92	1.01	0.51	0.40	0.00	1.92	1.52	0.00	0.00	0.00	0.00	19.59
CT_handtalc R	3.00	7.00	0.00	3.00	66.00	0.00	3.00	1.00	5.00	2.10	0.00	8.00	1.00	7.00	3.00	7.00	0.00	2.00	0.00	118.00
CT_Fisher	3.84	7.78	1.92	3.64	1.62	1.92	0.61	2.32	1.92	1.52	1.41	3.13	35.96	8.28	1.52	0.00	0.00	0.00	0.00	77.37
CT_tiretalc	1811.94	2930.72	6.06	25.55	3.54	0.81	30.81	5.35	2.12	1.82	1.41	11.62	41.31	2.22	0.10	0.81	0.00	1.01	1.11	4878.30
CT_FP_CSI	3.00	7.00	2.00	11.00	256.00	0.00	30.00	14.00	5.00	1.50	2.00	2.00	25.00	3.00	6.00	4.00	0.00	3.00	2.00	377.00
CT_Malincrodt	23.23	6.97	0.71	6.57	0.20	0.00	1.01	1.41	2.83	1.11	2.93	0.00	3.43	1.62	0.40	0.00	0.20	0.10	0.00	52.72
CT_Polyguard	3.92	6.72	0.70	9.38	111.44	4.62	149.94	8.86	2.10	0.14	2.10	4.62	27.86	3.92	0.00	1.12	0.00	1.40	0.00	338.84
CT_soap_BR	2089.64	2044.98	9.24	34.30	6.72	0.98	0.00	13.64	2.24	1.26	5.18	34.72	89.32	3.36	3.64	3.36	0.70	4.90	1.82	4350.00
CT_soap_coaster	5.27	17.74	6.24	21.21	105.89	57.38	51.70	456.90	50.03	40.06	32.29	6.93	4.16	40.75	221.62	390.30	241.86	102.43	27.30	1880.05
CT_soap_griddle	2572.50	3072.18	5.76	40.47	26.21	1.10	24.15	18.61	2.74	1.92	2.88	36.36	43.49	15.37	1.92	5.90	1.23	3.84	1.37	5878.01

	Ni	Cr	Sc	V	Ba	Rb	Sr	Zr	Y	Nb	Ga	Cu	Zn	Pb	La	Ce	Th	Nd	U	sum tr.
CT_soap_icecube	14.42	24.78	1.68	24.64	5.46	0.84	0.84	45.69	2.24	3.92	5.04	10.92	22.82	4.20	4.90	5.60	3.92	1.96	0.98	184.85
CT_soap_pizzastone	1538.88	2860.90	13.86	87.22	6.02	1.68	15.96	11.39	2.10	0.00	5.18	38.64	58.24	5.32	0.00	0.00	0.70	0.00	1.12	4647.21
CT_tiretalc	1768.00	2893.00	5.00	26.00	13.00	1.00	30.00	5.00	2.00	0.70	2.00	17.00	41.00	2.00	4.00	0.00	0.00	3.00	1.00	4838.00
CT_NYTAL_100	2.26	4.10	1.27	9.62	135.60	4.52	239.81	10.08	2.55	0.00	1.13	2.97	23.76	10.46	4.52	0.00	0.85	1.98	0.71	456.20
CT_NYTAL_200	10.32	3.25	0.85	9.19	124.57	4.81	136.17	9.94	1.41	1.41	1.27	4.52	25.31	1.84	0.00	0.99	0.71	4.10	2.40	343.08
CT_NYTAL_300	0.28	2.40	2.69	8.63	141.68	3.68	201.35	7.53	2.40	0.00	0.28	3.25	70.84	8.91	1.56	0.99	0.57	4.67	1.70	463.40
CT_NYTAL_400	3.68	3.11	0.57	9.19	129.66	4.24	193.29	10.22	2.69	0.71	0.99	3.82	27.57	2.40	1.27	0.00	0.00	3.68	0.00	397.09
CT_Mouldene	6.65	2.83	0.42	10.89	689.33	3.96	186.51	8.52	1.84	0.85	1.56	2.55	10.18	4.38	0.85	0.42	0.14	0.99	0.00	932.85
CT_Fibertal_1	5.51	1.84	2.12	12.73	978.63	4.81	201.64	7.24	1.13	0.00	1.27	2.26	8.63	4.38	5.51	0.00	0.71	2.26	0.14	1240.81
CT_Fibertal_2	6.08	4.52	1.27	11.31	1004.79	4.38	189.33	8.38	1.70	0.00	0.28	1.70	7.64	3.96	1.13	0.00	0.71	0.57	0.00	1247.75
CT_Fibertal_6	4.81	3.82	1.70	9.90	413.60	4.52	203.47	9.23	0.85	0.00	0.99	4.67	19.65	6.79	0.00	2.69	0.14	0.99	0.00	687.81
IL_Shin_White_snow	7.64	5.94	3.25	8.63	46.52	1.27	16.40	12.07	1.70	1.27	0.99	12.02	116.51	4.81	0.42	0.00	0.00	0.71	0.42	240.57
IL_Shin_White_snow R	8.86	5.63	2.11	11.54	51.92	0.70	16.74	11.73	2.81	1.55	0.70	13.09	114.81	5.21	6.19	0.00	0.00	1.41	0.00	255.00

Appendix C: Talc Electron Microprobe data

Weight percent oxides are listed in Part 1 and calculated APFU values are listed in Part 2.

(-) indicates that the element was not analyzed for in this sample, (bdl) indicates the values were below the detection limit

Part 1.

Sample Name	SiO2/MgO		SiO2	Al2O3	TiO2	ZnO	Cr2O3	FeO	NiO	MnO	MgO	CaO	Na2O	K2O	P2O5	SO3	Oxide Sum	F	Cl
AUS_Mt.Seabrook	2.00	Average	62.05	0.31	bdl	bdl	bdl	0.82	bdl	bdl	31.05	0.01	0.04	0.01	-	0.01	94.32	0.14	0.01
		Std. Dev.	0.98	0.56	0.00	0.01	0.00	0.08	0.00	0.01	0.65	0.01	0.01	0.02	-	0.00	0.59	0.02	0.01
AUS_ThreeSprings	2.04	Average	62.39	0.17	0.01	bdl	bdl	1.02	bdl	bdl	30.52	0.02	0.03	0.01	-	0.00	94.17	0.12	0.01
		Std. Dev.	0.60	0.01	0.01	0.01	0.00	0.04	0.01	0.01	0.53	0.00	0.01	0.00	-	0.00	0.89	0.01	0.00
AUSTRIA_Styria_Anger	2.08	Average	61.69	0.32	0.01	0.01	bdl	0.75	bdl	0.01	29.72	0.01	0.02	bdl	-	0.01	92.56	0.10	0.01
		Std. Dev.	0.78	0.16	0.01	0.01	0.01	0.18	0.00	0.00	0.94	0.02	0.01	0.01	-	0.02	1.48	0.02	0.00
AUSTRIA_Styria_Lassing	2.05	Average	61.15	0.12	bdl	0.01	bdl	1.09	bdl	bdl	29.89	0.01	0.06	0.01	-	0.01	92.35	0.10	0.04
		Std. Dev.	2.27	0.04	0.00	0.01	0.01	0.03	0.01	0.00	1.06	0.01	0.07	0.01	-	0.01	3.12	0.02	0.07
BRA_Bahia_78	2.03	Average	61.91	0.30	bdl	bdl	bdl	0.99	0.01	0.01	30.47	bdl	0.03	bdl	-	bdl	93.72	0.26	0.02
		Std. Dev.	0.78	0.04	0.00	0.01	0.01	0.02	0.00	0.01	0.59	0.01	0.01	0.00	-	0.00	1.31	0.02	0.02
BRA_Bahia_mill	2.05	Average	60.34	0.38	0.02	-	-	0.28	-	0.01	29.76	0.02	0.01	bdl	0.00	-	90.81	0.08	0.04
		Std. Dev.	1.59	0.29	0.02	-	-	0.06	-	0.01	0.96	0.02	0.01	0.01	0.00	-	2.37	0.03	0.05
CAN_Ontario_Madoc_80	2.03	Average	62.32	0.41	bdl	0.01	bdl	0.19	bdl	bdl	30.63	0.01	0.03	0.02	-	0.00	93.64	0.24	bdl
		Std. Dev.	0.35	0.18	0.00	0.01	0.01	0.01	0.01	0.01	0.25	0.01	0.01	0.06	-	0.00	0.32	0.03	0.00
CAN_Ontario_Madoc_170	2.03	Average	62.10	0.03	0.01	bdl	bdl	0.11	bdl	bdl	30.65	0.01	0.03	bdl	-	0.01	92.93	0.23	0.01
		Std. Dev.	0.58	0.01	0.00	0.01	0.00	0.01	0.01	0.01	0.38	0.01	0.01	0.00	-	0.00	0.56	0.02	0.01
CHI_94	1.98	Average	61.90	0.05	bdl	0.01	bdl	0.29	bdl	bdl	31.29	0.04	0.01	0.01	-	0.01	93.61	0.12	0.00
		Std. Dev.	0.31	0.02	0.01	0.01	0.01	0.02	0.01	0.00	0.66	0.07	0.01	0.01	-	0.01	0.55	0.02	0.01
CHI_Cuangai_86	2.01	Average	62.54	0.07	bdl	bdl	bdl	0.47	bdl	bdl	31.05	0.01	0.01	bdl	-	0.01	94.17	0.05	0.01
		Std. Dev.	0.38	0.03	0.00	0.01	0.01	0.02	0.00	0.01	0.35	0.01	0.01	0.00	-	0.00	0.35	0.02	0.00
CHI_Guangxi_mill	2.03	Average	58.70	0.03	bdl	-	-	0.71	-	bdl	28.52	0.04	0.01	0.01	0.01	-	88.04	0.11	0.04
		Std. Dev.	3.32	0.05	0.01	-	-	0.20	-	0.01	1.90	0.04	0.01	0.00	0.02	-	5.28	0.04	0.02

Sample Name	SiO2/MgO		SiO2	Al2O3	TiO2	ZnO	Cr2O3	FeO	NiO	MnO	MgO	CaO	Na2O	K2O	P2O5	SO3	Oxide Sum	F	Cl
CHI_Giangxi_G1_89	2.05	Average	62.52	0.32	bdl	bdl	bdl	0.46	bdl	bdl	30.48	0.01	0.01	bdl	-	0.00	93.80	0.04	bdl
		Std. Dev.	0.44	0.13	0.00	0.01	0.00	0.02	0.00	0.00	0.26	0.01	0.01	0.00	-	0.00	0.35	0.02	0.00
CHI_Guangxi_G3_91-dark	2.09	Average	61.02	2.74	bdl	bdl	bdl	0.03	bdl	bdl	29.23	0.03	0.08	0.01	-	0.05	93.19	1.31	0.05
		Std. Dev.	1.91	1.60	0.00	0.01	0.01	0.01	0.01	0.01	1.46	0.01	0.02	0.00	-	0.02	1.71	0.12	0.02
CHI_Guangxi_G3_91-light	2.02	Average	58.72	0.17	bdl	0.01	bdl	0.02	bdl	bdl	29.06	0.03	0.03	0.01	-	0.03	88.08	1.24	bdl
		Std. Dev.	2.49	0.05	0.00	0.01	0.00	0.01	0.01	0.00	0.90	0.01	0.01	0.00	-	0.04	3.30	0.09	0.59
CHI_Guangxi_G3_92	1.98	Average	61.82	0.13	bdl	bdl	bdl	0.01	bdl	bdl	31.16	0.01	0.03	0.01	-	0.01	93.17	1.38	0.03
		Std. Dev.	0.43	0.02	0.00	0.01	0.00	0.01	0.01	0.01	0.22	0.01	0.01	0.00	-	0.00	0.47	0.02	0.01
CHI_Guangxi_Longsheng_G1_88	2.01	Average	62.36	0.05	bdl	bdl	bdl	0.59	bdl	bdl	31.10	0.01	0.01	0.01	-	0.01	94.13	0.05	0.01
		Std. Dev.	0.36	0.02	0.00	0.01	0.01	0.02	0.01	0.01	0.24	0.00	0.02	0.02	-	0.00	0.32	0.01	0.01
CHI_Haicmen_84	1.97	Average	62.37	0.08	bdl	bdl	bdl	0.20	bdl	bdl	31.59	0.01	0.00	bdl	-	bdl	94.26	0.09	0.01
		Std. Dev.	0.37	0.02	0.00	0.01	0.00	0.03	0.01	0.00	0.28	0.01	0.01	0.00	-	0.00	0.45	0.02	0.00
CHI_Liaoning_87	2.02	Average	62.46	0.04	bdl	bdl	bdl	0.27	bdl	bdl	30.99	0.01	0.01	bdl	-	0.01	93.78	0.23	0.01
		Std. Dev.	0.46	0.01	0.00	0.01	0.01	0.02	0.01	0.00	0.32	0.00	0.01	0.00	-	0.00	0.38	0.03	0.00
CHI_Liaoning_Haicheng_G3_93	1.98	Average	62.63	0.02	bdl	bdl	bdl	0.03	bdl	bdl	31.56	0.01	bdl	bdl	-	0.01	94.25	0.10	0.00
		Std. Dev.	0.39	0.01	0.00	0.01	0.00	0.01	0.01	0.00	0.20	0.01	0.01	0.00	-	0.00	0.34	0.02	0.00
CHI_Liaoning_Yingkow_83	2.00	Average	62.64	0.02	bdl	bdl	bdl	0.31	bdl	bdl	31.31	0.01	0.01	bdl	-	0.01	94.31	0.16	0.01
		Std. Dev.	0.44	0.01	0.00	0.01	0.01	0.01	0.00	0.00	0.61	0.01	0.01	0.01	-	0.01	0.71	0.02	0.01
CHI_Shadong_Qixia_85	2.00	Average	62.50	0.07	bdl	bdl	bdl	0.08	bdl	bdl	31.28	bdl	0.03	bdl	-	0.00	93.96	0.06	0.01
		Std. Dev.	0.57	0.02	0.00	0.01	0.01	0.01	0.00	0.01	0.51	0.01	0.01	0.00	-	0.00	0.31	0.02	0.01
FIN_NKarelia	2.01	Average	61.12	0.16	0.01	0.01	0.07	1.50	0.04	bdl	30.37	0.01	0.02	bdl	-	0.02	93.32	bdl	0.01
		Std. Dev.	1.24	0.15	0.01	0.01	0.04	0.11	0.01	0.00	0.36	0.01	0.01	0.00	-	0.01	1.05	0.02	0.01
IND_Chainpura_mill	2.07	Average	58.13	0.09	0.01	-	-	0.48	-	bdl	28.12	0.04	0.04	0.02	0.02	-	86.96	bdl	0.08
		Std. Dev.	2.91	0.02	0.02	-	-	0.14	-	0.02	1.82	0.02	0.04	0.01	0.03	-	4.74	0.13	0.06
IND_Ghevaria_mill	2.03	Average	60.94	0.06	0.01	-	-	0.54	-	bdl	30.01	0.04	0.01	bdl	0.01	-	91.64	0.18	0.05
		Std. Dev.	2.64	0.06	0.02	-	-	0.06	-	0.01	1.66	0.02	0.01	0.01	0.01	-	4.31	0.04	0.05

Sample Name	SiO2/MgO		SiO2	Al2O3	TiO2	ZnO	Cr2O3	FeO	NiO	MnO	MgO	CaO	Na2O	K2O	P2O5	SO3	Oxide Sum	F	Cl
ITA_Gianna_A	2.09	Average	62.01	0.16	bdl	0.01	bdl	1.30	bdl	bdl	29.68	bdl	0.03	bdl	-	0.01	93.20	0.27	0.01
		Std. Dev.	0.39	0.06	0.00	0.01	0.00	0.13	0.01	0.00	0.31	0.01	0.02	0.01	-	0.01	0.39	0.02	0.00
ITA_Gianna_C	2.06	Average	62.00	0.13	bdl	bdl	bdl	0.72	bdl	bdl	30.15	bdl	0.02	bdl	-	0.00	93.04	0.27	0.01
		Std. Dev.	0.18	0.05	0.00	0.01	0.01	0.02	0.01	0.01	0.28	0.01	0.01	0.00	-	0.00	0.39	0.03	0.01
ITA_Paola_A	2.05	Average	62.04	0.15	bdl	bdl	bdl	0.80	bdl	bdl	30.21	0.01	0.02	bdl	-	0.01	93.23	0.25	0.01
		Std. Dev.	0.52	0.01	0.00	0.01	0.01	0.02	0.01	0.01	0.45	0.00	0.01	0.00	-	0.00	0.59	0.03	0.00
ITA_Paola_scop	2.04	Average	55.67	0.20	bdl	0.02	bdl	0.73	bdl	0.01	27.31	0.01	0.03	0.01	-	0.02	84.01	0.24	0.21
		Std. Dev.	8.13	0.09	0.00	0.01	0.00	0.16	0.00	0.00	3.62	0.00	0.01	0.00	-	0.00	11.86	0.02	0.33
ITA_Rodoretto_A1	2.05	Average	61.44	0.16	bdl	0.01	bdl	0.58	bdl	bdl	29.98	0.02	0.03	0.01	-	0.02	92.25	0.14	0.02
		Std. Dev.	0.49	0.08	0.00	0.01	0.01	0.26	0.00	0.00	0.45	0.01	0.01	0.00	-	0.02	0.39	0.08	0.01
ITA_Rodoretto_B1	2.06	Average	57.23	0.13	bdl	bdl	bdl	0.79	bdl	bdl	27.77	0.01	0.03	bdl	-	0.01	85.98	0.24	0.17
		Std. Dev.	3.82	0.06	0.00	0.01	0.00	0.15	0.00	0.00	2.33	0.01	0.02	0.00	-	0.01	6.08	0.02	0.23
KOR	2.04	Average	62.23	0.31	0.01	0.01	bdl	0.97	bdl	bdl	30.48	bdl	0.05	bdl	-	0.01	94.07	0.42	0.01
		Std. Dev.	0.35	0.05	0.00	0.01	0.00	0.01	0.01	0.00	0.32	0.00	0.01	0.01	-	0.00	0.40	0.02	0.00
MOR_109	2.08	Average	62.56	0.02	bdl	0.01	bdl	0.36	bdl	bdl	30.04	0.01	0.01	bdl	-	0.01	93.03	0.13	0.00
		Std. Dev.	0.74	0.01	0.00	0.01	0.01	0.10	0.01	0.00	0.42	0.01	0.01	0.00	-	0.00	0.85	0.03	0.00
NOR	2.08	Average	62.39	0.21	bdl	0.01	bdl	0.50	bdl	bdl	30.01	0.01	0.01	bdl	-	0.00	93.15	0.20	0.01
		Std. Dev.	0.78	0.05	0.00	0.01	0.01	0.03	0.00	0.00	0.55	0.01	0.01	0.00	-	0.01	0.81	0.02	0.01
SPA_110	2.04	Average	62.39	0.09	bdl	bdl	bdl	0.19	bdl	bdl	30.60	0.02	0.02	0.01	-	0.00	93.31	0.48	0.01
		Std. Dev.	0.50	0.02	0.00	0.01	0.00	0.04	0.00	0.00	0.42	0.00	0.02	0.00	-	0.01	0.57	0.07	0.01
SPA_111	2.02	Average	62.09	0.11	bdl	bdl	bdl	0.14	bdl	bdl	30.81	0.02	0.03	bdl	-	0.00	93.21	0.42	0.00
		Std. Dev.	0.48	0.01	0.00	0.01	0.01	0.02	0.01	0.00	0.51	0.00	0.01	0.00	-	0.00	0.41	0.06	0.00
USA_CA_Grantham	2.05	Average	61.96	0.63	bdl	bdl	bdl	0.24	bdl	0.01	30.29	0.06	0.06	0.03	-	0.01	93.29	0.46	bdl
		Std. Dev.	0.54	0.41	0.01	0.01	0.01	0.04	0.00	0.00	0.45	0.13	0.03	0.03	-	0.00	0.38	0.02	0.00
USA_CA_TalcCity_6_dark	2.13	Average	61.40	0.34	0.01	0.01	bdl	0.68	bdl	bdl	28.79	0.04	0.10	0.02	-	0.02	91.42	0.18	0.01
		Std. Dev.	1.37	0.19	0.01	0.00	0.01	0.21	0.01	0.00	0.87	0.01	0.04	0.01	-	0.01	1.70	0.05	0.00

Sample Name	SiO2/MgO		SiO2	Al2O3	TiO2	ZnO	Cr2O3	FeO	NiO	MnO	MgO	CaO	Na2O	K2O	P2O5	SO3	Oxide Sum	F	Cl
USA_CA_TalcCity_6_light	2.09	Average	62.24	0.28	bdl	0.01	bdl	0.91	bdl	bdl	29.86	0.03	0.09	0.02	-	0.01	93.46	0.26	0.00
		Std. Dev.	0.66	0.08	0.00	0.01	0.01	0.20	0.01	0.00	0.41	0.01	0.05	0.01	-	0.01	0.73	0.05	0.00
USA_CA_WesternTalc_3A	2.06	Average	60.85	0.14	bdl	bdl	bdl	0.20	bdl	bdl	29.59	0.03	0.10	0.07	-	0.03	91.01	0.12	0.08
		Std. Dev.	1.58	0.11	0.00	0.01	0.00	0.04	0.01	0.01	0.97	0.04	0.04	0.06	-	0.02	2.36	0.03	0.05
USA_CA_WesternTalc_3C	2.05	Average	62.61	0.04	bdl	bdl	bdl	0.08	bdl	bdl	30.57	0.02	0.04	0.02	-	0.00	93.40	0.05	0.01
		Std. Dev.	0.66	0.01	0.00	0.00	0.01	0.02	0.00	0.01	0.44	0.02	0.02	0.02	-	0.01	1.03	0.02	0.02
USA_CA_Victorville	2.05	Average	62.23	0.31	bdl	bdl	bdl	0.02	bdl	bdl	30.40	0.02	0.04	0.33	-	0.01	93.35	0.10	0.00
		Std. Dev.	1.09	0.30	0.00	0.01	0.00	0.01	0.01	0.00	0.39	0.01	0.01	0.35	-	0.01	0.74	0.03	0.00
USA_GA_Earnest_fibrous	2.32	Average	59.85	0.11	bdl	0.02	bdl	5.76	0.08	bdl	25.80	1.390	0.02	0.02	-	0.02	93.11	0.14	0.01
		Std. Dev.	1.13	0.06	0.00	0.01	0.01	0.22	0.02	0.01	0.99	1.158	0.01	0.01	-	0.01	1.10	0.02	0.01
USA_MT_Beaverhead County	2.10	Average	61.00	0.15	bdl	bdl	bdl	2.22	bdl	0.07	29.02	0.09	0.04	bdl	-	0.01	92.61	0.04	0.00
		Std. Dev.	0.58	0.04	0.01	0.01	0.01	0.43	0.00	0.10	0.60	0.20	0.02	0.00	-	0.00	0.90	0.03	0.00
USA_MT_Beaverhead_hi Fe	2.05	Average	62.06	0.06	bdl	bdl	bdl	1.06	bdl	bdl	30.24	bdl	0.02	bdl	-	0.00	93.46	0.11	0.01
		Std. Dev.	0.65	0.02	0.00	0.01	0.00	0.07	0.01	0.01	0.22	0.01	0.01	0.00	-	0.01	0.49	0.01	0.00
USA_MT_Beaverhead_low Fe	2.05	Average	62.24	0.18	bdl	bdl	bdl	0.27	bdl	bdl	30.42	0.008	0.03	bdl	-	0.00	93.16	0.11	0.00
		Std. Dev.	0.48	0.11	0.00	0.01	0.00	0.06	0.01	0.01	0.34	0.005	0.01	0.00	-	0.00	0.44	0.02	0.00
USA_MT_Regal_HG	2.04	Average	62.07	0.21	0.01	bdl	bdl	0.52	bdl	bdl	30.44	0.02	0.06	bdl	-	0.00	93.34	0.10	0.01
		Std. Dev.	0.63	0.05	0.00	0.01	0.01	0.13	0.00	0.01	0.41	0.01	0.01	0.00	-	0.01	0.72	0.01	0.00
USA_MT_Treasure_float	2.04	Average	61.87	0.19	0.01	-	-	2.70	-	0.05	30.34	0.03	0.03	0.01	bdl	-	95.23	0.20	0.01
		Std. Dev.	0.36	0.07	0.01	-	-	0.54	-	0.04	0.22	0.02	0.01	0.01	0.01	-	0.98	0.06	0.00
USA_MT_Treasure_G1_hi Fe	2.11	Average	61.93	0.04	bdl	0.01	bdl	2.30	0.01	bdl	29.31	bdl	0.01	bdl	-	0.01	93.63	0.29	0.00
		Std. Dev.	0.22	0.01	0.00	0.00	0.01	0.25	0.00	0.00	0.18	0.00	0.01	0.00	-	0.01	0.28	0.05	0.00
USA_MT_Treasure_G1_lo Fe	2.02	Average	62.11	0.12	0.01	bdl	bdl	0.24	bdl	bdl	30.69	0.009	0.03	bdl	-	0.01	93.22	0.11	0.00
		Std. Dev.	0.51	0.03	0.00	0.01	0.00	0.09	0.00	0.00	0.29	0.004	0.01	0.00	-	0.00	0.48	0.01	0.00
USA_MT_Treasure_G3	2.12	Average	61.88	0.16	bdl	bdl	bdl	2.24	0.01	bdl	29.19	0.02	0.05	bdl	-	0.00	93.55	0.20	0.00
		Std. Dev.	0.51	0.03	0.00	0.01	0.01	0.12	0.01	0.00	0.25	0.00	0.01	0.01	-	0.00	0.45	0.01	0.00

Sample Name	SiO2/MgO		SiO2	Al2O3	TiO2	ZnO	Cr2O3	FeO	NiO	MnO	MgO	CaO	Na2O	K2O	P2O5	SO3	Oxide Sum	F	Cl
USA_MT_Treasure_pseudo.	2.09	Average	62.06	0.17	0.01	bdl	bdl	1.93	bdl	bdl	29.63	0.01	0.04	bdl	-	bdl	93.85	0.13	bdl
		Std. Dev.	0.32	0.04	0.00	0.01	0.00	0.19	0.01	0.01	0.26	0.01	0.01	0.00	-	0.00	0.24	0.02	0.00
USA_MT_Willow Creek_1a	2.02	Average	62.24	0.06	0.01	-	-	1.63	-	0.01	30.83	0.02	0.01	0.01	bdl	-	94.82	0.19	0.02
		Std. Dev.	0.70	0.04	0.01	-	-	0.64	-	0.01	0.48	0.02	0.02	0.01	0.01	-	1.19	0.05	0.01
USA_MT_Willow Creek_8	2.03	Average	62.47	0.05	bdl	-	-	1.88	-	0.01	30.82	0.01	0.02	0.01	bdl	-	95.28	0.15	0.02
		Std. Dev.	0.56	0.08	0.01	-	-	0.51	-	0.01	0.41	0.01	0.01	0.01	0.01	-	1.03	0.02	0.01
USA_MT_WillowCreek_SF_N9A	2.17	Average	61.96	0.10	0.01	bdl	bdl	2.56	bdl	0.05	28.54	0.27	0.09	0.02	-	0.01	93.60	0.05	0.03
		Std. Dev.	0.94	0.05	0.01	0.01	0.00	0.16	0.00	0.00	0.65	0.14	0.03	0.00	-	0.01	0.59	0.01	0.02
USA_MT_WillowCreek_SF14	2.07	Average	61.47	0.08	bdl	bdl	bdl	1.76	0.01	0.01	29.63	0.01	0.02	bdl	-	bdl	93.00	0.10	0.01
		Std. Dev.	0.43	0.07	0.00	0.01	0.01	0.64	0.01	0.01	0.52	0.01	0.03	0.01	-	0.00	0.22	0.02	0.01
USA_MT_Yellowstone_HG	2.01	Average	62.13	0.14	bdl	-	-	1.09	-	bdl	30.93	0.03	0.03	bdl	0.01	-	94.37	0.29	bdl
		Std. Dev.	0.77	0.01	0.02	-	-	0.03	-	0.01	0.50	0.01	0.01	0.00	0.01	-	1.29	0.02	0.00
USA_MT_Yellowstone_LG	2.02	Average	62.66	0.07	bdl	-	-	1.36	-	bdl	31.08	0.04	bdl	bdl	bdl	-	95.20	0.31	0.00
		Std. Dev.	0.54	0.01	0.01	-	-	0.02	-	0.01	0.32	0.02	0.00	0.01	0.01	-	0.84	0.02	0.00
USA_NC_HC_CT_light	2.03	Average	60.78	0.16	0.01	-	-	1.10	-	bdl	29.91	0.04	0.04	0.01	0.01	-	92.06	0.14	0.04
		Std. Dev.	1.48	0.05	0.01	-	-	0.89	-	0.02	1.15	0.03	0.03	0.01	0.01	-	2.23	0.04	0.03
USA_NC_HC_dark rock	2.00	Average	62.61	0.33	bdl	-	-	1.18	-	bdl	31.27	0.02	0.02	bdl	0.01	-	95.42	0.36	0.00
		Std. Dev.	0.81	0.23	0.02	-	-	0.13	-	0.01	0.52	0.01	0.01	0.01	0.01	-	1.09	0.01	0.00
USA_NC_HC_light rock	2.00	Average	62.03	0.38	0.01	-	-	1.12	-	0.01	30.95	bdl	0.02	bdl	bdl	-	94.52	0.39	0.00
		Std. Dev.	0.53	0.05	0.01	-	-	0.02	-	0.01	0.39	0.01	0.01	0.01	0.01	-	0.92	0.02	0.00
USA_NC_crayon	1.99	Average	62.56	0.19	0.01	-	-	0.32	-	bdl	31.40	bdl	0.03	0.01	bdl	-	94.51	0.25	0.02
		Std. Dev.	0.34	0.08	0.01	-	-	0.03	-	0.01	0.23	0.01	0.01	0.01	0.01	-	0.51	0.01	0.01
USA_NC_CCLA	2.04	Average	60.37	0.15	0.01	-	-	0.50	-	0.01	29.61	0.02	0.03	0.02	bdl	-	90.73	0.29	0.03
		Std. Dev.	3.16	0.04	0.01	-	-	0.03	-	0.01	2.02	0.02	0.03	0.02	0.01	-	5.17	0.02	0.03
USA_NC_Dcrayon	2.02	Average	61.80	0.30	bdl	-	-	0.66	-	bdl	30.65	0.02	0.02	bdl	bdl	-	93.45	0.34	0.01
		Std. Dev.	1.08	0.12	0.01	-	-	0.03	-	0.01	0.71	0.02	0.01	0.01	0.01	-	1.76	0.02	0.01

Sample Name	SiO2/MgO		SiO2	Al2O3	TiO2	ZnO	Cr2O3	FeO	NiO	MnO	MgO	CaO	Na2O	K2O	P2O5	SO3	Oxide Sum	F	Cl
USA_NC_Foote	2.01	Average	61.99	0.14	bdl	-	-	0.95	-	bdl	30.84	0.01	0.02	0.01	bdl	-	93.96	0.51	0.01
		Std. Dev.	1.11	0.08	0.01	-	-	0.08	-	0.01	0.84	0.01	0.02	0.01	0.01	-	1.82	0.03	0.00
USA_NC_Murphy_124	2.07	Average	62.24	0.11	bdl	bdl	bdl	0.91	bdl	bdl	30.03	0.01	0.02	bdl	-	0.01	93.32	0.35	0.01
		Std. Dev.	0.59	0.05	0.00	0.01	0.00	0.19	0.01	0.01	0.34	0.01	0.01	0.00	-	0.01	0.48	0.02	0.01
USA_NC_Murphy_129	2.09	Average	62.53	0.27	0.01	bdl	bdl	0.86	bdl	bdl	29.95	0.01	0.03	bdl	-	0.00	93.67	0.37	0.00
		Std. Dev.	0.50	0.04	0.00	0.01	0.01	0.03	0.00	0.00	0.45	0.00	0.01	0.01	-	0.00	0.51	0.03	0.00
USA_NC_Murphy_132	2.06	Average	62.50	0.11	bdl	bdl	bdl	0.11	bdl	bdl	30.38	0.01	0.04	bdl	-	0.00	93.16	0.19	0.00
		Std. Dev.	0.39	0.03	0.00	0.01	0.01	0.01	0.01	0.01	0.23	0.00	0.01	0.00	-	0.00	0.48	0.02	0.00
USA_TX_VanHorn_black	2.04	Average	61.63	0.21	bdl	bdl	bdl	0.08	bdl	bdl	30.22	0.04	0.05	0.07	-	0.01	92.31	0.36	0.00
		Std. Dev.	0.52	0.02	0.00	0.01	0.00	0.01	0.01	0.00	0.52	0.01	0.01	0.01	-	0.00	0.53	0.03	0.00
USA_TX_VanHorn_gray	2.03	Average	62.32	0.09	bdl	bdl	bdl	0.01	bdl	bdl	30.73	0.09	0.06	0.02	-	0.02	93.35	0.32	0.01
		Std. Dev.	0.82	0.02	0.00	0.01	0.00	0.01	0.00	0.00	0.50	0.06	0.05	0.02	-	0.01	1.06	0.08	0.00
USA_TX_VanHorn_pink	2.00	Average	60.73	0.05	bdl	bdl	bdl	0.03	bdl	bdl	30.42	0.05	0.08	0.01	-	0.01	91.39	0.20	0.01
		Std. Dev.	0.96	0.02	0.00	0.01	0.00	0.02	0.00	0.00	0.91	0.03	0.04	0.01	-	0.00	1.47	0.12	0.00
USA_TX_Llano	2.04	Average	60.68	0.34	bdl	bdl	0.02	2.49	0.21	0.01	29.74	bdl	0.06	bdl	-	bdl	93.55	bdl	bdl
		Std. Dev.	0.71	0.14	0.01	0.01	0.02	0.21	0.02	0.00	0.46	0.00	0.03	0.00	-	0.01	0.54	0.02	0.00
USA_VT_Argonaut_BB_T1	2.09	Average	60.33	0.03	0.01	-	-	2.72	-	0.01	28.94	0.03	0.02	0.01	bdl	-	92.09	0.04	0.05
		Std. Dev.	2.14	0.05	0.01	-	-	0.28	-	0.01	1.22	0.02	0.00	0.01	0.00	-	3.43	0.04	0.06
USA_VT_Argonaut_flake	2.04	Average	62.30	bdl	bdl	-	-	1.78	-	bdl	30.59	0.01	0.03	0.01	bdl	-	94.72	0.03	0.01
		Std. Dev.	0.30	0.01	0.00	-	-	0.07	-	0.01	0.26	0.02	0.01	0.01	0.01	-	0.51	0.01	0.01
USA_VT_Argonaut_HG	2.07	Average	62.11	0.01	bdl	-	-	2.45	-	0.01	30.08	0.02	0.02	bdl	bdl	-	94.68	0.03	0.01
		Std. Dev.	0.35	0.01	0.01	-	-	0.06	-	0.02	0.23	0.02	0.01	0.01	0.01	-	0.52	0.01	0.00
USA_VT_Argonaut_LG	2.11	Average	62.81	0.01	bdl	-	-	2.72	-	bdl	29.81	0.01	0.02	0.01	-	-	95.39	0.04	0.01
		Std. Dev.	0.55	0.02	0.01	-	-	0.06	-	0.01	0.24	0.01	0.01	0.01	-	-	0.76	0.02	0.00
USA_VT_Argonaut_SGR	2.17	Average	62.42	0.11	bdl	-	-	4.46	-	0.05	28.72	0.02	0.02	0.01	-	-	95.81	0.11	0.01
		Std. Dev.	0.83	0.03	0.01	-	-	0.13	-	0.01	0.63	0.01	0.01	0.01	-	-	1.47	0.02	0.01

Sample Name	SiO2/MgO		SiO2	Al2O3	TiO2	ZnO	Cr2O3	FeO	NiO	MnO	MgO	CaO	Na2O	K2O	P2O5	SO3	Oxide Sum	F	Cl
USA_VT_Argonaut_underflow	2.13	Average	62.01	0.05	0.01	-	-	2.89	-	0.01	29.10	0.04	0.02	0.01	-	-	94.14	0.06	0.02
		Std. Dev.	1.32	0.05	0.01	-	-	0.28	-	0.01	0.71	0.02	0.02	0.01	-	-	2.09	0.02	0.01
USA_VT_Argonaut-W71	2.11	Average	63.11	0.03	bdl	-	-	2.86	-	0.01	29.87	0.02	0.01	bdl	-	-	95.91	0.10	0.01
		Std. Dev.	0.31	0.12	0.01	-	-	0.32	-	0.01	0.27	0.01	0.01	0.01	-	-	0.49	0.03	0.00
UA_VT_Argonaut_W83	2.06	Average	62.22	bdl	0.01	-	-	2.27	-	bdl	30.27	0.02	0.03	0.02	bdl	-	94.82	0.05	0.03
		Std. Dev.	0.80	0.02	0.01	-	-	0.16	-	0.01	0.63	0.02	0.04	0.02	0.01	-	1.32	0.02	0.03
USA_VT_Johnson_black	2.10	Average	62.55	0.02	0.01	-	-	3.37	-	bdl	29.86	0.01	0.01	0.01	-	-	95.83	0.10	0.00
		Std. Dev.	0.52	0.02	0.01	-	-	0.06	-	0.01	0.44	0.01	0.01	0.01	-	-	0.92	0.02	0.00
USA_VT_CT_Johnson_E42	2.12	Average	60.40	0.02	0.01	-	-	2.40	-	0.01	28.49	0.03	0.01	0.01	-	-	91.37	0.07	0.06
		Std. Dev.	1.48	0.02	0.02	-	-	0.09	-	0.01	0.79	0.01	0.01	0.01	-	-	2.18	0.02	0.04
USA_VT_CT_Johnson_E42 R	2.13	Average	60.44	0.05	0.01	-	-	2.64	-	0.03	28.40	0.05	0.03	0.01	-	-	91.65	0.14	0.07
		Std. Dev.	1.46	0.02	0.02	-	-	0.57	-	0.02	0.74	0.02	0.01	0.01	-	-	2.51	0.05	0.03
USA_VT_Johnson_green	2.09	Average	61.94	bdl	bdl	-	-	3.57	-	0.02	29.70	0.01	0.01	0.01	-	-	95.25	0.09	0.01
		Std. Dev.	0.36	0.01	0.01	-	-	0.37	-	0.02	0.35	0.01	0.01	0.01	-	-	0.56	0.02	0.01
USA_VT_Johnson-LesW	2.06	Average	62.40	bdl	bdl	-	-	2.48	-	bdl	30.24	0.01	0.01	0.01	-	-	95.12	0.06	0.01
		Std. Dev.	0.35	0.01	0.01	-	-	0.09	-	0.01	0.23	0.01	0.01	0.01	-	-	0.54	0.02	0.01
USA_VT_Johnson_CT_J50	2.06	Average	62.38	bdl	bdl	-	-	2.52	-	bdl	30.25	0.01	0.02	0.01	-	-	95.17	0.07	0.01
		Std. Dev.	0.68	0.01	0.01	-	-	0.10	-	0.02	0.38	0.01	0.01	0.01	-	-	1.01	0.02	0.01
USA_VT_Johnson_UVM	2.11	Average	62.20	0.02	0.01	-	-	3.83	-	0.02	29.50	0.02	0.06	0.04	-	-	95.69	0.11	0.05
		Std. Dev.	0.51	0.03	0.01	-	-	0.17	-	0.01	0.34	0.01	0.03	0.02	-	-	0.80	0.02	0.03
USA_VT_Johnson_CT_E500	2.11	Average	57.52	0.02	0.01	-	-	2.27	-	bdl	27.32	0.04	0.06	0.02	-	-	87.27	0.08	0.15
		Std. Dev.	3.48	0.02	0.02	-	-	0.11	-	0.01	1.85	0.02	0.02	0.01	-	-	5.21	0.04	0.11
USA_VT_Johnson_mill pipe	2.11	Average	61.86	0.00	0.01	-	-	2.87	-	bdl	29.35	0.02	0.01	0.01	-	-	94.12	0.09	0.03
		Std. Dev.	0.90	0.02	0.01	-	-	0.10	-	0.01	0.44	0.01	0.01	0.01	-	-	1.37	0.02	0.04
USA_VT_Johnson_mill rafters	2.13	Average	60.85	0.04	bdl	-	-	2.43	-	bdl	28.53	0.04	0.04	0.01	-	-	91.95	0.05	0.05
		Std. Dev.	2.56	0.10	0.01	-	-	0.64	-	0.01	1.60	0.04	0.04	0.01	-	-	3.94	0.04	0.05

Sample Name	SiO2/MgO		SiO2	Al2O3	TiO2	ZnO	Cr2O3	FeO	NiO	MnO	MgO	CaO	Na2O	K2O	P2O5	SO3	Oxide Sum	F	Cl
USA_VT_Johnson_W23_USGS	2.16	Average	62.56	0.01	bdl	-	-	4.49	-	0.07	28.96	0.01	0.03	0.02	-	-	96.14	0.08	0.03
		Std. Dev.	1.04	0.03	0.01	-	-	0.23	-	0.01	0.67	0.01	0.03	0.01	-	-	1.78	0.02	0.03
USA_VT_CT_Engelhard	2.15	Average	44.73	0.07	bdl	-	-	1.72	-	0.01	21.01	0.04	0.04	0.03	0.02	-	67.66	bdl	0.58
		Std. Dev.	16.10	0.15	0.02	-	-	0.46	-	0.01	8.04	0.02	0.02	0.02	0.02	-	24.42	0.24	0.54
USA_WA_Totem Talc	2.09	Average	62.72	0.03	bdl	bdl	bdl	0.48	bdl	bdl	30.08	0.01	bdl	bdl	-	0.01	93.32	0.07	0.00
		Std. Dev.	0.73	0.01	0.00	0.01	0.01	0.06	0.01	0.00	0.54	0.01	0.01	0.00	-	0.00	0.76	0.02	0.00
USA_WA_Totem Gulch	2.06	Average	62.27	0.05	bdl	0.00	bdl	0.45	bdl	bdl	30.31	0.01	bdl	bdl	-	0.01	93.11	0.07	0.00
		Std. Dev.	0.97	0.01	0.00	0.01	0.01	0.06	0.00	0.00	0.90	0.01	0.01	0.00	-	0.00	0.72	0.01	0.00
CT_Johnson's bp	2.05	Average	57.31	0.08	0.01	-	-	0.75	-	bdl	27.96	0.04	0.02	0.02	bdl	-	86.19	0.11	0.17
		Std. Dev.	7.44	0.08	0.02	-	-	0.13	-	0.01	3.51	0.01	0.02	0.01	0.01	-	11.00	0.03	0.29
CT_CSI_fingerprint	2.18	Average	60.65	0.14	0.02	-	-	0.80	-	bdl	29.62	0.10	0.13	0.06	0.01	-	91.53	0.09	0.16
		Std. Dev.	1.68	0.13	0.02	-	-	0.22	-	0.01	0.89	0.05	0.06	0.02	0.01	-	2.61	0.02	0.06
CT_marker_Moscow	2.05	Average	62.69	0.06	bdl	bdl	bdl	0.49	bdl	bdl	30.60	0.01	bdl	bdl	-	0.01	93.86	0.04	bdl
		Std. Dev.	0.62	0.01	0.00	0.01	0.01	0.02	0.01	0.01	0.29	0.00	0.01	0.00	-	0.00	0.70	0.01	0.00
CT_Protech	2.10	Average	61.31	0.24	0.01	0.03	bdl	0.24	bdl	bdl	29.17	0.66	0.08	0.08	-	0.03	91.86	0.47	0.02
		Std. Dev.	0.88	0.14	0.02	0.03	0.01	0.05	0.01	0.01	1.27	1.08	0.06	0.08	-	0.03	1.24	0.22	0.01
CT_WhiteSnow	2.11	Average	55.52	0.21	0.01	0.02	bdl	1.25	bdl	bdl	26.29	0.05	0.03	bdl	-	0.03	83.42	0.27	0.21
		Std. Dev.	5.90	0.09	0.01	0.01	0.00	0.17	0.01	0.01	2.97	0.05	0.02	0.00	-	0.01	8.88	0.05	0.16

Atoms per formula unit values were calculated based on Dyar, Gunter, and Tasa (Table 10.6)
(-) indicates that the element was not analyzed for in this sample
Part 2.

Sample Name		Si4+	Al3+	Ti4+	Zn2+	Cr3+	Fe2+	Ni2+	Mn2+	Mg2+	Ca2+	Na+	K+	P5+	S6+	F-	OH-	Tet	Oct
AUS_Mt.Seabrook	Average	3.97	0.02	0.00	0.00	0.00	0.04	0.00	0.00	2.97	0.00	0.01	0.00	-	0.00	0.03	1.97	3.99	3.02
	Std. Dev.	0.05	0.04	0.00	0.00	0.00	0.00	0.00	0.00	0.06	0.00	0.00	0.00	-	0.00	0.00	0.00	0.02	0.05
AUS_ThreeSprings	Average	4.00	0.01	0.00	0.00	0.00	0.05	0.00	0.00	2.92	0.00	0.00	0.00	-	0.00	0.02	1.98	4.01	2.99
	Std. Dev.	0.02	0.00	0.00	0.00	0.00	0.00	0.00	0.00	0.04	0.00	0.00	0.00	-	0.00	0.00	0.00	0.02	0.03
AUSTRIA_Styria_Anger	Average	4.02	0.02	0.00	0.00	0.00	0.04	0.00	0.00	2.88	0.00	0.00	0.00	-	0.00	0.02	1.98	4.02	2.95
	Std. Dev.	0.03	0.01	0.00	0.00	0.00	0.01	0.00	0.00	0.06	0.00	0.00	0.00	-	0.00	0.00	0.00	0.02	0.05
AUSTRIA_Styria_Lassing	Average	4.00	0.01	0.00	0.00	0.00	0.06	0.00	0.00	2.92	0.00	0.01	0.00	-	0.00	0.02	1.98	4.01	2.99
	Std. Dev.	0.03	0.00	0.00	0.00	0.00	0.00	0.00	0.00	0.06	0.00	0.01	0.00	-	0.00	0.00	0.00	0.03	0.06
BRA_Bahia_78	Average	3.99	0.02	0.00	0.00	0.00	0.05	0.00	0.00	2.93	0.00	0.00	0.00	-	0.00	0.05	1.95	4.00	3.00
	Std. Dev.	0.01	0.00	0.00	0.00	0.00	0.00	0.00	0.00	0.02	0.00	0.00	0.00	-	0.00	0.00	0.00	0.01	0.02
BRA_Bahia_mill	Average	4.00	0.03	0.00	-	-	0.02	-	0.00	2.94	0.00	0.00	0.00	0.00	-	0.02	1.98	4.01	2.98
	Std. Dev.	0.02	0.02	0.00	-	-	0.00	-	0.00	0.03	0.00	0.00	0.00	0.00	-	0.01	0.01	0.01	0.02
CAN_Ontario_Madoc_80	Average	4.00	0.03	0.00	0.00	0.00	0.01	0.00	0.00	2.93	0.00	0.00	0.00	-	0.00	0.05	1.95	4.01	2.98
	Std. Dev.	0.01	0.01	0.00	0.00	0.00	0.00	0.00	0.00	0.03	0.00	0.00	0.01	-	0.00	0.01	0.01	0.01	0.02
CAN_Ontario_Madoc_170	Average	4.02	0.00	0.00	0.00	0.00	0.01	0.00	0.00	2.95	0.00	0.00	0.00	-	0.00	0.05	1.95	4.02	2.97
	Std. Dev.	0.02	0.00	0.00	0.00	0.00	0.00	0.00	0.00	0.04	0.00	0.00	0.00	-	0.00	0.00	0.00	0.02	0.04
CHI_94	Average	3.99	0.00	0.00	0.00	0.00	0.02	0.00	0.00	3.00	0.00	0.00	0.00	-	0.00	0.03	1.97	3.99	3.03
	Std. Dev.	0.03	0.00	0.00	0.00	0.00	0.00	0.00	0.00	0.05	0.00	0.00	0.00	-	0.00	0.00	0.00	0.02	0.05
CHI_Cuangai_86	Average	4.00	0.01	0.00	0.00	0.00	0.03	0.00	0.00	2.96	0.00	0.00	0.00	-	0.00	0.01	1.99	4.00	2.99
	Std. Dev.	0.02	0.00	0.00	0.00	0.00	0.00	0.00	0.00	0.03	0.00	0.00	0.00	-	0.00	0.00	0.00	0.01	0.03
CHI_Guangxi_mill	Average	4.02	0.00	0.00	-	-	0.04	-	0.00	2.91	0.00	0.00	0.00	0.00	-	0.02	1.98	4.02	2.96
	Std. Dev.	0.01	0.00	0.00	-	-	0.01	-	0.00	0.02	0.00	0.00	0.00	0.00	-	0.01	0.01	0.01	0.03

Sample Name		Si4+	Al3+	Ti4+	Zn2+	Cr3+	Fe2+	Ni2+	Mn2+	Mg2+	Ca2+	Na+	K+	P5+	S6+	F-	OH-	Tet	Oct
CHI_Giangxi_G1_89	Average	4.01	0.02	0.00	0.00	0.00	0.02	0.00	0.00	2.92	0.00	0.00	0.00	-	0.00	0.01	1.99	4.01	2.96
	Std. Dev.	0.01	0.01	0.00	0.00	0.00	0.00	0.00	0.00	0.03	0.00	0.00	0.00	-	0.00	0.00	0.00	0.01	0.02
CHI_Guangxi_G3_91-dark	Average	3.93	0.21	0.00	0.00	0.00	0.00	0.00	0.00	2.81	0.00	0.01	0.00	-	0.00	0.27	1.73	4.01	2.96
	Std. Dev.	0.07	0.13	0.00	0.00	0.00	0.00	0.00	0.00	0.11	0.00	0.00	0.00	-	0.00	0.02	0.02	0.02	0.05
CHI_Guangxi_G3_91-light	Average	4.01	0.01	0.00	0.00	0.00	0.00	0.00	0.00	2.96	0.00	0.00	0.00	-	0.00	0.27	1.73	4.01	2.97
	Std. Dev.	0.02	0.00	0.00	0.00	0.00	0.00	0.00	0.00	0.04	0.00	0.00	0.00	-	0.00	0.02	0.02	0.02	0.04
CHI_Guangxi_G3_92	Average	3.99	0.01	0.00	0.00	0.00	0.00	0.00	0.00	3.00	0.00	0.00	0.00	-	0.00	0.28	1.72	4.00	3.01
	Std. Dev.	0.01	0.00	0.00	0.00	0.00	0.00	0.00	0.00	0.02	0.00	0.00	0.00	-	0.00	0.00	0.00	0.01	0.02
CHI_Guangxi_Longsheng_G1_88	Average	4.00	0.00	0.00	0.00	0.00	0.03	0.00	0.00	2.97	0.00	0.00	0.00	-	0.00	0.01	1.99	4.00	3.01
	Std. Dev.	0.01	0.00	0.00	0.00	0.00	0.00	0.00	0.00	0.02	0.00	0.00	0.00	-	0.00	0.00	0.00	0.01	0.02
CHI_Haicmen_84	Average	3.98	0.01	0.00	0.00	0.00	0.01	0.00	0.00	3.01	0.00	0.00	0.00	-	0.00	0.02	1.98	3.99	3.02
	Std. Dev.	0.01	0.00	0.00	0.00	0.00	0.00	0.00	0.00	0.02	0.00	0.00	0.00	-	0.00	0.00	0.00	0.01	0.02
CHI_Liaoning_87	Average	4.01	0.00	0.00	0.00	0.00	0.01	0.00	0.00	2.96	0.00	0.00	0.00	-	0.00	0.05	1.95	4.01	2.98
	Std. Dev.	0.02	0.00	0.00	0.00	0.00	0.00	0.00	0.00	0.03	0.00	0.00	0.00	-	0.00	0.01	0.01	0.02	0.03
CHI_Liaoning_Haicheng_G3_93	Average	4.00	0.00	0.00	0.00	0.00	0.00	0.00	0.00	3.00	0.00	0.00	0.00	-	0.00	0.02	1.98	4.00	3.01
	Std. Dev.	0.01	0.00	0.00	0.00	0.00	0.00	0.00	0.00	0.02	0.00	0.00	0.00	-	0.00	0.00	0.00	0.01	0.02
CHI_Liaoning_Yingkow_83	Average	4.00	0.00	0.00	0.00	0.00	0.02	0.00	0.00	2.98	0.00	0.00	0.00	-	0.00	0.03	1.97	4.00	3.00
	Std. Dev.	0.02	0.00	0.00	0.00	0.00	0.00	0.00	0.00	0.05	0.00	0.00	0.00	-	0.00	0.00	0.00	0.02	0.05
CHI_Shadong_Qixia_85	Average	4.00	0.01	0.00	0.00	0.00	0.00	0.00	0.00	2.98	0.00	0.00	0.00	-	0.00	0.01	1.99	4.00	3.00
	Std. Dev.	0.03	0.00	0.00	0.00	0.00	0.00	0.00	0.00	0.05	0.00	0.00	0.00	-	0.00	0.00	0.00	0.03	0.05
FIN_NKarelia	Average	3.97	0.01	0.00	0.00	0.00	0.08	0.00	0.00	2.94	0.00	0.00	0.00	-	0.00	0.00	2.00	3.99	3.03
	Std. Dev.	0.03	0.01	0.00	0.00	0.00	0.01	0.00	0.00	0.05	0.00	0.00	0.00	-	0.00	0.00	0.00	0.02	0.05
IND_Chainpura_mill	Average	4.02	0.01	0.00	-	-	0.03	-	0.00	2.90	0.00	0.01	0.00	0.00	-	0.01	1.99	4.03	2.95
	Std. Dev.	0.02	0.00	0.00	-	-	0.01	-	0.00	0.04	0.00	0.01	0.00	0.00	-	0.01	0.01	0.02	0.03
IND_Ghevaria_mill	Average	4.01	0.00	0.00	-	-	0.03	-	0.00	2.94	0.00	0.00	0.00	0.00	-	0.04	1.96	4.01	2.98
	Std. Dev.	0.02	0.00	0.00	-	-	0.00	-	0.00	0.03	0.00	0.00	0.00	0.00	-	0.01	0.01	0.01	0.03

Sample Name		Si4+	Al3+	Ti4+	Zn2+	Cr3+	Fe2+	Ni2+	Mn2+	Mg2+	Ca2+	Na+	K+	P5+	S6+	F-	OH-	Tet	Oct
ITA_Gianna_A	Average	4.02	0.01	0.00	0.00	0.00	0.07	0.00	0.00	2.87	0.00	0.00	0.00	-	0.00	0.06	1.94	4.02	2.96
	Std. Dev.	0.01	0.00	0.00	0.00	0.00	0.01	0.00	0.00	0.03	0.00	0.00	0.00	-	0.00	0.00	0.00	0.01	0.03
ITA_Gianna_C	Average	4.02	0.01	0.00	0.00	0.00	0.04	0.00	0.00	2.91	0.00	0.00	0.00	-	0.00	0.05	1.95	4.02	2.96
	Std. Dev.	0.01	0.00	0.00	0.00	0.00	0.00	0.00	0.00	0.02	0.00	0.00	0.00	-	0.00	0.01	0.01	0.01	0.02
ITA_Paola_A	Average	4.01	0.01	0.00	0.00	0.00	0.04	0.00	0.00	2.91	0.00	0.00	0.00	-	0.00	0.05	1.95	4.01	2.97
	Std. Dev.	0.02	0.00	0.00	0.00	0.00	0.00	0.00	0.00	0.04	0.00	0.00	0.00	-	0.00	0.01	0.01	0.02	0.04
ITA_Paola_scop	Average	4.00	0.02	0.00	0.00	0.00	0.04	0.00	0.00	2.93	0.00	0.00	0.00	-	0.00	0.05	1.95	4.01	2.98
	Std. Dev.	0.03	0.01	0.00	0.00	0.00	0.00	0.00	0.00	0.06	0.00	0.00	0.00	-	0.00	0.00	0.00	0.02	0.05
ITA_Rodoretto_A1	Average	4.01	0.01	0.00	0.00	0.00	0.03	0.00	0.00	2.92	0.00	0.00	0.00	-	0.00	0.03	1.97	4.01	2.97
	Std. Dev.	0.01	0.01	0.00	0.00	0.00	0.01	0.00	0.00	0.04	0.00	0.00	0.00	-	0.00	0.02	0.02	0.01	0.03
ITA_Rodoretto_B1	Average	4.01	0.01	0.00	0.00	0.00	0.05	0.00	0.00	2.90	0.00	0.00	0.00	-	0.00	0.05	1.95	4.02	2.96
	Std. Dev.	0.05	0.00	0.00	0.00	0.00	0.01	0.00	0.00	0.09	0.00	0.00	0.00	-	0.00	0.01	0.01	0.04	0.09
KOR	Average	4.00	0.02	0.00	0.00	0.00	0.05	0.00	0.00	2.92	0.00	0.01	0.00	-	0.00	0.09	1.91	4.00	2.99
	Std. Dev.	0.01	0.00	0.00	0.00	0.00	0.00	0.00	0.00	0.03	0.00	0.00	0.00	-	0.00	0.00	0.00	0.01	0.02
MOR_109	Average	4.04	0.00	0.00	0.00	0.00	0.02	0.00	0.00	2.89	0.00	0.00	0.00	-	0.00	0.03	1.97	4.04	2.92
	Std. Dev.	0.02	0.00	0.00	0.00	0.00	0.01	0.00	0.00	0.04	0.00	0.00	0.00	-	0.00	0.01	0.01	0.02	0.04
NOR	Average	4.03	0.02	0.00	0.00	0.00	0.03	0.00	0.00	2.89	0.00	0.00	0.00	-	0.00	0.04	1.96	4.03	2.93
	Std. Dev.	0.03	0.00	0.00	0.00	0.00	0.00	0.00	0.00	0.05	0.00	0.00	0.00	-	0.00	0.00	0.00	0.02	0.05
SPA_110	Average	4.02	0.01	0.00	0.00	0.00	0.01	0.00	0.00	2.94	0.00	0.00	0.00	-	0.00	0.10	1.90	4.02	2.96
	Std. Dev.	0.02	0.00	0.00	0.00	0.00	0.00	0.00	0.00	0.04	0.00	0.00	0.00	-	0.00	0.02	0.02	0.02	0.04
SPA_111	Average	4.01	0.01	0.00	0.00	0.00	0.01	0.00	0.00	2.96	0.00	0.00	0.00	-	0.00	0.08	1.92	4.01	2.98
	Std. Dev.	0.02	0.00	0.00	0.00	0.00	0.00	0.00	0.00	0.05	0.00	0.00	0.00	-	0.00	0.01	0.01	0.02	0.05
USA_CA_Grantham	Average	4.00	0.05	0.00	0.00	0.00	0.01	0.00	0.00	2.91	0.00	0.01	0.00	-	0.00	0.09	1.91	4.01	2.98
	Std. Dev.	0.02	0.03	0.00	0.00	0.00	0.00	0.00	0.00	0.05	0.01	0.00	0.00	-	0.00	0.00	0.00	0.01	0.03
USA_CA_TalcCity_6_dark	Average	4.04	0.03	0.00	0.00	0.00	0.04	0.00	0.00	2.83	0.00	0.01	0.00	-	0.00	0.04	1.96	4.04	2.91
	Std. Dev.	0.04	0.01	0.00	0.00	0.00	0.01	0.00	0.00	0.07	0.00	0.01	0.00	-	0.00	0.01	0.01	0.04	0.07

Sample Name		Si4+	Al3+	Ti4+	Zn2+	Cr3+	Fe2+	Ni2+	Mn2+	Mg2+	Ca2+	Na+	K+	P5+	S6+	F-	OH-	Tet	Oct
USA_CA_TalcCity_6_light	Average	4.02	0.02	0.00	0.00	0.00	0.05	0.00	0.00	2.87	0.00	0.01	0.00	-	0.00	0.05	1.95	4.02	2.96
	Std. Dev.	0.02	0.01	0.00	0.00	0.00	0.01	0.00	0.00	0.04	0.00	0.01	0.00	-	0.00	0.01	0.01	0.02	0.04
USA_CA_WesternTalc_3A	Average	4.02	0.01	0.00	0.00	0.00	0.01	0.00	0.00	2.91	0.00	0.01	0.01	-	0.00	0.02	1.98	4.02	2.96
	Std. Dev.	0.01	0.01	0.00	0.00	0.00	0.00	0.00	0.00	0.03	0.00	0.01	0.01	-	0.00	0.01	0.01	0.01	0.03
USA_CA_WesternTalc_3C	Average	4.03	0.00	0.00	0.00	0.00	0.00	0.00	0.00	2.93	0.00	0.01	0.00	-	0.00	0.01	1.99	4.03	2.95
	Std. Dev.	0.01	0.00	0.00	0.00	0.00	0.00	0.00	0.00	0.02	0.00	0.00	0.00	-	0.00	0.00	0.00	0.01	0.02
USA_CA_Victorville	Average	4.01	0.02	0.00	0.00	0.00	0.00	0.00	0.00	2.92	0.00	0.00	0.03	-	0.00	0.02	1.98	4.02	2.97
	Std. Dev.	0.03	0.02	0.00	0.00	0.00	0.00	0.00	0.00	0.03	0.00	0.00	0.03	-	0.00	0.01	0.01	0.02	0.05
USA_GA_Earnest_fibrous	Average	3.99	0.01	0.00	0.00	0.00	0.32	0.00	0.00	2.57	0.10	0.00	0.00	-	0.00	0.03	1.97	4.00	3.01
	Std. Dev.	0.04	0.00	0.00	0.00	0.00	0.01	0.00	0.00	0.09	0.08	0.00	0.00	-	0.00	0.00	0.00	0.04	0.08
USA_MT_Beaverhead County	Average	4.00	0.01	0.00	0.00	0.00	0.12	0.00	0.00	2.84	0.01	0.00	0.00	-	0.00	0.01	1.99	4.01	2.98
	Std. Dev.	0.01	0.00	0.00	0.00	0.00	0.02	0.00	0.01	0.04	0.01	0.00	0.00	-	0.00	0.01	0.01	0.01	0.02
USA_MT_Beaverhead_hi Fe	Average	4.01	0.00	0.00	0.00	0.00	0.06	0.00	0.00	2.91	0.00	0.00	0.00	-	0.00	0.02	1.98	4.01	2.98
	Std. Dev.	0.02	0.00	0.00	0.00	0.00	0.00	0.00	0.00	0.03	0.00	0.00	0.00	-	0.00	0.00	0.00	0.02	0.04
USA_MT_Beaverhead_low Fe	Average	4.02	0.01	0.00	0.00	0.00	0.01	0.00	0.00	2.93	0.00	0.00	0.00	-	0.00	0.02	1.98	4.02	2.96
	Std. Dev.	0.02	0.01	0.00	0.00	0.00	0.00	0.00	0.00	0.03	0.00	0.00	0.00	-	0.00	0.00	0.00	0.02	0.04
USA_MT_Regal_HG	Average	4.01	0.02	0.00	0.00	0.00	0.03	0.00	0.00	2.93	0.00	0.01	0.00	-	0.00	0.02	1.98	4.01	2.98
	Std. Dev.	0.02	0.00	0.00	0.00	0.00	0.01	0.00	0.00	0.03	0.00	0.00	0.00	-	0.00	0.00	0.00	0.01	0.03
USA_MT_Treasure_float	Average	3.96	0.01	0.00	-	-	0.14	-	0.00	2.90	0.00	0.00	0.00	0.00	-	0.04	1.96	3.98	3.05
	Std. Dev.	0.01	0.00	0.00	-	-	0.03	-	0.00	0.01	0.00	0.00	0.00	0.00	-	0.01	0.01	0.01	0.02
USA_MT_Treasure_G1_hi Fe	Average	4.02	0.00	0.00	0.00	0.00	0.12	0.00	0.00	2.83	0.00	0.00	0.00	-	0.00	0.06	1.94	4.02	2.96
	Std. Dev.	0.01	0.00	0.00	0.00	0.00	0.01	0.00	0.00	0.01	0.00	0.00	0.00	-	0.00	0.01	0.01	0.01	0.02
USA_MT_Treasure_G1_lo Fe	Average	4.01	0.01	0.00	0.00	0.00	0.01	0.00	0.00	2.95	0.00	0.00	0.00	-	0.00	0.02	1.98	4.01	2.98
	Std. Dev.	0.01	0.00	0.00	0.00	0.00	0.00	0.00	0.00	0.03	0.00	0.00	0.00	-	0.00	0.00	0.00	0.01	0.03
USA_MT_Treasure_G3	Average	4.02	0.01	0.00	0.00	0.00	0.12	0.00	0.00	2.82	0.00	0.01	0.00	-	0.00	0.04	1.96	4.02	2.96
	Std. Dev.	0.01	0.00	0.00	0.00	0.00	0.01	0.00	0.00	0.03	0.00	0.00	0.00	-	0.00	0.00	0.00	0.01	0.03

Sample Name		Si4+	Al3+	Ti4+	Zn2+	Cr3+	Fe2+	Ni2+	Mn2+	Mg2+	Ca2+	Na+	K+	P5+	S6+	F-	OH-	Tet	Oct
USA_MT_Treasure_pseudo.	Average	4.01	0.01	0.00	0.00	0.00	0.10	0.00	0.00	2.85	0.00	0.01	0.00	-	0.00	0.03	1.97	4.01	2.98
	Std. Dev.	0.01	0.00	0.00	0.00	0.00	0.01	0.00	0.00	0.02	0.00	0.00	0.00	-	0.00	0.00	0.00	0.01	0.02
USA_MT_Willow Creek_1a	Average	3.98	0.00	0.00	-	-	0.09	-	0.00	2.94	0.00	0.00	0.00	0.00	-	0.04	1.96	3.99	3.03
	Std. Dev.	0.00	0.00	0.00	-	-	0.03	-	0.00	0.03	0.00	0.00	0.00	0.00	-	0.01	0.01	0.01	0.01
USA_MT_Willow Creek_8	Average	3.98	0.00	0.00	-	-	0.10	-	0.00	2.93	0.00	0.00	0.00	0.00	-	0.03	1.97	3.99	3.03
	Std. Dev.	0.01	0.01	0.00	-	-	0.03	-	0.00	0.02	0.00	0.00	0.00	0.00	-	0.00	0.00	0.01	0.02
USA_MT_WillowCreek_SF_N9A	Average	4.03	0.01	0.00	0.00	0.00	0.14	0.00	0.00	2.77	0.02	0.01	0.00	-	0.00	0.01	1.99	4.03	2.95
	Std. Dev.	0.04	0.00	0.00	0.00	0.00	0.01	0.00	0.00	0.07	0.01	0.00	0.00	-	0.00	0.00	0.00	0.04	0.07
USA_MT_WillowCreek_SF14	Average	4.01	0.01	0.00	0.00	0.00	0.10	0.00	0.00	2.88	0.00	0.00	0.00	-	0.00	0.02	1.98	4.01	2.98
	Std. Dev.	0.02	0.01	0.00	0.00	0.00	0.04	0.00	0.00	0.04	0.00	0.00	0.00	-	0.00	0.00	0.00	0.02	0.04
USA_MT_Yellowstone_HG	Average	3.98	0.01	0.00	-	-	0.06	-	0.00	2.96	0.00	0.00	0.00	0.00	-	0.06	1.94	3.99	3.02
	Std. Dev.	0.01	0.00	0.00	-	-	0.00	-	0.00	0.01	0.00	0.00	0.00	0.00	-	0.00	0.00	0.00	0.01
USA_MT_Yellowstone_LG	Average	3.99	0.00	0.00	-	-	0.07	-	0.00	2.95	0.00	0.00	0.00	0.00	-	0.06	1.94	3.99	3.02
	Std. Dev.	0.00	0.00	0.00	-	-	0.00	-	0.00	0.01	0.00	0.00	0.00	0.00	-	0.00	0.00	0.01	0.01
USA_NC_HC_CT_light	Average	3.99	0.01	0.00	-	-	0.06	-	0.00	2.93	0.00	0.01	0.00	0.00	-	0.03	1.97	4.00	3.00
	Std. Dev.	0.01	0.00	0.00	-	-	0.05	-	0.00	0.05	0.00	0.00	0.00	0.00	-	0.01	0.01	0.00	0.01
USA_NC_HC_dark rock	Average	3.97	0.02	0.00	-	-	0.06	-	0.00	2.96	0.00	0.00	0.00	0.00	-	0.07	1.93	3.99	3.02
	Std. Dev.	0.01	0.02	0.00	-	-	0.01	-	0.00	0.02	0.00	0.00	0.00	0.00	-	0.00	0.00	0.01	0.01
USA_NC_HC_light rock	Average	3.97	0.03	0.00	-	-	0.06	-	0.00	2.95	0.00	0.00	0.00	0.00	-	0.08	1.92	4.00	3.02
	Std. Dev.	0.01	0.00	0.00	-	-	0.00	-	0.00	0.01	0.00	0.00	0.00	0.00	-	0.00	0.00	0.00	0.01
USA_NC_crayon	Average	3.99	0.01	0.00	-	-	0.02	-	0.00	2.98	0.00	0.00	0.00	0.00	-	0.05	1.95	4.00	3.01
	Std. Dev.	0.01	0.01	0.00	-	-	0.00	-	0.00	0.01	0.00	0.00	0.00	0.00	-	0.00	0.00	0.00	0.01
USA_NC_CCLA	Average	4.01	0.01	0.00	-	-	0.03	-	0.00	2.93	0.00	0.00	0.00	0.00	-	0.06	1.94	4.01	2.98
	Std. Dev.	0.02	0.00	0.00	-	-	0.00	-	0.00	0.04	0.00	0.00	0.00	0.00	-	0.00	0.00	0.02	0.04
USA_NC_Dcrayon	Average	3.99	0.02	0.00	-	-	0.04	-	0.00	2.95	0.00	0.00	0.00	0.00	-	0.07	1.93	4.00	3.00
	Std. Dev.	0.01	0.01	0.00	-	-	0.00	-	0.00	0.02	0.00	0.00	0.00	0.00	-	0.00	0.00	0.00	0.01

Sample Name		Si4+	Al3+	Ti4+	Zn2+	Cr3+	Fe2+	Ni2+	Mn2+	Mg2+	Ca2+	Na+	K+	P5+	S6+	F-	OH-	Tet	Oct
USA_NC_Foote	Average	3.99	0.01	0.00	-	-	0.05	-	0.00	2.96	0.00	0.00	0.00	0.00	-	0.10	1.90	3.99	3.01
	Std. Dev.	0.01	0.01	0.00	-	-	0.00	-	0.00	0.03	0.00	0.00	0.00	0.00	-	0.01	0.01	0.01	0.02
USA_NC_Murphy_124	Average	4.02	0.01	0.00	0.00	0.00	0.05	0.00	0.00	2.89	0.00	0.00	0.00	-	0.00	0.07	1.93	4.02	2.95
	Std. Dev.	0.02	0.00	0.00	0.00	0.00	0.01	0.00	0.00	0.04	0.00	0.00	0.00	-	0.00	0.00	0.00	0.02	0.03
USA_NC_Murphy_129	Average	4.02	0.02	0.00	0.00	0.00	0.05	0.00	0.00	2.87	0.00	0.00	0.00	-	0.00	0.08	1.92	4.02	2.94
	Std. Dev.	0.02	0.00	0.00	0.00	0.00	0.00	0.00	0.00	0.04	0.00	0.00	0.00	-	0.00	0.01	0.01	0.02	0.04
USA_NC_Murphy_132	Average	4.03	0.01	0.00	0.00	0.00	0.01	0.00	0.00	2.92	0.00	0.01	0.00	-	0.00	0.04	1.96	4.03	2.94
	Std. Dev.	0.01	0.00	0.00	0.00	0.00	0.00	0.00	0.00	0.02	0.00	0.00	0.00	-	0.00	0.00	0.00	0.01	0.02
USA_TX_VanHorn_black	Average	4.01	0.02	0.00	0.00	0.00	0.00	0.00	0.00	2.93	0.00	0.01	0.01	-	0.00	0.07	1.93	4.02	2.97
	Std. Dev.	0.02	0.00	0.00	0.00	0.00	0.00	0.00	0.00	0.05	0.00	0.00	0.00	-	0.00	0.00	0.00	0.02	0.05
USA_TX_VanHorn_gray	Average	4.01	0.01	0.00	0.00	0.00	0.00	0.00	0.00	2.95	0.01	0.01	0.00	-	0.00	0.07	1.93	4.01	2.97
	Std. Dev.	0.02	0.00	0.00	0.00	0.00	0.00	0.00	0.00	0.03	0.00	0.01	0.00	-	0.00	0.02	0.02	0.02	0.03
USA_TX_VanHorn_pink	Average	4.00	0.00	0.00	0.00	0.00	0.00	0.00	0.00	2.99	0.00	0.01	0.00	-	0.00	0.04	1.96	4.00	3.00
	Std. Dev.	0.03	0.00	0.00	0.00	0.00	0.00	0.00	0.00	0.07	0.00	0.01	0.00	-	0.00	0.02	0.02	0.03	0.06
														-					
USA_TX_Llano	Average	3.96	0.03	0.00	0.00	0.00	0.14	0.01	0.00	2.89	0.00	0.01	0.00	-	0.00	0.00	2.00	3.98	3.05
	Std. Dev.	0.03	0.01	0.00	0.00	0.00	0.01	0.00	0.00	0.04	0.00	0.00	0.00	-	0.00	0.00	0.00	0.02	0.04
USA_VT_Argonaut_BB_T1	Average	3.99	0.00	0.00	-	-	0.15	-	0.00	2.85	0.00	0.00	0.00	0.00	-	0.01	1.99	3.99	3.01
	Std. Dev.	0.01	0.00	0.00	-	-	0.01	-	0.00	0.03	0.00	0.00	0.00	0.00	-	0.01	0.01	0.01	0.02
USA_VT_Argonaut_flake	Average	3.99	0.00	0.00	-	-	0.10	-	0.00	2.92	0.00	0.00	0.00	0.00	-	0.01	1.99	3.99	3.02
	Std. Dev.	0.01	0.00	0.00	-	-	0.00	-	0.00	0.01	0.00	0.00	0.00	0.00	-	0.00	0.00	0.00	0.01
USA_VT_Argonaut_HG	Average	3.99	0.00	0.00	-	-	0.13	-	0.00	2.88	0.00	0.00	0.00	0.00	-	0.01	1.99	3.99	3.02
	Std. Dev.	0.01	0.00	0.00	-	-	0.00	-	0.00	0.01	0.00	0.00	0.00	0.00	-	0.00	0.00	0.01	0.01
USA_VT_Argonaut_LG	Average	4.01	0.00	0.00	-	-	0.15	-	0.00	2.84	0.00	0.00	0.00	-	-	0.01	1.99	4.01	2.99
	Std. Dev.	0.01	0.00	0.00	-	-	0.00	-	0.00	0.01	0.00	0.00	0.00	-	-	0.00	0.00	0.01	0.01
USA_VT_Argonaut_SGR	Average	4.00	0.01	0.00	-	-	0.24	-	0.00	2.74	0.00	0.00	0.00	-	-	0.02	1.98	4.00	2.99
	Std. Dev.	0.01	0.00	0.00	-	-	0.01	-	0.00	0.02	0.00	0.00	0.00	-	-	0.00	0.00	0.01	0.02

Sample Name		Si4+	Al3+	Ti4+	Zn2+	Cr3+	Fe2+	Ni2+	Mn2+	Mg2+	Ca2+	Na+	K+	P5+	S6+	F-	OH-	Tet	Oct
USA_VT_Argonaut_underflow	Average	4.01	0.00	0.00	-	-	0.16	-	0.00	2.81	0.00	0.00	0.00	-	-	0.01	1.99	4.01	2.97
	Std. Dev.	0.01	0.00	0.00	-	-	0.02	-	0.00	0.02	0.00	0.00	0.00	-	-	0.00	0.00	0.01	0.02
USA_VT_Argonaut-W71	Average	4.01	0.00	0.00	-	-	0.15	-	0.00	2.83	0.00	0.00	0.00	-	-	0.02	1.98	4.01	2.98
	Std. Dev.	0.01	0.01	0.00	-	-	0.02	-	0.00	0.02	0.00	0.00	0.00	-	-	0.01	0.01	0.01	0.02
UA_VT_Argonaut_W83	Average	3.99	0.00	0.00	-	-	0.12	-	0.00	2.89	0.00	0.00	0.00	0.00	-	0.01	1.99	3.99	3.02
	Std. Dev.	0.01	0.00	0.00	-	-	0.01	-	0.00	0.03	0.00	0.00	0.00	0.00	-	0.00	0.00	0.01	0.02
USA_VT_Johnson_black	Average	3.99	0.00	0.00	-	-	0.18	-	0.00	2.84	0.00	0.00	0.00	-	-	0.02	1.98	3.99	3.02
	Std. Dev.	0.01	0.00	0.00	-	-	0.00	-	0.00	0.01	0.00	0.00	0.00	-	-	0.00	0.00	0.01	0.01
USA_VT_CT_Johnson_E42	Average	4.02	0.00	0.00	-	-	0.13	-	0.00	2.82	0.00	0.00	0.00	-	-	0.02	1.98	4.02	2.97
	Std. Dev.	0.02	0.00	0.00	-	-	0.00	-	0.00	0.04	0.00	0.00	0.00	-	-	0.00	0.00	0.02	0.04
USA_VT_CT_Johnson_E42	Average	4.01	0.00	0.00	-	-	0.15	-	0.00	2.81	0.00	0.00	0.00	-	-	0.03	1.97	4.01	2.97
	Std. Dev.	0.01	0.00	0.00	-	-	0.03	-	0.00	0.02	0.00	0.00	0.00	-	-	0.01	0.01	0.01	0.02
USA_VT_Johnson_green	Average	3.98	0.00	0.00	-	-	0.19	-	0.00	2.85	0.00	0.00	0.00	-	-	0.02	1.98	3.98	3.04
	Std. Dev.	0.01	0.00	0.00	-	-	0.02	-	0.00	0.02	0.00	0.00	0.00	-	-	0.00	0.00	0.01	0.01
USA_VT_Johnson-LesW	Average	3.99	0.00	0.00	-	-	0.13	-	0.00	2.88	0.00	0.00	0.00	-	-	0.01	1.99	3.99	3.02
	Std. Dev.	0.00	0.00	0.00	-	-	0.00	-	0.00	0.01	0.00	0.00	0.00	-	-	0.00	0.00	0.00	0.00
USA_VT_Johnson_CT_J50	Average	3.99	0.00	0.00	-	-	0.13	-	0.00	2.88	0.00	0.00	0.00	-	-	0.02	1.98	3.99	3.02
	Std. Dev.	0.01	0.00	0.00	-	-	0.01	-	0.00	0.01	0.00	0.00	0.00	-	-	0.00	0.00	0.01	0.02
USA_VT_Johnson_UVM	Average	3.98	0.00	0.00	-	-	0.21	-	0.00	2.82	0.00	0.01	0.00	-	-	0.02	1.98	3.99	3.03
	Std. Dev.	0.00	0.00	0.00	-	-	0.01	-	0.00	0.01	0.00	0.00	0.00	-	-	0.00	0.00	0.00	0.01
USA_VT_Johnson_CT_E500	Average	4.01	0.00	0.00	-	-	0.13	-	0.00	2.84	0.00	0.01	0.00	-	-	0.02	1.98	4.01	2.99
	Std. Dev.	0.01	0.00	0.00	-	-	0.01	-	0.00	0.02	0.00	0.00	0.00	-	-	0.01	0.01	0.01	0.02
USA_VT_Johnson_mill pipe	Average	4.00	0.00	0.00	-	-	0.16	-	0.00	2.83	0.00	0.00	0.00	-	-	0.02	1.98	4.00	2.99
	Std. Dev.	0.01	0.00	0.00	-	-	0.00	-	0.00	0.02	0.00	0.00	0.00	-	-	0.00	0.00	0.01	0.01
USA_VT_Johnson_mill rafters	Average	4.02	0.00	0.00	-	-	0.14	-	0.00	2.81	0.00	0.01	0.00	-	-	0.01	1.99	4.02	2.96
	Std. Dev.	0.01	0.01	0.00	-	-	0.04	-	0.00	0.05	0.00	0.00	0.00	-	-	0.01	0.01	0.01	0.02

Sample Name		Si4+	Al3+	Ti4+	Zn2+	Cr3+	Fe2+	Ni2+	Mn2+	Mg2+	Ca2+	Na+	K+	P5+	S6+	F-	OH-	Tet	Oct
USA_VT_Johnson_W23_USGS	Average	4.00	0.00	0.00	-	-	0.24	-	0.00	2.76	0.00	0.00	0.00	-	-	0.02	1.98	4.00	3.01
	Std. Dev.	0.01	0.00	0.00	-	-	0.01	-	0.00	0.02	0.00	0.00	0.00	-	-	0.00	0.00	0.01	0.01
USA_VT_CT_Engelhard	Average	4.02	0.02	0.00	-	-	0.14	-	0.00	2.79	0.01	0.01	0.00	0.00	-	0.00	2.00	4.02	2.96
	Std. Dev.	0.03	0.04	0.00	-	-	0.02	-	0.00	0.08	0.01	0.01	0.00	0.00	-	0.00	0.00	0.02	0.05
USA_WA_Totem Talc	Average	4.04	0.00	0.00	0.00	0.00	0.03	0.00	0.00	2.89	0.00	0.00	0.00	-	0.00	0.01	1.99	4.04	2.92
	Std. Dev.	0.03	0.00	0.00	0.00	0.00	0.00	0.00	0.00	0.05	0.00	0.00	0.00	-	0.00	0.00	0.00	0.03	0.05
USA_WA_Totem Gulch	Average	4.02	0.00	0.00	0.00	0.00	0.02	0.00	0.00	2.92	0.00	0.00	0.00	-	0.00	0.01	1.99	4.03	2.95
	Std. Dev.	0.05	0.00	0.00	0.00	0.00	0.00	0.00	0.00	0.09	0.00	0.00	0.00	-	0.00	0.00	0.00	0.04	0.09
CT_Johnson's bp	Average	4.01	0.01	0.00	-	-	0.04	-	0.00	2.92	0.00	0.00	0.00	0.00	-	0.03	1.97	4.01	2.97
	Std. Dev.	0.02	0.01	0.00	-	-	0.01	-	0.00	0.04	0.00	0.00	0.00	0.00	-	0.01	0.01	0.02	0.04
CT_CSI_fingerprint	Average	4.00	0.01	0.00	-	-	0.04	-	0.00	2.91	0.01	0.02	0.00	0.00	-	0.02	1.98	4.01	3.00
	Std. Dev.	0.01	0.01	0.00	-	-	0.01	-	0.00	0.02	0.00	0.01	0.00	0.00	-	0.00	0.00	0.01	0.01
CT_marker_Moscow	Average	4.02	0.00	0.00	0.00	0.00	0.03	0.00	0.00	2.92	0.00	0.00	0.00	-	0.00	0.01	1.99	4.02	2.96
	Std. Dev.	0.01	0.00	0.00	0.00	0.00	0.00	0.00	0.00	0.03	0.00	0.00	0.00	-	0.00	0.00	0.00	0.01	0.03
CT_Protech	Average	4.02	0.02	0.00	0.00	0.00	0.01	0.00	0.00	2.85	0.05	0.01	0.01	-	0.00	0.10	1.90	4.03	2.94
	Std. Dev.	0.04	0.01	0.00	0.00	0.00	0.00	0.00	0.00	0.09	0.08	0.01	0.01	-	0.00	0.05	0.05	0.04	0.08
CT_WhiteSnow	Average	4.02	0.02	0.00	0.00	0.00	0.08	0.00	0.00	2.84	0.00	0.00	0.00	-	0.00	0.06	1.94	4.02	2.94
	Std. Dev.	0.03	0.01	0.00	0.00	0.00	0.01	0.00	0.00	0.06	0.00	0.00	0.00	-	0.00	0.01	0.01	0.03	0.06

Appendix D: Accessory Mineral Electron Microprobe Analysis Data

Weight percent oxides are listed in Part 1 and calculated APFU values are listed in Part 2.

(-) indicates that the element was not analyzed for in this sample, (bdl) indicates the values were below the detection limit

Part 1.

Sample #	Mineral	SiO2/MgO		SiO2	Al2O3	TiO2	ZnO	Cr2O3	FeO	NiO	MnO	MgO	CaO	Na2O	K2O	P2O5	SO3	Oxide Sum	F wt%	Cl wt%
	AMPHIBOLE																			
USA_CA_WesternTalc_C	Richterite	2.44		57.16	0.18	0.02	0.00	0.01	0.94	0.00	0.05	23.46	5.66	5.82	1.06	-	0.07	94.43	0.43	0.02
USA_GA_Earnest_fibrous	Actinolite	3.00	Average	56.33	0.27	0.02	0.01	0.00	8.23	0.04	0.29	18.81	13.14	0.06	0.05	-	0.00	97.27	0.09	0.00
			Std. Dev.	0.43	0.11	0.01	0.01	0.00	0.42	0.02	0.03	0.38	0.06	0.02	0.01	-	0.01	0.37	0.02	0.00
USA_GA_Earnest_platy	Actinolite	2.84	Average	57.24	0.34	0.02	0.01	0.04	6.25	0.10	0.22	20.13	12.61	0.06	0.07	-	0.01	97.10	0.13	0.00
			Std. Dev.	0.35	0.02	0.00	0.01	0.01	0.16	0.01	0.01	0.33	0.26	0.00	0.02	-	0.00	0.52	0.02	0.00
USA_NC_Murphy_129	Tremolite	2.54	Average	57.81	1.54	0.03	0.00	0.00	1.10	0.00	0.00	22.78	13.81	0.14	0.02	-	0.00	97.24	0.24	0.00
			Std. Dev.	0.79	0.23	0.01	0.01	0.01	0.04	0.00	0.00	0.44	0.05	0.03	0.01	-	0.00	0.51	0.03	0.00
USA_MT_WC_SF_N9A	Tremolite	2.57	Average	57.51	0.40	0.02	0.00	0.00	2.31	0.00	0.83	22.40	13.37	0.11	0.01	-	0.00	96.97	0.11	0.01
			Std. Dev	0.28	0.03	0.00	0.01	0.01	0.10	0.01	0.06	0.07	0.07	0.02	0.01	-	0.00	0.26	0.03	0.00
Sample #	Mineral	SiO2/MgO		SiO2	Al2O3	TiO2	ZnO	Cr2O3	FeO	NiO	MnO	MgO	CaO	Na2O	K2O	P2O5	SO3	Oxide Sum	F wt%	Cl wt%
	MICA																			
CHI-94	Phlogopite	1.57	Average	45.89	9.26	0.02	0.00	0.00	0.28	0.00	0.00	29.28	0.04	0.06	7.56	-	0.00	92.40	0.56	0.09
			Std Dev	0.73	0.29	0.00	0.00	0.00	0.15	0.01	0.01	0.44	0.03	0.02	0.07	-	0.00	1.51	0.07	0.02
ITA_Paola_scop	Muscovite	10.52	Average	49.88	26.14	0.19	0.01	0.01	0.24	0.01	0.00	4.74	0.01	0.25	10.80	-	0.01	92.29	0.13	0.03
			Std. Dev.	0.98	0.60	0.04	0.00	0.01	0.01	0.01	0.00	0.10	0.00	0.03	0.17	-	0.01	1.62	0.02	0.02
ITA_Rodoretto_A1	Muscovite	17.35	Average	48.01	31.36	0.20	0.00	0.00	0.41	0.00	0.01	2.78	0.01	0.46	10.55	-	0.01	93.80	0.08	0.03
			Std. Dev.	0.73	0.32	0.04	0.00	0.01	0.02	0.00	0.00	0.25	0.00	0.11	0.16	-	0.01	0.56	0.02	0.00
USA_CA_Victorville	Phlogopite	1.81	Average	48.40	8.14	0.07	0.00	0.00	0.02	0.00	0.00	26.78	0.07	0.05	9.41	-	0.01	92.95	0.84	0.00
			Std. Dev.	0.63	0.24	0.01	0.01	0.00	0.01	0.00	0.01	0.29	0.01	0.01	0.40	-	0.00	0.44	0.06	0.00
ITA_Gianna_in place contact	Muscovite	14.78	Average	49.70	28.50	0.12	0.00	0.00	0.52	0.00	0.00	3.51	0.00	0.47	10.66	-	0.00	93.48	0.14	0.01
			Std. Dev	1.34	2.27	0.02	0.01	0.00	0.16	0.00	0.01	0.78	0.01	0.15	0.21	-	0.00	0.80	0.04	0.01
USA_CA_Western Talc_3A	Phlogopite	1.78	Average	46.76	9.08	0.13	0.00	0.00	0.63	0.00	0.00	26.31	0.05	0.09	9.91	-	0.01	92.98	0.97	0.02
			Std. Dev	0.99	0.39	0.08	0.01	0.00	0.26	0.00	0.00	0.57	0.03	0.05	0.33	-	0.01	1.26	0.07	0.03

Sample #	Mineral			SiO2	Al2O3	TiO2	ZnO	Cr2O3	FeO	NiO	MnO	MgO	CaO	Na2O	K2O	P2O5	SO3	Oxide Sum	F wt%	Cl wt%
USA_CA_Western Talc_3C	Phlogopite	1.74	Average	48.22	7.71	0.08	0.00	0.00	0.27	0.00	0.01	27.71	0.10	0.18	8.31	-	0.02	92.60	0.48	0.02
			Std. Dev	1.65	1.16	0.03	0.01	0.00	0.09	0.01	0.01	0.40	0.15	0.14	1.15	-	0.00	0.94	0.06	0.02
USA_MT_WC_SF_24_rx	Phlogopite	1.56	Average	40.36	14.44	0.64	0.00	0.01	1.92	0.00	0.12	25.90	0.38	0.99	8.24	-	0.00	92.99	1.53	0.02
			Std. Dev.	0.29	0.70	0.09	0.01	0.00	0.29	0.00	0.01	0.11	0.22	0.15	0.50	-	0.00	0.74	0.30	0.00
	CARBONATE			SiO2	Al2O3	TiO2	ZnO	Cr2O3	FeO	NiO	MnO	MgO	CaO	Na2O	K2O	P2O5	SO3	Oxide Sum	F wt%	Cl wt%
AUS_ThSprings	Magnesite		Average	1.21	0.20	0.01	0.00	0.00	0.08	0.00	0.00	1.11	53.75	0.00	0.00	-	0.00	56.36	3.16	0.01
			Std. Dev	1.28	0.29	0.02	0.00	0.01	0.07	0.01	0.00	1.23	0.17	0.02	0.00	-	0.00	2.68	0.37	0.01
AUSTRIA_Styria_Lassing	Dolomite		Average	1.63	0.02	0.00	0.00	0.00	1.63	0.00	0.11	19.69	31.47	0.01	0.01	-	0.01	54.56	-0.02	0.05
			Std. Dev	1.56	0.01	0.01	0.00	0.00	0.43	0.01	0.03	1.10	1.25	0.01	0.01	-	0.01	1.75	0.05	0.03
CAN_Ontario_Madoc_170	Dolomite			0.03	0.00	0.01	0.00	0.00	0.12	0.00	0.07	20.69	31.31	0.00	0.00		-0.01	52.24	-0.05	0.00
CAN_Ontario_Madoc_170	Calcite			0.00	-0.01	0.00	-0.02	0.00	0.00	0.01	0.12	0.23	55.58	0.01	0.00		0.01	55.95	0.03	-0.02
CHI_Guangxi_G3_91	Calcite			0.00	0.00	-0.01	0.00	0.00	0.03	0.02	0.00	27.67	0.03	0.09	0.01	-	0.07	27.91	0.60	0.06
CHI_Cuangai_86	Calcite		Average	0.29	0.00	-0.01	0.00	-0.01	0.02	0.01	0.00	0.23	54.36	-0.01	0.00	-	0.01	54.90	2.18	0.05
			Std. Dev	0.10	0.00	0.00	0.01	0.00	0.02	0.00	0.01	0.07	0.17	0.02	0.00	-	0.02	0.04	0.28	0.00
CHI_Liaoning_90	Magnesite		Average	0.06	0.02	0.00	0.00	0.00	0.21	0.00	0.01	38.88	0.03	0.00	0.00	-	0.00	39.21	-0.01	0.00
			Std. Dev	0.02	0.01	0.00	0.00	0.00	0.02	0.00	0.01	0.32	0.00	0.00	0.00	-	0.00	0.29	0.01	0.00
FIN_Nkarelia	Magnesite		Average	0.06	0.00	-0.01	0.00	0.00	6.09	0.02	0.11	38.53	0.12	0.00	0.00	-	0.00	44.92	0.00	0.00
			Std. Dev	0.01	0.01	0.00	0.01	0.01	1.91	0.01	0.07	0.56	0.03	0.00	0.00	-	0.01	1.51	0.01	0.00
IND_Ghevaria_mill	Dolomite		Average	-0.21	-0.04	-0.01	-	-	0.27	-	0.02	23.19	32.91	0.00	0.00	0.01	-	56.13	0.04	0.01
			Std. Dev	0.05	0.00	0.01	-	-	0.17	-	0.00	0.09	3.24	0.00	0.00	0.01	-	2.94	0.00	0.01
ITA_Paola_A	Calcite			0.04	0.00	-0.01	0.01	-0.01	0.05	-0.01	0.00	0.05	54.58	0.00	0.00	-	0.10	54.81	3.95	0.01
ITA_Rodoretto_A1	Dolomite		Avg.	0.06	0.00	0.00	0.00	0.00	1.96	0.00	0.24	19.86	31.19	-0.01	0.00	-	0.01	53.31	0.02	0.01
			Std. Dev.	0.02	0.01	0.00	0.00	0.01	0.53	0.01	0.05	0.59	0.05	0.01	0.01	-	0.00	0.01	0.02	0.00
ITA_Rodoretto_B1	Dolomite			0.05	-0.01	0.00	0.00	0.02	1.23	0.00	0.11	21.39	31.64	0.00	0.00	-	0.03	54.47	-0.01	0.02

	CARBONATE			SiO2	Al2O3	TiO2	ZnO	Cr2O3	FeO	NiO	MnO	MgO	CaO	Na2O	K2O	P2O5	SO3	Oxide Sum	F wt%	Cl wt%
ITA_Rodoretto_B1	Calcite			0.09	0.00	-0.01	0.00	0.00	0.03	-0.01	0.00	0.07	51.16	0.02	-0.01	-	0.02	51.37	3.01	0.06
MOR_109	Calcite		Avg.	0.38	0.00	-0.01	-0.01	0.00	0.02	0.01	0.06	0.58	57.10	0.01	0.00	-	0.16	58.30	0.90	0.00
			Std. Dev.	0.31	0.00	0.01	0.01	0.00	0.02	0.01	0.07	0.61	3.14	0.01	0.00	-	0.25	4.27	1.54	0.02
USA_CA_Grantham	Calcite		Avg	0.11	-0.01	-0.21	-0.01	-0.04	0.02	0.03	0.12	0.90	54.81	0.00	-0.01	-	-0.09	55.61	0.06	-0.08
			Std. Dev.	0.09	0.01	0.48	0.01	0.08	0.01	0.04	0.06	0.27	1.29	0.02	0.01	-	0.23	1.17	0.05	0.18
USA_MT_Beaverhead	Calcite			0.19	-0.01	0.00	0.01	0.00	0.03	-0.01	-0.01	0.29	53.94	0.00	-0.01	-	0.00	54.43	3.10	0.15
USA_NC_Murphy_129	Calcite			0.21	0.01	-0.01	0.00	0.00	0.04	0.01	0.00	0.20	54.38	-0.01	-0.01	-	0.00	54.83	2.83	0.06
USA_TX_VanHorn_black	Dolomite			9.18	0.04	0.00	0.01	0.00	0.10	0.00	0.01	18.82	27.56	0.01	0.01	-	0.02	55.75	0.07	0.01
USA_VT_CT_Johnson_E42	Magnesite			0.37	-0.03	0.01	-	-	10.18	-	0.04	39.61	0.14	0.00	0.01	-	-	50.33	-0.06	0.01
USA_VT_CT_Johnson_E42	Magnesite			0.12	-0.03	-0.01	-	-	3.88	-	0.01	41.25	0.25	0.01	0.02	-	-	45.49	-0.03	0.02
USA_VT_Johnson_rafters	Magnesite			0.57	-0.04	0.00	-	-	4.34	-	0.06	41.76	0.02	0.01	0.00	-	-	46.71	0.00	0.01
							-	-		-						-	-			
USA_VT_Johnson_pipe	Magnesite		Average	0.99	0.08	0.00	-	-	9.57	-	0.13	39.03	0.60	0.01	0.00	-	-	50.40	-0.03	0.01
			Std. Dev	0.95	0.07	0.00	-	-	2.84	-	0.09	2.00	0.72	0.00	0.01	-	-	2.10	0.03	0.00
USA_VT_Argonaut_HG	Magnesite		Average	0.14	-0.03	0.00	-	-	8.84	-	0.13	40.03	0.32	0.00	0.01	0.00	-	49.43	-0.03	0.00
			Std. Dev	0.03	0.01	0.00	-	-	1.16	-	0.02	0.60	0.16	0.00	0.00	0.00	-	0.49	0.01	0.00
CT_BP_Johnson	Dolomite			0.62	0.06	0.00			0.26		0.02	17.45	30.86	0.02	0.03	0.22		49.55	0.07	0.06
CT_FP_CSI	Calcite		Average	-0.18	-0.03	0.00	-	-	0.44	-	0.14	10.86	44.45	0.01	0.00	0.02	-	55.70	-0.07	0.03
			Std. Dev	0.14	0.01	0.01	-	-	0.56	-	0.04	14.76	15.64	0.01	0.00	0.01	-	0.13	0.02	0.02
Sample #		SiO2/MgO		SiO2	Al2O3	TiO2	ZnO	Cr2O3	FeO	NiO	MnO	MgO	CaO	Na2O	K2O	P2O5	SO3	Oxide Sum	F wt%	Cl wt%
	CLINOCHLORE																			
AUS_Mt.Seabrook		0.96	Average	31.54	17.64	0.00	0.01	0.01	1.58	0.00	0.01	32.88	0.03	0.03	0.03	-	0.02	83.79	0.12	0.03
			St. Dev.	0.61	0.76	0.00	0.01	0.01	0.24	0.01	0.00	0.83	0.01	0.02	0.06	-	0.01	1.07	0.02	0.03
AUSTRIA_Styria_Lassing		1.05	Average	32.04	16.47	0.00	0.04	0.01	2.82	0.00	0.01	30.62	0.05	0.06	0.01	-	0.02	82.15	0.12	0.07
			St. Dev.	0.49	1.63	0.00	0.03	0.00	0.42	0.00	0.00	0.95	0.04	0.09	0.01	-	0.02	2.11	0.01	0.09

Sample #	CLINOCHLORE	SiO2/MgO		SiO2	Al2O3	TiO2	ZnO	Cr2O3	FeO	NiO	MnO	MgO	CaO	Na2O	K2O	P2O5	SO3	Oxide Sum	F wt%	Cl wt%
AUSTRIA_Styria_Anger		0.94	Average	29.14	21.06	0.03	0.01	0.01	1.91	0.00	0.02	31.08	0.00	0.00	0.00	-	0.01	83.28	0.05	0.01
			St. Dev.	0.60	0.71	0.00	0.01	0.01	0.06	0.01	0.00	0.55	0.00	0.01	0.00	-	0.01	0.52	0.02	0.00
CHI_Cuangai		1.07		34.74	17.24	0.01	0.00	0.01	1.21	0.01	0.00	32.41	0.02	0.00	0.01	-	0.03	85.69	0.01	0.01
CHI_Guangxi_product		0.95	Average	29.66	21.87	0.03	-	-	5.34	-	0.00	31.17	0.02	0.02	0.01	0.00	-	88.12	0.04	0.03
			Std. Dev	0.73	0.32	0.01	-	-	2.03	-	0.01	1.53	0.01	0.01	0.01	0.01	-	1.32	0.02	0.01
ITA_Gianna_in place contact		1.00	Average	28.29	21.74	0.02	0.00	0.00	5.57	-0.01	0.04	28.19	0.00	0.00	0.01	-	0.01	83.85	0.14	0.01
			St. Dev.	0.18	0.02	0.00	0.01	0.00	0.06	0.00	0.00	0.11	0.00	0.01	0.01	-	0.01	0.22	0.03	0.01
ITA_Paola_A		0.99	Average	30.47	20.17	0.01	0.00	0.00	2.18	0.00	0.01	30.87	0.01	0.00	0.00	-	0.01	83.72	0.17	0.01
			Std. Dev.	0.33	0.58	0.00	0.01	0.01	0.04	0.01	0.00	1.11	0.00	0.01	0.00	-	0.00	0.50	0.02	0.00
ITA_Rodoretto_A1		1.00	Average	29.55	19.66	0.01	0.03	0.00	1.96	0.00	0.01	29.69	0.01	0.00	0.00	-	0.04	80.95	0.10	0.04
			Std. dev.	0.16	0.64	0.00	0.04	0.00	1.13	0.00	0.00	0.02	0.01	0.00	0.00	-	0.03	1.52	0.10	0.02
ITA_Rodoretto_B1		0.99		31.06	17.04	0.00	0.05	0.14	2.14	0.00	0.00	31.51	0.02	0.01	0.00	-	0.06	82.03	0.25	0.02
USA_NC_CCFoote		0.92		29.41	21.86	0.02			2.68		0.00	31.90	0.02	0.03	0.05	0.00		85.98	0.30	0.03
USA_NC_light rock		0.91	Average	28.67	23.46	0.03	-	-	2.93	-	0.01	31.64	0.02	0.00	0.02	0.00	-	86.77	0.18	0.01
			Std. Dev	0.69	0.46	0.01	-	-	0.04	-	0.01	0.30	0.01	0.00	0.02	0.01	-	1.45	0.01	0.01
USA_NC_HC_CT_light		0.96	Average	29.37	20.47	0.04	-	-	4.30	-	0.15	30.66	0.01	0.03	0.01	0.02	-	85.06	0.08	0.02
			Std. Dev	0.04	2.44	0.03	-	-	2.96	-	0.07	2.34	0.02	0.04	0.01	0.03	-	1.80	0.25	0.01
USA_VT_Argonaut_brokenbag		1.03	Average	28.61	17.17	0.03	-	-	8.58	-	0.03	27.81	0.03	0.02	0.01	0.00	-	82.29	-0.01	0.09
			St. Dev.	3.16	3.49	0.03	-	-	0.64	-	0.02	3.01	0.00	0.00	0.00	0.00	-	2.00	0.01	0.09
USA_VT_Argonaut_underflow		1.04	Average	31.40	16.82	0.01	-	-	8.93	-	0.02	30.32	0.01	0.02	0.00	-	-	87.53	0.00	0.02
			Std. Dev	1.36	2.49	0.02	-	-	0.51	-	0.01	1.14	0.01	0.01	0.01	-	-	1.29	0.01	0.01
USA_VT_CT_Johnson-E42		1.01		31.59	17.48	-0.01			7.03		0.04	31.40	0.02	-0.01	0.00			87.53	0.00	0.01
USA_VT_Johnson_black		1.04	Average	30.46	17.10	0.02	-	-	9.61	-	0.08	29.34	0.02	0.01	0.00	-	-	86.64	0.05	0.01
			Std. Dev	0.25	0.60	0.01	-	-	0.14	-	0.01	0.36	0.01	0.01	0.01	-	-	1.04	0.01	0.00

Sample #	CLINOCHLORE	SiO2/MgO		SiO2	Al2O3	TiO2	ZnO	Cr2O3	FeO	NiO	MnO	MgO	CaO	Na2O	K2O	P2O5	SO3	Oxide Sum	F wt%	Cl wt%
USA_VT_Johnson_pipe		1.03	Average	31.62	14.26	0.01	-	-	7.64	-	0.04	30.57	0.04	0.01	0.01	-	-	84.21	0.05	0.01
			Std. Dev	2.51	0.90	0.02	-	-	0.27	-	0.00	1.29	0.02	0.00	0.00	-	-	4.44	0.00	0.00
USA_VT_Johnson_UVM		1.09	Average	29.94	15.45	0.03	-	-	10.54	-	0.14	27.41	0.01	0.03	0.02	-	-	83.56	0.07	0.01
			Std. Dev	0.83	1.51	0.01	-	-	0.16	-	0.01	0.52	0.01	0.01	0.01	-	-	0.53	0.01	0.01
USA_VT_Johnson_W23		1.17	Average	31.63	14.62	0.01	-	-	10.83	-	0.33	27.13	0.01	0.02	0.01	-	-	84.60	0.03	0.02
			Std. Dev	0.87	0.97	0.01	-	-	0.04	-	0.06	0.67	0.02	0.01	0.01	-	-	0.82	0.01	0.01
USA_MT_Beaverhead_123		1.01	Average	34.26	12.19	0.01	0.00	0.02	2.19	0.00	0.03	33.85	0.07	0.02	0.00	-	0.02	82.65	0.10	0.55
			Std. Dev.	1.35	0.21	0.00	0.01	0.00	0.16	0.00	0.00	0.50	0.03	0.01	0.00	-	0.02	1.09	0.02	0.19
USA_MT_WC_Sep		1.08		34.60	13.07	0.13	-0.01	0.01	4.56	0.01	0.12	31.93	0.19	0.01	0.29	-	0.00	84.90	0.50	0.01
USA_MT_WC_SF-2		0.98	Average	30.96	9.83	0.34	0.00	0.02	7.96	0.00	0.25	31.47	0.05	0.01	0.14	-	0.03	81.07	0.23	0.19
			Std. Dev.	0.45	0.49	0.09	0.01	0.00	0.13	0.00	0.03	0.18	0.01	0.01	0.03	-	0.00	0.12	0.03	0.02
USA_MT_WC_SF_9		1.02	Average	29.76	19.26	0.01	0.00	0.00	5.88	0.00	0.07	29.23	0.01	0.00	0.00	-	0.00	84.23	0.17	0.00
			Std. Dev.	0.71	0.79	0.00	0.01	0.00	0.24	0.01	0.02	0.35	0.01	0.01	0.00	-	0.01	0.27	0.07	0.00
USA_MT_WC_SF_14		1.03	Average	30.78	17.38	0.01	0.00	0.00	6.22	0.01	0.05	29.84	0.01	0.01	0.00	-	0.00	84.32	0.06	0.01
			Std. Dev.	0.53	0.56	0.01	0.01	0.00	0.94	0.01	0.02	0.79	0.01	0.01	0.00	-	0.01	0.50	0.02	0.00
USA_MT_WC_SF_24_rx		0.98	Average	32.14	10.40	0.27	0.00	0.01	7.49	0.00	0.30	32.63	0.11	0.03	0.42	-	0.01	83.81	0.48	0.15
			Std. Dev.	0.32	0.33	0.09	0.00	0.00	0.59	0.00	0.03	0.19	0.08	0.00	0.14	-	0.00	0.25	0.15	0.02
USA_MT_WC_SF_N4		1.00	Average	34.17	11.96	0.22	0.00	0.01	2.46	0.00	0.24	34.16	0.05	0.02	1.15	-	0.00	84.44	0.04	0.17
			Std. Dev.	0.19	0.22	0.01	0.00	0.00	0.06	0.00	0.02	0.15	0.01	0.01	0.13	-	0.01	0.30	0.01	0.02
USA_MT_WC_SF_N9A		1.07	Average	33.33	14.06	0.03	0.00	0.01	5.64	0.00	0.17	31.18	0.05	0.01	0.22	-	0.00	84.72	0.01	0.00
			Std. Dev.	0.94	1.11	0.02	0.01	0.01	0.85	0.01	0.02	0.82	0.04	0.02	0.14	-	0.00	0.29	0.02	0.00
CT_BP_Johnson		0.93		30.44	21.00	0.01	-	-	2.06	-	0.01	32.84	0.00	0.02	0.01	0.00	-	86.37	0.06	0.02
CT_marker_MBS		0.99	Average	31.57	19.82	0.01	0.00	0.00	1.23	0.00	0.00	31.85	0.01	-0.01	0.00	-	0.01	84.49	0.04	0.00
			St. Dev.	0.13	0.45	0.01	0.01	0.01	0.11	0.00	0.00	0.12	0.01	0.00	0.00	-	0.01	0.30	0.01	0.00

Sample #	Mineral	SiO2/MgO		SiO2	Al2O3	TiO2	ZnO	Cr2O3	FeO	NiO	MnO	MgO	CaO	Na2O	K2O	P2O5	SO3	Oxide Sum	F wt%	Cl wt%
	SEPIOLITE																			
WC_Sep		2.73	Average	48.43	0.26	0.00	-0.01	0.00	3.70	0.00	0.07	17.80	0.09	0.01	0.02	-	0.00	70.38	0.43	0.02
			Std. Dev.	4.82	0.09	0.00	0.01	0.00	0.33	0.01	0.01	2.12	0.07	0.01	0.01	-	0.00	6.95	0.07	0.01
SF_24_bu		2.91	Average	52.07	0.07	0.00	0.01	0.00	7.62	0.00	0.08	17.92	0.05	0.01	0.01	-	0.00	77.82	0.22	0.02
			Std. Dev	3.63	0.01	0.00	0.01	0.00	0.39	0.01	0.02	1.33	0.02	0.00	0.00	-	0.00	5.17	0.08	0.00
USA_MT_Reg_Sep		2.44	Average	54.04	0.03	0.00	0.00	0.00	0.98	0.00	0.10	22.17	0.02	0.02	0.01	-	0.01	77.37	0.27	0.02
			Std. Dev	3.86	0.01	0.00	0.01	0.01	0.11	0.00	0.02	2.11	0.01	0.01	0.00	-	0.00	6.06	0.05	0.01
USA_MT_WC_Sep_N		2.72	Average	49.79	0.20	0.00	-0.01	0.00	4.85	0.00	0.10	18.31	0.10	0.01	0.01	-	0.00	73.37	0.49	0.05
			Std. Dev	6.69	0.09	0.00	0.01	0.00	0.87	0.00	0.03	2.59	0.05	0.01	0.01	-	0.01	9.96	0.08	0.02
Sample #	Mineral	SiO2/MgO		SiO2	Al2O3	TiO2	ZnO	Cr2O3	FeO	NiO	MnO	MgO	CaO	Na2O	K2O	P2O5	SO3	Oxide Sum	F wt%	Cl wt%
	SERPENTINE																			
WC_Sep-serpentine		1.17	Average	43.40	0.32	0.00	0.00	0.00	3.92	0.00	0.27	37.15	0.22	0.00	0.00	-	0.00	85.29	0.15	0.01
			Std. Dev.	0.19	0.04	0.00	0.01	0.00	0.30	0.01	0.04	0.50	0.14	0.01	0.00	-	0.00	0.28	0.02	0.01
USA_MT_WC_SF_24_rx		1.09	Average	42.34	0.46	0.00	0.02	0.00	2.14	0.00	0.10	38.98	0.16	0.00	0.01	-	0.00	84.21	0.13	0.08
			Std. Dev.	0.22	0.13	0.00	0.01	0.00	0.23	0.00	0.01	0.44	0.06	0.01	0.00	-	0.00	0.24	0.04	0.01
USA_MT_WC_SF_N9A		1.18	Average	43.35	0.33	0.00	0.00	0.00	4.37	0.00	0.68	36.59	0.14	0.01	0.00	-	0.00	85.49	0.03	0.03
			Std. Dev.	0.22	0.19	0.00	0.01	0.00	0.21	0.01	0.07	0.23	0.04	0.01	0.00	-	0.00	0.29	0.01	0.01
USA_MT_WC_SF_N7		1.08	Average	42.49	0.05	0.00	0.00	0.00	1.64	0.00	0.21	39.49	0.05	0.00	0.00	-	0.01	83.94	0.07	0.05
			Std. Dev.	0.54	0.05	0.01	0.01	0.01	0.54	0.01	0.12	0.79	0.03	0.01	0.00	-	0.01	0.59	0.03	0.02
USA_MT_WC_SF_N4		1.07	Average	42.51	0.23	0.00	0.00	0.00	1.57	0.00	0.18	39.58	0.05	0.00	0.00	-	0.00	84.13	0.06	0.04
			Std. Dev	0.60	0.35	0.00	0.00	0.01	0.70	0.01	0.15	0.98	0.02	0.01	0.00	-	0.00	0.60	0.01	0.04
USA_MT_SF_N4_T6		1.13	Average	43.12	0.27	0.02	0.00	0.00	2.09	0.00	0.32	38.29	0.11	0.00	0.00	-	0.01	84.22	0.07	0.03
			Std. Dev	0.37	0.21	0.03	0.01	0.01	0.96	0.00	0.18	1.74	0.06	0.01	0.00	-	0.01	0.62	0.06	0.01
USA_MT_WC_SF-2		1.12	Average	42.57	0.08	0.01	0.00	0.00	2.59	0.00	0.26	38.14	0.09	0.00	0.01	-	0.01	83.77	0.10	0.07
			Std. Dev	0.91	0.05	0.01	0.01	0.01	0.37	0.00	0.13	0.71	0.03	0.01	0.01	-	0.01	0.96	0.02	0.02
WC_Sep_N		1.20	Average	44.03	0.12	0.00	-0.01	0.00	3.75	0.01	0.26	36.74	0.09	0.01	0.01	-	0.00	85.01	0.18	0.01
			Std. Dev	0.50	0.03	0.00	0.00	0.00	0.15	0.00	0.02	0.77	0.01	0.01	0.01	-	0.00	0.44	0.05	0.01

Atoms per formula unit values were calculated based on Dyar, Gunter, and Tasa (Table 10.6)
(-) indicates that the element was not analyzed for in this sample
Part 2.

Sample #	Mineral		Si4+	Al3+	Ti4+	Zn2+	Cr3+	Fe2+	Ni2+	Mn2+	Mg2+	Ca2+	Na+	K+	P5+	S6+	F-	OH-	A	B	C	T
	AMPHIBOLE																	2.00	0.0-1.0	2.00	5.00	8.00
USA_CA_WesternTalc_C	Richterite		8.06	0.03	0.00	0.00	0.00	0.11	0.00	0.01	4.93	0.86	1.59	0.19	0.00	0.01	0.19	1.81	0.72	2.00	5.00	8.06
USA_GA_Earnest_fibrous	Actinolite	Average	7.97	0.05	0.00	0.00	0.00	0.97	0.00	0.04	3.97	1.99	0.02	0.01	0.00	0.00	0.04	1.96	0.01	2.00	5.00	8.00
		Std. Dev.	0.02	0.02	0.00	0.00	0.00	0.05	0.00	0.00	0.07	0.02	0.01	0.00	0.00	0.00	0.01	0.01	0.00	0.01	0.00	0.01
USA_GA_Earnest_platy	Actinolite	Average	8.01	0.06	0.00	0.00	0.00	0.73	0.01	0.03	4.20	1.89	0.02	0.01	0.00	0.00	0.06	1.94	0.00	1.92	5.00	8.02
		Std. Dev.	0.03	0.00	0.00	0.00	0.00	0.02	0.00	0.00	0.05	0.04	0.00	0.00	0.00	0.00	0.01	0.01	0.00	0.03	0.00	0.02
USA_NC_Murphy_129	Tremolite	Average	7.90	0.25	0.00	0.00	0.00	0.13	0.00	0.00	4.64	2.02	0.04	0.00	0.00	0.00	0.10	1.90	0.04	2.02	5.00	8.00
		Std. Dev.	0.06	0.04	0.00	0.00	0.00	0.01	0.00	0.00	0.10	0.02	0.01	0.00	0.00	0.00	0.01	0.01	0.01	0.02	0.00	0.01
USA_MT_WC_SF_N9A	Tremolite	Average	7.96	0.07	0.00	0.00	0.00	0.27	0.00	0.10	4.62	1.98	0.03	0.00	0.00	0.00	0.05	1.95	0.00	2.00	5.00	8.00
		Std. Dev	0.01	0.01	0.00	0.00	0.00	0.01	0.00	0.01	0.02	0.01	0.00	0.00	0.00	0.00	0.01	0.01	0.00	0.00	0.00	0.00

Sample #	Mineral		Si4+	Al3+	Ti4+	Zn2+	Cr3+	Fe2+	Ni2+	Mn2+	Mg2+	Ca2+	Na+	K+	P5+	S6+	F-	OH-	Tet	Oct	I
	MICA																	2.00	4.00	2.0-3.0	0.6-1.0
CHI-94	Phlogopite	Average	3.22	0.77	0.00	0.00	0.00	0.02	0.00	0.00	3.06	0.00	0.01	0.68	0.00	0.00	0.12	1.88	3.96	3.09	0.69
		Std. Dev	0.05	0.02	0.00	0.00	0.00	0.01	0.00	0.00	0.05	0.00	0.00	0.01	0.00	0.00	0.02	0.02	0.05	0.08	0.01
ITA_Paola_scop	Muscovite	Average	3.50	2.16	0.01	0.00	0.00	0.01	0.00	0.00	0.50	0.00	0.03	0.97	0.00	0.00	0.03	1.97	4.00	2.18	1.00
		Std. Dev.	0.07	0.05	0.00	0.00	0.00	0.00	0.00	0.00	0.01	0.00	0.00	0.01	0.00	0.00	0.00	0.00	0.00	0.11	0.01
ITA_Rodoretto_A1	Muscovite	Average	3.37	2.59	0.01	0.00	0.00	0.02	0.00	0.00	0.29	0.00	0.06	0.94	0.00	0.00	0.02	1.98	4.00	2.28	1.01
		Std. Dev.	0.05	0.03	0.00	0.00	0.00	0.00	0.00	0.00	0.03	0.00	0.02	0.01	0.00	0.00	0.00	0.00	0.00	0.05	0.00
USA_CA_Victorville	Phlogopite	Average	3.39	0.67	0.00	0.00	0.00	0.00	0.00	0.00	2.80	0.01	0.01	0.84	0.00	0.00	0.19	1.81	4.00	2.87	0.85
		Std. Dev.	0.04	0.02	0.00	0.00	0.00	0.00	0.00	0.00	0.03	0.00	0.00	0.04	0.00	0.00	0.01	0.01	0.00	0.04	0.04
ITA_Gianna_in place contact	Muscovite	Average	3.48	2.35	0.01	0.00	0.00	0.03	0.00	0.00	0.37	0.00	0.06	0.95	0.00	0.00	0.03	1.97	4.00	2.24	1.02
		Std. Dev	0.09	0.19	0.00	0.00	0.00	0.01	0.00	0.00	0.08	0.00	0.02	0.02	0.00	0.00	0.01	0.01	0.00	0.05	0.01
USA_CA_Western Talc_3A	Phlogopite	Average	3.28	0.75	0.01	0.00	0.00	0.04	0.00	0.00	2.75	0.00	0.01	0.89	0.00	0.00	0.22	1.78	3.98	2.84	0.90
		Std. Dev	0.07	0.03	0.00	0.00	0.00	0.02	0.00	0.00	0.06	0.00	0.01	0.03	0.00	0.00	0.02	0.02	0.03	0.08	0.02

Sample #	Mineral		Si4+	Al3+	Ti4+	Zn2+	Cr3+	Fe2+	Ni2+	Mn2+	Mg2+	Ca2+	Na+	K+	P5+	S6+	F-	CO3	Oct		
USA_CA_Western Talc_3C	Phlogopite	Average	3.38	0.64	0.00	0.00	0.00	0.02	0.00	0.00	2.90	0.01	0.02	0.74	0.00	0.00	0.11	1.89	3.99	2.93	0.77
		Std. Dev	0.12	0.10	0.00	0.00	0.00	0.01	0.00	0.00	0.04	0.01	0.02	0.10	0.00	0.00	0.01	0.01	0.02	0.05	0.13
USA_MT_WC_SF_24_rx	Phlogopite	Average	2.83	1.19	0.03	0.00	0.00	0.11	0.00	0.01	2.71	0.03	0.13	0.74	0.00	0.00	0.35	1.65	4.00	2.89	0.90
		Std. Dev.	0.02	0.06	0.00	0.00	0.00	0.02	0.00	0.00	0.01	0.02	0.02	0.04	0.00	0.00	0.07	0.07	0.01	0.05	0.05
CARBONATE	CARBONATE		Si4+	Al3+	Ti4+	Zn2+	Cr3+	Fe2+	Ni2+	Mn2+	Mg2+	Ca2+	Na+	K+	P5+	S6+	F-	CO3	Oct		
AUS_ThSprings	Magnesite	Average	0.04	0.01	0.00	0.00	0.00	0.00	0.00	0.00	0.05	1.86	0.00	0.00	0.00	0.00	0.32	1.68	1.96		
		Std. Dev	0.04	0.01	0.00	0.00	0.00	0.00	0.00	0.00	0.06	0.15	0.00	0.00	0.00	0.00	0.01	0.01	0.04		
AUSTRIA_Styria_Lassing	Dolomite	Average	0.05	0.00	0.00	0.00	0.00	0.04	0.00	0.00	0.87	1.00	0.00	0.00	0.00	0.00	0.00	2.00	1.95		
		Std. Dev	0.04	0.00	0.00	0.00	0.00	0.01	0.00	0.00	0.00	0.08	0.00	0.00	0.00	0.00	0.00	0.00	0.04		
CAN_Ontario_Madoc_170	Dolomite		0.00	0.00	0.00	0.00	0.00	0.00	0.00	0.00	0.95	1.04	0.00	0.00	0.00	0.00	0.00	2.00	2.00		
CAN_Ontario_Madoc_170	Calcite		0.00	0.00	0.00	0.00	0.00	0.00	0.00	0.00	0.01	1.98	0.00	0.00	0.00	0.00	0.00	2.00	2.00		
CHI_Guangxi_G3_91	Calcite		0.00	0.00	0.00	0.00	0.00	0.00	0.00	0.00	1.98	0.00	0.01	0.00	0.00	0.00	0.09	1.91	2.00		
CHI_Cuangai_86	Calcite	Average	0.01	0.00	0.00	0.00	0.00	0.00	0.00	0.00	0.01	1.97	0.00	0.00	0.00	0.00	0.23	1.77	1.99		
		Std. Dev	0.00	0.00	0.00	0.00	0.00	0.00	0.00	0.00	0.00	0.01	0.00	0.00	0.00	0.00	0.03	0.03	0.00		
CHI_Liaoning_90	Magnesite	Average	0.00	0.00	0.00	0.00	0.00	0.01	0.00	0.00	1.99	0.00	0.00	0.00	0.00	0.00	0.00	2.00	2.00		
		Std. Dev	0.00	0.00	0.00	0.00	0.00	0.00	0.00	0.00	0.00	0.00	0.00	0.00	0.00	0.00	0.00	0.00	0.00		
FIN_Nkarelia	Magnesite	Average	0.00	0.00	0.00	0.00	0.00	0.16	0.00	0.00	1.83	0.00	0.00	0.00	0.00	0.00	0.00	2.00	2.00		
		Std. Dev	0.00	0.00	0.00	0.00	0.00	0.05	0.00	0.00	0.05	0.00	0.00	0.00	0.00	0.00	0.00	0.00	0.00		
IND_Ghevaria_mill	Dolomite	Average	-0.01	0.00	0.00	0.00	0.00	0.01	0.00	0.00	0.99	1.01	0.00	0.00	0.00	0.00	0.00	2.00	2.01		
		Std. Dev	0.00	0.00	0.00	0.00	0.00	0.00	0.00	0.00	0.05	0.05	0.00	0.00	0.00	0.00	0.00	0.00	0.00		
ITA_Paola_A	Calcite		0.00	0.00	0.00	0.00	0.00	0.00	0.00	0.00	0.00	1.99	0.00	0.00	0.00	0.00	0.42	1.58	1.99		
ITA_Rodoretto_A1	Dolomite	Avg.	0.00	0.00	0.00	0.00	0.00	0.05	0.00	0.01	0.91	1.03	0.00	0.00	0.00	0.00	0.00	2.00	2.00		
		Std. Dev.	0.00	0.00	0.00	0.00	0.00	0.01	0.00	0.00	0.02	0.00	0.00	0.00	0.00	0.00	0.00	0.00	0.00		
ITA_Rodoretto_B1	Dolomite		0.00	0.00	0.00	0.00	0.00	0.03	0.00	0.00	0.95	1.01	0.00	0.00	0.00	0.00	0.00	2.00	2.00		

CARBONATE	CARBONATE		Si4+	Al3+	Ti4+	Zn2+	Cr3+	Fe2+	Ni2+	Mn2+	Mg2+	Ca2+	Na+	K+	P5+	S6+	F-	CO3	Oct
ITA_Rodoretto_B1	Calcite		0.00	0.00	0.00	0.00	0.00	0.00	0.00	0.00	0.00	1.99	0.00	0.00	0.00	0.00	0.35	1.65	2.00
MOR_109	Calcite	Avg.	0.01	0.00	0.00	0.00	0.00	0.00	0.00	0.00	0.03	1.94	0.00	0.00	0.00	0.00	0.10	1.90	1.98
		Std. Dev.	0.01	0.00	0.00	0.00	0.00	0.00	0.00	0.00	0.03	0.06	0.00	0.00	0.00	0.01	0.17	0.17	0.02
USA_CA_Grantham	Calcite	Avg	0.00	0.00	-0.01	0.00	0.00	0.00	0.00	0.00	0.04	1.96	0.00	0.00	0.00	0.00	0.01	1.99	2.01
		Std. Dev.	0.00	0.00	0.01	0.00	0.00	0.00	0.00	0.00	0.01	0.03	0.00	0.00	0.00	0.01	0.00	0.00	0.03
USA_MT_Beaverhead	Calcite		0.01	0.00	0.00	0.00	0.00	0.00	0.00	0.00	0.01	1.97	0.00	0.00	0.00	0.00	0.33	1.67	1.99
USA_NC_Murphy_129	Calcite		0.01	0.00	0.00	0.00	0.00	0.00	0.00	0.00	0.01	1.97	0.00	0.00	0.00	0.00	0.30	1.70	1.99
USA_TX_VanHorn_black	Dolomite		0.24	0.00	0.00	0.00	0.00	0.00	0.00	0.00	0.74	0.78	0.00	0.00	0.00	0.00	0.01	1.99	1.76
USA_VT_CT_Johnson_E42	Magnesite		0.01	0.00	0.00	0.00	0.00	0.25	0.00	0.00	1.73	0.00	0.00	0.00	0.00	0.00	0.00	2.00	1.99
USA_VT_CT_Johnson_E42	Magnesite		0.00	0.00	0.00	0.00	0.00	0.10	0.00	0.00	1.89	0.01	0.00	0.00	0.00	0.00	0.00	2.00	2.00
USA_VT_Johnson_rafters	Magnesite		0.02	0.00	0.00	0.00	0.00	0.11	0.00	0.00	1.86	0.00	0.00	0.00	0.00	0.00	0.00	2.00	1.98
USA_VT_Johnson_pipe	Magnesite	Average	0.03	0.00	0.00	0.00	0.00	0.26	0.00	0.00	1.63	0.02	0.00	0.00	0.00	0.00	0.00	2.00	1.96
		Std. Dev	0.03	0.00	0.00	0.00	0.00	0.02	0.00	0.00	0.02	0.02	0.00	0.00	0.00	0.00	0.00	0.00	0.03
USA_VT_Argonaut_HG	Magnesite	Average	0.00	0.00	0.00	0.00	0.00	0.22	0.00	0.00	1.76	0.01	0.00	0.00	0.00	0.00	0.00	2.00	2.00
		Std. Dev	0.00	0.00	0.00	0.00	0.00	0.03	0.00	0.00	0.03	0.00	0.00	0.00	0.00	0.00	0.00	0.00	0.00
CT_BP_Johnson	Dolomite		0.02	0.00	0.00	0.00	0.00	0.01	0.00	0.00	0.85	1.08	0.00	0.00	0.01	0.00	0.01	1.99	1.96
CT_FP_CSI		Average	-0.01	0.00	0.00	0.00	0.00	0.01	0.00	0.00	0.48	1.52	0.00	0.00	0.00	0.00	0.00	2.00	2.01
		Std. Dev	0.00	0.00	0.00	0.00	0.00	0.01	0.00	0.00	0.64	0.67	0.00	0.00	0.00	0.00	0.00	0.00	0.01

Sample #			Si4+	Al3+	Ti4+	Zn2+	Cr3+	Fe2+	Ni2+	Mn2+	Mg2+	Ca2+	Na+	K+	P5+	S6+	F-	OH-	Tet	Oct
	CLINOCHLORE		3.00	2.00							5.00							8.00	4.00	6.00
AUS_Mt.Seabrook		Average	3.05	2.01	0.00	0.00	0.00	0.13	0.00	0.00	4.74	0.00	0.01	0.00	0.00	0.00	0.04	7.96	4.00	5.93
		St. Dev.	0.06	0.07	0.00	0.00	0.00	0.02	0.00	0.00	0.09	0.00	0.00	0.01	0.00	0.00	0.00	0.00	0.00	0.04
AUSTRIA_Styria_Lassing		Average	3.17	1.92	0.00	0.00	0.00	0.23	0.00	0.00	4.52	0.01	0.01	0.00	0.00	0.00	0.04	7.96	4.00	5.85
		St. Dev.	0.09	0.16	0.00	0.00	0.00	0.03	0.00	0.00	0.11	0.00	0.02	0.00	0.00	0.00	0.00	0.00	0.00	0.03

Sample #	CLINOCHLORE		Si4+	Al3+	Ti4+	Zn2+	Cr3+	Fe2+	Ni2+	Mn2+	Mg2+	Ca2+	Na+	K+	P5+	S6+	F-	OH-	Tet	Oct
AUSTRIA_Styria_Anger		Average	2.84	2.42	0.00	0.00	0.00	0.16	0.00	0.00	4.52	0.00	0.00	0.00	0.00	0.00	0.01	7.99	4.00	5.94
		St. Dev.	0.05	0.09	0.00	0.00	0.00	0.01	0.00	0.00	0.07	0.00	0.00	0.00	0.00	0.00	0.00	0.00	0.00	0.02
CHI_Cuangai			3.26	1.90	0.00	0.00	0.00	0.09	0.00	0.00	4.53	0.00	0.00	0.00	0.00	0.00	0.00	8.00	4.00	5.78
CHI_Guangxi_product		Average	2.79	2.42	0.00	0.00	0.00	0.42	0.00	0.00	4.36	0.00	0.00	0.00	0.00	0.00	0.01	7.99	4.00	6.00
		Std. Dev	0.03	0.03	0.00	0.00	0.00	0.17	0.00	0.00	0.15	0.00	0.00	0.00	0.00	0.00	0.01	0.01	0.00	0.02
ITA_Gianna_in place contact		Average	2.79	2.53	0.00	0.00	0.00	0.46	0.00	0.00	4.15	0.00	0.00	0.00	0.00	0.00	0.04	7.96	4.00	5.94
		St. Dev.	0.01	0.01	0.00	0.00	0.00	0.00	0.00	0.00	0.02	0.00	0.00	0.00	0.00	0.00	0.01	0.01	0.00	0.01
ITA_Paola_A		Average	2.95	2.30	0.00	0.00	0.00	0.18	0.00	0.00	4.46	0.00	0.00	0.00	0.00	0.00	0.05	7.95	4.00	5.89
		Std. Dev.	0.04	0.07	0.00	0.00	0.00	0.00	0.00	0.00	0.15	0.00	0.00	0.00	0.00	0.00	0.01	0.01	0.00	0.06
ITA_Rodoretto_A1		Average	2.96	2.32	0.00	0.00	0.00	0.16	0.00	0.00	4.43	0.00	0.00	0.00	0.00	0.00	0.03	7.97	4.00	5.87
		Std. dev.	0.05	0.05	0.00	0.00	0.00	0.09	0.00	0.00	0.05	0.00	0.00	0.00	0.00	0.00	0.03	0.03	0.00	0.03
ITA_Rodoretto_B1			3.08	1.99	0.00	0.00	0.01	0.18	0.00	0.00	4.66	0.00	0.00	0.00	0.00	0.00	0.08	7.92	4.00	5.91
USA_NC_CCFoote			2.79	2.45	0.00	0.00	0.00	0.21	0.00	0.00	4.52	0.00	0.01	0.01	0.00	0.00	0.09	7.91	4.00	5.97
USA_NC_light rock		Average	2.70	2.61	0.00	0.00	0.00	0.23	0.00	0.00	4.45	0.00	0.00	0.00	0.00	0.00	0.05	7.95	4.00	5.99
		Std Dev	0.02	0.02	0.00	0.00	0.00	0.00	0.00	0.00	0.04	0.00	0.00	0.00	0.00	0.00	0.00	0.00	0.00	0.02
USA_NC_HC_CT_light		Average	2.85	2.33	0.00	0.00	0.00	0.35	0.00	0.01	4.42	0.00	0.01	0.00	0.00	0.00	0.04	7.96	4.00	5.97
		Std Dev	0.11	0.19	0.00	0.00	0.00	0.25	0.00	0.00	0.18	0.00	0.01	0.00	0.00	0.00	0.05	0.05	0.00	0.02
USA_VT_Argonaut_brokenbag		Average	2.93	2.08	0.00	0.00	0.00	0.74	0.00	0.00	4.25	0.00	0.00	0.00	0.00	0.00	0.00	8.00	4.00	6.01
		St. Dev.	0.24	0.48	0.00	0.00	0.00	0.08	0.00	0.00	0.34	0.00	0.00	0.00	0.00	0.00	0.00	0.00	0.00	0.01
USA_VT_Argonaut_underflow		Average	3.03	1.91	0.00	0.00	0.00	0.72	0.00	0.00	4.36	0.00	0.00	0.00	0.00	0.00	0.00	8.00	4.00	6.01
		Std. Dev	0.14	0.27	0.00	0.00	0.00	0.04	0.00	0.00	0.17	0.00	0.00	0.00	0.00	0.00	0.00	0.00	0.00	0.00
USA_VT_CT_Johnson-E42			3.01	1.96	0.00	0.00	0.00	0.56	0.00	0.00	4.46	0.00	0.00	0.00	0.00	0.00	0.00	8.00	4.00	6.00
USA_VT_Johnson_black		Average	2.98	1.97	0.00	0.00	0.00	0.79	0.00	0.01	4.28	0.00	0.00	0.00	0.00	0.00	0.02	7.98	4.00	6.03
		Std. Dev	0.03	0.05	0.00	0.00	0.00	0.02	0.00	0.00	0.00	0.00	0.00	0.00	0.00	0.00	0.00	0.00	0.00	0.00

Sample #	CLINOCHLORE		Si4+	Al3+	Ti4+	Zn2+	Cr3+	Fe2+	Ni2+	Mn2+	Mg2+	Ca2+	Na+	K+	P5+	S6+	F-	OH-	Tet	Oct
USA_VT_Johnson_pipe		Average	3.15	1.67	0.00	0.00	0.00	0.64	0.00	0.00	4.54	0.00	0.00	0.00	0.00	0.00	0.02	7.98	4.00	6.01
		Std. Dev	0.06	0.01	0.00	0.00	0.00	0.06	0.00	0.00	0.08	0.00	0.00	0.00	0.00	0.00	0.00	0.00	0.00	0.07
USA_VT_Johnson_UVM		Average	3.06	1.86	0.00	0.00	0.00	0.90	0.00	0.01	4.17	0.00	0.01	0.00	0.00	0.00	0.02	7.98	4.00	6.01
		Std. Dev	0.09	0.18	0.00	0.00	0.00	0.01	0.00	0.00	0.09	0.00	0.00	0.00	0.00	0.00	0.00	0.00	0.00	0.01
USA_VT_Johnson_W23		Average	3.19	1.74	0.00	0.00	0.00	0.91	0.00	0.03	4.08	0.00	0.00	0.00	0.00	0.00	0.01	7.99	4.00	5.94
		Std. Dev	0.09	0.10	0.00	0.00	0.00	0.01	0.00	0.01	0.11	0.00	0.00	0.00	0.00	0.00	0.00	0.00	0.00	0.06
USA_MT_Beaverhead_123		Average	3.36	1.41	0.00	0.00	0.00	0.18	0.00	0.00	4.96	0.01	0.00	0.00	0.00	0.00	0.03	7.97	4.00	5.92
		Std. Dev.	0.08	0.04	0.00	0.00	0.00	0.01	0.00	0.00	0.11	0.00	0.00	0.00	0.00	0.00	0.00	0.00	0.00	0.07
USA_MT_WC_Sep			3.35	1.49	0.01	0.00	0.00	0.37	0.00	0.01	4.62	0.02	0.00	0.04	0.00	0.00	0.15	7.85	4.00	5.85
USA_MT_WC_SF-2		Average	3.24	1.21	0.03	0.00	0.00	0.70	0.00	0.02	4.91	0.01	0.00	0.02	0.00	0.00	0.08	7.92	4.00	6.10
		Std. Dev.	0.04	0.06	0.01	0.00	0.00	0.01	0.00	0.00	0.02	0.00	0.00	0.00	0.00	0.00	0.01	0.01	0.00	0.00
USA_MT_WC_SF_9		Average	2.93	2.24	0.00	0.00	0.00	0.48	0.00	0.01	4.29	0.00	0.00	0.00	0.00	0.00	0.05	7.95	4.00	5.95
		Std. Dev.	0.07	0.09	0.00	0.00	0.00	0.02	0.00	0.00	0.05	0.00	0.00	0.00	0.00	0.00	0.02	0.02	0.00	0.03
USA_MT_WC_SF_14		Average	3.03	2.02	0.00	0.00	0.00	0.51	0.00	0.00	4.38	0.00	0.00	0.00	0.00	0.00	0.02	7.98	4.00	5.95
		Std. Dev.	0.04	0.06	0.00	0.00	0.00	0.08	0.00	0.00	0.11	0.00	0.00	0.00	0.00	0.00	0.01	0.01	0.00	0.03
USA_MT_WC_SF_24_rx		Average	3.24	1.24	0.02	0.00	0.00	0.63	0.00	0.03	4.91	0.01	0.01	0.05	0.00	0.00	0.15	7.85	4.00	6.07
		Std. Dev.	0.02	0.04	0.01	0.00	0.00	0.05	0.00	0.00	0.04	0.01	0.00	0.02	0.00	0.00	0.05	0.05	0.00	0.04
USA_MT_WC_SF_N4		Average	3.33	1.37	0.02	0.00	0.00	0.20	0.00	0.02	4.96	0.01	0.00	0.14	0.00	0.00	0.01	7.99	4.00	5.89
		Std. Dev.	0.01	0.02	0.00	0.00	0.00	0.00	0.00	0.00	0.03	0.00	0.00	0.02	0.00	0.00	0.00	0.00	0.00	0.01
USA_MT_WC_SF_N9A		Average	3.26	1.62	0.00	0.00	0.00	0.46	0.00	0.01	4.55	0.01	0.00	0.03	0.00	0.00	0.00	8.00	4.00	5.91
		Std. Dev.	0.09	0.13	0.00	0.00	0.00	0.07	0.00	0.00	0.11	0.00	0.00	0.02	0.00	0.00	0.01	0.01	0.00	0.03
CT_BP_Johnson			2.87	2.33	0.00	0.00	0.00	0.16	0.00	0.00	4.61	0.00	0.00	0.00	0.00	0.00	0.02	7.98	4.00	5.97
CT_marker_MBS		Average	3.01	2.23	0.00	0.00	0.00	0.10	0.00	0.00	4.53	0.00	0.00	0.00	0.00	0.00	0.01	7.99	4.00	5.87
		St. Dev.	0.02	0.04	0.00	0.00	0.00	0.01	0.00	0.00	0.03	0.00	0.00	0.00	0.00	0.00	0.00	0.00	0.00	0.00

Sample #	Mineral		Si4+	Al3+	Ti4+	Zn2+	Cr3+	Fe2+	Ni2+	Mn2+	Mg2+	Ca2+	Na+	K+	P5+	S6+	F-	OH-	Tet	Oct
	SEPIOLITE		6.00								4.00							2.00	6.00	4.00
WC_Sep		Average	6.10	0.04	0.00	0.00	0.00	0.39	0.00	0.01	3.33	0.01	0.00	0.00	0.00	0.00	0.17	1.83	6.10	3.77
		Std. Dev.	0.04	0.01	0.00	0.00	0.00	0.05	0.00	0.00	0.08	0.01	0.00	0.00	0.00	0.00	0.04	0.04	0.04	0.08
SF_24_bu		Average	6.06	0.01	0.00	0.00	0.00	0.74	0.00	0.01	3.11	0.01	0.00	0.00	0.00	0.00	0.08	1.92	6.06	3.87
		Std. Dev	0.03	0.00	0.00	0.00	0.00	0.04	0.00	0.00	0.06	0.00	0.00	0.00	0.00	0.00	0.03	0.03	0.03	0.06
USA_MT_Reg_Sep		Average	6.08	0.00	0.00	0.00	0.00	0.09	0.00	0.01	3.72	0.00	0.00	0.00	0.00	0.00	0.10	1.90	6.08	3.82
		Std. Dev	0.04	0.00	0.00	0.00	0.00	0.01	0.00	0.00	0.09	0.00	0.00	0.00	0.00	0.00	0.02	0.02	0.04	0.09
USA_MT_WC_Sep_N		Average	6.06	0.03	0.00	0.00	0.00	0.49	0.00	0.01	3.32	0.01	0.00	0.00	0.00	0.00	0.19	1.81	6.06	3.85
		Std. Dev	0.04	0.02	0.00	0.00	0.00	0.05	0.00	0.00	0.07	0.01	0.00	0.00	0.00	0.00	0.05	0.05	0.03	0.07
Sample #	Mineral		Si4+	Al3+	Ti4+	Zn2+	Cr3+	Fe2+	Ni2+	Mn2+	Mg2+	Ca2+	Na+	K+	P5+	S6+	F-	OH-	Tet	Oct
	SERPENTINE																	4.00	2.00	3.00
WC_Sep-serpentine		Average	2.07	0.02	0.00	0.00	0.00	0.16	0.00	0.01	2.65	0.01	0.00	0.00	0.00	0.00	0.02	3.98	2.07	2.83
		Std. Dev.	0.01	0.00	0.00	0.00	0.00	0.01	0.00	0.00	0.03	0.01	0.00	0.00	0.00	0.00	0.00	0.00	0.01	0.02
USA_MT_WC_SF_24_rx		Average	2.03	0.03	0.00	0.00	0.00	0.09	0.00	0.00	2.79	0.01	0.00	0.00	0.00	0.00	0.02	3.98	2.03	2.91
		Std. Dev.	0.01	0.01	0.00	0.00	0.00	0.01	0.00	0.00	0.02	0.00	0.00	0.00	0.00	0.00	0.01	0.01	0.01	0.01
USA_MT_WC_SF_N9A		Average	2.08	0.02	0.00	0.00	0.00	0.18	0.00	0.03	2.61	0.01	0.00	0.00	0.00	0.00	0.00	4.00	2.08	2.83
		Std. Dev.	0.01	0.01	0.00	0.00	0.00	0.01	0.00	0.00	0.01	0.00	0.00	0.00	0.00	0.00	0.00	0.00	0.01	0.01
USA_MT_WC_SF_N7		Average	2.04	0.00	0.00	0.00	0.00	0.07	0.00	0.01	2.83	0.00	0.00	0.00	0.00	0.00	0.01	3.99	2.04	2.91
		Std. Dev.	0.01	0.00	0.00	0.00	0.00	0.02	0.00	0.00	0.05	0.00	0.00	0.00	0.00	0.00	0.00	0.00	0.01	0.03
USA_MT_WC_SF_N4		Average	2.04	0.01	0.00	0.00	0.00	0.06	0.00	0.01	2.83	0.00	0.00	0.00	0.00	0.00	0.01	3.99	2.04	2.91
		Std. Dev	0.01	0.02	0.00	0.00	0.00	0.03	0.00	0.01	0.07	0.00	0.00	0.00	0.00	0.00	0.00	0.00	0.01	0.03
USA_MT_SF_N4_T6		Average	2.07	0.02	0.00	0.00	0.00	0.08	0.00	0.01	2.74	0.01	0.00	0.00	0.00	0.00	0.01	3.99	2.07	2.85
		Std. Dev	0.02	0.01	0.00	0.00	0.00	0.04	0.00	0.01	0.11	0.00	0.00	0.00	0.00	0.00	0.01	0.01	0.02	0.05
USA_MT_WC_SF-2		Average	2.06	0.00	0.00	0.00	0.00	0.10	0.00	0.01	2.75	0.00	0.00	0.00	0.00	0.00	0.02	3.98	2.06	2.87
		Std. Dev	0.02	0.00	0.00	0.00	0.00	0.01	0.00	0.01	0.06	0.00	0.00	0.00	0.00	0.00	0.00	0.00	0.02	0.04
WC_Sep_N		Average	2.10	0.01	0.00	0.00	0.00	0.15	0.00	0.01	2.62	0.00	0.00	0.00	0.00	0.00	0.03	3.97	2.10	2.78
		Std. Dev	0.02	0.00	0.00	0.00	0.00	0.01	0.00	0.00	0.05	0.00	0.00	0.00	0.00	0.00	0.01	0.01	0.02	0.05